SAND2023-04826

SANDIA REPORT

Printed June 2023

Sandia National Laboratories

Improved Modeling of Waste Isolation Pilot Plant Disposal Room Porosity

Chet Vignes, James Bean, Benjamin Reedlunn

Prepared by
Sandia National Laboratories
Albuquerque, New Mexico 87185
Livermore, California 94550

Issued by Sandia National Laboratories, operated for the United States Department of Energy by National Technology & Engineering Solutions of Sandia, LLC.

NOTICE: This report was prepared as an account of work sponsored by an agency of the United States Government. Neither the United States Government, nor any agency thereof, nor any of their employees, nor any of their contractors, subcontractors, or their employees, make any warranty, express or implied, or assume any legal liability or responsibility for the accuracy, completeness, or usefulness of any information, apparatus, product, or process disclosed, or represent that its use would not infringe privately owned rights. Reference herein to any specific commercial product, process, or service by trade name, trademark, manufacturer, or otherwise, does not necessarily constitute or imply its endorsement, recommendation, or favoring by the United States Government, any agency thereof, or any of their contractors or subcontractors. The views and opinions expressed herein do not necessarily state or reflect those of the United States Government, any agency thereof, or any of their contractors.

Printed in the United States of America. This report has been reproduced directly from the best available copy.

Available to DOE and DOE contractors from

U.S. Department of Energy
Office of Scientific and Technical Information
P.O. Box 62
Oak Ridge, TN 37831

Telephone: (865) 576-8401
Facsimile: (865) 576-5728
E-Mail: reports@osti.gov
Online ordering: http://www.osti.gov/scitech

Available to the public from

U.S. Department of Commerce
National Technical Information Service
5301 Shawnee Road
Alexandria, VA 22312

Telephone: (800) 553-6847
Facsimile: (703) 605-6900
E-Mail: orders@ntis.gov
Online order: https://classic.ntis.gov/help/order-methods





ABSTRACT

Disposal rooms at the Waste Isolation Pilot Plant (WIPP) contain waste and gas, and their porosity evolves over time. This report presents several improvements to the disposal room porosity model and presents new porosity predictions for use in future WIPP Performance Assessment activities. The improvements pertain to three sub-models: the geomechanical model, the waste compaction model, and the gas pressurization model. The impacts of each major improvement were quantified and the new porosity predictions were shown to be both mesh and domain size converged. Also, sensitivity studies on the disposal room horizon, clay seam friction coefficients, and homogenized waste representation were performed to support assumptions in the disposal room porosity model. To compare the legacy and new porosity predictions, the simulation results were plotted as a response surface, where gas pressure and time are inputs and porosity is the output. The new porosity response surface is insensitive to pressures beneath lithostatic pressure and highly sensitive to pressures above lithostatic pressure. The legacy porosity response surface, on the other hand, has moderate porosity gradients over all pressures. The new porosity response surface has a stronger scientific foundation than the legacy surface and may now be used for Compliance Decision Analyses.

Acknowledgment

The authors would like to acknowledge several individuals for their contributions. Courtney Herrick and Richard Jensen provided useful comments on the disposal room porosity model and the analysis of the results. Seth King helped us understand the manner in which the porosity response surface is used in the WIPP Performance Assessment. Todd Zeitler produced the official simulation results on the qualified computer system. Last but not least, Jibril Coulibaly formally reviewed a draft of the report.

CONTENTS

1. Introduction **11**

2. Disposal Room Porosity Model **14**
2.1. Geomechanical Model 14
2.1.1. Background 14
2.1.2. Scope 14
2.1.3. Stratigraphy 15
2.1.4. Model Geometry, Boundary Conditions, and Initial Conditions 15
2.1.5. Geomaterial Models 18
2.1.6. Frictional Sliding Models 19
2.2. Waste Compaction Model 20
2.2.1. Scope 20
2.2.2. Homogenized Waste Block 21
2.2.3. Waste Material Model 22
2.3. Gas Pressurization Model 24
2.3.1. Gas Generation Potential 24
2.3.2. Gas Constitutive Model 25
2.3.3. Surfaces Subject to Gas Pressure 26
2.4. Numerical Approach 26
2.5. Summary 28

3. Results **30**
3.1. Progression from the Legacy Toward the New Model 31
3.1.1. Recreated Legacy Model Simulations 31
3.1.2. Impact of Improved Numerical Setup 32
3.1.3. Impact of New Geomechanical Model 32
3.1.4. Impact of New Waste Compaction Model 34
3.1.5. Impact of New Gas Pressurization Model 35
3.2. New Porosity Response Surface 35
3.3. Legacy vs. New Porosity Response Surface 40
3.4. Sensitivity Studies 40
3.4.1. Lower vs. Upper Horizon 40
3.4.2. Clay Seam Friction Coefficient 43
3.4.3. Homogenized vs. Discrete Containers 44

4. Summary **50**

Bibliography **53**

Appendices 56

A. Geomechanical Model Validation Simulations 56

B. Numerical Details 58
B.1. Miscellaneous Details 58
B.2. Solution Scheme 60
B.3. Mesh Convergence Study 62
B.4. Domain Size Study 64

C. Example Simulation Files 67
C.1. Mesh Generation Files 67
C.1.1. Recreated Legacy Model 67
C.1.2. New Model 73
C.2. Sierra/SM Input Files 88
C.2.1. Recreated Legacy Model 88
C.2.2. New Model 97

D. New Porosity Response Surface Raw Data 122

LIST OF FIGURES

Figure 1-1. Photo and schematic of a disposal room filled with waste containers, magnesium oxide sacks, and gas. 11

Figure 2-1. Legacy and new stratigraphies. 16
Figure 2-2. Layout of a WIPP disposal panel. 17
Figure 2-3. Initial model geometry and boundary conditions. 17
Figure 2-4. A hexagonal array of containers (with MgO and gas) versus a homogenized waste block (with gas). 22
Figure 2-5. Legacy and new gas generation potentials, $f = 1$, for a disposal room. 24
Figure 2-6. Legacy finite element mesh and new (base) finite element mesh for lower horizon disposal room and waste. The recreated legacy mesh is essentially the same as the mesh shown in (a). (The image in (a) was modified from Stone (1997a, Fig. 5).) 27

Figure 3-1. Comparison of Eulerian porosity and pressure histories between the legacy model and recreated legacy model for a lower horizon disposal room. 31
Figure 3-2. Comparison of porosity histories between the recreated legacy model and models which progressively switch to the new numerical model, new geomechanical model, and new waste compaction model for zero gas generation, $f = 0$, over 10,000 years. All results correspond to a lower horizon disposal room. 33
Figure 3-3. Comparison of lower horizon room volume histories between the recreated legacy model and the new model for zero gas generation, $f = 0$. 34
Figure 3-4. Comparison of a deformed lower horizon disposal room between the recreated legacy model (left) and new model (right) at 10,000 years for zero gas generation, $f = 0$. 35
Figure 3-5. Lower horizon Eulerian and Lagrangian porosity histories over 10,000 years for the new model. 36
Figure 3-6. Lower horizon disposal room deformations at select years for three gas generation factors. 37
Figure 3-7. Lower horizon disposal room gas pressure histories for the new model. 38
Figure 3-8. Lower horizon disposal room Eulerian and Lagrangian porosity intensity maps for the new model. 39
Figure 3-9. Lower horizon Eulerian and Lagrangian porosity intensity maps for the recreated legacy model. 41
Figure 3-10. Comparison of Eulerian porosity histories between a lower horizon and an upper horizon disposal room over 10,000 years and the first 1,000 years. 42
Figure 3-11. Comparison of Eulerian porosity histories for different clay seam friction coefficients (see Table 2-1) and disposal room horizons. 43
Figure 3-12. Discrete container arrangements. 44

Figure 3-13. Discrete container mesh. 45
Figure 3-14. Comparison of room closure histories between discrete container waste arrangements and a homogeneous waste block over 600 years for an upper horizon disposal room with zero gas generation, $f = 0$. 46
Figure 3-15. Comparison of porosity histories between discrete container waste arrangements and a homogeneous waste block over 600 years for an upper horizon disposal room with zero gas generation, $f = 0$. 47
Figure 3-16. Upper horizon disposal room deformations at select years with zero gas generation for the discrete container hexagonal arrangement shown in the stratigraphy (left) and with the room surface boundary (right). 48
Figure 3-17. Upper horizon disposal room deformations at select years with zero gas generation for the discrete container triangular arrangement shown in the stratigraphy (left) and with the room surface boundary (right). 49

Figure A-1. Room D, G, and Q nominal initial cross-sectional geometries and locations within the stratigraphy. 56
Figure A-2. Simulation predictions of Room D, G, and Q horizontal and vertical closure compared against experimental measurements. 57

Figure B-1. Full and enlarged views of the coarse (left), base (center), and fine (right) meshes for a lower horizon disposal room. 63
Figure B-2. Comparison of Eulerian porosity histories between coarse, base, and fine meshes for a lower horizon disposal room with various gas generation factors over 1,000 and 10,000 years. 64
Figure B-3. Schematics of the four upper horizon domains considered. 65
Figure B-4. Comparison of room closure histories and room volume histories between the $\approx$ 100 m domain size and larger domains for an upper horizon, empty disposal room. 66

LIST OF TABLES

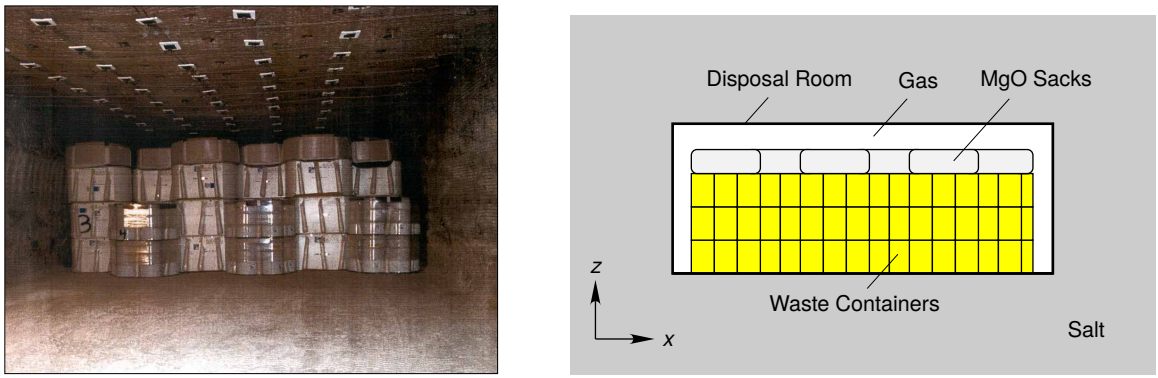
Table 2-1. Clay seam friction coefficients 20
Table 2-2. Gas generation potential parameters 25
Table 2-3. Summary of major changes between the legacy model, recreated legacy model, and new model 29

Table B-1. Material model implementation information 59
Table B-2. Mesh properties and computational times 62

Table D-1. Eulerian porosity data at each gas generation factor, f 122
Table D-2. Lagrangian porosity data at each gas generation factor, f 128
Table D-3. Pressure data at each gas generation factor, f 135

1. INTRODUCTION

The Waste Isolation Pilot Plant (WIPP) is a repository for defense-related nuclear waste located in southeastern New Mexico. The repository is about 650 m underground in the Salado rock salt formation. As shown in Fig. 1-1, the waste disposal rooms within the repository have a rectangular cross-section and typically contain waste containers, magnesium oxide sacks, and various amounts of gas that might be generated due to container degradation and brine radiolysis. These rooms gradually close and compact their contents over the course of decades to centuries because salt viscoplastically deforms under deviatoric stress. The compaction process continues until the room contents supply sufficient back pressure to resist the lithostatic pressure $p^{\text{litho}} \approx 14.7$ MPa at the repository horizon.



(a) Photo **(b) Schematic**

Figure 1-1. Photo and schematic of a disposal room filled with waste containers, magnesium oxide sacks, and gas.

The spatially averaged porosity within a disposal room, hereafter referred to as disposal room porosity, is an input to the WIPP Performance Assessment (PA). Disposal room porosity principally affects the potential for radionuclide releases due to, what are known as, spallings and direct brine releases (DBR). "Spallings are solid materials blown into the borehole by gas flow through the waste at the time of a drilling intrusion." (Hansen et al., 2004) "Direct brine releases are volumes of contaminated brine that may flow from the waste into a borehole during and immediately after a drilling intrusion." (Hansen et al., 2004) Greater disposal room porosity has the potential to decrease spalling releases, due to the decreased gas pressure within the repository, and increase direct brine releases, due to the increased volume of brine permitted within the repository.

This link between porosity and potential releases led Sandia National Laboratories to develop a method to predict disposal room porosity in the 1990's. Room porosity depends on the lithostatic pressure p^{litho}, the mechanical behavior of the rock surrounding the room, the waste's mechanical

behavior as it compacts, and the gas pressure within the room. Gas pressure depends on the volume of the room, the temperature, and number of moles of gas n_g. Ideally, n_g would depend on the number of moles of gas generated n_{gg} and the net number of moles of gas that has flowed into the room, but including gas flow would require coupling solid mechanics simulations to fluid flow simulations. Running 1000's of such coupled simulations for the WIPP Performance Assessment would be very computationally demanding. Instead, an alternative uncoupled approach was and continues to be used.

In the uncoupled approach, a series of disposal room porosity simulations are performed, followed by a series of PA flow simulations. The disposal room porosity simulations do not allow gas to escape from the room ($n_g = n_{gg}$), and the gas generation history is prescribed a-priori. Each simulation utilizes a different multiple of the maximum expected gas generation history in order to compute a series of porosity and gas pressure histories. A porosity response surface, where porosity is a function of both time and the gas pressure in the room, is then constructed. The PA flow simulations use this porosity response surface as a look-up table to determine the volume available to store gas at a given gas pressure and time. The coupled and uncoupled approaches give the same response if the n_g history predicted by the PA flow simulation matches the n_g history used in the disposal room porosity simulation. The PA flow simulations, however, are not constrained to follow the same n_g histories considered in the disposal room porosity simulations. Consider a scenario, for example, where n_g is small and then suddenly increases at $t = 1,000$ yr, causing an increase in gas pressure. A fully coupled approach would predict a gradual increase in porosity after $t = 1,000$ yr because it includes rock salt's viscoplastic path dependence. The uncoupled approach, on the other hand, would likely predict a nearly instantaneous porosity increase directly following $t = 1,000$ yr because it obtains the porosity from a look-up table that was computed using qualitatively different n_g histories. Nevertheless, the error incurred by ignoring such transient effects is assumed to be acceptably small for the uncoupled approach's computational savings.

The porosity surface computed in 1997, referred to in this report as the legacy porosity response surface, was documented in Stone (1997a), with supporting documentation in Butcher (1997a,b). This legacy porosity response surface was used in the PA calculations for the original Compliance Certification Application (CCA) and each Compliance Recertification Application (CRA) since then, including the most recent CRA-2019 (CBFO, 2019). Despite the continued use of the legacy porosity surface, the geomechanical model and waste compaction model within the greater disposal room porosity model have each been revisited once.

In 2004, Park and Holland (2007)[1] studied the impact of mining disposal rooms 2.43 m higher, such that the ceilings of these upper horizon rooms were coincident with Clay Seam G. They found this change had a relatively minor impact on room porosity, so the CRAs continued to use the legacy porosity response surface for simplicity.

In 2005, Park and Hansen (2005) computed porosity response surfaces of rooms filled with different types of waste containers, such as standard waste containers, super-compacted waste from the Advanced Mixed Waste Treatment Project (AMWTP), and Pipe Overpack (POP)

[1]Park and Holland originally released their study as SAND2003-3409 in January 2004, but they later released a corrected version as SAND2007-3334 in September 2007.

containers. They considered rooms entirely filled with one container type, a room filled with 1/3 super-compacted waste and 2/3 standard waste, and a room filled with 2/3 super-compacted waste and 1/3 standard waste. The super-compacted and POP waste forms tended to hold open the rooms, resulting in significantly greater room porosity than rooms full of standard waste containers. As an aside, the Park and Hansen (2005) model for the POP containers was later found to be far too stiff (see Reedlunn and Bean (2019, pg. 27) and Reedlunn et al. (2023, Chapter 1)), so the POP porosity response surfaces in Park and Hansen (2005) should be considered an upper bound.

Hansen et al. (2004) studied how a heterogenous distribution of the waste forms considered in Park and Hansen (2005) might impact WIPP's performance. In each heterogeneously distributed waste performance assessment (HDWPA) realization, they assigned one porosity response surface to a single waste panel (a collection of seven rooms), and another porosity response surface to the rest of the repository. The probability of assigning a particular waste form's porosity surface was roughly based on the expected volume fraction of that waste form within the repository. Hansen et al. (2004) compared their HDWPA results to results from a PA calculation that used all the same models and waste inventory, except it used homogeneously distributed waste and the standard waste container (legacy) porosity response surface. They found the HDWPA predicted a negligible decrease in spalling releases and a small, roughly 30 %, increase in DBR (Hansen et al., 2004, Section 4.3.2) (note that releases are measured on a logarithmic scale, so a 30 % increase is relatively small). Consequently, subsequent PA calculations, including CRA-2019, have used only the legacy porosity response surface.

More recently, however, significant improvements have been made to the geomechanical model, waste compaction model, and gas pressurization model that make up the disposal room porosity model. These improvements, which are discussed in the following chapter, substantially improve the scientific basis behind the disposal room porosity model, but they do not constitute a departure from the Creep Closure and Gas Generation Conceptual Models discussed in Hansen (2021, Sections 20 and 22). All the same general concepts are involved; the new disposal room porosity model is simply more credible.

The primary purpose of this report is to document the new porosity response surface computed from the new disposal room porosity model, according to AP-197 (Reedlunn, 2022). Chapter 2 reviews the improvements to the geomechanical model, waste compaction model, gas pressurization model, and the numerical approach used in the simulations. Chapter 3 presents a re-creation of the legacy porosity response surface, the impact of each major model change, the new porosity response surface, a comparison of the legacy and new surfaces, and several sensitivity studies. Chapter 4 summarizes the improvements to the disposal room porosity model and the simulation results.

2. DISPOSAL ROOM POROSITY MODEL

This chapter reviews the geomechanical model, waste compaction model, gas pressurization model, and the numerical approach employed in the simulations.

2.1. Geomechanical Model

This section defines the new geomechanical model and notes differences between the legacy vs. new geomechanical model. The new geomechanical model is largely documented in Reedlunn et al. (2022), but this section specializes it to disposal rooms.

2.1.1. Background

The legacy geomechanical model was based on models developed by Munson and colleagues. As discussed in Reedlunn et al. (2022, Section 2.2), the Munson models produced room closure histories that agreed quite well with experimental measurements of room closure, but the models contained speculative assumptions, the models were not always consistent between simulations, and the numerical details often were not documented. Munson disclosed these speculations and inconsistencies when they were first introduced, but he did not discuss them in his capstone paper (Munson, 1997). In addition, significant differences exist between the Munson models and the legacy geomechanical model utilized by Stone (1997a).

The new geomechanical model, by contrast, is more faithful to the laboratory test measurements, uses a more detailed stratigraphy, is based on numerically converged simulations, and, perhaps most importantly, includes the low stress creep behavior of salt. Reedlunn et al. (2022) simulated the Room D, G, and Q experiments at the WIPP with both the legacy model and a close variant of the new geomechanical model utilized herein. Appendix A revises those Reedlunn et al. (2022) simulations to be consistent with the new geomechanical model. As shown in Fig. A-2, the new geomechanical model reduced the under-prediction of the measured closure rates at $t = 5.7$ yr, averaged over the three experiments, from 2.48× to 1.02×.

2.1.2. Scope

The new geomechanical model, similar to the legacy model, attempts to capture room closure due to salt viscoplasticity, clay seam sliding, and anhydrite deformation. These models do not attempt to capture micro or macro-cracks within the salt strata. Salt forms cracks when exposed to shear stress without sufficient confining pressure. Consequently, cracks form in the excavation damaged

zone (EDZ), also known as disturbed rock zone (DRZ), surrounding the room, before the salt comes into contact with the room contents. These cracks can possibly lead to blocks of salt detaching from the surrounding rock formation, but full detachments are typically prevented by installing rock bolts (see the ceiling in Fig. 1-1a). Rock bolts secure partially detached blocks to intact rock further from the room. Even if these bolts break and allow a block to fall into a filled room, the block does not fall far before landing on the waste and MgO. (The gap between the room surfaces and solid room contents is always less than that shown in Fig. 1-1b because some vertical room closure always occurs before any blocks detach.) It is, therefore, reasonable to assume that partially and fully detached blocks would mate up fairly well with the surrounding rock formation as the room closes. For these reasons, the error caused by ignoring salt fracturing around filled rooms is thought to be acceptably small.

2.1.3. Stratigraphy

Figure 2-1 compares the legacy and new stratigraphies. Layers are color coded as to whether they are salt, anhydrite, or polyhalite. Some layers have clay seams between them, marked with brown lines. All elevations are referenced off of Clay Seam G, which is about 648 m beneath the earth's surface (Munson et al., 1989b). The legacy stratigraphy is relatively simple. It comprises of mostly argillaceous salt, two layers of clean salt, and two layers of anhydrite. No clay seams are included. The new stratigraphy, on the other hand, contains significantly more detail. It has twelve clay seams, seven anhydrite layers, a polyhalite base, and many salt layers. The new stratigraphy does not distinguish between argillaceous and clean salt, but it is otherwise consistent with the 1983 reference stratigraphy (Krieg, 1984), which was agreed upon by representatives from the Department of Energy, Bechtel, TSC/D'Appolonia, and Sandia.

2.1.4. Model Geometry, Boundary Conditions, and Initial Conditions

A WIPP disposal panel is an array of seven parallel rooms connected by two perpendicular access drifts, as shown in Fig. 2-2. The seven rooms are spaced $D_x = 40.54$ m apart, and each room is $R_y = 91.44$ m long in the y-direction.

Rather than simulate an entire panel, both the legacy and new models employ the following three simplifications to reduce the domain size to that shown in Fig. 2-3. First, the rooms are treated as infinitely long, such that room cross-sections deform only in the x-z plane, thereby reducing the three-dimensional deformations to two-dimensional plane strain deformations. Second, if the seven room array is treated as an infinite array of rooms in the x-direction, then only one half of one disposal room may be considered. The right half of a disposal room is shown in Fig. 2-3, where the rollers along the left and right domain boundaries are symmetry boundary conditions. Third, a domain size convergence study (see Appendix B.4) showed that the rollers at the bottom of the domain and the prescribed traction of $p_{top} = 13.57$ MPa, representing the overburden pressure, are far enough away from the disposal room that they have negligible impact on the room deformation. The domain top and bottom are $D_{z1} = 52.87$ m and $D_{z2} = 54.19$ m from Clay Seam G, respectively. The last boundary condition, the gas pressure within the room p_g is discussed further in Section 2.3.

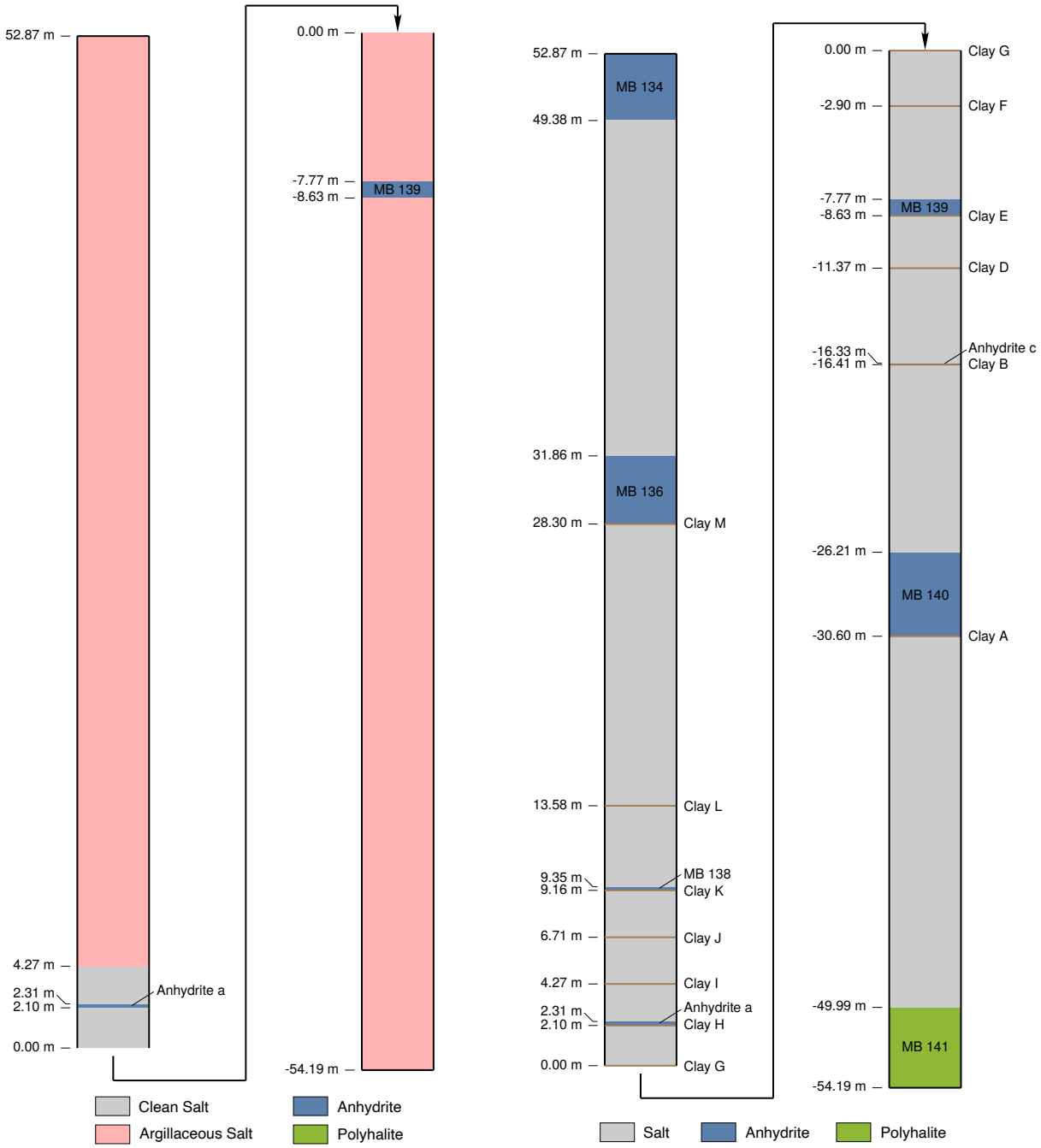


Figure 2-1. Legacy and new stratigraphies.

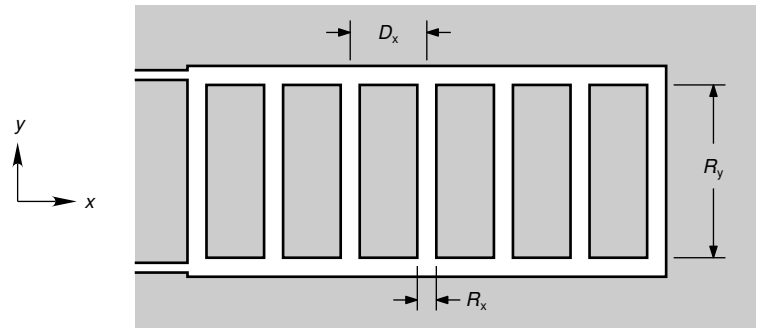


Figure 2-2. Layout of a WIPP disposal panel.

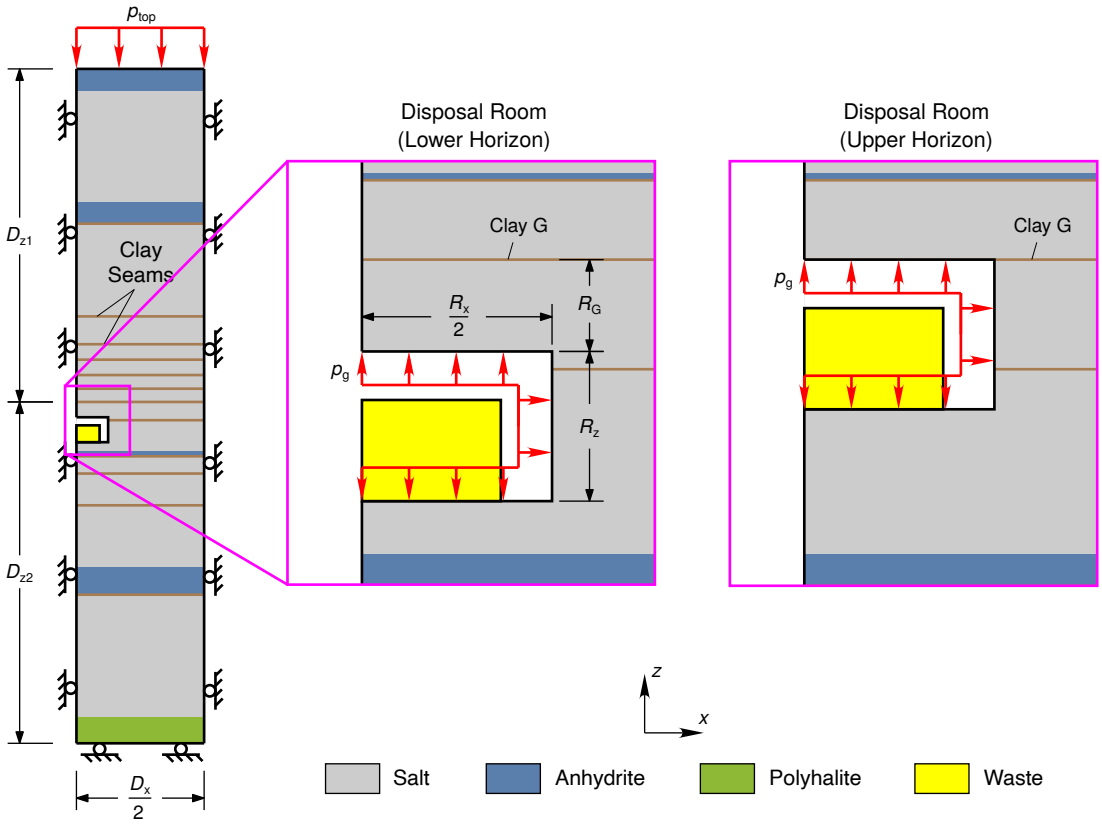


Figure 2-3. Initial model geometry and boundary conditions.

Two disposal room horizons are considered: the lower horizon and the upper horizon shown schematically in Fig. 2-3. The lower horizon disposal room is the initial mined configuration at the WIPP with the disposal room ceiling located $R_G = 2.43$ m below Clay Seam G. The upper horizon room, a subsequent mined configuration, has the disposal room ceiling coincident with Clay Seam G ($R_G = 0$). The as-excavated dimensions of rooms on both horizons are $R_x = 10.06$ m wide and $R_z = 3.96$ m tall. The room corners are square, instead of rounded, in order to avoid severe finite element distortions as the room closes.

The waste block shown in Fig. 2-3 is discussed in Section 2.2.

All geological material points are initialized with a lithostatic stress state that varies linearly from

p_{top} = 13.57 MPa at the domain top to p_{bot} = 15.97 MPa at the domain bottom. This lithostatic pressure gradient is consistent with a uniform rock density of $\rho = 2300$ kg/m^3 and an applied gravity body force of $g = 9.79$ m/s^2. The rock mass temperature is spatially uniform at $T = 300$ K.

The traction-free room boundary conditions are introduced into the simulation at time $t = t_0 = 0$. Instantaneous numerical excavation was not possible because it would have made implicit quasi-static convergence difficult and would have caused inertial effects in explicit dynamic simulations. Instead, the mining excavation process is modeled numerically over multiple time steps by applying a time-varying fluid pressure to the surfaces of the room. At the very start of the simulation ($t = t_{-1} < t_0$), the fluid pressure varies linearly from the top to the bottom of the room according to the lithostatic pressure that exists prior to room excavation. Then the fluid mass density ρ_{fluid} was reduced from the salt mass density ρ to zero according to

$$\rho_{fluid} = \frac{\rho}{2}\left[1 - \cos\left(\frac{\pi t}{t_0 - t_{-1}}\right)\right], \tag{2.1}$$

between $t = t_{-1}$ and $t = t_0$. The salt responds virtually elastically to this fluid density reduction because $t_{-1} = -10$ ms and $t_0 = 0$ s. Once $t > t_0$, the fluid density is held to zero.

2.1.5. Geomaterial Models

The legacy and new geomechanical models capture the mechanical behavior of the salt using the Munson-Dawson (M-D) model, but with different M-D model calibrations. The legacy model utilizes the Legacy Clean Salt and Legacy Arg. Salt calibrations listed in Reedlunn et al. (2022, Table 1). The new geomechanical model, on the other hand, uses an enhanced M-D model formulation (Reedlunn, 2018; Reedlunn et al., 2022), which has three differences from the legacy M-D model:

1. It includes an extra transient strain limit term to capture transient creep at low equivalent stresses.
2. It includes an extra steady-state strain rate term to capture steady-state creep at low equivalent stresses.
3. It uses the more flexible Hosford equivalent stress instead of the Tresca equivalent stress.

Once the enhancements were calibrated against experimental data, Reedlunn et al. (2022, Section 3.3) showed that the new low stress steady-state strain rate term had the most dramatic effect on room closure. Herein, the new geomechanical model utilizes a single M-D model calibration, listed as Calibration 3B in Reedlunn et al. (2022, Table 1), for all WIPP salt, instead of distinguishing between clean and argillaceous salt like the legacy geomechanical model. Although some uncertainty remains about potential geomechanical differences between clean and argillaceous salt (see Reedlunn (2016b, Section 4.1.4)), both Düsterloh et al. (2015) and Reedlunn et al. (2022) found that the creep behaviors were nearly identical; therefore, the new geomechanical model does not distinguish between these salt types.

For anhydrite, the legacy and new geomechanical models use similar Drucker-Prager (D-P) plasticity model calibrations that are respectively listed as Legacy Anhydrite and Calibration 1 in Reedlunn et al. (2022, Table B.4). The only difference between the calibrations is the legacy model utilizes a non-associated flow rule with a dilatation angle of $\omega = 0$, while the new model utilizes an associated flow rule with $\omega = 0.423$. As discussed in Reedlunn et al. (2022, Appendix B), an associated flow rule was needed in empty disposal room closure simulations to avoid strain localizations within anhydrite "a" when fine finite element meshes were employed. Fortunately, the empty room closure was insensitive to ω in the simulations that successfully ran with strain localizations present. The Calibration 1 model was adopted for the new model herein since fine finite element meshes were also used for anhydrite "a".

The legacy geomechanical model does not include polyhalite, while the new geomechanical model uses an old non-associated D-P plasticity model calibration for the polyhalite. This calibration is listed as Legacy Polyhalite in Reedlunn et al. (2022, Table B.4), even though it is used by the new geomechanical model.

2.1.6. Frictional Sliding Models

Coulomb friction is used to model all sliding in the legacy and new geomechanical models. In Coulomb friction, the tangential traction magnitude t_t and normal traction magnitude t_n at the interface are related as

$$t_\mathrm{t} \leq \mu\, t_\mathrm{n}, \tag{2.2}$$

where μ is the friction coefficient for the interface. Various subscripts and superscripts on μ are used to designate to which interface(s) a given friction coefficient pertains.

Although the legacy model does not include clay seams, as mentioned in Section 2.1.3, the clay seams in the new geomechanical model are represented as sliding contact surfaces with Coulomb friction. See Sobolik et al. (2022, Section 5) for a short discussion of the rationale behind this simple model.

Table 2-1 lists the lower bound, nominal, and upper bound friction coefficients for Clay Seam F $\mu_\mathrm{c}^\mathrm{F}$ and for all other clay seams $\mu_\mathrm{c}^\mathrm{other}$. The lower and upper bounds in Table 2-1 are derived from a set of direct shear experiments on (weak) artificial clay seams and (strong) diffuse natural clay seams (Sobolik et al., 2022). In all cases, $\mu_\mathrm{c}^\mathrm{F} = 0.42$ because Clay Seam F is 10 to 50 cm thick, it resembles the diffuse natural clay seams tested in the experiments, and it has not perceptibly slid in either lower or upper horizon disposal rooms (Carrasco, 2020). Clay Seam G, by contrast, is roughly 1 cm thick, is quite distinct, and is known to slide in the WIPP underground (Carrasco, 2020). The remaining clay seams in the new geomechanical model are assumed to behave more similarly to Clay Seam G than Clay Seam F, and clay seams similar to Clay Seam G have not been experimentally characterized, so $\mu_\mathrm{c}^\mathrm{other}$ is varied in the sensitivity study presented in Section 3.4.2. Aside from that sensitivity study, all simulations with the new disposal room porosity model utilized the column of nominal values in Table 2-1.

The nominal friction coefficient of 0.2 was originally proposed by Munson et al. (1989a) using engineering judgement and analysts have used it ever since to consider clay seam sliding. When

Reedlunn et al. (2022) used $\mu_c^F = \mu_c^{other} = 0.2$ in their simulations of Room D, G, and Q's closure, their simulations predicted plausible amounts of clay seam sliding and reasonably predicted the Room D, G, and Q closure rates. Recognizing that $\mu_c^F = 0.2$ differs from the 0.42 utilized herein, Appendix A presents new Room D, G, and Q closure simulations using the nominal set in Table 2-1 to ensure the geomechanical model validation is consistent with the geomechanical model used in the disposal room porosity simulations.

Table 2-1. Clay seam friction coefficients

Parameter	Low	Nominal	High
μ_c^F	0.42	0.42	0.42
μ_c^{other}	0.028	0.2	0.42

Salt-on-salt sliding can occur when the surfaces of the room contact each other. Salt surfaces with a little water can bond together (heal) when held in contact under sufficient pressure for a sufficient time, but the Coulomb friction model utilized herein does not include this behavior for simplicity. The legacy model assumed frictionless salt-to-salt sliding[1], but salt-to-salt friction should be higher than clay seam friction ($\mu_{ss} > \mu_c$) and a large value of μ_{ss} is desired to roughly approximate the effects of interface bonding, so the new geomechanical model uses $\mu_{ss} = 0.5$.

Salt-on-waste sliding can occur when surfaces of the room contact the waste block. The legacy model assumed a salt-to-waste friction coefficient of $\mu_{sw} = 0$, which seems too small. The salt-to-metal coefficient of friction is probably somewhere between $\mu_c = 0.2$ and $\mu_{ss} = 0.5$ once significant waste compaction occurs, so the new geomechanical model uses $\mu_{sw} = 0.4$.

2.2. Waste Compaction Model

This section presents the new waste compaction model scope, the homogenized waste block, and the waste material model. The scope and waste block are the same in the legacy and new waste compaction models. Only the waste material models differ.

2.2.1. Scope

The legacy and new waste compaction models only consider the mechanical behavior of non-degraded waste. A simplistic argument for neglecting degradation of mechanical strength is that the physical processes responsible for degradation can generate significant amounts of gas and the waste compaction behavior is not very important when significant gas pressures build up within the room. Butcher (1997a, Section 3.2.2) presented further arguments for focusing on

[1] Stone (1997a); Park and Hansen (2005); Park and Holland (2007) do not mention the friction coefficients they utilized for salt-to-salt or salt-to-waste sliding. The SANTOS input files in the appendix of Stone (1997a); Park and Hansen (2005); Park and Holland (2007) along with the SANTOS user manual (Stone, 1997b), however, make it clear they used $\mu_{ss} = \mu_{sw} = 0$.

non-degraded waste. Regardless, if predicting the porosity (and permeability) of disposal rooms filled with degraded waste becomes a high priority, Broome et al. (2014) presented a series of uniaxial strain, triaxial stress, and hydrostatic stress compaction experiments on surrogate, degraded, waste. It might be possible to create another waste material model that captures the results from those degraded waste experiments.

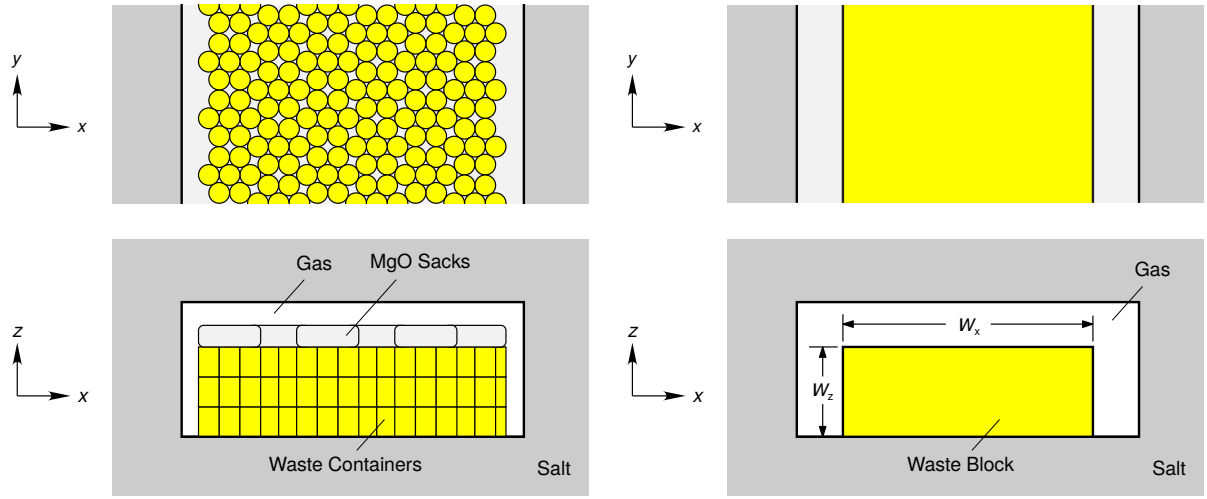
The legacy and new waste compaction models consider only standard 55-gallon waste containers. The legacy model ignored other container types because, as discussed in Chapter 1, Hansen et al. (2004, Section 4.3.2) found that super-compacted and POP waste resulted in room porosity increases that caused only a small DBR increase ($\approx$ 30 %). The small DBR increase was especially negligible in 2004 because DBR were not considered to be the dominant release type at that time (Hansen et al., 2004, Section 4.3.1). Although DBR are now the dominant release type for low probability (10^{-3}) events (CBFO, 2019, Figure PA-72), the present report assumes the *sensitivity* of DBR to super-compacted and POP waste would still be less than or equal to the 30 % increase in radionuclide releases found in Hansen et al. (2004, Section 4.3.2) if a similar study was performed with today's PA assumptions. A 30 % increase is considered too small to warrant the large effort required to compute porosity response surfaces for mixed waste forms and incorporate them into the PA. By contrast, the legacy model of disposal rooms filled with standard waste containers can be updated much more expeditiously.

Note that the legacy and new waste compaction models both ignore the sacks filled with granular MgO that are placed on top of the waste containers (see Fig. 2-4). One potential difficulty with modeling the MgO is room closure will likely cause the sacks to split open and spill their contents into the interstices between the containers. Continuum numerical methods, such as the finite element method, would struggle to capture such behavior. In addition, a material model for the compaction of confined granular MgO has not been developed. Nevertheless, it might be fruitful to consider ways to model the MgO within the room in future work.

2.2.2. Homogenized Waste Block

In reality, standard 55-gallon containers are emplaced in WIPP disposal rooms as shown in Fig. 2-4a. The containers are bundled together in hexagon shaped 7-packs: six containers surround one container in the center. The 7-packs are stacked three-high and arranged in a hexagonal array. A given room contains 972 7-packs for a total of $n_{\text{con}} = 6{,}804$ containers that occupy an initial volume of $V_{\text{w0}} = 1{,}728$ m^3 (Stone, 1997a, pg. 11).

Both the legacy and new waste compaction models employ the same idealization of the standard 55-gallon containers within a room: they replace the complexity in Fig. 2-4a with the geometry in Fig. 2-4b. Instead of modeling every individual container, all the containers are represented by a single, homogenized, waste block. The waste block's initial height is equal to the initial height of three containers $W_{\text{z}} = 2.676$ m, while the waste block's initial width $W_{\text{x}} = 7.35$ m is computed by preserving V_{w0} (see Stone (1997a, pg. 18)). This value of W_{x} is roughly 0.85$\times$ the width of the hexagonal container array. A study of the validity of this homogenization scheme is presented in Section 3.4.3.



(a) Hexagonal array of containers **(b) Homogenized waste block**

Figure 2-4. A hexagonal array of containers (with MgO and gas) versus a homogenized waste block (with gas).

2.2.3. Waste Material Model

The mechanical behavior of each material point within the waste block is represented with a waste material model.

The legacy waste material model utilizes the Soil and Foam (SAF) constitutive model (see Stone (1997b, Section 4.6) or LAMÉ Team (2021, Section 4.24)) parameterized to be a D-P plasticity model with an end cap[2]. As compaction progresses, the end cap translates along the hydrostat according to a pressure p vs. volume strain ε^{vol} relationship. This relationship is a weighted average of oedometer measurements on individual, non-degraded, waste components. The legacy waste material model parameters can be found in Stone (1997a, pg. 21–23)[3].

A review of the legacy waste material model in Jensen et al. (2023, Chapter 1) uncovered seven shortcomings:

1. Butcher (1997b) assumed a waste composition that was substantially different from recent, more accurate, estimates. In particular, Butcher (1997b) assumed a 0.43× smaller weight percentage of metals than the most recent estimate.

[2]Stone (1997a) incorrectly wrote that the legacy waste material model uses an associated flow rule. The SAF model combines a D-P yield surface with a von Mises flow potential, which results in a non-associated flow rule.

[3]Stone (1997a, Table 5) and Butcher (1997b, Table 7) made two mistakes when they listed the elastic shear and bulk moduli as $G = 333$ MPa and $K = 222$ MPa, respectively. The precise values for the elastic moduli should have minimal impact on the disposal room porosity predictions, so we note these two mistakes primarily in the spirit of accurate documentation. First, Butcher (1997b, Table 7) cites Weatherby et al. (1991) for the elastic properties of the waste, yet Weatherby et al. (1991) actually lists $G = 222$ MPa and $K = 333$ MPa. Second, the input file for the disposal room porosity simulation (Stone, 1997a, Appendix A), however, shows he actually used $G = 333/2 = 166.5$ MPa. The recreated legacy model simulations presented herein utilized $G = 166.5$ MPa and $K = 222$ MPa to be consistent with the simulations performed by Stone (1997a, Appendix A).

2. Butcher (1997b) assumed an initial waste porosity of $\phi_{w0} = 0.681$, which is 0.83× smaller than a more recent, more accurate, estimate of $\phi_{w0} = 0.825$.

3. Butcher (1997a, Section 3.2.2) assumed the waste produced zero lateral stress (and zero lateral strain) in the oedometer tests used to derive the model's p vs. ε^{vol} relationship.

4. The oedometer tests used for the p vs. ε^{vol} relationship only reached $p = 4.93$ MPa with the zero lateral stress assumption, yet $p^{litho} \approx 14.7$ MPa.

5. The Drucker-Prager yield surface was not calibrated against experimental measurements.

6. The legacy model predicts non-physical tensile out-of-plane stresses when in-plane compression is applied under plane strain conditions, which occurs in disposal room porosity simulations.

7. The legacy model assumes waste compaction does not depend on strain rate.

Jensen et al. (2023) addressed these issues by first performing a suite of new experiments on surrogate, non-degraded, waste. The waste composition and density were chosen to agree with recent waste inventory estimates. The waste was subjected to uniaxial, triaxial, and hydrostatic stress compaction. Special care was taken to measure the volume strain during the uniaxial and triaxial experiments so that the lateral strain could be inferred from the volume and axial strains. In addition, the strain rate was varied from 10^{-7} to 10^{-4} in the uniaxial stress tests. As expected, the mechanical responses were initially quite compliant, but then stiffened when the waste was sufficiently compacted. Similarly, the waste did not expand laterally significantly until the waste became relatively stiff and strong.

Once the new experiments were complete, Jensen et al. (2023) calibrated the Foam Damage (FD) constitutive model (LAMÉ Team, 2021, Section 4.29) against the measurements to create a new waste material model. The calibration effort focused primarily on capturing the triaxial and hydrostatic compression tests, and, to a lesser degree, the lateral strain vs. axial strain curves from the uniaxial stress tests. The new waste material model parameters are listed as Calibration 1 in Jensen et al. (2023, Section 3.2.2). Note that the new model does not capture the waste's uniaxial stress vs. strain behavior, but Jensen et al. (2023) showed that the average stress state within the waste deviated from uniaxial stress long before the waste supplied sufficient back pressure to affect the room closure process. The uniaxial stress response, therefore, is thought to be unimportant during disposal room porosity simulations.

Once calibrated, the new waste material model largely resolves the issues with the legacy model. The new model is based on experiments that utilized more accurate approximations of the waste composition and porosity. The new model's hydrostatic response agrees far better with the experimental measurements and does not involve unsupported extrapolation to p^{litho}. The new model predicts reasonable compressive out-of-plane stresses, instead of tensile stresses, when using plane strain conditions to simulate those applied to the waste in a disposal room. Finally, the new model includes a mild degree of strain rate dependence.

As discussed in the next section, the volume of solid waste within the room plays a role in computing the room porosity and gas pressure. The new waste material model increases the initial

waste porosity from $\phi_{w0} = 0.681$ to 0.825, which decreases the volume of solid waste within the room from $V_{sw} = V_{w0}(1 - \phi_{w0}) = 551.2$ m^3 to 302.4 m^3.

2.3. Gas Pressurization Model

This section defines the new gas pressurization model and discusses differences with the legacy model.

2.3.1. Gas Generation Potential

Anoxic corrosion of the waste drums, microbial activity in the waste, and brine radiolysis can all produce gas within a disposal room (King, 2021). The amount of gas generated by any one source is uncertain so a wide range of gas generation realizations are considered in the WIPP PA. These individual gas generation realizations are not input into the disposal room porosity model because, as discussed in Chapter 1, the PA calculations are uncoupled from the disposal room porosity calculations. Instead, a gas generation potential is constructed that bounds the individual gas generation realizations, and a series of disposal room porosity simulations are run, each with some fraction f of the total gas generation potential.

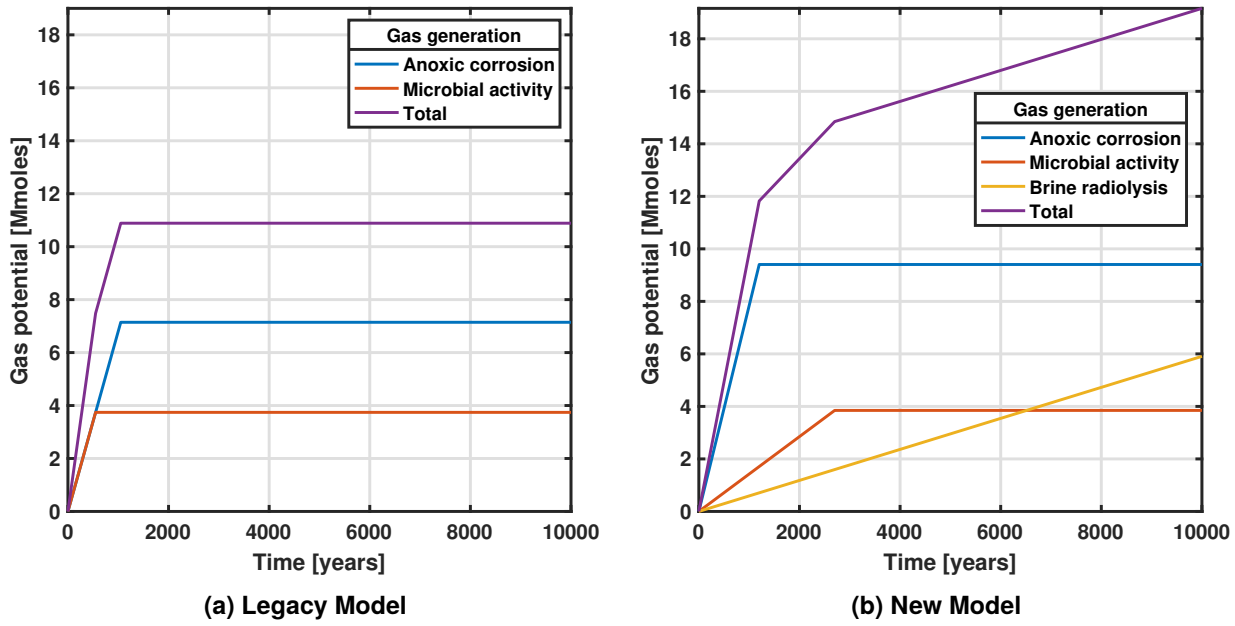


Figure 2-5. Legacy and new gas generation potentials, $f = 1$, for a disposal room.

The legacy and new gas generation potentials are compared in Fig. 2-5, along with the contributions from each of the three gas sources. Each total gas generation potential has three phases, each with a different gas generation rate. The new gas generation potential Eq. (2.3) has an increased iron corrosion rate, an increased iron inventory, a decreased microbial rate, and the addition of brine radiolysis (King, 2021). Anoxic corrosion and microbial activity are inventory

Table 2-2. Gas generation potential parameters

Phase	N_{i0} mol	N_{i1} mol/yr	t_i yr
$i = 0$	0	9846.38	0
$i = 1$	11815656	2015.65	1200
$i = 2$	14839131	590.65	2700

limited, so the gas due to those processes plateaus after a certain period of time. Radiolysis, on the other hand, is not inventory limited because brine can continually flow into the repository from the surrounding rock formations and the exponential decay of radionuclide activity extends beyond the 10,000 year regulatory period. By the end of the 10,000 year regulatory period, the gas generation potential for the current analysis has 1.76× more moles than the legacy potential.

For reference, the three phases of the new gas generation potential are given as

$$n_{\mathrm{gg}}^{\mathrm{pot}} = \begin{cases} N_{00} + N_{01}\,(t - t_0) & \text{for } t_0 \le t \le t_1 \\ N_{10} + N_{11}\,(t - t_1) & \text{for } t_1 < t \le t_2 \\ N_{20} + N_{21}\,(t - t_2) & \text{for } t_2 < t, \end{cases} \tag{2.3}$$

where $n_{\mathrm{gg}}^{\mathrm{pot}}$ is the potential number of moles of gas generated, and the values of N_{i0}, N_{i1}, and t_i are listed in Table 2-2. Note, Eq. (2.3) corrects King (2021, Equation (1)) in which the time shifts, $(t - t_1)$ and $(t - t_2)$, for the latter two phases were accidentally omitted.

As mentioned in Chapter 1, gas is not permitted to escape the room, so the potential number of moles of gas is equal to the potential number of moles of gas generated ($n_{\mathrm{g}}^{\mathrm{pot}} = n_{\mathrm{gg}}^{\mathrm{pot}}$).

2.3.2. Gas Constitutive Model

The legacy and new model both compute the gas pressure p_{g} in the disposal room using the ideal gas law

$$p_{\mathrm{g}} = \frac{f\, n_{\mathrm{g}}^{\mathrm{pot}}\, R\, T}{V_{\mathrm{g}}}, \tag{2.4}$$

where R is the universal gas constant, $T = 300$ K is the absolute temperature of the gas, and V_{g} is the current gas storage volume of the disposal room. The gas generation factor f is a multiplier used to scale the amount of gas generation ($n_{\mathrm{g}} = f\, n_{\mathrm{g}}^{\mathrm{pot}}$). A value of $f = 0$ corresponds to zero gas within the room, while $f = 1$ corresponds to the full gas generation potential.

The current gas storage volume of the disposal room is computed as $V_{\mathrm{g}} = V_{\mathrm{r}} - V_{\mathrm{sw}}$, where V_{r} is the current volume of the disposal room, including the waste, and V_{sw} is the solid volume of the waste. See Appendix B.1 for a description of how V_{r} is numerically computed. V_{sw} is treated as a constant when calculating V_{g}, because the vast majority of the waste deformation is accommodated by changes in waste porosity. This approach effectively assumes the pore space within the waste is fully permeable to gas flow, such that p_{g} is uniform throughout the disposal room gas storage volume, including inside the waste pore space.

2.3.3. Surfaces Subject to Gas Pressure

The gas pressure is applied to the boundary of the disposal room. The room boundary is composed only of the room surfaces in the legacy model; in the new model, the room boundary is composed not only of the room surfaces, but also includes any upper or lower clay seam surfaces exposed to gas pressure by clay seam sliding.

The gas pressure is not applied to the waste block surfaces in order to account for pore pressure effects within the waste block. Assuming the pore pressure is spatially uniform, not applying gas pressure to the waste block is equivalent to replacing the Cauchy stress with the Terzaghi effective stress within the waste material model (Jensen et al., 2023, Section 3.1.2).

The gas pressure boundary conditions on the room surfaces (see Fig. 2-3) remain active throughout the simulation. That is, even if the room surfaces contact each other, such as a portion of the disposal room roof contacting the disposal room wall at the room corner, p_g remains applied to the surfaces in contact. This assumption, which is consistent with the legacy geomechanical model, implies a layer of salt forming the boundary of the disposal room remains permeable to gas flow.

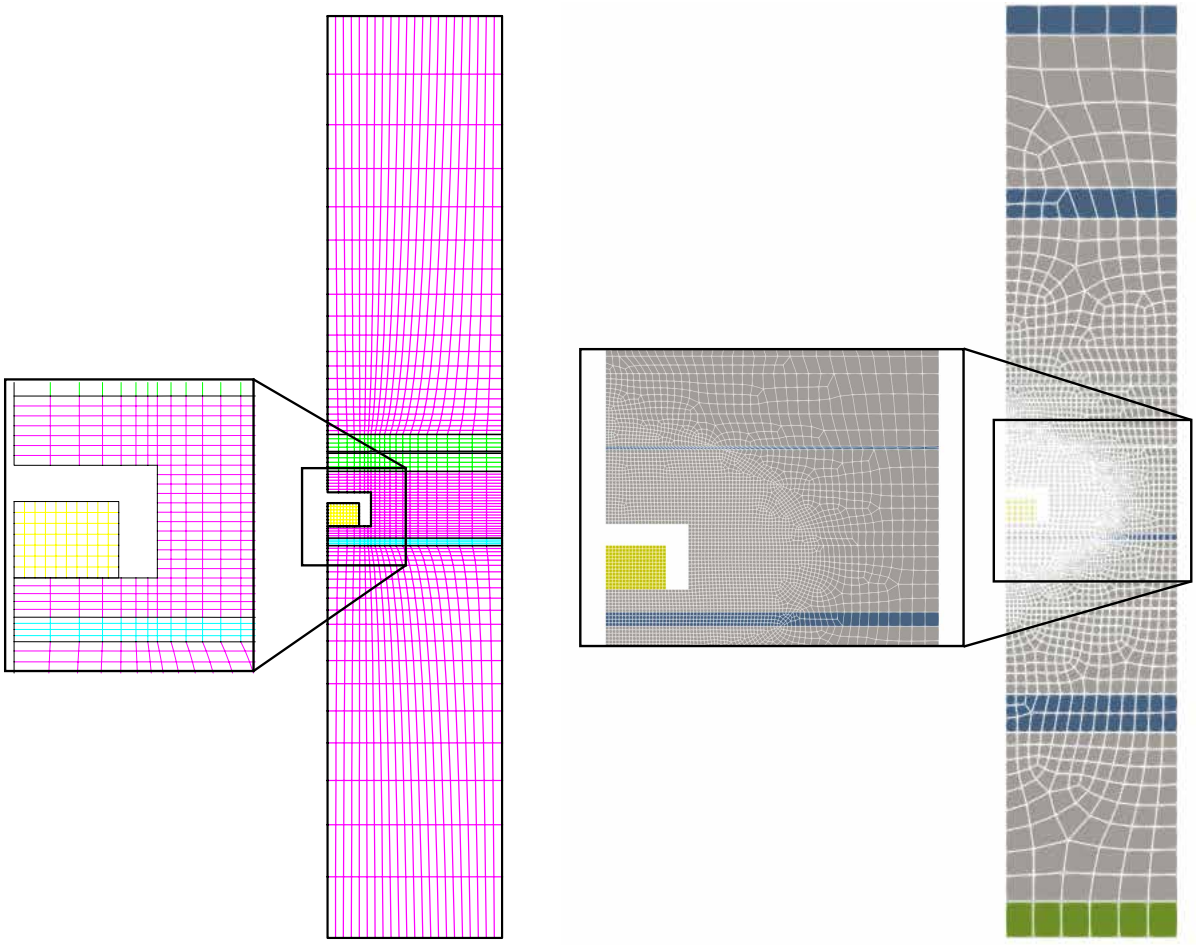
A pressure masking technique is used to apply gas pressure to exposed clay seam surfaces. Sierra/SolidMechanics (2022) computes a quantity called contact strength, c_s, which ranges from 0 (no contact) to 1 (full contact). This contact strength is used to linearly reduce the applied gas pressure on the clay seam from full gas pressure on exposed clay seam surfaces to zero gas pressure on portions of the clay seam in full contact. The pressure applied to the clay seam, p_c, is simply

$$p_c = (1 - c_s)\, p_g. \tag{2.5}$$

2.4. Numerical Approach

The set of equations resulting from the legacy and new models defined in Sections 2.1 to 2.3 were solved using large deformation finite element codes. The legacy simulations utilized SANTOS (Stone, 1997b), which is no longer supported at Sandia. Sierra/SolidMechanics (2022) is the current day successor to SANTOS, so Sierra/SolidMechanics (2022) version 5.4.1 was used to recreate the legacy simulations as well as run the new simulations. An example SANTOS input file can be found in Stone (1997a, Appendix A), while example Sierra/SM input files can be found in Appendix C.2.

The recreated legacy simulations used essentially the same finite element mesh as the legacy simulations, but the new simulations used a mesh with significantly more elements near the room than the legacy mesh, as shown in Fig. 2-6. The number of elements across the room half-width, for example, increased from 7 to 25 elements. The size of the elements in the new mesh was selected based on the mesh convergence study presented in Appendix B.3. The scripts used to generate the recreated legacy mesh and the new base mesh using Cubit (2021) can be found in Appendix C.1.



(a) Legacy Mesh (b) New Mesh

Figure 2-6. Legacy finite element mesh and new (base) finite element mesh for lower horizon disposal room and waste. The recreated legacy mesh is essentially the same as the mesh shown in (a). (The image in (a) was modified from Stone (1997a, Fig. 5).)

Each set of simulations used a different element type. The legacy simulations utilized uniform-strain elements, while the recreated legacy simulations utilized mean quadrature (uniform-strain) elements. These two elements should be roughly equivalent, as both employ hourglass control and the hourglass stiffness was set to 0.005 in both cases, but the authors have not investigated whether the hourglass implementations are truly equivalent. The new simulations, on the other hand, used the selective deviatoric (SD) element. The SD element under-integrates the pressure response, but fully-integrates the deviatoric response, which increases its computational cost, increases its accuracy, and obviates its need for hourglass control.

See Appendix B for additional numerical details thought to be of minor importance.

2.5. Summary

A summary of the major changes from the legacy disposal room model to the new disposal room model are collected in Table 2-3.

Table 2-3. Summary of major changes between the legacy model, recreated legacy model, and new model

Component	Category	Factor	Legacy Model	Recreated Legacy Model	New Model
Geomechanical model	Stratigraphy	Type	Simplified	Simplified	Full 1983 reference
		Clay seams	None	None	All 12
		Anhydrite layers	2	2	All 7
		Polyhalite base	Replaced with salt	Replaced with salt	Polyhalite
	Material model	Clean salt	M-D, Legacy Clean Cal.	M-D, Legacy Clean Cal.	M-D, Calibration 3B
		Arg. salt	M-D, Legacy Arg. Cal.	M-D, Legacy Arg. Cal.	M-D, Calibration 3B
		Anhydrite	D-P, Legacy Cal.	D-P, Legacy Cal.	D-P, Calibration 1
		Polyhalite	M-D, Legacy Arg. Cal.	M-D, Legacy Arg. Cal.	D-P, Legacy Cal.
	Friction Coefficient	Salt-on-salt	$\mu_{ss} = 0$	$\mu_{ss} = 0$	$\mu_{ss} = 0.5$
		Salt-on-waste	$\mu_{sw} = 0$	$\mu_{sw} = 0$	$\mu_{sw} = 0.4$
Waste compaction model	Material model		SAF, Legacy Cal.	SAF, Legacy Cal.	FD, Calibration 1
	Initial porosity		$\phi_{w0} = 0.681$	$\phi_{w0} = 0.681$	$\phi_{w0} = 0.825$
	Solid volume per room		$V_{sw} = 551.2$ m^3	$V_{sw} = 551.2$ m^3	$V_{sw} = 302.4$ m^3
Gas pressurization model	Anoxic corrosion	Active (years)	1,050	1,050	1,200
		Rate (moles/yr)	6,804	6,804	7,830.73
	Microbial activity	Active (years)	550	550	2,700
		Rate (moles/year)	6,804	6,804	1,425
	Brine radiolysis	Active (years)	0	0	10,000
		Rate (moles/year)	0	0	590.65
	Pressure masking		None	None	Clay seams
Numerical approach	Software	Code name	SANTOS	Sierra/SolidMechanics	Sierra/SolidMechanics
		Solver	Explicit, dynamic relaxation	Implicit	Explicit, viscoplastic scaling
		Contact	ACME	ACME	DASH
	Finite element mesh	Type	Structured	Structured	Unstructured
		Elements	1,608	1,608	5,576
		Element type	Uniform strain	Mean quadrature	Selective deviatoric

3. RESULTS

The disposal room porosity, as discussed in Chapter 1, is the spatially averaged porosity within the disposal room and is an input to the WIPP Performance Assessment. This chapter presents the recreated legacy porosity response surface, the impact of the major sub-model changes, the new porosity response surface, a comparison between the legacy and new porosity response surfaces, and several sensitivity studies. The new porosity response surface may be used for Compliance Decision Analyses, per. NP 9-1 (Nielsen, 2020). All files associated with the results in this chapter are archived at `/data/cvs/CVSLIB/WIPP_EXTERNAL/ap197_files` on Sandia Carlsbad's Linux server.

The Eulerian porosity ϕ_{E} (or true porosity) of the disposal room is defined as the ratio of the current gas storage volume of the disposal room to the current volume of the room,

$$\phi_{\mathrm{E}} = \frac{V_{\mathrm{g}}}{V_{\mathrm{r}}}. \tag{3.1}$$

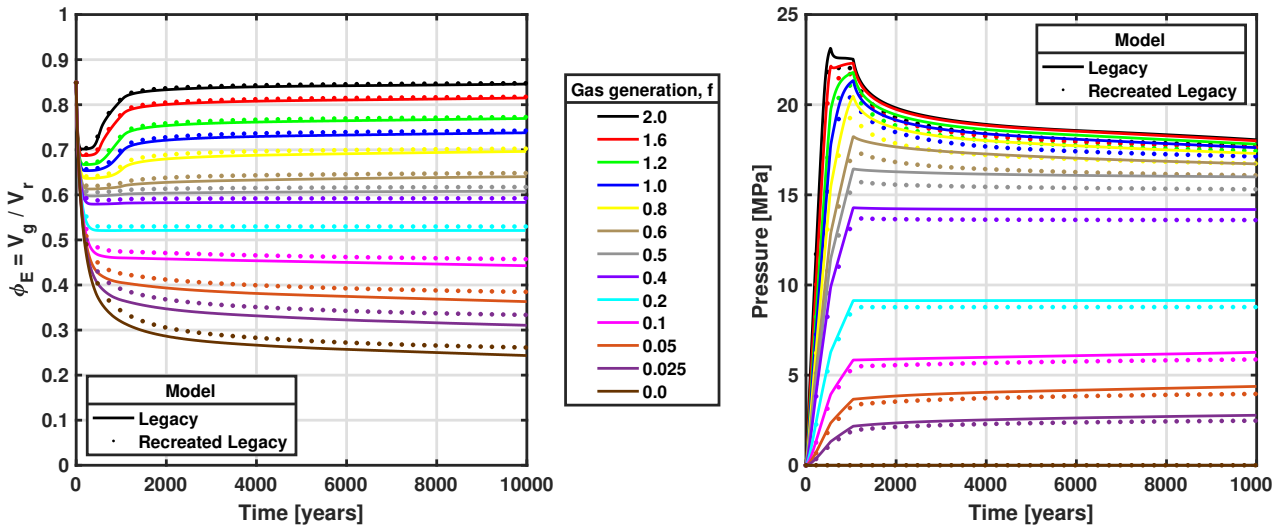
The Eulerian porosity was used to report the legacy porosity response surface (Stone, 1997a). However, for PA flow simulations, the Lagrangian porosity is required as an input. The Lagrangian porosity ϕ_{L} (or engineering porosity) of the disposal room is defined as the ratio of the current gas storage volume of the disposal room to the initial volume of the room V_{r0},

$$\phi_{\mathrm{L}} = \frac{V_{\mathrm{g}}}{V_{\mathrm{r0}}}. \tag{3.2}$$

The Lagrangian porosity is related to the Eulerian porosity by the transform,

$$\phi_{\mathrm{L}} = \frac{(1-\phi_{\mathrm{E0}})\,\phi_{\mathrm{E}}}{1-\phi_{\mathrm{E}}}, \tag{3.3}$$

where ϕ_{E0} is the Eulerian porosity at the initial time $t = t_0$. Both measures of porosity are displayed in this report.



(a) Porosity History

(b) Pressure History

Figure 3-1. Comparison of Eulerian porosity and pressure histories between the legacy model and recreated legacy model for a lower horizon disposal room.

3.1. Progression from the Legacy Toward the New Model

3.1.1. Recreated Legacy Model Simulations

The intermediate step in the progression from the legacy model to the new model was to recreate the legacy model simulations in Sierra/SM. As listed in Table 2-3, the recreated legacy simulations use the same parameters, material models and calibrations, and finite element mesh as the legacy simulations. As discussed in Section 2.4 and Appendix B.1, potential sources of difference between the recreated legacy model and legacy model, such as variations in implementation of the hourglass control, contact algorithms, and material models, remained, but were deemed sufficiently minor. The recreated legacy Eulerian porosity histories and pressure histories are compared to the legacy histories in Fig. 3-1a and Fig. 3-1b, respectively. The absolute difference in porosity ranged between 0.5% and 3% for the various gas generation factors.

In Fig. 3-1a, the porosity histories for gas generation factors $f \leq 0.2$ decrease monotonically over time as the disposal room closes and compresses the waste. For gas generation factors $f > 0.2$, the porosity histories decrease for a few hundred years, after which time, the porosity increases. In fact, for a gas generation of $f = 2.0$, the porosity at 10,000 years is essentially the same as the initial porosity. For these gas generation factors, the disposal room closes initially as gas is generated. Eventually, the gas generation and reduction in room volume pressurize the disposal room enough to arrest further room closure. As gas continues to be generated, the disposal room pressurizes further, expands the room, and increases the porosity.

From the disposal room pressure histories Fig. 3-1b, it should be noted that most room pressures at 10,000 years are either significantly smaller or greater than $p^{\text{litho}} \approx 14.7$ MPa. A significant gas pressure difference indicates that the disposal room has not yet reached its long-term equilibrium size and shape.

3.1.2. Impact of Improved Numerical Setup

The numerical setup was improved from the recreated legacy model to the new model. From the numerical approaches summarized in Table 2-3, compared to the recreated legacy model, the new model uses a different solution scheme and contact algorithm as well as a finer finite element mesh, resolved nearest the disposal room, with higher-order integration elements.

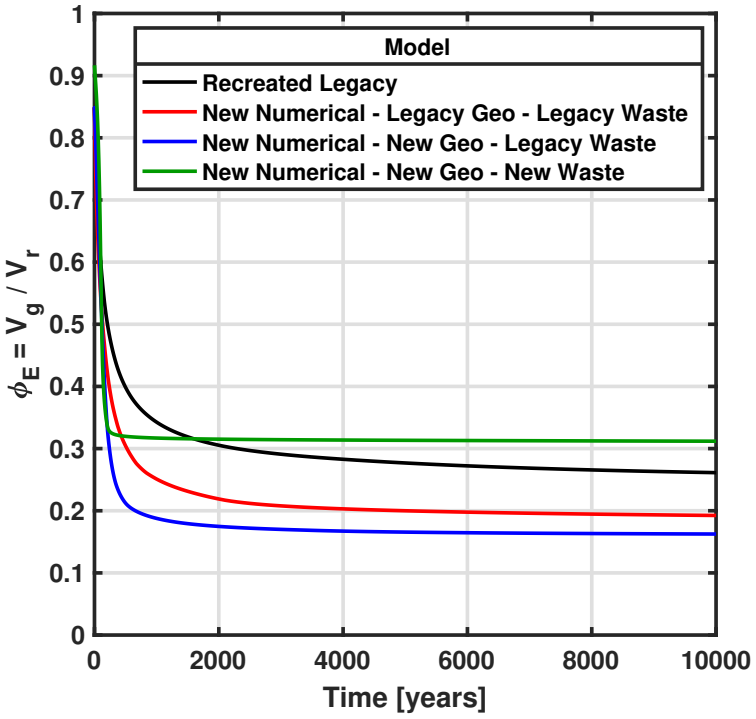
The disposal room porosities for the recreated legacy model and the recreated legacy model with improvements only to the numerical setup (“New Numerical - Legacy Geo - Legacy Waste") are compared in Fig. 3-2 for the case of zero gas generation. The improved numerical setup alone increases the compliance of the model. The impact is quite pronounced in the Eulerian porosity (up to 0.08 difference) and a few percent absolute difference in the Lagrangian porosity.

The primary sources of the porosity differences with the improved numerical setup are probably the higher-order integration elements and finer mesh. As discussed in Appendix B.2, differences in the solution scheme and contact algorithm are expected to have minor effect on the results. Related to the discussion in Section 2.4, the under-integrated mean quadrature element requires an artificial hourglass stiffness to avoid spurious hourglass modes. When a finite element mesh is too coarse, the artificial hourglass stiffness can have a substantial effect on the results, yet a mesh convergence study was not documented for the legacy mesh and the stiffness appears to have been chosen without justification. The selective deviatoric element, by contrast, does not have an artificial hourglass stiffness to set and, the finer, unstructured mesh of selective deviatoric elements was chosen based on a mesh convergence study (see Appendix B.3). The new numerical setup then can be regarded as a closer approximation of the exact solution.

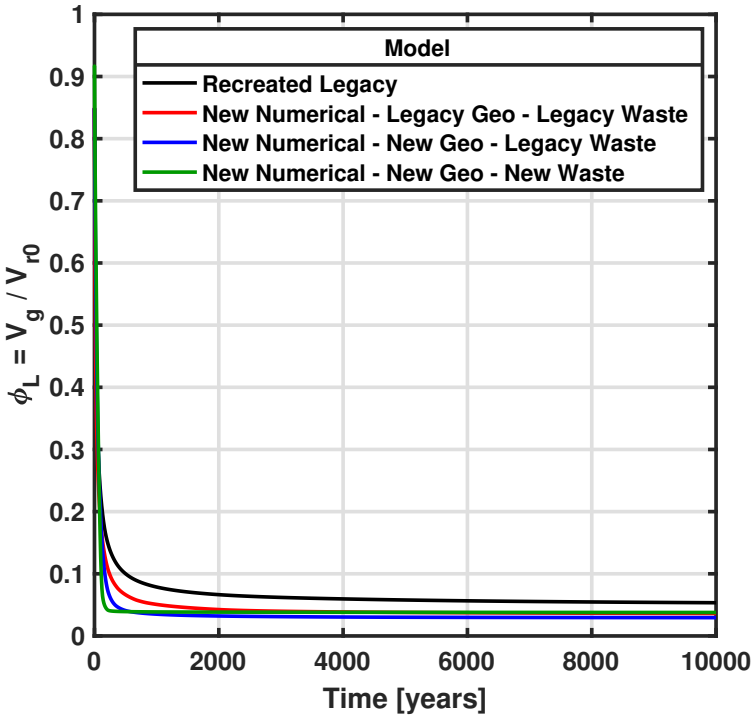
3.1.3. Impact of New Geomechanical Model

The disposal room porosities for the recreated legacy model with improved numerical setup (“New Numerical - Legacy Geo - Legacy Waste") and the recreated legacy model with improved numerical setup and new geomechanical model (“New Numerical - New Geo - Legacy Waste") are also compared in Fig. 3-2 for the case of zero gas generation.

The new geomechanical model further increases the compliance of the geology, beyond that of only the new numerical setup. Switching from the recreated legacy with improved numerical setup model to the new geomechanical model causes the Eulerian porosity to drop from 0.304 to 0.211 at $t = 500$ yr and drop from 0.192 to 0.163 at $t = 10,000$ yr. Apparently, the increased compliance of the new geomechanical model has its most significant impact in the first ≈ 500 years, but it still has a moderate impact at 10,000 years. Although the relative impact of each change to the new geomechanical model, as applied to disposal room closure, was not isolated herein, Reedlunn (2016a, Appendix A.9.3) and Reedlunn et al. (2022, Section 3) performed such sensitivity studies of the new geomechanical model, as applied to Room D closure. They found the new low stress creep behavior in the M-D model increased the predicted Room D closure rates for $0.1 \leq t \leq 7.8$ yr more than any other factor.



(a) Eulerian Porosity History



(b) Lagrangian Porosity History

Figure 3-2. Comparison of porosity histories between the recreated legacy model and models which progressively switch to the new numerical model, new geomechanical model, and new waste compaction model for zero gas generation, $f = 0$, over 10,000 years. All results correspond to a lower horizon disposal room.

3.1.4. *Impact of New Waste Compaction Model*

The disposal room porosities for the model with improved numerical setup, new geomechanical model, and legacy waste compaction model ("New Numerical - New Geo - Legacy Waste") and the new model ("New Numerical - New Geo - New Waste"), which is simply the former with the new waste model, are compared in Fig. 3-2 for the case of zero gas generation.

The new waste compaction model has a significant impact on the Eulerian porosity. As noted in Section 2.2.3, by selecting the waste composition and density to agree with recent waste inventory estimates, the new waste material model has a higher initial porosity and a lower solid waste volume than the legacy waste material model (see Table 2-3). This higher initial waste porosity raises the initial room porosity from 0.849 to 0.917. As expected with a higher initial porosity waste, the new waste compaction model is more compliant than the legacy model for moderate levels of compaction. Once the waste porosity drops beneath about 0.32, however, the new waste compaction model becomes stronger for the same porosity under plane strain compression (Jensen et al., 2023, Figure 3-12b). As a result, the new model significantly increases the room's Eulerian porosity at 10,000 years from 0.163 to 0.312.

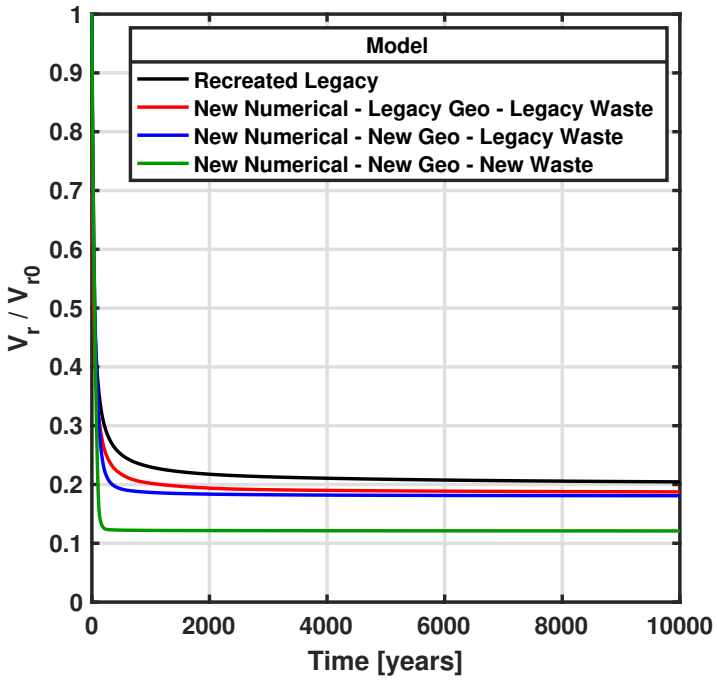


Figure 3-3. Comparison of lower horizon room volume histories between the recreated legacy model and the new model for zero gas generation, $f = 0$.

Although the new waste model caused a substantial increase in Eulerian porosity relative to the legacy waste model, the new waste model only causes a small, 0.0083, shift in Lagrangian porosity at 10,000 years. Similarly, the aggregate effect of all the improvements to arrive at the new model from the recreated legacy model produce only a 0.0157 difference in the Lagrangian porosity at 10,000 years. This surprising result is due to two competing effects: the new waste model's resistance reaches p^{litho} at a higher waste porosity, but the new waste block also compacts to a smaller final volume at 10,000 years (see Fig. 3-3). Compacting to a smaller waste block

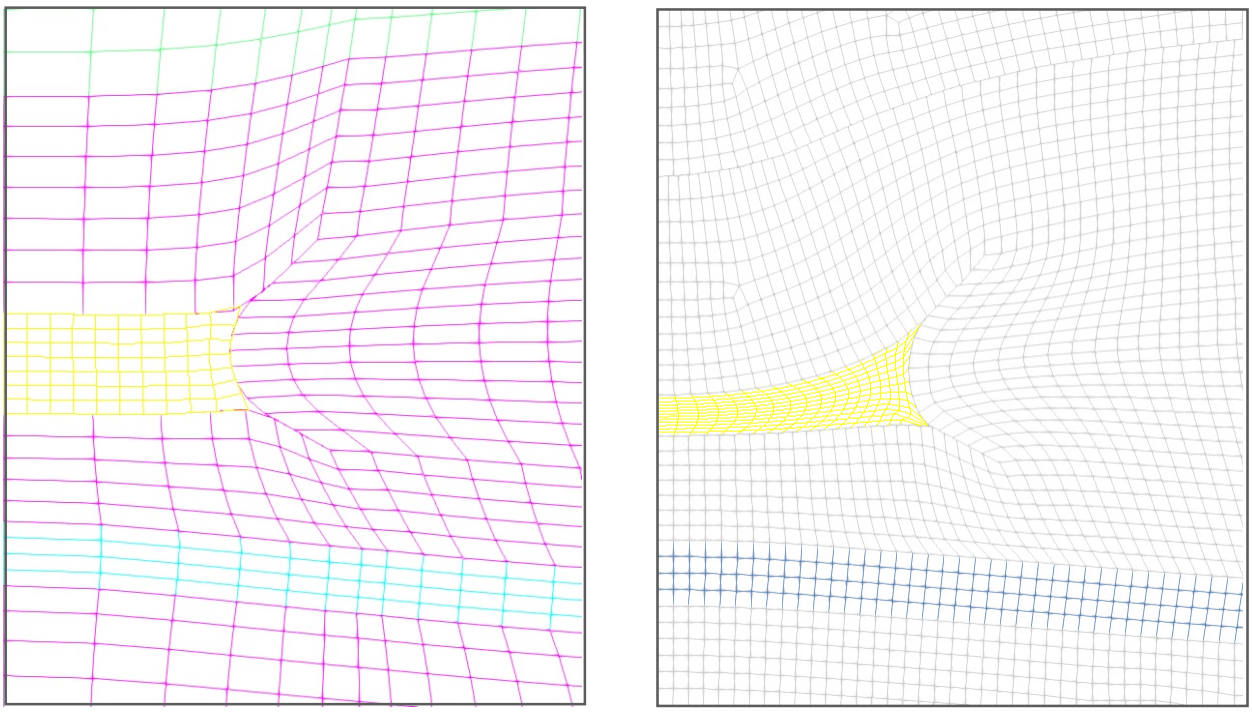


Figure 3-4. Comparison of a deformed lower horizon disposal room between the recreated legacy model (left) and new model (right) at 10,000 years for zero gas generation, $f = 0$.

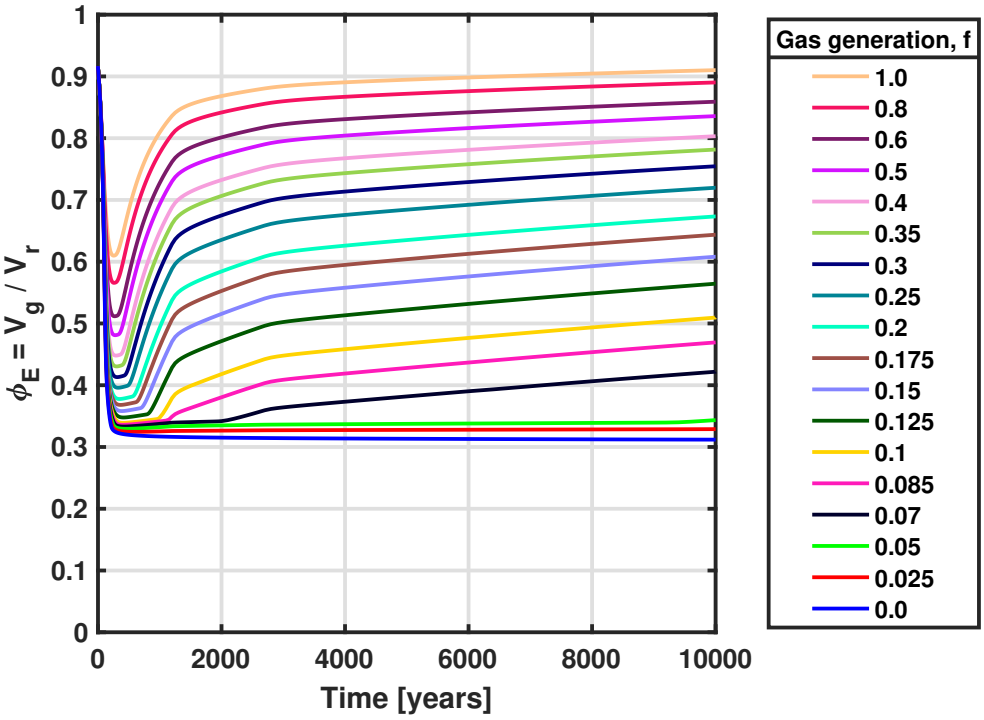
volume means more of the volume within the original room boundary fills with solid salt (see Fig. 3-4), reducing the Lagrangian porosity. The two reasons the new waste block compacts to a smaller volume are (1) the geology is more compliant after improving the numerical setup and geomechanical model (see Fig. 3-3), and (2) the new waste model is more compliant when compared at the same strain (Jensen et al., 2023, Figure 3-12a), instead of at the same porosity.

3.1.5. Impact of New Gas Pressurization Model

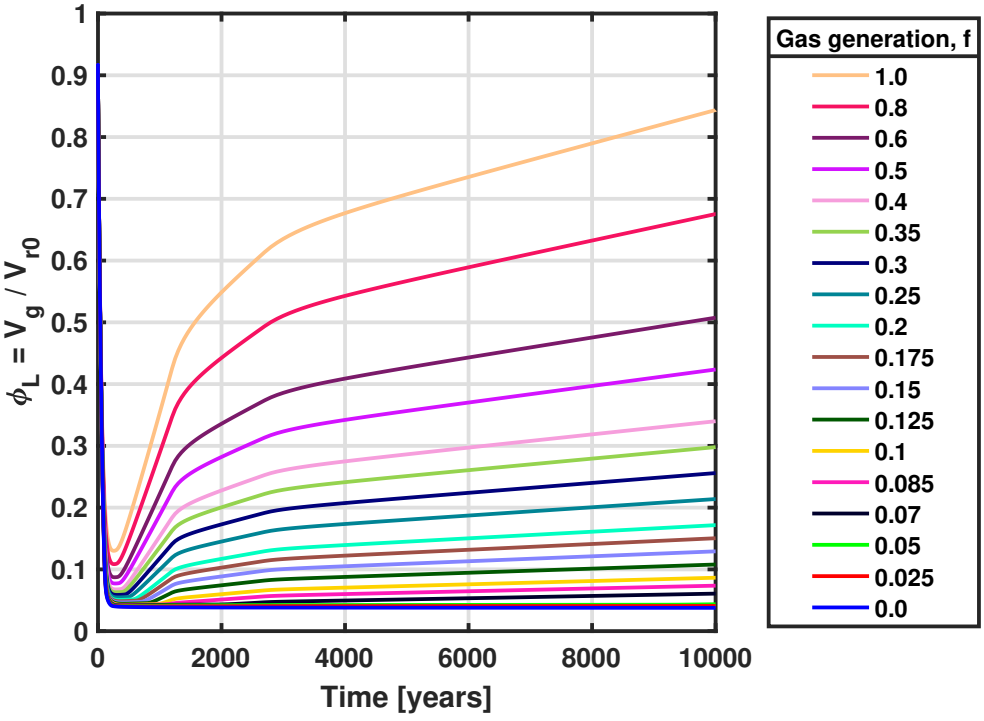
The gas generation factor f corresponds to different amounts of gas for the legacy and new gas pressurization models because the gas generation potentials differ. It is, therefore, not meaningful to directly compare porosity histories from each model for the same values of f. Instead, a later section (Section 3.3) compares the porosity predictions at the same values of time and gas pressure. First, however, the new porosity and pressure histories at each f are presented.

3.2. New Porosity Response Surface

Twenty-one gas generation factors, f, were used to construct the new porosity response surface. The Eulerian and Lagrangian room porosity histories for all gas generation factors throughout the 10,000 year regulatory period are shown in Fig. 3-5a and Fig. 3-5b, respectively. The Eulerian porosity decreases for the first 200-500 years, at which time, with the exception of the zero gas generation case, $f = 0.0$, the porosity increases. Similar to the explanation in Section 3.1.1, the



(a) Eulerian Porosity History



(b) Lagrangian Porosity History

Figure 3-5. Lower horizon Eulerian and Lagrangian porosity histories over 10,000 years for the new model.

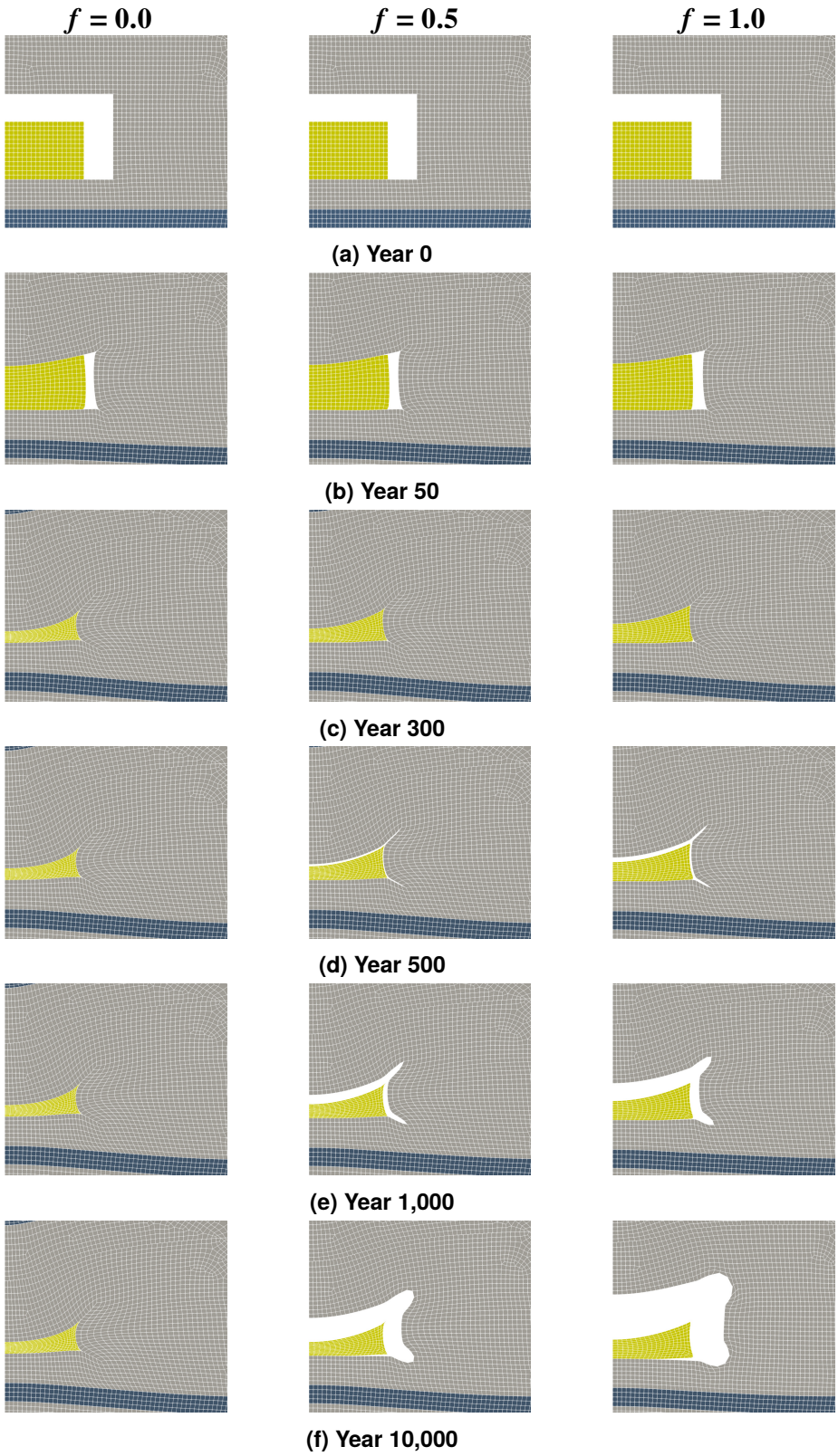


Figure 3-6. Lower horizon disposal room deformations at select years for three gas generation factors.

disposal room closes initally as gas is generated. Eventually, the gas generation and reduction in room volume pressurize the disposal room enough to arrest further room closure. As gas continues to be generated, the disposal room pressurizes further, expands the room, and increases the porosity. The disposal room deformations in Fig. 3-6 show this process.

The initial disposal room porosity is 0.917 for the new model. For the reference gas generation case, $f = 1.0$, the final disposal room Eulerian porosity at 10,000 years is 99.3 % of the initial porosity. That is, for the maximum theoretical gas generation, the disposal room porosity decreases to 0.61 at year 270 and then inflates to a final porosity of 0.91 at year 10,000. For gas generation factors exceeding the reference case, $f > 1.0$, the final disposal room Eulerian porosity exceeds the initial porosity.

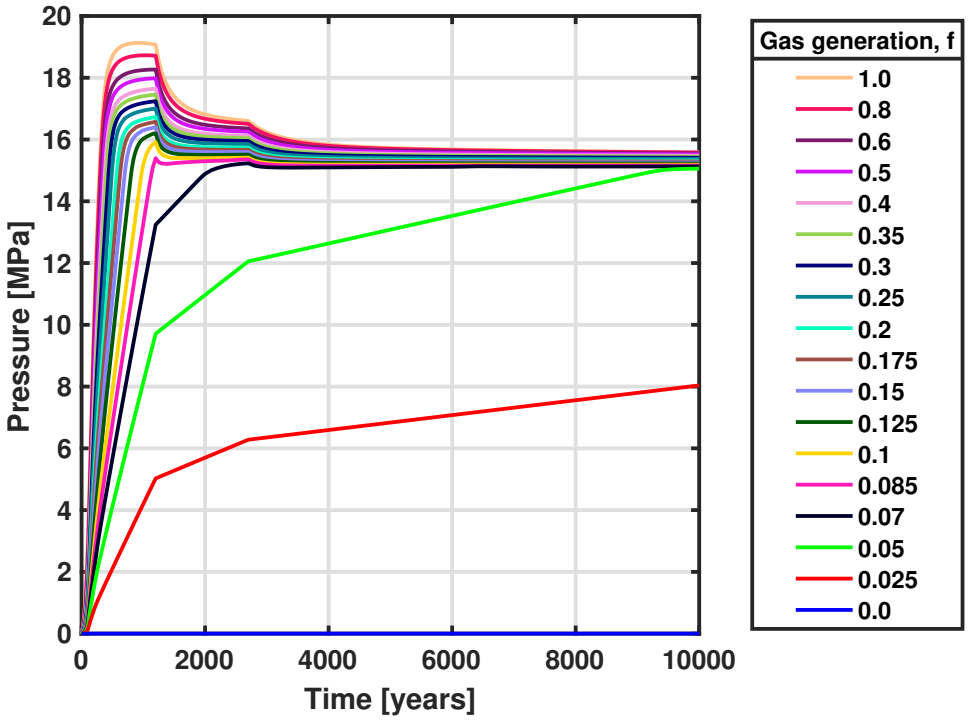
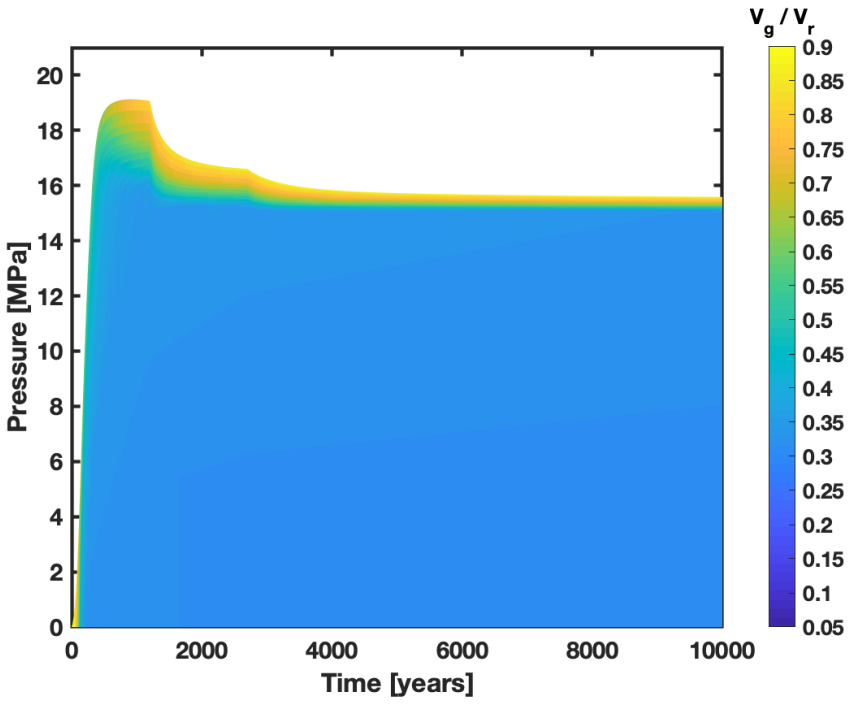


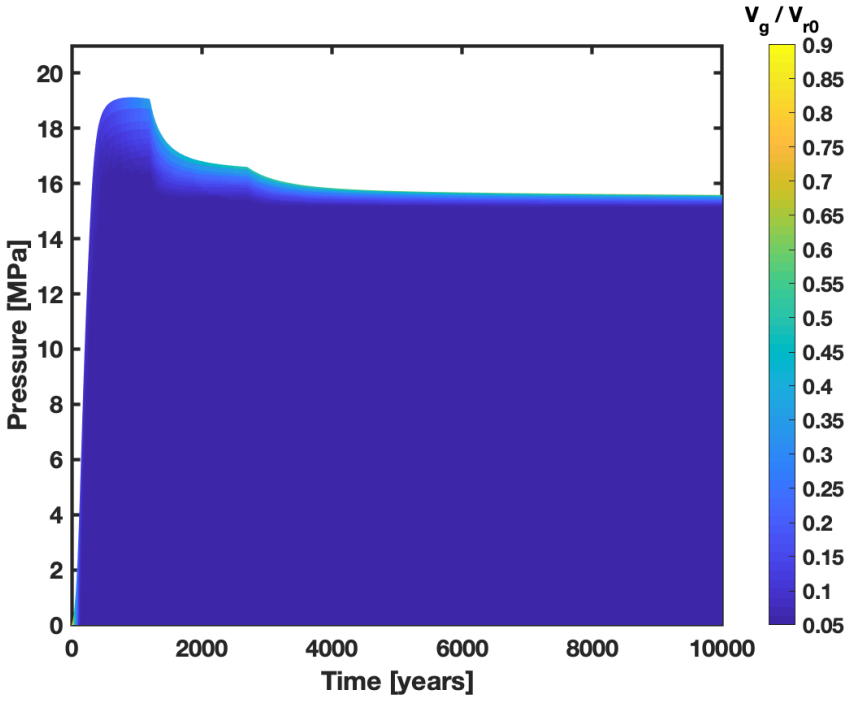
Figure 3-7. Lower horizon disposal room gas pressure histories for the new model.

The gas pressure histories in the room for the twenty-one gas generation factors, f, over the 10,000 year regulatory period are shown in Fig. 3-7. For $f \leq 0.05$, the room pressure increases monotonically for the duration of the simulation. For $f \geq 0.07$, the room pressure increases to a maximum and then decreases as the gas pressure and overburden approach equilibrium. Two sharp changes in the gas pressure rate for a given f are noted at 1,200 years and 2,700 years where the gas generation contributions from anoxic corrosion and microbial activity, respectively, end. At 10,000 years, the room pressures are greater than p^{litho} for $f \geq 0.05$, which is consistent with the increasing porosities for $f \geq 0.05$ in Fig. 3-5.

The porosity response surface is a function of both time and the gas pressure in the room. Fig. 3-8 shows intensity maps of the porosity. In a PA calculation, at a given time and pressure, the Lagrangian porosity value would be used. Intensity maps provide a visual representation of the porosity response surface look-up table.



(a) Eulerian Porosity



(b) Lagrangian Porosity

Figure 3-8. Lower horizon disposal room Eulerian and Lagrangian porosity intensity maps for the new model.

3.3. Legacy vs. New Porosity Response Surface

As previously mentioned, a given value of f corresponds to a different amount of gas for each model, because the gas generation potential has been updated between the legacy model and the new model. A direct comparison of the porosity histories for each model based on gas generation factor is not meaningful. Instead, the porosity intensity maps for the new model, Fig. 3-8, are compared to the porosity intensity maps for the recreated legacy model, Fig. 3-9.

The porosity intensity maps for the recreated legacy model show a porosity gradient over the entire pressure range. In contrast, the porosity intensity maps for the new model show very little change in porosity below p^{litho}, but a very sharp increase in porosity with increasing pressures above p^{litho}. The new model also reaches higher porosity values than the recreated legacy. The pressure histories provide further insight into the intensity maps.

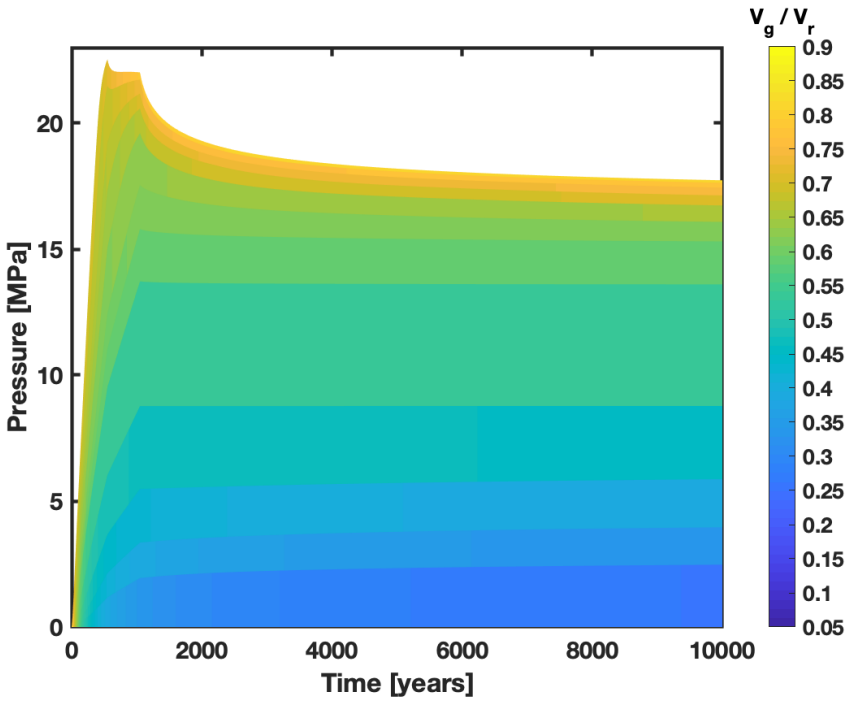
Note that in the new pressure histories, Fig. 3-7, for all $f \geq 0.05$, the pressure at 10,000 years is in the range 15.1 MPa - 15.6 MPa. These pressures are all above $p^{\text{litho}} \approx 14.7$ MPa by 2.7 % to 5.4 %. The disposal room has not yet reached equilibrium at 10,000 years, but the pressures are close. In contrast, the recreated legacy pressure histories, Fig. 3-1b, vary in the range 4.0 MPa to 17.7 MPa at 10,000 years for all $f \geq 0.05$. These pressures are -73.1 % to 20.6 % of $p^{\text{litho}} \approx 14.7$ MPa and the rate of change of these pressure histories is very small. The recreated legacy pressure histories also do not reach equilibrium in 10,000 years and will require significantly more time than the new model to eventually reach equilibrium. These observations show the geology in the new model is significantly more compliant than the geology in the legacy model.

3.4. Sensitivity Studies

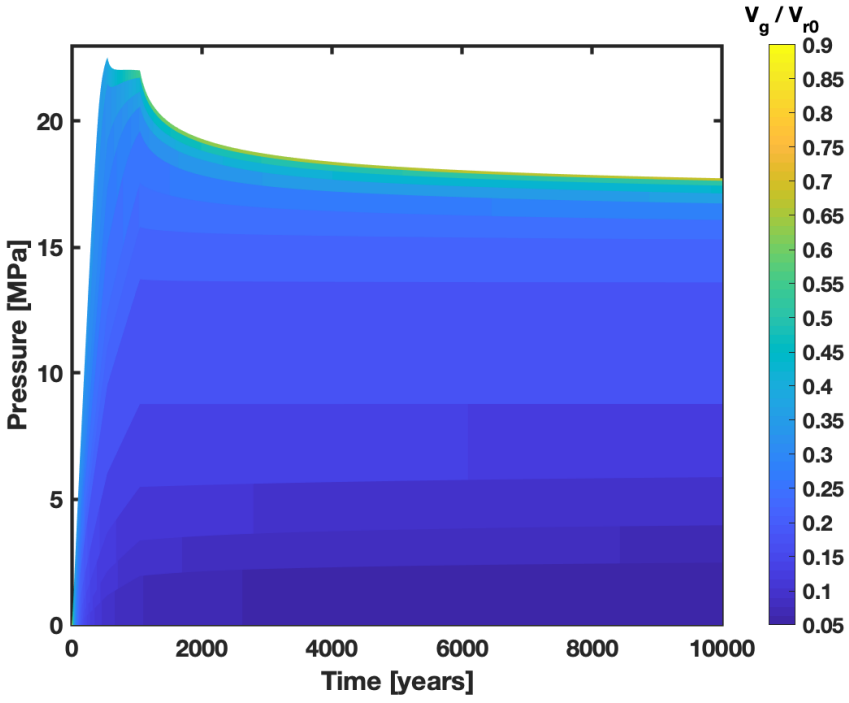
3.4.1. Lower vs. Upper Horizon

The results presented up to this point of the report have all been for a lower horizon disposal room (see Fig. 2-3). As mentioned in Chapter 1, Park and Holland (2007) previously studied the impact of changing the disposal room horizon. They concluded that the disposal room horizon had a relatively minor impact on room porosity, so the CRAs used the legacy porosity response surface for both horizons for simplicity. With the updated geomechanical, waste compaction, and gas pressurization models, it is worthwhile to check whether this result still holds. One potential cause for different lower and upper horizon behavior is that the clay seams intersect the upper and lower horizon rooms at different locations along the room walls, and neither Stone (1997a) nor Park and Holland (2007) included clay seams in their simulations.

The porosity histories for an upper horizon disposal room are compared to the porosity histories for a lower horizon disposal room over 10,000 years in Fig. 3-10a and for the first 1,000 years in Fig. 3-10b. A reduced set of gas generation factors is shown to aid in visualization. During the first 330 years, there are minor differences in porosity. After 330 years, the difference in porosities between the lower and upper horizons is negligible. The absolute difference in porosities between the lower and upper horizons is less than 0.01 for all times outside 50-330 years and less than 0.03

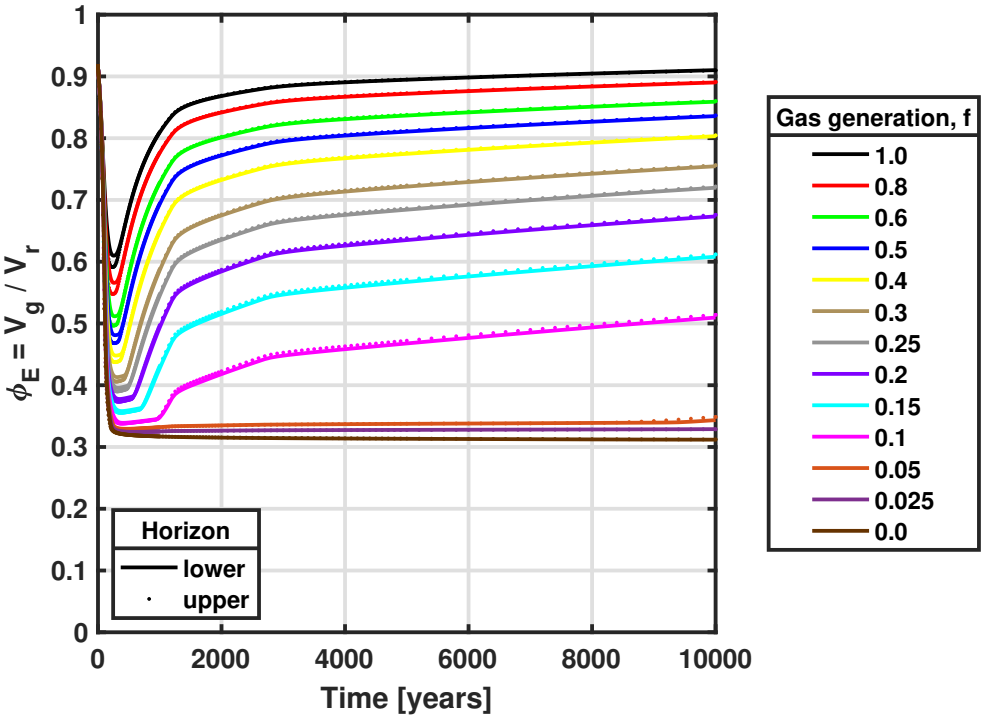


(a) Eulerian Porosity

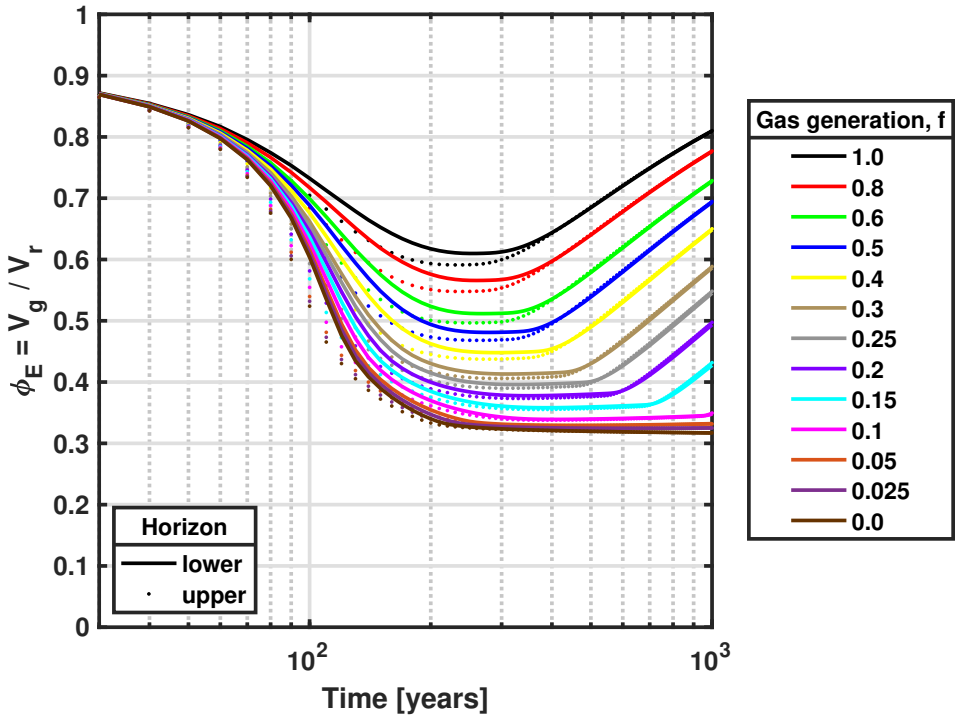


(b) Lagrangian Porosity

Figure 3-9. Lower horizon Eulerian and Lagrangian porosity intensity maps for the recreated legacy model.



(a) Porosity History over 10,000 Years



(b) Porosity History over 1,000 Years

Figure 3-10. Comparison of Eulerian porosity histories between a lower horizon and an upper horizon disposal room over 10,000 years and the first 1,000 years.

for all times outside 70 to 180 years. In the time period 70 to 180 years, the difference in porosities is a maximum of 0.08 for the zero gas generation case, $f = 0.0$, and decreases with increasing gas generation factor. The analysis and conclusions for the upper horizon disposal room are the same as for the lower horizon disposal room.

The pressure histories (not shown) support this conclusion as well. After 330 years, the maximum relative pressure difference between the upper and lower horizons is less than 4.5%. In the time period 70-180 years, the maximum relative pressure difference is 37.4% for the lowest, non-zero gas generation factor and decreases with increasing gas generation factor.

3.4.2. Clay Seam Friction Coefficient

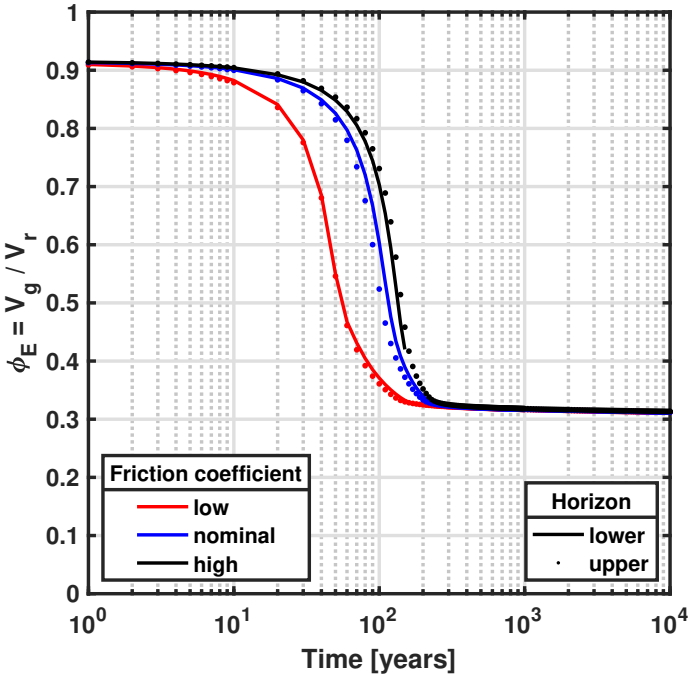


Figure 3-11. Comparison of Eulerian porosity histories for different clay seam friction coefficients (see Table 2-1) and disposal room horizons.

For the results presented thus far, the clay seam friction coefficient was $\mu_c^{\text{other}} = 0.2$ for all clay seams except Clay Seam F which had a friction coefficient of $\mu_c^{\text{F}} = 0.42$. As discussed in Section 2.1.6, the clay seam friction coefficient of $\mu_c^{\text{other}} = 0.2$ was set using engineering judgement to produce qualitatively realistic amounts of clay seam sliding. It is, therefore, prudent to investigate the porosity's sensitivity to this value.

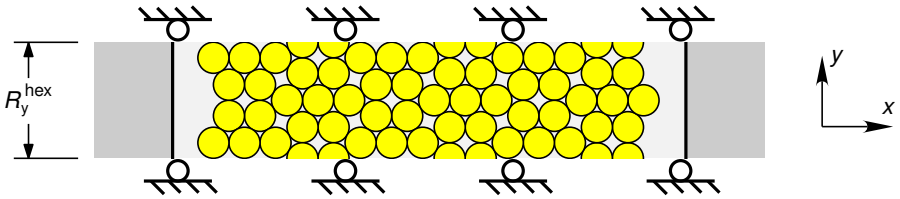
Fig. 3-11 shows the porosity histories for the bounding clay seam friction coefficients and nominal clay seam friction coefficient listed in Table 2-1. These simulations utilized zero gas generation for simplicity. For times less than 300 years, the porosity histories are sensitive to the clay seam friction coefficient. A maximum porosity difference of 0.40 between the lower and upper friction bounds is observed in year 80. After 300 years, the porosity histories become insensitive to the clay seam friction coefficient. As expected, the friction coefficient influences the rate at which the

porosity reaches the final state, but not the final state itself. The final Eulerian porosity is controlled by the lithostatic pressure and the waste (Eulerian) porosity required for the waste to resist the lithostatic pressure. After 300 years with zero gas generation, the disposal room has closed around the waste (see Fig. 3-3 and Fig. 3-6) and the clay seams have no more effect.

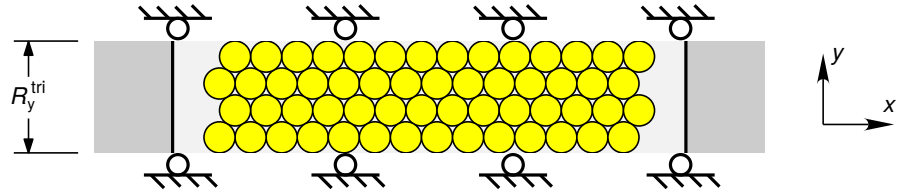
3.4.3. Homogenized vs. Discrete Containers

The results presented have all used the homogeneous waste block representation of the waste described in Section 2.2. The validity of this assumption is examined by comparing the porosity history for a disposal room with a homogeneous waste block to the porosity history for a disposal room with the waste modeled as discrete containers. The porosity histories to be compared correspond to an upper horizon disposal room with no gas generation.

The discrete containers have the geometry of a DOT 17C 55-gal container (see (Sandia WIPP Project, 1992, p. 3-10)). The initial container diameter, height, and volume are 0.602 m, 0.892 m, and 0.254 m^3, respectively. For the numerical model, the diameter was increased to 0.610 m to account for faceting in the mesh (see Fig. 3-13), such that the container volume remained constant. The height of three stacked containers is the same as the height of the homogeneous waste block.



(a) Hexagonal arrangement



(b) Triangular arrangement

Figure 3-12. Discrete container arrangements.

Two different container packing arrangements, as shown in Fig. 3-12, were considered for their impact on room porosity. The hexagonal arrangement has 153 complete containers and 36 half-containers at the front and back row, for a total of $n_{con}^{hex} = 171$ containers. The modeled room length is $R_y^{hex} = 2.295$ m for the hexagonal array. The triangular arrangement has $n_{con}^{tri} = 168$ complete containers and a modeled room length of $R_y^{tri} = 2.208$ m. In order to approximate an infinitely long room, mirror (roller) boundary conditions were enforced on the front and back x-z planes.

The number of containers per unit length of room for the hexagonal and triangular arrays are similar, but not identical to the homogenized case: $n_{\text{con}}^{\text{hex}}/R_{\text{y}}^{\text{hex}} = 74.5\ \text{m}^{-1}$ and $n_{\text{con}}^{\text{tri}}/R_{\text{y}}^{\text{tri}} = 76.1\ \text{m}^{-1}$ versus $n_{\text{con}}/R_{\text{y}} = 74.4\ \text{m}^{-1}$. A greater number of containers within a room yields a greater volume of solid waste within the room, so hexagonal and triangular array solid waste volumes are computed as

$$V_{\text{sw}}^{\text{hex}} = V_{\text{sw}} \frac{n_{\text{con}}^{\text{hex}}/R_{\text{y}}^{\text{hex}}}{n_{\text{con}}/R_{\text{y}}} = 302.8\,\text{m}^3$$

$$V_{\text{sw}}^{\text{tri}} = V_{\text{sw}} \frac{n_{\text{con}}^{\text{tri}}/R_{\text{y}}^{\text{tri}}}{n_{\text{con}}/R_{\text{y}}} = 309.2\,\text{m}^3.$$

A greater number of containers within a room should have only a minor impact on the final Eulerian porosity since each additional unit of waste volume must still reach the same (Eulerian) porosity before it can resist the lithostatic pressure. That is, for a greater number of containers, both the volume of solid waste within the room and the volume of the room at closure increase, but their ratio remains nearly constant for the waste porosity required to resist lithostatic pressure. A greater number of containers within a room should, however, lead to less room closure and larger Lagrangian porosity, since less salt will be allowed to flow into the original volume of the room.

The waste constitutive model is the foam damage model described in Section 2.2. The contact model is the same as for the homogeneous waste block simulations, using nominal clay seam friction coefficients, with the addition of a container-to-container friction coefficient of 0.3.

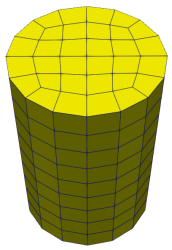
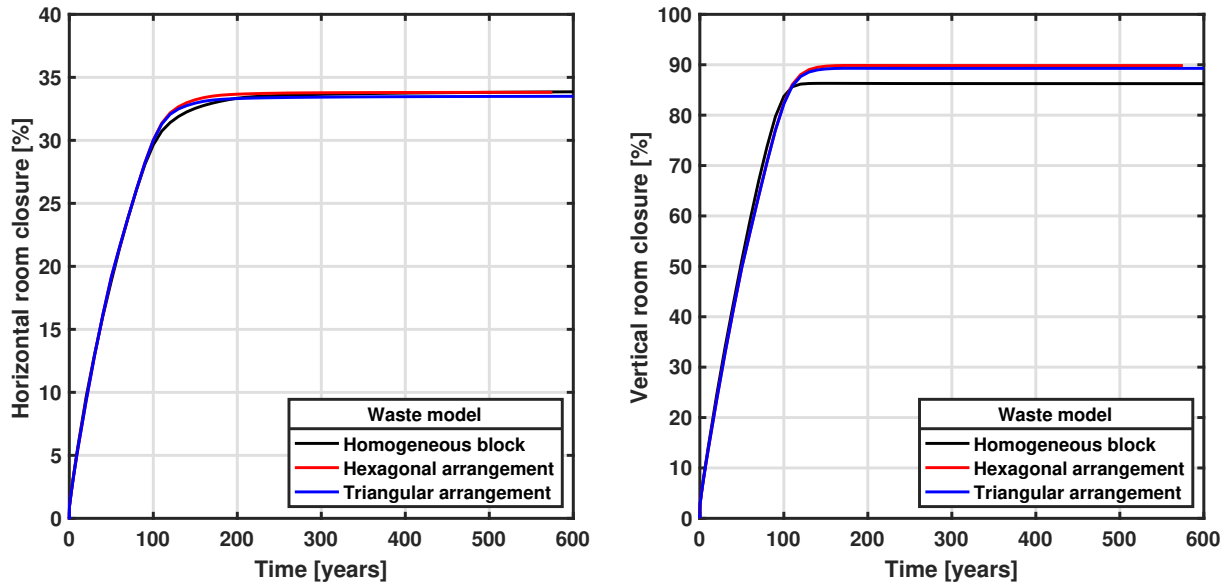


Figure 3-13. Discrete container mesh.

In the numerical model, the full disposal room width R_{x} is modeled due to the container arrangements breaking symmetry. This contrasts with the half-width model for the homogeneous waste block (Fig. 2-3). The disposal room mesh was approximately the resolution of the coarse mesh in Appendix B.3 and used for both arrangements. The hexagonal arrangement used 63,348 elements and the triangular arrangement used 62,484 elements for the entire geometry. Fig. 3-13 shows the mesh for a discrete container. The disposal room closure simulations required 4 days of run time on 192 processors each to reach years 580 and 690 for the hexagonal and triangular arrangement, respectively. Severely distorted container elements were removed by an element death procedure to allow the simulation to proceed. Typically, the removed elements were located at the left and right walls of the disposal room and were pinched as the room corners closed. The hexagonal arrangement simulation removed 4 % of container elements and the triangular arrangement simulation removed 0.5 % of container elements. Analogous to removing containers,



(a) Horizontal Room Closure

(b) Vertical Room Closure

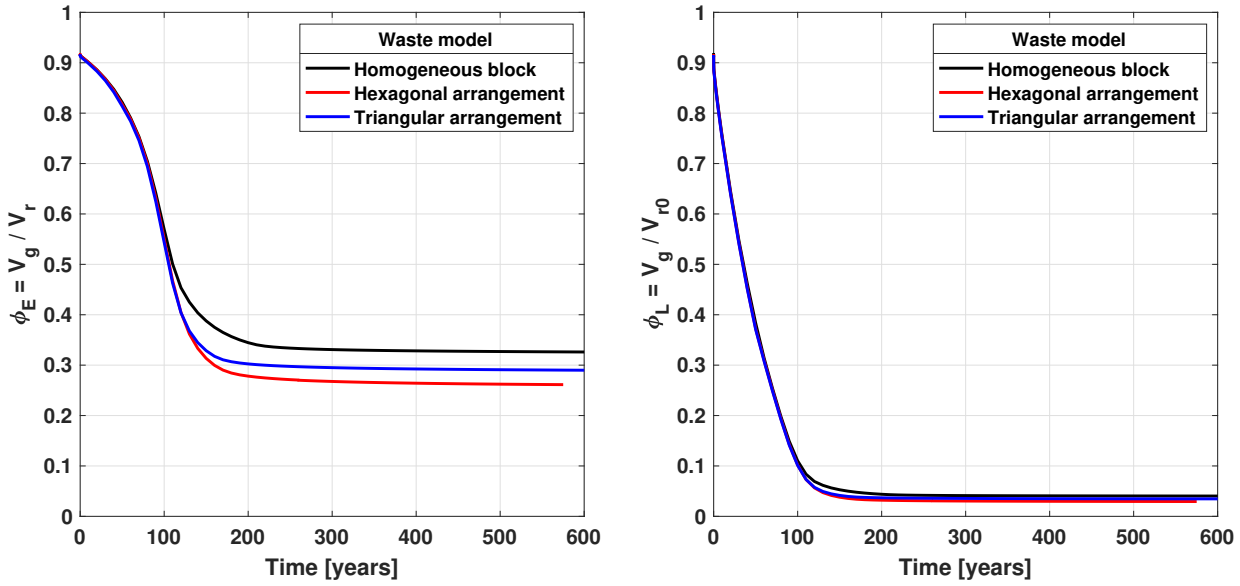
Figure 3-14. Comparison of room closure histories between discrete container waste arrangements and a homogeneous waste block over 600 years for an upper horizon disposal room with zero gas generation, $f = 0$.

deleting elements slightly increase room closure and decrease Lagrangian porosity, but should have minor to negligible impact on Eulerian porosity.

The disposal room horizontal closure histories and vertical closure histories for the discrete container arrangements are compared to the homogeneous waste block closure histories in Fig. 3-14. The homogeneous waste block simulation in this section utilized the coarse finite element mesh shown in Fig. B-1 in order to be consistent with the coarse meshes used in the discrete container simulations. Vertical closure is the sum of the vertical displacement magnitudes measured at mid-width on the floor and ceiling, while horizontal closure is the sum of the horizontal displacement magnitudes measured at mid-height on the left and right walls. The horizontal and vertical closure histories are normalized by the initial disposal room width and height, respectively. The closures for the discrete containers and homogeneous waste block are the same for the first 90 years. After 90 years, the horizontal closure of the discrete containers is less than 0.4 % lower than the homogeneous waste block closure and the vertical closure of the discrete containers is less than 3.1 % higher than the homogeneous waste block closure.

The deformation of the discrete waste containers at different times are shown in Fig. 3-16 and Fig. 3-17 for the hexagonal arrangement and triangular arrangement, respectively. The deformation at 500 years for the discrete container simulations is visually simular to the deformation in the homogeneous waste block simulation Fig. 3-6d.

The disposal room porosity histories, both Eulerian and Lagrangian, for the discrete container arrangements are compared to the homogeneous waste block porosity history in Fig. 3-15. The discrete container Eulerian porosity histories agree well with the homogeneous waste block porosity history until roughly 120 years, after which the discrete container Eulerian porosity



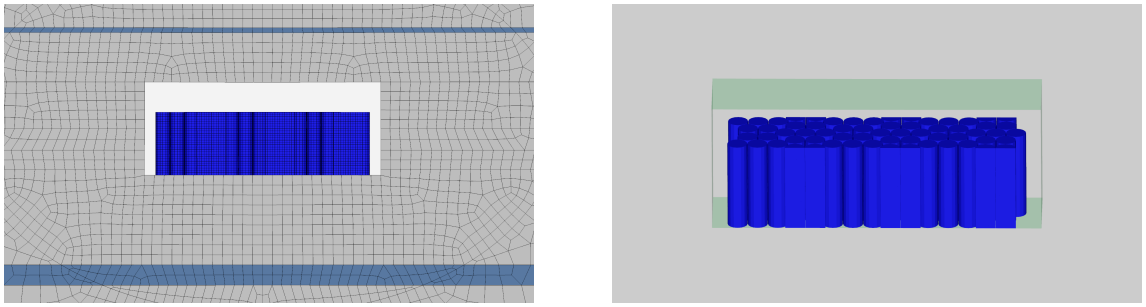
(a) Eulerian Porosity History **(b) Lagrangian Porosity History**

Figure 3-15. Comparison of porosity histories between discrete container waste arrangements and a homogeneous waste block over 600 years for an upper horizon disposal room with zero gas generation, $f = 0$.

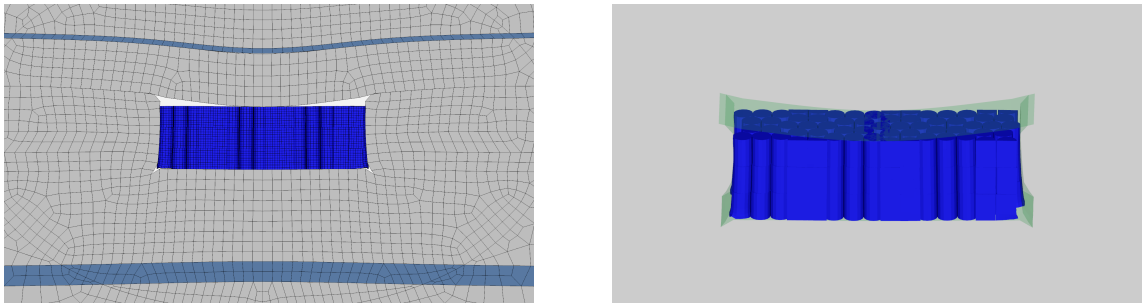
decreases to a lower plateau than the homogenized porosities. By 500 years, the discrete hexagonal arrangement and triangular arrangement Eulerian porosities are less than 0.076 and 0.06 lower, respectively. The differences in Lagrangian porosity histories in Fig. 3-15b are more muted. The difference in Lagrangian porosity between the discrete hexagonal and triangular arrangements versus the homogeneous waste block are less than 0.015 and 0.013, respectively.

As expected, the waste homogenization appears to artificially stiffen the waste behavior. Some potential reasons are discrete containers can slide past one another; discrete containers can squeeze into the void space between one another; and discrete containers have a lower concentration of material to resist to vertical room closure at room mid-width, where the pinching between the floor and roof is most severe. Although these differences are interesting to discuss, only the Lagrangian porosity is used in the PA flow simulations and the Lagrangian porosity differences are minimal.

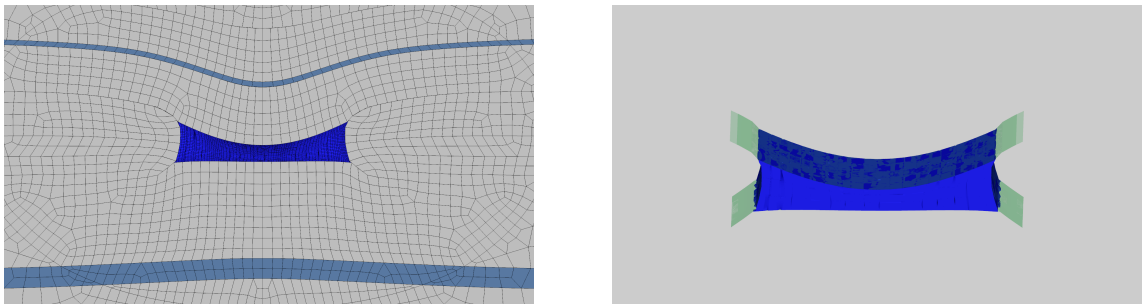
For less than 0.015 difference in Lagrangian porosity between the discrete and homogeneous model predictions, the additional computational cost of the discrete container model is deemed unnecessary and the assumption of a homogeneous waste block is considered acceptable. If, however, it becomes necessary to consider different types of waste containers (Standard, Criticality Control Overpack, Pipe Overpack) placed together in a waste disposal room, the different structural characteristics of each waste container type may require a discrete container model and the homogeneous waste block assumption should be revisited.



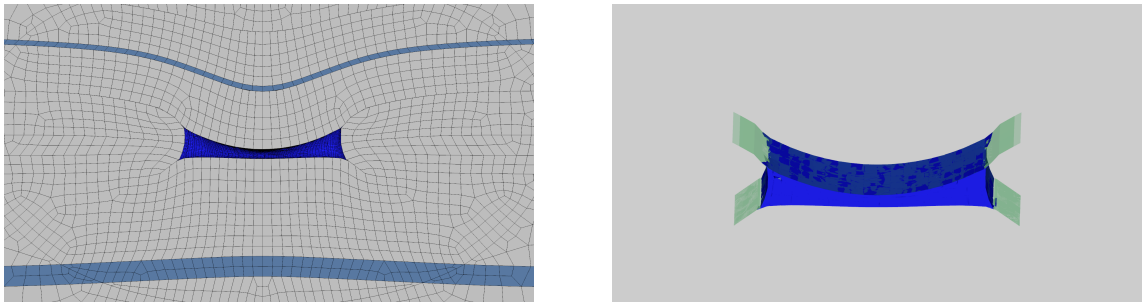
(a) Year 0



(b) Year 30

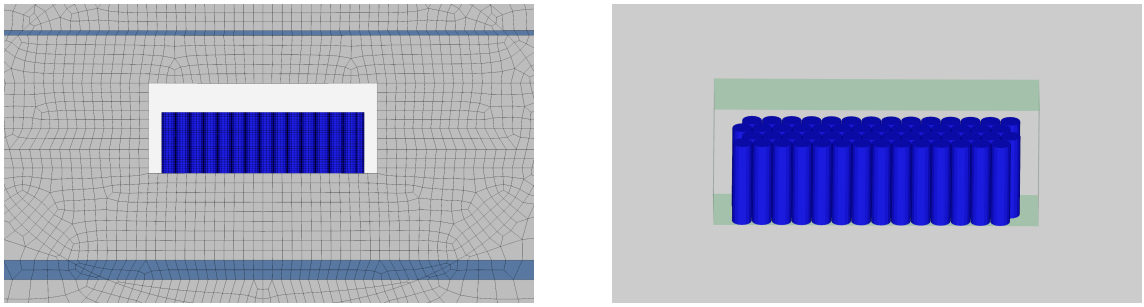


(c) Year 100

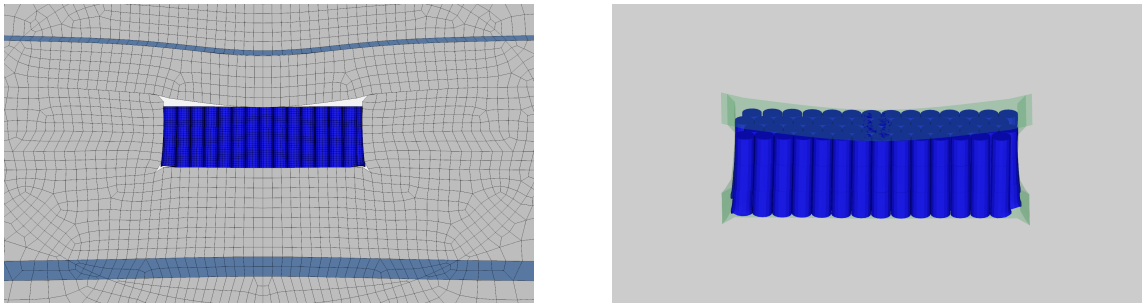


(d) Year 500

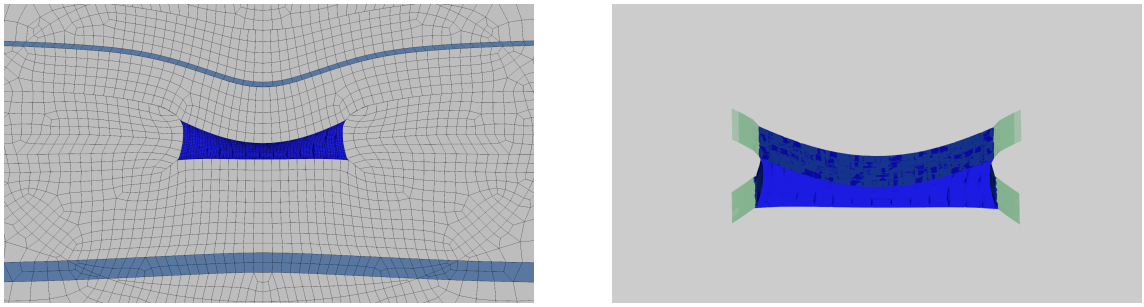
Figure 3-16. Upper horizon disposal room deformations at select years with zero gas generation for the discrete container hexagonal arrangement shown in the stratigraphy (left) and with the room surface boundary (right).



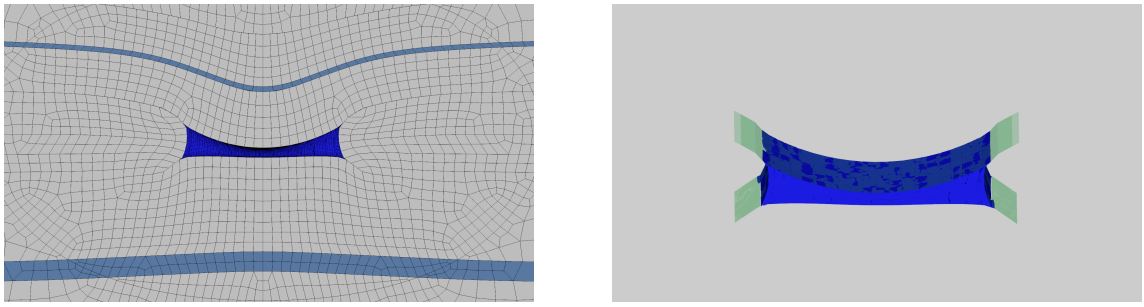
(a) Year 0



(b) Year 30



(c) Year 100



(d) Year 500

Figure 3-17. Upper horizon disposal room deformations at select years with zero gas generation for the discrete container triangular arrangement shown in the stratigraphy (left) and with the room surface boundary (right).

4. SUMMARY

A new porosity response surface was computed from simulations of the evolution of a disposal room filled with waste and gas at the WIPP. This is the first update to the porosity response surface since the legacy surface was computed in 1997.

The disposal room porosity model, used to construct the new porosity response surface, was updated with significant improvements to three sub-models: the geomechanical model, waste compaction model, and gas pressurization model. The improved geomechanical model uses the full stratigraphy, an enhanced salt constitutive model which captures low stress creep behavior, and a frictional sliding model for clay seams. The improved waste compaction model is based on new experiments that included both axial and lateral strain measurements on containers filled with a more representative waste composition. The improved gas pressurization model includes brine radiolysis as a new gas generation source and updates the gas generation rates and durations of sources based on recent studies. In addition, the numerical set-up was improved and the porosity response surface shown to be both mesh converged and domain size converged.

The impacts of each major step from the legacy to the new disposal room porosity model were investigated. Switching from the legacy finite element code, SANTOS, to a newer finite element code, Sierra/SolidMechanics, caused only minor changes in the porosity predictions. The improved numerical setup and the new geomechanical model both made the disposal room porosity model more compliant, so that the room evolved toward its long-term equilibrium geometry more rapidly than in the legacy model. The new waste compaction model had minimal impact on the disposal room porosity because two effects largely cancelled each other out: the waste block compacted to a smaller final volume, yet the porosity within that volume was higher.

The new porosity response surface was constructed from of a series of porosity and pressure histories for various gas generation factors. If gas was not generated within the room, the porosity decreased sharply during the first 200-500 years to near its equilibrium value after which it remained nearly constant. If gas was generated, the porosity dropped to a local minimum and then increased with time and the amount of gas generated. Similarly, the gas pressure in the non-zero gas generation cases increased sharply during the first 200-500 years, and then asymptoted toward the lithostatic pressure.

A comparison of the legacy and new porosity response surface revealed distinctly different behavior. At a given time, the legacy surface predicted a moderate increase in porosity for increases in pressure. The new surface, by contrast, predicted a shallow porosity gradient for pressures beneath lithostatic pressure, and a steep porosity gradient for pressures above lithostatic pressure. These differences appear to be due to the increased compliance of the new geomechanical model and improved numerical setup.

Sensitivity studies for lower versus upper horizon disposal rooms, clay seam friction coefficient, and a homogenized waste block versus discrete waste containers were performed. These sensitivity studies supported the assumptions made in the disposal room porosity model. Horizon had a minor impact: the lower and upper horizon disposal room porosity histories differed by less than 0.01 for all times outside 50-330 years. Inside this time period, the maximum porosity difference was 0.08 for the zero gas generation case and decreased with increasing gas generation. The porosity histories were sensitive to the clay seam friction coefficient for times less than 300 years. After 300 years, the porosity histories became insensitive to the clay seam friction coefficient. The Lagrangian porosity history for the discrete container waste model differed by less than 0.015 from the homogeneous waste block model, which shows the homogeneous waste block model was a sufficiently accurate substitution.

The new porosity response surface has a stronger scientific foundation than the legacy surface, differs significantly from the legacy surface, and is ready to be used for Compliance Decision Analyses.

BIBLIOGRAPHY

R. M. Brannon, T. J. Fuller, A. F. Fossum, and O. E. Strack. Kayenta: theory and user's guide. Technical Report SAND2015-0803, Sandia National Laboratories, Albuquerque, NM, USA; Livermore, CA, USA, 2015.

S. T. Broome, D. R. Bronowski, S. J. Kuthakun, T. W. Pfeifle, and C. G. Herrick. Compaction behavior of surrogate degraded emplaced WIPP waste. Technical Report SAND2014-1897, Sandia National Laboratories (SNL-NM), Albuquerque, NM (United States), March 2014.

B. Butcher. Waste Isolation Pilot Plant disposal room model. Technical report SAND97-0794, Sandia National Laboratories, Albuquerque, New Mexico 87185 and Livermore, California 94550, Aug. 1997a.

B. Butcher. A summary of the sources of input parameter values for the Waste Isolation Pilot Plant final porosity surface calculations. Technical report SAND97-0796, Sandia National Laboratories, Albuquerque, New Mexico 87185 and Livermore, California 94550, Aug. 1997b.

R. Carrasco. Clay seam observations. Personal Communication, March 2020.

CBFO. Title 40 CFR part 191, subparts B and C, compliance recertification application 2019 for the Waste Isolation Pilot Plant, appendix pa-2019 performance assessment. Technical report, United States Department of Energy, Waste Isolation Pilot Plant, 2019.

Cubit. *Cubit 15.9 User Documentation*. Sandia National Laboratories, Albuquerque, NM, USA; Livermore, CA, USA, 15.9 edition, 2021.

U. Düsterloh, K. Herchen, and K.-H. Lux. Joint project III on the comparison of constitutive models for the mechanical behavior of rock salt III. Extensive laboratory test program with argillaceous salt from WIPP and comparison of test results. In L. Roberts, K. Mellegard, and F. Hansen, editors, *Mechanical Behavior of Salt VIII*, pages 13–21. CRC Press, London, May 2015.

C. Hansen. Review of conceptual models for the additional panels performance assessment. Analysis Report ERMS 575130, Sandia National Laboratories, 2021.

C. Hansen, L. Brush, M. Gross, F. Hansen, B. Park, J. Stein, and T. Thompson. Effects of supercompacted waste and heterogeneous waste emplacement on repository performance, revision 2. WIPP Records Center ERMS #533551, Sandia National Laboratories, Carlsbad, NM, Jan. 2004.

R. Jensen, S. Broome, C. Herrick, and B. Reedlunn. Improved compaction experiments and modeling of Waste Isolation Pilot Plant standard, non-degraded, waste containers. Technical Report SAND2023-04823, Sandia National Laboratories, Albuquerque, New Mexico 87185 and Livermore, California 94550, June 2023.

S. King. Gas generation function for calculating waste creep closure. WIPP Records Center ERMS #575793, Sandia National Laboratories, Carlsbad, NM, Aug. 2021.

R. Krieg. Reference stratigraphy and rock properties for the Waste Isolation Pilot Plant (WIPP) project. Technical report SAND83-1908, Sandia National Laboratories, Albuquerque, New Mexico 87185 and Livermore, California 94550, Jan. 1984.

LAMÉ Team. Library of advanced materials for engineering (LAMÉ) 5.4. Technical Report SAND2021-16079, Sandia National Lab.(SNL-NM), Albuquerque, NM (United States), December 2021.

D. Munson, A. Fossum, and P. Senseny. Advances in resolution of discrepancies between predicted and measured in situ WIPP room closures. Technical report SAND88-2948, Sandia National Laboratories, Albuquerque, New Mexico 87185 and Livermore, California 94550, Feb. 1989a.

D. Munson, R. Jones, D. Hoag, and J. Ball. Mining development test (Room D): in situ data report (March 1984 - May 1988); Waste Isolation Pilot Plant (WIPP) thermal/structural interactions program. Technical report SAND88-1460, Sandia National Laboratories, Albuquerque, New Mexico 87185 and Livermore, California 94550, Sept. 1989b.

D. E. Munson. Constitutive model of creep in rock salt applied to underground room closure. *International Journal of Rock Mechanics and Mining Sciences*, 34(2):233–247, 1997.

S. R. Nielsen. *Nuclear Waste Management Procedure NP 9-1 Analyses, Revision 11*. Sandia National Laboratories, Albuquerque, New Mexico 87185 and Livermore, California 94550, September 2020.

B. Y. Park and F. D. Hansen. Determination of the porosity surfaces of the disposal room containing various waste inventories for WIPP PA. Technical report SAND2005-4236, Sandia National Laboratories, Albuquerque, New Mexico 87185 and Livermore, California 94550, 2005.

B.-Y. Park and J. Holland. Structural evaluation of WIPP disposal room raised to Clay Seam G. Technical report SAND2007-3334, Sandia National Laboratories, Albuquerque, New Mexico 87185 and Livermore, California 94550, September 2007.

B. Reedlunn. Reinvestigation into closure predictions of Room D at the Waste Isolation Pilot Plant. Technical Report SAND2016-9961, Sandia National Laboratories, Albuquerque, NM, USA, 2016a.

B. Reedlunn. Reinvestigation into closure predictions of Room D at the Waste Isolation Pilot Plant. Technical report SAND2016-9961, Sandia National Laboratories, Albuquerque, New Mexico 87185 and Livermore, California 94550, Oct. 2016b.

B. Reedlunn. Enhancements to the Munson-Dawson model for rock salt. Technical report SAND2018-12601, Sandia National Laboratories, Albuquerque, New Mexico 87185 and Livermore, California 94550, Nov. 2018.

B. Reedlunn. Analysis plan for improvements to the disposal room porosity model. WIPP Analysis Plan AP-197 Rev. 0, ERMS 577517, Sandia National Laboratories, June 2022.

B. Reedlunn and J. Bean. Simulations of Pipe Overpack container compaction at the Waste Isolation Pilot Plant. Technical report SAND2019-12111, Sandia National Laboratories, Albuquerque, New Mexico 87185 and Livermore, California 94550, October 2019.

B. Reedlunn, J. G. Argüello, and F. D. Hansen. A reinvestigation into Munson's model for room closure in bedded rock salt. *International Journal of Rock Mechanics and Mining Sciences*, 151, March 2022. doi: 10.1016/j.ijrmms.2021.105007.

B. Reedlunn, J. Bean, J. Wilkes, and J. Bignell. Simulations of Criticality Control Overpack container compaction at the Waste Isolation Pilot Plant. Technical Report SAND2023-10477, Sandia National Laboratories, January 2023.

Sandia WIPP Project. Preliminary performance assessment for the Waste Isolation Pilot Plant, December 1992, volume 3: model parameters. Technical report SAND92-0700/3, Sandia National Laboratories, Albuquerque, New Mexico 87185 and Livermore, California 94550, Dec. 1992.

Sierra/SolidMechanics. *Sierra/SolidMechanics 5.4 User's Guide*. Sandia National Laboratories, Albuquerque, New Mexico 87185 and Livermore, California 94550, 5.4.1 edition, January 2022.

S. R. Sobolik, C. Vignes, S. A. Buchholz, E. Keffeler, and B. Reedlunn. Weimos: Shear behaviors of bedded salt clay seams and their impact on disposal room porosity. In J. de Bresser, M. Drury, P. A. Fokker, M. Gazzani, S. Hangx, A. Niemeijer, and C. Spiers, editors, *The Mechanical Behavior of Salt X*, 2022. doi: 10.1201/9781003295808.

C. M. Stone. Final disposal room structural response calculations. Technical report SAND97-0795, Sandia National Laboratories, Albuquerque, New Mexico 87185 and Livermore, California 94550, August 1997a.

C. M. Stone. *SANTOS: a two-dimensional finite element program for the quasistatic, large deformation, inelastic response of solids*. Sandia National Laboratories, Albuquerque, New Mexico 87185 and Livermore, California 94550, July 1997b.

J. Weatherby, D. E. Munson, and J. G. Arg´uello. Three-dimensional finite element simulation of creep deformation in rock salt. *Engineering computations*, 13(8):82–105, 1996. doi: 10.1108/02644409610153023.

J. R. Weatherby, W. T. Brown, and B. M. Butcher. The closure of WIPP disposal rooms filled with various waste and backfill combinations. In *The 32nd US Symposium on Rock Mechanics (USRMS)*. American Rock Mechanics Association, 1991.

APPENDIX A. Geomechanical Model Validation Simulations

As mentioned in Sections 2.1.1 and 2.1.6, the geomechanical model Reedlunn et al. (2022) validated against the Room D, G, and Q experiments was not quite consistent with the new geomechanical model used herein. Reedlunn et al. (2022) utilized a Clay Seam F friction coefficient of $\mu_c^F = 0.2$, but the new model herein utilized $\mu_c^F = 0.42$ because Clay Seam F resembles diffuse natural clay seams whose friction coefficient was measured as 0.42 (Sobolik et al., 2022).

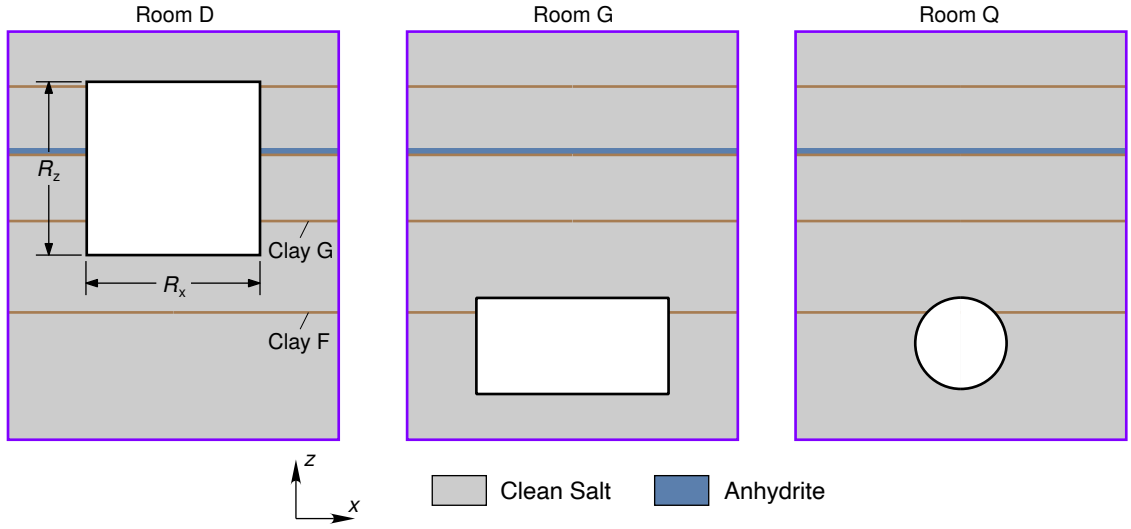


Figure A-1. Room D, G, and Q nominal initial cross-sectional geometries and locations within the stratigraphy.

To resolve this inconsistency, new simulations of Room D, G, and Q were performed with $\mu_c^F = 0.42$. All other details of the new simulations, including numerical details and the friction coefficient for the other clay seams ($\mu_c^{other} = 0.2$), were identical to the respective Room D, G, and Q simulations in Reedlunn et al. (2022, Simulations 17, 22, and 23). The only differences between each of the new Room D, G, and Q simulations were the initial geometries of the rooms and the rooms' position within the stratigraphy, as shown in Fig. A-1. Room G was perhaps the most relevant of the three rooms because Room G's R_x/R_z aspect ratio, as well as its location within the stratigraphy, was similar to lower horizon disposal rooms (see Fig. 2-3). All three rooms were long and slender in the y-direction, such that plane strain conditions were assumed.

Fig. A-2 compares the measured Room D, G, and Q room closures against simulation predictions. The top row of plots depicts the horizontal closure δ_x at room mid-height, normalized by the initial room width R_x, for each room. The bottom row of plots depicts the vertical closure δ_z at

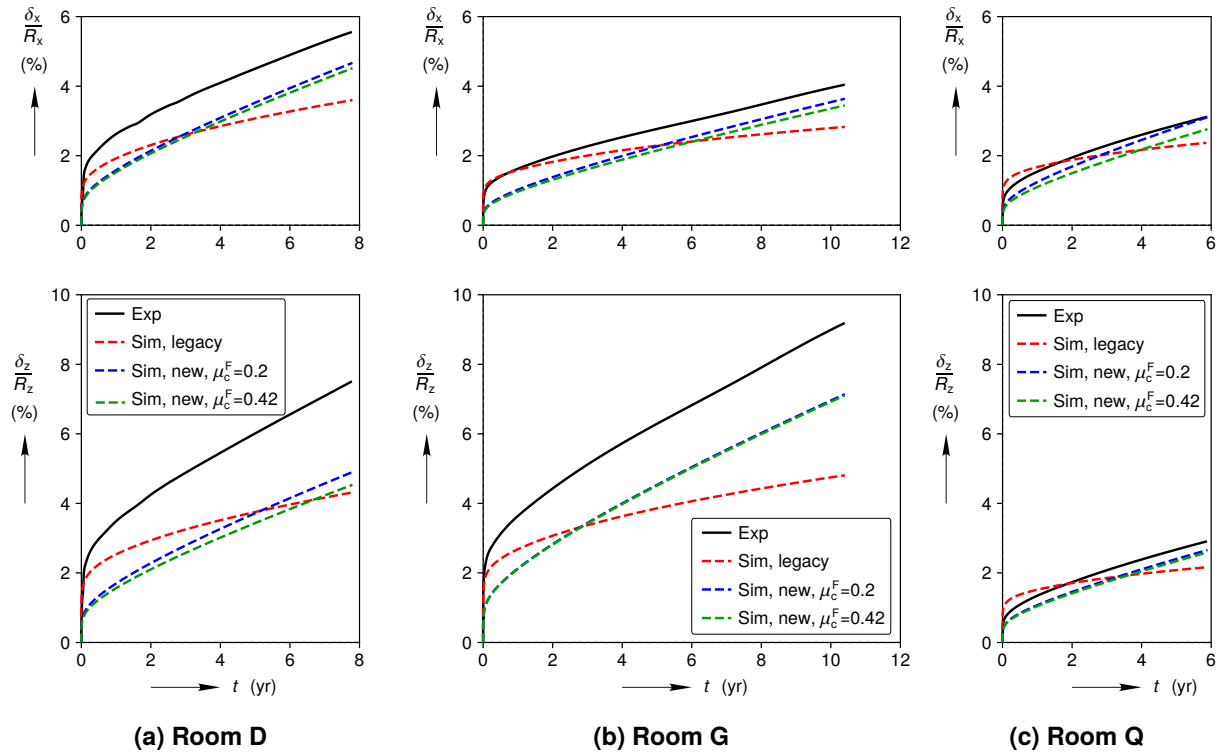


Figure A-2. Simulation predictions of Room D, G, and Q horizontal and vertical closure compared against experimental measurements.

room mid-width, normalized by the initial room height R_z, for each room. The horizontal axis in each plot is the time t since the closure measurement station was excavated. Each room was simulated with three different numerical setups: the legacy setup (see Reedlunn et al. (2022, Simulations 19, 20, and 21)), the new setup with $\mu_c^F = 0.2$ (see Reedlunn et al. (2022, Simulations 17, 22, and 23)), and the new setup with $\mu_c^F = 0.42$.

The new simulation setups under-predict the closure histories during $0 < t < 1$ month, but capture the closure *rates* for $t > 1$ month far better than the legacy simulation setup. Accurate predictions of long-term closure rates are far more important than predictions of the short-term closures because these geomechanical models are used to extrapolate hundreds to thousands of years into the future. This study, therefore, elects to compare the closure rates at $t = 5.7$ yr because it is the maximum time that measurements were collected in all three rooms. Switching from the legacy setup to the new setup with $\mu_c^F = 0.2$ reduces the under-prediction of the closure rates, on average, from 2.48× to 0.97× (a 1.03× over-prediction) at $t = 5.7$ yr.

Increasing μ_c^F from 0.2 to 0.42 has a minor impact on the closure rate predictions. The closure rate under-prediction at $t = 5.7$ yr increases from 0.97× to 1.02×, on average. The new geomechanical model with $\mu_c^F = 0.42$ is therefore sufficiently predictive for careful engineering use.

APPENDIX B. Numerical Details

This section presents various numerical details of the legacy simulations, recreated legacy simulations, and new simulations. Appendix B.1 discusses a variety of numerical details, Appendix B.2 covers the solution schemes, and Appendix B.3 describes a mesh convergence study.

B.1. Miscellaneous Details

Although Sierra/SM has many more capabilities than SANTOS, it does not include two-dimensional plane strain elements. To closely approximate plane strain conditions, the recreated and new finite element meshes used with Sierra/SM consisted of a single layer of hexahedral elements, and the y displacements of the front and back surfaces of the single layer were held to zero. This single layer was $e_y = 1$ m thick in the y-direction for the coarse mesh and base mesh, and $e_y = 10.06/96$ m thick for the fine mesh. (See Appendix B.3 for descriptions of the coarse, base, and fine meshes.) This single layer applies to all the homogeneous waste block simulations; the discrete container simulations meshed the actual dimensions of the containers (see Section 3.4.3).

The name of each material model's numerical implementation, ordinary differential equation (ODE) integration method, and references are listed in Table B-1 for both the legacy and new models. The implementation name corresponds to the name included in the SANTOS and Sierra/SM input files listed in Stone (1997a, Appendix A) and Appendices C.2.1 and C.2.2. Note that, for the same material model and same calibration, differences in accuracy from one implementation to another are expected to be negligible. Nevertheless, the legacy and new material model implementations are not identical, so they are documented here for completeness.

The legacy, recreated legacy, and new simulations used different contact enforcement algorithms to capture contact between the waste, room surfaces, and clay seams (new model only). SANTOS used the ACME contact algorithm, which is a master-slave, node-to-face, kinematic enforcement method. Sierra/SM used the DASH contact algorithm, which is a face-to-face, augmented Lagrangian enforcement method, for the new simulations. DASH is the Sierra/SM default contact algorithm; however, Sierra/SM also has an ACME contact implementaion which was used for the recreated legacy simulations. Similar to the material model implementations, accuracy differences between these two algorithms are expected to be negligible.

The gas pressure p_g was coupled to the disposal room volume V_r through the ideal gas law, as indicated in Section 2.3.2. Rather than update p_g and V_r simultaneously (strong coupling), p_g was computed at the start of a time step based on V_r from the end of the previous time step (weak

Table B-1. Material model implementation information

Material	Item	Legacy	Recreated Legacy	New
Salt	Implementation Name	`m-d creep model`	`munson_dawson`	`md_viscoplastic`
	ODE Integration	Explicit with sub-stepping	Explicit with sub-stepping	Implicit with line search
	Reference	Weatherby et al. (1996)	Weatherby et al. (1996)	Reedlunn (2018, Chapter 3)
Anhydrite	Implementation Name	`soil_n_foams`	`soil_foam`	`kayenta`
	ODE Integration	Implicit (radial return)	Implicit (radial return)	Explicit with sub-stepping
	Reference	Stone (1997b, Section 4.6)	LAMÉ Team (2021, Section 4.24)	Brannon et al. (2015, Chapter 8)
Polyhalite	Implementation Name	–	–	`soil_foam`
	ODE Integration	–	–	Implicit (radial return)
	Reference	–	–	LAMÉ Team (2021, Section 4.24)
Waste	Implementation Name	`soil_n_foams`	`soil_foam`	`foam_damage`
	ODE Integration	Implicit (radial return)	Implicit (radial return)	Explicit with sub-stepping
	Reference	Stone (1997b, Section 4.6)	LAMÉ Team (2021, Section 4.24)	LAMÉ Team (2021, Section 4.29)

coupling). Weak coupling is believed to be sufficient since V_r and n_g change gradually relative to the time step size.

The current room volume V_r was computed using a specialized subroutine. Although Stone (1997a,b) does not precisely explain how the room volume was computed in the legacy simulations, it was likely very similar to the method employed in the new simulations with Sierra/SM. In Sierra/SM, the element faces that comprise the room boundary and a reference point along the leftmost symmetry boundary condition in Fig. 2-3 were supplied to the user subroutine `aupst_cavity_volume`. Note that Clay Seam F element faces were included in the lower horizon room boundary, while Clay Seam F and G element faces were included in the upper horizon room boundary. The `aupst_cavity_volume` subroutine constructed a pentahedron for each element face in the room boundary. The reference point defined the apex of each pentahedron, while the coordinates of the four nodes that made up each element face defined each pentahedron's base. The subroutine then computed the room volume as $V_r = f_v \sum_i^I V_i^{ph}$, where V_i^{ph} is the volume of pentahedron i, I is the total number of pentahedrons, and f_v is a scale factor. If the room were a fully enclosed cavity, then $f_v = 1$ would produce the correct room volume. In this case, the room was open on the front, back, and left sides, so $f_v = 3\,R_y/e_y$ was used to obtain the correct room volume.

B.2. Solution Scheme

Different approaches were used to solve the quasi-static equilibrium equations in the legacy, recreated legacy, and new simulations. In the legacy simulations, SANTOS explicitly integrated the equations of motion (with inertia effects) and then used a dynamic relaxation scheme to obtain the equilibrium solution for a given time step (Stone, 1997b, Section 4.6). In the recreated legacy simulations, Sierra/SM implicitly solved the equilibrium equations. For each time step, Sierra/SM accepted a solution if

$$\frac{\sqrt{\boldsymbol{R}\cdot\boldsymbol{R}}}{\sqrt{\boldsymbol{F}^{re}\cdot\boldsymbol{F}^{re}}} = \hat{R} \le \hat{R}_{max}. \tag{B.1}$$

where $\boldsymbol{R}$ is the residual from the discretized equilibrium equations, $\boldsymbol{F}^{re}$ is the reaction force vector, $\hat{R}$ is the relative residual norm, and $\hat{R}_{max} = 10^{-4}$. The new simulations attempted to also use Sierra/SM's implicit solver, but it often had difficulty converging on solutions that satisfied Eq. (B.1). The lack of convergence may have been related to difficulty satisfying contact constraints between the disposal room and the waste, contact between disposal room surfaces, or contact slippage along clay seams. Regardless of the source, the implicit solver convergence issues were avoided by switching the solution scheme to an explicit dynamics solver with viscoplastic rate scaling for the salt and waste.

Explicit dynamics solvers use very small time steps, typically on the order of 1 μs, which usually restricts explicit dynamics to simulations of short duration events. Viscoplastic rate scaling, however, sidesteps this restriction by compressing physical time t to a reduced code simulation time, termed the momentum balance time t^{mb} (Reedlunn et al., 2023, Section 2.3.2). In this time

compression scheme, the physical viscoplastic strain rate $\mathrm{d}\tilde{\varepsilon}^{\mathrm{vp}}/\mathrm{d}t$ is increased into a scaled viscoplastic strain rate $\mathrm{d}\tilde{\varepsilon}^{\mathrm{vp}}/\mathrm{d}t^{\mathrm{mb}}$. The viscoplastic scale factor $s = s(t^{\mathrm{mb}})$ is defined as

$$s = \frac{\dfrac{\mathrm{d}\tilde{\varepsilon}^{\mathrm{vp}}}{\mathrm{d}t^{\mathrm{mb}}}}{\dfrac{\mathrm{d}\tilde{\varepsilon}^{\mathrm{vp}}}{\mathrm{d}t}} = \frac{\mathrm{d}t}{\mathrm{d}t^{\mathrm{mb}}}, \tag{B.2}$$

so the current physical time can be calculated from the scale factor history as

$$t = \int_{t_{\mathrm{i}}^{\mathrm{mb}}}^{t^{\mathrm{mb}}} s \, \mathrm{d}\hat{t}^{\mathrm{mb}} + t_{\mathrm{i}}, \tag{B.3}$$

where t_{i} and $t_{\mathrm{i}}^{\mathrm{mb}}$, respectively, are the physical and momentum balance time at the start of the time period of interest. Increasing s, reduces the simulation period, but also increases inertial effects. Selecting the viscoplastic rate scaling must, therefore, balance completion of the room closure simulation in a reasonable period of computational time against inertial effect deviations from the quasi-static solution. This balance may generally be achieved by keeping the ratio $E_{\mathrm{k}}/E_{\mathrm{i}}$ of the kinetic energy, E_{k}, to the internal energy, E_{i}, low.

Reedlunn et al. (2023, Appendix A.2.1) ran a series of empty room closure simulations with a viscoplastic rate scaling profile described by:

$$s = \begin{cases} S_0 & \text{for } t^{\mathrm{mb}} \leq 0 \\ S_0 + S_1 t^{\mathrm{mb}} & \text{for } t^{\mathrm{mb}} > 0, \end{cases} \tag{B.4}$$

where S_0 and S_1 are constant numerical parameters. They set $S_0 = 10^{-2}$, varied S_1, compared the viscoplastic rate scaled explicit dynamics solutions against a reference implicit quasi-static solution, and concluded that $S_1 = 2 \times 10^9$ s^{-1} sufficiently approximated the quasi-static solution. Herein, these values for S_0 and S_1 were used to compress the 10,000 year physical time period to 17.8 seconds of momentum balance (simulation) time.

Different methods were used to control the viscoplastic rate scaling in the salt and waste material models (all other material models were rate-independent). The enhanced Munson-Dawson model implementation, `md_viscoplastic`, includes s as an internal variable, and it is straightforward to vary material internal variables during a simulation using Sierra/SM input file commands. The `foam_damage` model implementation, on the other hand, does not have an internal variable that corresponds to s. Fortunately, the Foam Damage model's viscoplastic strain rate depends on the temperature and the disposal room porosity model only considers isothermal conditions, so an artificial temperature history was specified to effectively change s during the simulation.

Rather than specify a complex temperature history, a specific temperature dependence for the Foam Damage model's viscoplastic strain rate can be constructed such that the artificial temperature history $T = s$ may be used. According to LAMÉ Team (2021, Section 4.29), the Foam Damage's viscoplastic strain rate, with respect to momentum balance time, is defined as

$$\frac{\mathrm{d}\tilde{\varepsilon}^{\mathrm{vp}}}{\mathrm{d}t^{\mathrm{mb}}} = \exp(h) \left\langle \frac{\sigma^*}{a} - 1 \right\rangle^n, \tag{B.5}$$

where $< \cdot >$ are Macaulay brackets, σ^* is the effective stress, a is a user defined function of the relative density, h is a user defined function of the (artificial) temperature, and n is another user defined function of the (artificial) temperature. The viscoplastic strain rate, with respect to physical time, is

$$\frac{\mathrm{d}\tilde{\varepsilon}^{\mathrm{vp}}}{\mathrm{d}t} = \exp\left(h_{\mathrm{ns}}\right) \left\langle \frac{\sigma^*}{a} - 1 \right\rangle^n, \tag{B.6}$$

where h_{ns} is a material constant for the isothermal conditions of the disposal room porosity model. Solving Eq. (B.6) for the Macaulay bracket and substituting into Eq. (B.5) gives the relation

$$\frac{\mathrm{d}\tilde{\varepsilon}^{\mathrm{vp}}}{\mathrm{d}t^{\mathrm{mb}}} = \exp\left(h - h_{\mathrm{ns}}\right) \frac{\mathrm{d}\tilde{\varepsilon}^{\mathrm{vp}}}{\mathrm{d}t}. \tag{B.7}$$

Comparing Eqs. (B.2) and (B.7),

$$s = \exp\left(h - h_{\mathrm{ns}}\right). \tag{B.8}$$

Selecting h in the form,

$$h = h_{\mathrm{ns}} + \ln(T), \tag{B.9}$$

reduces Eq. (B.8) to $s = T$. When no viscoplastic scaling is used, $s = T = 0$ and $h = h_{\mathrm{ns}}$ recovering the unscaled viscoplastic strain rate Eq. (B.6). Thus, viscoplastic rate scaling can be implemented in the Foam Damage model for the isothermal disposal room porosity model by prescribing an (artificial) temperature history equal to the viscoplastic scale factor.

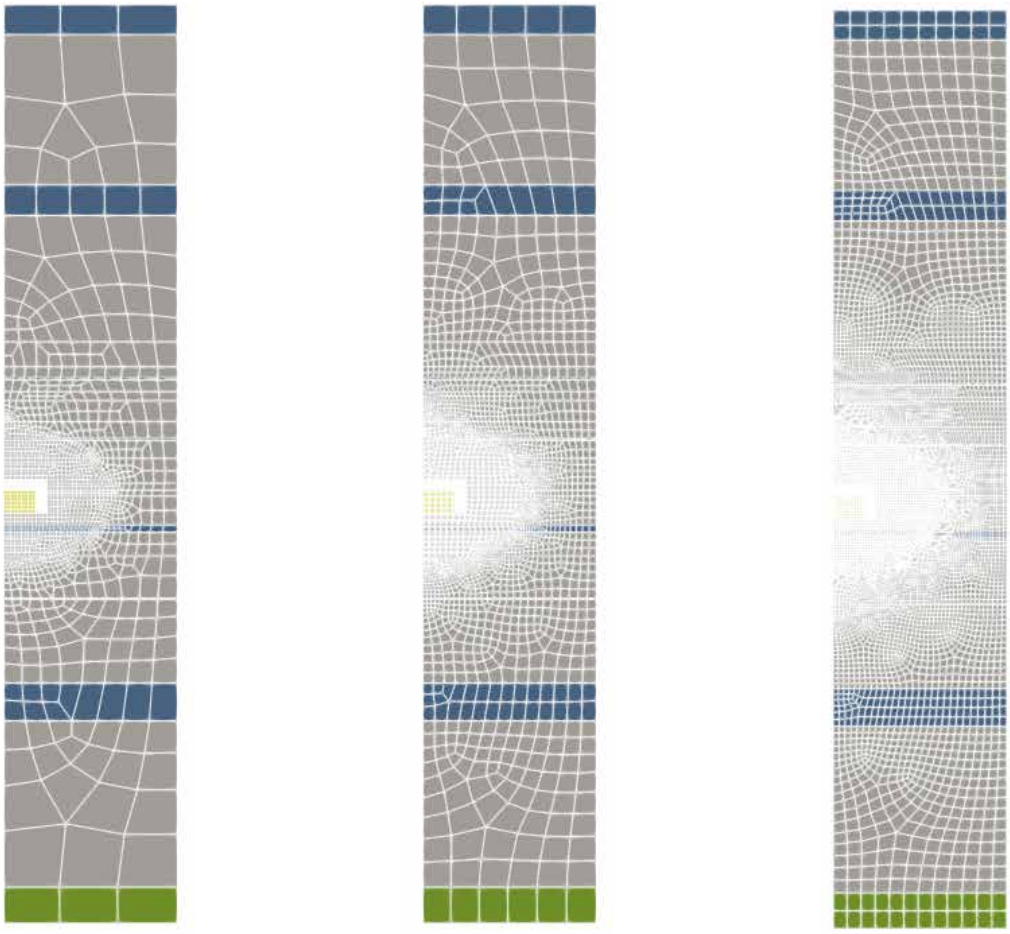
With this formulation, h_{ns} must be set to the value of h that would have been used without any viscoplastic scaling. Herein, $h_{\mathrm{ns}} = -55.0$, per Jensen et al. (2023, Table 3-1).

B.3. Mesh Convergence Study

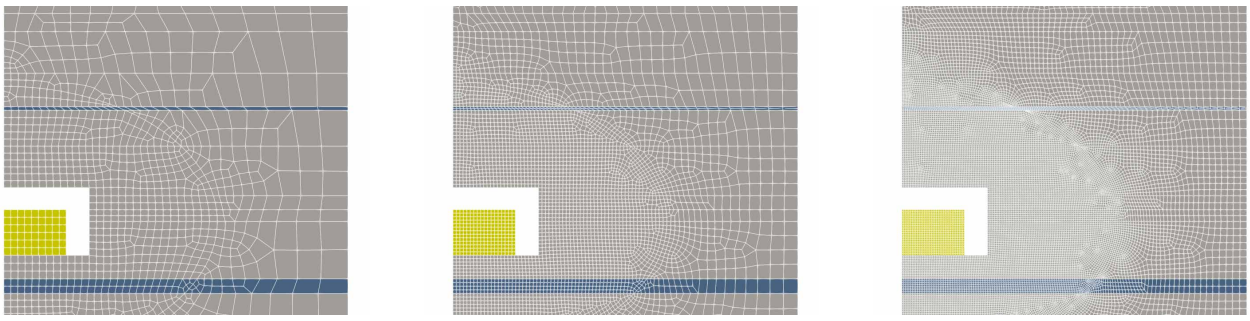
A mesh convergence study was performed to find the proper balance between accuracy and computational efficiency for the new model simulations. Fig. B-1a depicts a coarse mesh, base mesh, and fine mesh for a lower horizon disposal room filled with waste. Fig. B-1b depicts close up views near the disposal room for the same three respective meshes. The mesh properties are

Table B-2. Mesh properties and computational times

Mesh	Nodes	Elements	Processors	Run time (hrs)
Coarse	3,690	1,495	16	28
Base	12,510	5,576	16	58
Fine	47,296	22,304	32	180



(a) Full view



(b) Enlarged view of room

Figure B-1. Full and enlarged views of the coarse (left), base (center), and fine (right) meshes for a lower horizon disposal room.

tabulated in Table B-2. The porosity histories from simulations utilizing the coarse mesh, base mesh, and fine mesh are compared for three gas generation factors in Fig. B-2.

Between the fine mesh and the base mesh, the difference in porosities is less than 0.005 for all times outside 60-160 years. In the time period 60-160 years, the difference in porosities is a maximum of 0.021 for the zero gas generation case, $f = 0.0$, and decreases with increasing gas generation factor.

Between the fine and coarse meshes, the difference in porosities is less than 0.02 for all times outside 60-160 years. In the time period 60-160 years, the maximum difference in porosities is 0.074 for the zero gas generation case, $f = 0.0$.

Table B-2 also lists the computational run time for each of the three meshes. The base mesh solution requires under half the run time on half the processors as the fine mesh solution. Consequently, the base mesh is deemed a reasonable balance between accuracy and ease of computation, and it was used for for all simulations documented in Chapter 3, except the legacy simulations, the recreated legacy simulations, and the simulations presented in Section 3.4.3.

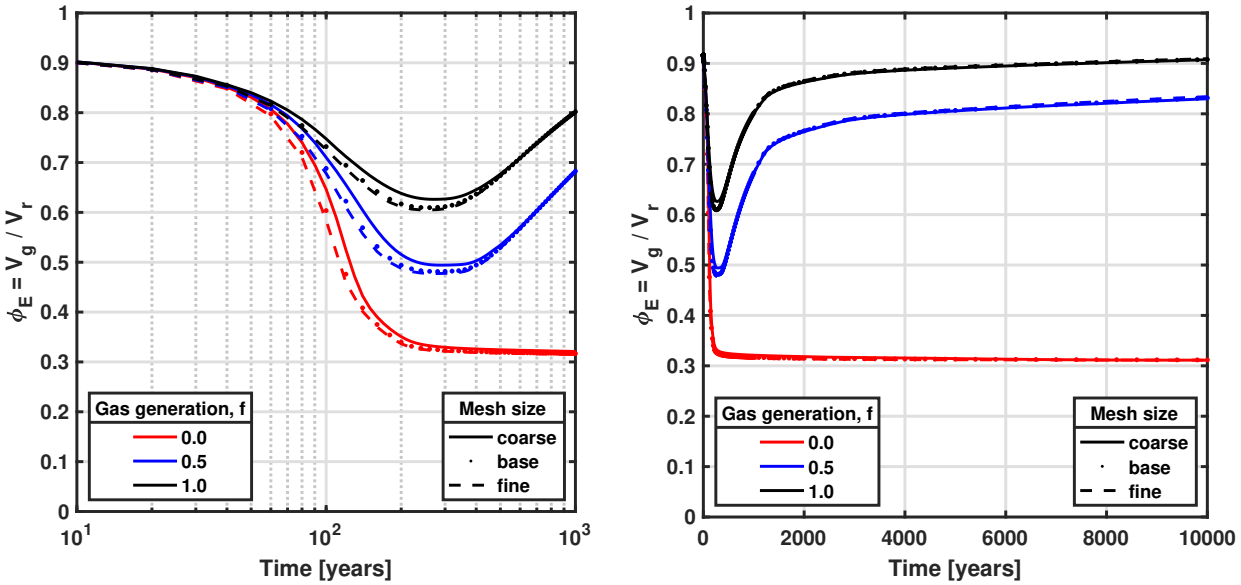


Figure B-2. Comparison of Eulerian porosity histories between coarse, base, and fine meshes for a lower horizon disposal room with various gas generation factors over 1,000 and 10,000 years.

B.4. Domain Size Study

A domain size convergence study was performed to ensure the top and bottom domain boundaries were far enough away from the disposal room as to have negligible impact on the room deformation. The horizontal domain width was held fixed at $D_x/2 = 20.27$ m to be consistent with the assumption of an infinite array of rooms spaced D_x apart, where each room is symmetric about the y-z plane (see discussion in Section 2.1.4). As shown in Fig. B-3, four domain heights

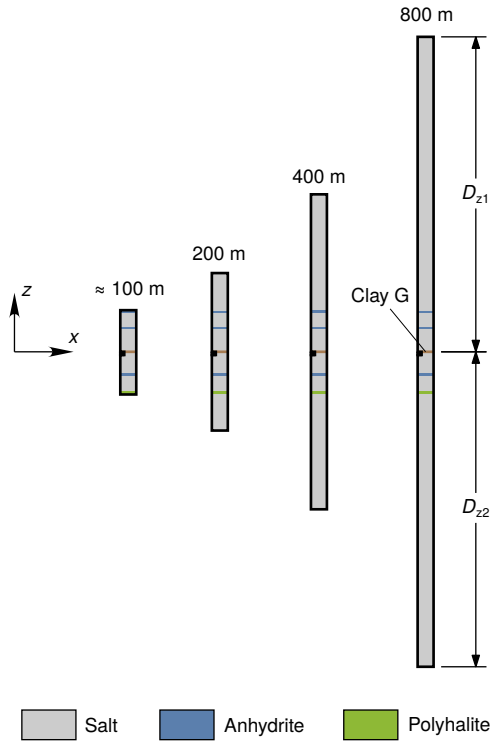
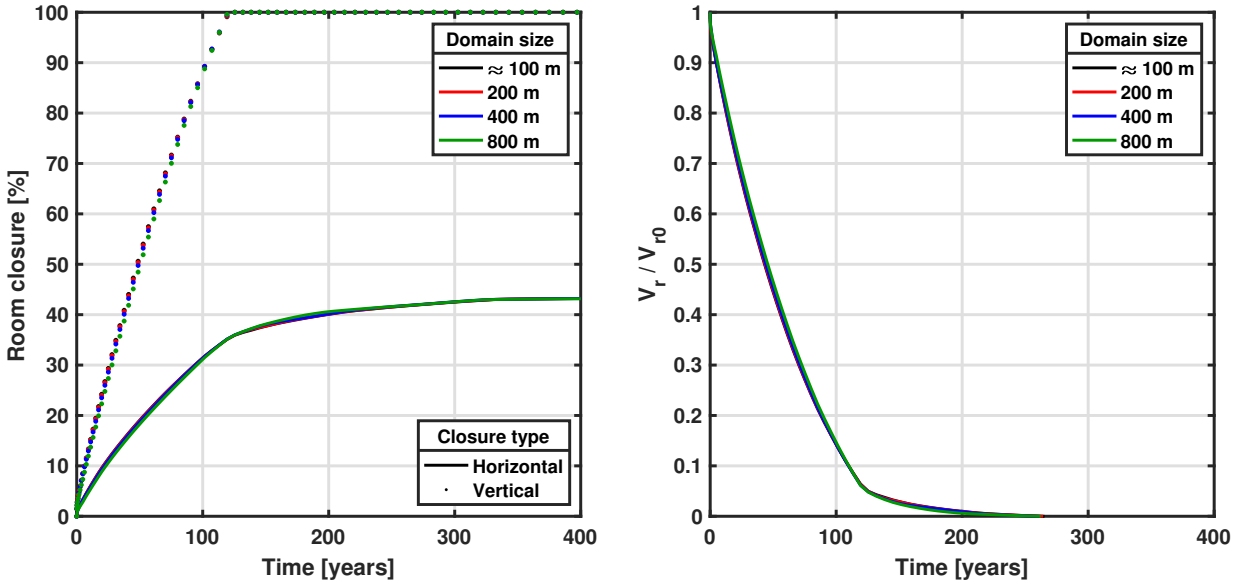


Figure B-3. Schematics of the four upper horizon domains considered.

were considered: ≈ 100 m, 200 m, 400 m, and 800 m. The ≈ 100 m domain size has slightly asymmetric distances from Clay Seam G (D_{z1} = 52.87 m and D_{z2} = 54.19 m), while the larger three domains sizes have symmetric distances from Clay Seam G (D_{z1} = D_{z2} =100 m, 200 m, and 400 m). The domains were discretized similar to the base mesh shown in Fig. B-1. Element size coarsening with respect to distance from the room was extended at the same rate for elements outside the $-54.19 \leq z \leq 52.87$ m range.

Fig. B-4 compares the room closure histories, both horizontal and vertical, as well as the room volume history for an upper horizon disposal room with no waste. The horizontal closure of the room is the horizontal displacement of the midpoint of the disposal room wall. The vertical closure of the room is the sum of the vertical displacement magnitudes of the roof and floor at the left plane of symmetry. Fig. B-4 shows negligible differences in the room deformation for the various domain sizes. The ≈ 100 m domain size is sufficiently large to prevent boundary effects so it was used for all other simulations in this report.



(a) Room Closure History

(b) Room Volume History

Figure B-4. Comparison of room closure histories and room volume histories between the ≈ 100 m domain size and larger domains for an upper horizon, empty disposal room.

APPENDIX C. Example Simulation Files

C.1. Mesh Generation Files

C.1.1. Recreated Legacy Model

C.1.1.1. Main Script

```
#! /bin/bash
module load seacas

#Generate 2D mesh using fastq

#Mesh generated is in X-Y plane
# input (text) file name = fastq_CMStone.i
# output (binary) file name = fastq_CMStone.g (exodus 2 format)

fastq -input fastq_CMStone_new.i -mesh fastq_CMStone.g -exodus 2

#Convert 2D (X-Y) mesh to 3D (X-Y-Z) mesh using gen3d.
#Plane strain model with 1 element in Z direction
# thickness = 1.0 is defined in gen3d.i
# input exodus file name = fastq_CMStone.g
# output exodus file name = gen3d_CMStone.g
# input commands file name = gen3d.i

gen3d fastq_CMStone.g gen3d_CMStone.g < gen3d.i > gen3d.o

#Use grepos to reorient the 3D mesh so that:
# X-axis is to right, Y-axis into page and Z axis is up
# input exodus file name = gen3d_CMStone.g
# ouput exodus file name = grepos_CMStone.g
# input commands file name = grepos.i

grepos gen3d_CMStone.g grepos_CMStone.g < grepos.i > grepos.o

#Run cubit to add boundary node sets, side sets and block names
#Use the journal file: disposal_room_CMStone_new.jou

/projects/cubit/cubit-15.4 disposal_room_CMStone_new.jou
```

C.1.1.2. fastq_CMStone_new.i

```
TITLE
 DISPOSAL ROOM MODEL FOR JAS3D- MULTIMATERIAL STRATIGRAPHY - SLIDELINES
POINT    1     0.00    -54.19
POINT    2    20.27    -54.19
POINT    3     0.00     -8.63
POINT    4    20.27     -8.63
POINT    5     0.00     -8.63
POINT    6    20.27     -8.63
POINT    7     0.00     -7.77
POINT    8    20.27     -7.77
```

```
POINT    9     0.00     -6.39
POINT   10     5.03     -6.39
POINT   11     0.00     -6.39
POINT   12     3.675    -6.39
POINT   13     0.00     -3.71
POINT   14     3.675    -3.71
POINT   15     5.03     -2.43
POINT   16     0.00     -2.43
POINT   17     0.00      0.00
POINT   18    20.27      0.00
POINT   19     0.00      4.27
POINT   20    20.27      4.27
POINT   21     0.00     52.87
POINT   22    20.27     52.87
POINT   23    20.27     -2.43
POINT   24    20.27     -6.39
POINT   25     5.03      0.00
POINT   26     5.03     -7.77
POINT   27     5.03      4.27
POINT   28     5.03     -8.63
POINT   29     0.0       2.10
POINT   30     5.03      2.10
POINT   31    20.27      2.10
POINT   32     0.0       2.31
POINT   33     5.03      2.31
POINT   34    20.27      2.31
LINE     1     STR    1    2    0    22   1.0
LINE     2     STR    1    5    0    20   0.85
LINE     3     STR    2    6    0    20   0.85
$LINE    4     STR    5    6    0    15
LINE     5     STR   28    6    0    15   1.1
LINE     6     STR    5    7    0     4
LINE     7     STR    6    8    0     4
LINE     8     STR    7    9    0     5
LINE     9     STR   26    8    0    15   1.1
LINE    10     STR   24    8    0     5
LINE    11     STR   10   24    0    15   1.1
LINE    12     STR    9   10    0     7   0.8
LINE    13     STR   11   12    0    10
LINE    14     STR   12   14    0     7
LINE    15     STR   13   14    0    10
LINE    16     STR   11   13    0     7
LINE    17     STR   10   15    0    12
LINE    18     STR   24   23    0    12
LINE    19     STR    8   18    0    12
LINE    20     STR   16   17    0     7
LINE    21     STR   16   15    0     7   0.8
LINE    22     STR   15   23    0    15   1.1
LINE    23     STR   18   23    0     7
LINE    24     STR   25   18    0    15   1.1
LINE    25     STR   17   19    0     8
LINE    26     STR   18   20    0     8
LINE    27     STR   27   20    0    15   1.1
$LINE   28     STR   25   20    0     8
LINE    29     STR   19   21    0    20   1.15
LINE    30     STR   20   22    0    20   1.15
LINE    31     STR   21   22    0    22   1.0
LINE    32     STR   17   25    0     7   0.8
LINE    33     STR   19   27    0     7   0.8
LINE    34     STR    7   26    0     7   0.8
LINE    35     STR    5   28    0     7   0.8
LINE    36     STR   17   29    0     4
LINE    37     STR   18   31    0     4
LINE    38     STR   29   30    0     7   0.8
LINE    39     STR   30   31    0    15   1.1
LINE    40     STR   29   32    0     1
LINE    41     STR   31   34    0     1
LINE    42     STR   32   33    0     7   0.8
```

```
LINE    43     STR   33   34    0    15   1.1
LINE    44     STR   32   19    0     4
LINE    45     STR   34   20    0     4
SIDE   100    11  12
SIDE   101    21  22
SIDE   102    32  24
SIDE   103    33  27
SIDE   104    35   5
SIDE   105    34   9
SIDE   106    38  39
SIDE   107    42  43
$ NODEBC CARDS
NODEBC   2    1
NODEBC   1    2    6    8   16   20   36   40   44   29
NODEBC   1    3    7   10   18   23   37   41   45   30
$ SIDEBC CARDS
SIDEBC  10   31
SIDEBC  20    1   $ adding on Sep 25 by B.Y.Park
SIDEBC 100   12
SIDEBC 200   17
SIDEBC 300   21
SIDEBC 400   13
SIDEBC 500   14
SIDEBC 600   15
SIDEBC 700   12   17   21
$ SIDEBC 800   13 14 15      $ ADDING ON OCT 29 BY B.Y.PARK
$ REGION CARDS
REGION   1    1   -1   -3  104   -2
REGION   2    2  104   -7  105   -6
REGION   3    5  105  -10  100   -8
REGION   4    6  -11  -18  -22  -17
REGION   5    7  101  -23  102  -20
REGION   6    3  102  -37  106  -36
REGION   7    1  103  -30  -31  -29
REGION   8    4  -13  -14  -15  -16
REGION   9    2  106  -41  107  -40
REGION  10    3  107  -45  103  -44
SCHEME   P
EXIT
}
```

C.1.1.3. gen3d.i

```
translate 1
end
```

C.1.1.4. disposal_room_CMStone_new.jou

```
#!python
#Cubit v15.0, and v15.3 (v15.1 and v15.2 don't always mesh the surfaces)
cubit.cmd('reset')
cubit.set_playback_paused_on_error(False)
error_old = cubit.get_error_count()
cubit.cmd('undo off')
import numpy as np
import math
import re

mesh_name = 'disposal_room_CMStone'
#Import mesh
cubit.cmd('import mesh geometry "grepos_CMStone.g" ')
#Remove sidesets, nodesets and give blocks useful names
```

```
cubit.cmd('delete sideset 10 20 100 200 300 400 500 600 700')
cubit.cmd('delete nodeset 1 2')
cubit.cmd('block 1 name "b_arg_halite"')
cubit.cmd('block 2 name "b_anhydrite"')
cubit.cmd('block 3 name "b_halite"')
cubit.cmd('block 4 name "b_homogenized_can_block"')
cubit.cmd('block 5 name "b_arg_halite_a"')
cubit.cmd('block 6 name "b_arg_halite_b"')
cubit.cmd('block 7 name "b_arg_halite_c"')

#Initialize dictionary to store geometry values
#(All dimensions are in meters.)
g = dict()

#Define whether to split each element into 4 elements
split_elements = False
#Define the clay seam slip definition
seam_slip_defn = 'all'
#Define whether to create blocks for the layer of elements on the room surface
room_surf_blocks = False
#Define whether to assume symmetry across the X=0 plane
x_sym = True
#Define how to determine thickness
thickness_determined_by = 'element_size'
#Define stratigraphy
strat_defn = 'SAND88_2948'

#Define the room dimensions as defined in SAND97-0795
#(elevations relative to clay seam G)
g['room_top_elev'] = -2.43
g['room_bot_elev'] = -6.39
g['room_width'] = 5.03 * 2.0
g['room_fillet_radius'] = 0.00001 #18.0 * 25.4 / 1000.0
#Define the coordinates of the center of the room
g['room_ctr'] = [0.0, (g['room_bot_elev'] + g['room_top_elev']) / 2.0]

#Define the total simulation dimensions as defined in SAND97-0795
#(elevations relative to the bottom of the bottom halite layer)
g['top_elev'] = 52.87
g['bot_elev'] = -54.19
g['width'] = 20.27 * 2.0
if thickness_determined_by == 'num_can_rows':
    can_dia = 24.0 * 25.4 / 1000.0
    seven_pack_depth = can_dia + can_dia * math.cos(math.pi/6) * 2.0
    num_can_rows = 0.01
    can_row_depth = seven_pack_depth * 1.5
    g['thickness'] = can_row_depth * num_can_rows * 1.1

#Define the fine element size in the X-Z plane
H_xz = g['room_width'] / 48.0
#Define the fine element size in the Y-direction
H_y = H_xz * 2.0
if thickness_determined_by == 'element_size':
    #g['thickness'] = H_xz
    g['thickness'] = 1.0

if not x_sym:
    #Mirror and merge
    cubit.cmd('volume all copy reflect x')
    cubit.cmd('merge all')

#Define some functions to help with meshing.
tol = 0.0001

#Identify interior room surfaces
roof_surf = cubit.parse_cubit_list('surface', \
    'with z_coord <= ' + str(g['room_top_elev'] + tol) \
    + ' and with z_coord >= ' + str(g['room_top_elev']-tol) \
```

```
    + ' and with y_coord > 0.0 ' \
    + ' and with y_coord < ' + str(g['thickness']) \
    + ' and with x_coord <= ' + str(g['room_width']/2.0 + tol) \
    + ' and with x_coord >= ' + str(-(g['room_width']/2.0 + tol)))
floor_surf = cubit.parse_cubit_list('surface', \
    'with z_coord <= ' + str(g['room_bot_elev'] + tol) \
    + ' and with z_coord >= ' + str(g['room_bot_elev']-tol) \
    + ' and with y_coord > 0.0 ' \
    + ' and with y_coord < ' + str(g['thickness']) \
    + ' and with x_coord <= ' + str(g['room_width']/2.0 + tol) \
    + ' and with x_coord >= ' + str(-(g['room_width']/2.0 + tol)))
right_wall_surf = cubit.parse_cubit_list('surface', \
    'with z_coord <= ' + str(g['room_top_elev'] + tol) \
    + ' and with z_coord >= ' + str(g['room_bot_elev'] - tol) \
    + ' and with y_coord > 0.0 ' \
    + ' and with y_coord < ' + str(g['thickness']) \
    + ' and with x_coord <= ' + str(g['room_width']/2.0 + tol) \
    + ' and with x_coord >= ' + str(g['room_width']/2.0 -
        g['room_fillet_radius']))
if not x_sym:
    left_wall_surf = cubit.parse_cubit_list('surface', \
        'with z_coord <= ' + str(g['room_top_elev'] + tol) \
        + ' and with z_coord >= ' + str(g['room_bot_elev'] - tol) \
        + ' and with y_coord > 0.0 ' \
        + ' and with y_coord < ' + str(g['thickness']) \
        + ' and with x_coord >= ' + str(-(g['room_width']/2.0 + tol)) \
        + ' and with x_coord <= ' + str(-(g['room_width']/2.0 -
            g['room_fillet_radius'])))
room_surf = []
room_surf.extend(roof_surf)
room_surf.extend(floor_surf)
if not x_sym:
    room_surf.extend(left_wall_surf)
room_surf.extend(right_wall_surf)
room_surf_str = str(room_surf)[1:-1]


#Create the nodesets and sidesets
#Plane strain surfaces
front_surf = cubit.parse_cubit_list('surface', 'with y_coord <= ' +
             str(0 + tol))
cubit.cmd('nodeset 1 surface ' + str(front_surf)[1:-1])
cubit.cmd('nodeset 1 name \'NS_front_surf\'')
back_surf = cubit.parse_cubit_list('surface', 'with y_coord >= ' +
            str(g['thickness']-tol))
cubit.cmd('nodeset 2 surface ' + str(back_surf)[1:-1])
cubit.cmd('nodeset 2 name \'NS_back_surf\'')
#Left and right surfaces
if not x_sym:
    left_surf_x = g['width']/2.0
else:
    left_surf_x = 0.0
left_surf = cubit.parse_cubit_list('surface', "with x_coord <= " +
            str(-(left_surf_x - tol)))
cubit.cmd('nodeset 3 surface ' + str(left_surf)[1:-1])
cubit.cmd('nodeset 3 name \'NS_left_surf\'')
cubit.cmd('sideset 3 surface ' + str(left_surf)[1:-1])
cubit.cmd('sideset 3 name \'SS_left_surf\'')
right_surf = cubit.parse_cubit_list('surface', 'with x_coord >= ' +
             str(g['width']/2.0 - tol))
cubit.cmd('nodeset 4 surface ' + str(right_surf)[1:-1])
cubit.cmd('nodeset 4 name \'NS_right_surf\'')
cubit.cmd('sideset 4 surface ' + str(right_surf)[1:-1])
cubit.cmd('sideset 4 name \'SS_right_surf\'')
#Top and bottom surfaces
bot_surf = cubit.parse_cubit_list('surface', 'with z_coord <= ' +
           str(g['bot_elev'] + tol))
cubit.cmd('nodeset 5 surface ' + str(bot_surf)[1:-1])
```

```
cubit.cmd('nodeset 5 name \'NS_bot_surf\'')
cubit.cmd('sideset 5 surface ' + str(bot_surf)[1:-1])
cubit.cmd('sideset 5 name \'SS_bot_surf\'')
top_surf = cubit.parse_cubit_list('surface', 'with z_coord >= ' +
           str(g['top_elev'] - tol))
cubit.cmd('nodeset 6 surface ' + str(top_surf)[1:-1])
cubit.cmd('nodeset 6 name \'NS_top_surf\'')
cubit.cmd('sideset 6 surface ' + str(top_surf)[1:-1])
cubit.cmd('sideset 6 name \'SS_top_surf\'')


#Interior room surface
cubit.cmd('sideset 7 surface 300 700 100')
cubit.cmd('sideset 7 name \'SS_room_surf\'')

#add sidesets for salt-salt contact as room creeps inward
cubit.cmd('sideset 8 surface ' + str(roof_surf)[1:-1])
cubit.cmd('sideset 8 name \'SS_roof_surf\'')

cubit.cmd('sideset 9 surface ' + str(right_wall_surf)[1:-1])
cubit.cmd('sideset 9 name \'SS_right_wall_surf\'')

#Need to do floor manually since the search also get surfaces on waste volume
cubit.cmd('sideset 10 surface 100')
cubit.cmd('sideset 10 name \'SS_floor_surf\'')

if not x_sym:
  cubit.cmd('sideset 11 surface ' + str(left_wall_surf)[1:-1])
  cubit.cmd('sideset 11 name \'SS_left_wall_surf\'')

#Room nodesets for history traces
roof_vertex = cubit.parse_cubit_list('vertex', \
    'with y_coord <= 0 \
    and with x_coord >= ' + str(0 - tol) \
    + ' and with x_coord <= ' + str(0 + tol) \
    + ' and with z_coord >= ' + str(g['room_top_elev'] - tol) \
    + ' and with z_coord <= ' + str(g['room_top_elev'] + tol))
cubit.cmd('nodeset 8 vertex ' + str(roof_vertex)[1:-1])
cubit.cmd('nodeset 8 name \'NS_roof_ctr\'')
floor_vertex = cubit.parse_cubit_list('vertex', \
    'with y_coord <= 0 \
    and with x_coord >= ' + str(0 - tol) \
    + ' and with x_coord <= ' + str(0 + tol) \
    + ' and with z_coord >= ' + str(g['room_bot_elev'] - tol) \
    + ' and with z_coord <= ' + str(g['room_bot_elev'] + tol))
cubit.cmd('nodeset 9 vertex ' + str(floor_vertex)[1:-1])
cubit.cmd('nodeset 9 name \'NS_floor_ctr\'')
right_wall_node = cubit.parse_cubit_list('node', \
    'with y_coord <= 0 \
    and with x_coord >= ' + str(g['room_width']/2.0 - tol) \
    + ' and with x_coord <= ' + str(g['room_width']/2.0 + tol) \
    + ' and with z_coord >= ' + str(g['room_ctr'][1] - tol) \
    + ' and with z_coord <= ' + str(g['room_ctr'][1] + tol))
cubit.cmd('nodeset 10 node ' + str(right_wall_node)[1:-1])
cubit.cmd('nodeset 10 name \'NS_right_wall_ctr\'')
if not x_sym:
    left_wall_node = cubit.parse_cubit_list('node', \
        'with y_coord <= 0 \
        and with x_coord >= ' + str(-(g['room_width']/2.0 + tol)) \
        + ' and with x_coord <= ' + str(-(g['room_width']/2.0 - tol)) \
        + ' and with z_coord >= ' + str(g['room_ctr'][1] - tol) \
        + ' and with z_coord <= ' + str(g['room_ctr'][1] + tol))
    cubit.cmd('nodeset 11 node ' + str(left_wall_node)[1:-1])
    cubit.cmd('nodeset 11 name \'NS_left_wall_ctr\'')

#Generate mesh entities on the waste block
cubit.cmd('nodeset 11 surface 47')
cubit.cmd('nodeset 11 name \'NS_homogenized_can_block_front_surf\'')
```

```
cubit.cmd('nodeset 12 surface 48')
cubit.cmd('nodeset 12 name \'NS_homogenized_can_block_back_surf\'')

cubit.cmd('nodeset 13 surface 46')
cubit.cmd('nodeset 13 name \'NS_homogenized_can_block_left_surf\'')

cubit.cmd('nodeset 14 surface 500')
cubit.cmd('nodeset 14 name \'NS_homogenized_can_block_right_surf\'')

cubit.cmd('nodeset 15 surface 400')
cubit.cmd('nodeset 15 name \'NS_homogenized_can_block_bot_surf\'')

cubit.cmd('nodeset 16 surface 600')
cubit.cmd('nodeset 16 name \'NS_homogenized_can_block_top_surf\'')

cubit.cmd('sideset 1 surface 600 500 400')
cubit.cmd('sideset 1 name \'SS_homogenized_can_block_exposed_surf\'')

#Export the Mesh
import os
pwd = os.getcwd()
if thickness_determined_by == 'num_can_rows':
    base_file_name = mesh_name + '-%d_cco_row_deep.g' %(num_can_rows)
elif thickness_determined_by == 'element_size':
    base_file_name = mesh_name + '-1_element_deep.g'
export_path = os.path.join(pwd, base_file_name )
print export_path
cubit.cmd('export genesis \'%s\' overwrite' % export_path)
if room_surf_blocks:
    export_path = os.path.join(pwd, base_file_name +
                  '-room_surf-%d_elements.g' %(g['room_width'] / H_xz))
    cubit.cmd("export genesis \'%s\' block 6 7 overwrite" % export_path)

#Save the geometry values
import cPickle
geom_path = os.path.join(pwd, base_file_name + '-geom_values.pkl')
geom_file = open(geom_path,'wb')
cPickle.dump(g, geom_file, protocol = 2)
geom_file.close()

#Print the pressures at the top and bottom surfaces
p1 = -15.97e6
p2 = -13.57e6
z1 = -54.19
z2 = 52.87
p = lambda z: (p2 - p1) / (z2 - z1) * (z - z1) + p1
print 'At z = ' + str(g['bot_elev']) + ' p = ' + str(p(g['bot_elev']))
print 'At z = ' + str(g['top_elev']) + ' p = ' + str(p(g['top_elev']))

#Print the error count
error_new = cubit.get_error_count()
print 'Cubit error count = %r' %(error_new - error_old)

exit
```

C.1.2. New Model

C.1.2.1. Reedlunn_2022-stratigraphy.csv

```
material, bot_elev_wrt_G, clay, name, comments
halite, -1000.0, none, none, this depth was made up and assumed to be all halite
polyhalite, -54.19, none, MB 141, none,
halite, -49.99, none, none, none
```

```
anhydrite, -30.60, A, MB 140, none
halite, -26.21, none, none, none
anhydrite, -16.41, B, anhydrite c, none
halite, -16.33, none, none, none
halite, -11.37, D, none, none
anhydrite, -8.63, E, MB 139, none
halite, -7.77, none, none, none
halite, -3.72, none, none, none
halite, -2.90, F, none, none
halite, 0.0, G, none, none
anhydrite, 2.10, H, anhydrite a, none
halite, 2.31, none, none, none
halite, 4.27, I, none, none
halite, 6.71, J, none, none
halite, 7.77, none, none, none
anhydrite, 9.16, K, MB 138, none
halite, 9.35, none, none, none
halite, 10.67, none, none, none
halite, 13.58, L, none, none
anhydrite, 28.3, M, MB 136, none
halite, 31.86, none, none, none
anhydrite, 49.38, none, MB 134, none
halite, 52.87, none, none, this was just assumed to be all halite
```

C.1.2.2. disposal_room.jou

```
#!python
#Cubit v15.9
cubit.cmd('reset')
#cubit.set_playback_paused_on_error(False)
cubit.set_playback_paused_on_error(True)
error_old = cubit.get_error_count()
cubit.cmd('undo off')
import numpy as np
import math
import re

# Define conversion factors
in_m = 0.0254

# Mesh uses smaller elements near the excavated disposal room (where equivalent stresses are the highest)
# Order of mesh refinement
# refinedMesh => split each base mesh element into 4 elements
# baseMesh     =  ~3.6* (number of coarseMesh elements)

# 1) Choose the level of refinement
refine_level    = 'baseMesh'      # ~24 elements across the room half-width
#refine_level = 'coarseMesh'   # ~12 elements across the room half-width
#refine_level = 'refinedMesh'  # ~48 elements across the room half-width

split_elements = False
if refine_level == 'refinedMesh':
  split_elements = True

mesh_name = 'disposal_room-' + refine_level

# 2) Choose whether to include homogeneous waste block
#empty_room = True
empty_room = False
if empty_room:
  mesh_name = mesh_name + '-noWasteBlock'
else:
  mesh_name = mesh_name + '-WasteBlock'

# 3) Choose room location: upper or lower horizon
```

```
#Define which horizon room is on
#horizon_defn = 'lower'
horizon_defn = 'upper'

# 4) Choose vertical extent of mesh for domain size study
#     define variable that will set the top and bottom mesh boundaries
# Example: the 100m case has a total vertical extent of 200m
# The 50m case is approximate (slightly larger than 100m vertical extent) and coincides with previous mesh
↪  models
domain_extent = '50m'
#domain_extent = '100m'
#domain_extent = '200m'
#domain_extent = '400m'

# 5) Define whether this is a plane strain mesh (1-element in y-direction)
# If not plane strain then this is a discrete drum case
plane_strain = True
#plane_strain = False

# 6) Define whether to assume symmetry across the X=0 plane
x_sym = True
#x_sym = False
if x_sym:
  mesh_name = mesh_name + '-Sym'
else:
  mesh_name = mesh_name + '-noSym'

#Initialize dictionary to store geometry values
#(All dimensions are in meters.)
g = dict()

# 7) Set some other variables for additional control
#Define whether to rapidly coarsen away from the room.
#(This is useful when you want to have failure around the room.)
rapidly_coarsen = False

#Define the clay seam slip definition
seam_slip_defn = 'all'
#Define whether to create blocks for the layer of elements on the room surface
room_surf_blocks = False

#Define stratigraphy
strat_defn = 'Reedlunn_2022'
#Define whether to have rounded room corners
rounded_corners = False

#Define the room dimensions as defined in SAND97-0795
#(elevations relative to clay seam G)
if horizon_defn == 'lower':
    #(Figure 3 in SAND97-0795 has the room top elevation as -1.96 m and the bottom as
    #-5.92 m, while Figure 4 has the room top elevation at -2.43 m and the bottom at -6.39 m.
    #This discrepancy is discussed in a March 4 memo from Charles Stone to B. Butcher, which
    #is in Appendix B-8 of SAND97-0796.  Apparently they decided to move the room elevation
    #because they felt it was most important to have the distance between marker band 139 and
    #the disposal room floor be 1.39 m.)
    g['room_top_elev'] = -2.43
    g['room_bot_elev'] = -6.39
elif horizon_defn == 'upper':
    #(Then in SAND2007-3334 they moved it again to avoid ground control issues.  The room top
    #elevation is 0.0, and the bottom is at -3.96 m.)
    g['room_top_elev'] = 0.0
    g['room_bot_elev'] = -3.96
g['room_width'] = 5.03 * 2.0
#(The cutting head radius used in room D was 18.0 * 25.4 / 1000.0.  I do not
#know if the disposal rooms used the same cutting head as Room D, but it seems like a
#safe bet.)
if rounded_corners:
    if horizon_defn == 'upper':
```

```
        g['room_fillet_radius'] = 18.0 * 25.4 / 1000.0
    elif horizon_defn == 'lower':
        #The lower horizon ends up with an awful element due to a short section with
        #a 0.0128 m length beneath the fillet radius.  To avoid this one can add 0.0128 to the fillet
        #radius.  Alternatively, can also use a sharp room radius to avoid element inversions at
        #the corner as the room surfaces come together.
        g['room_fillet_radius'] =18.0 * 25.4 / 1000.0 + 0.0128
    else:
        raise ValueError("ERROR: did not recognize horizon_defn")
else:
    g['room_fillet_radius'] = 0.0
#Define the coordinates of the center of the room
g['room_ctr'] = [0.0, (g['room_bot_elev'] + g['room_top_elev']) / 2.0]

#Define the total simulation dimensions as defined in SAND97-0795
#(elevations relative to the bottom of the bottom halite layer)
if domain_extent == '50m':
  g['top_elev'] =  52.87
  g['bot_elev'] = -54.19
elif domain_extent == '100m':
  g['top_elev'] =  100
  g['bot_elev'] = -100
elif domain_extent == '200m':
  g['top_elev'] =  200
  g['bot_elev'] = -200
elif domain_extent == '400m':
  g['top_elev'] =  400
  g['bot_elev'] = -400
else:
    raise IOError("Error: did not recognize 'domain_extent' variable")

g['width'] = 20.27 * 2.0

#Define the fine element size in the X-Z plane
nx = 48
if refine_level =='coarseMesh':
  nx = 24

H_xz = g['room_width'] / nx
H_xz_o = H_xz # Save for use in waste block meshing if needed

if plane_strain:
    #The thickness is somewhat arbitrary for plane strain simulations, but
    #it does impact Sierra's relative residual, since a thicker domain creates
    #a bigger reaction force, so we make sure to use a fixed  value.
    g['thickness'] = 1.0   # 5.5 / 48
    #Define the fine element size in the Y-direction (1-element thick)
    H_y = g['thickness']
else:
   # This case is for treating 4 rows of discrete drums
   #Define the center-to-center distance between 55 gal drums
   gap = 5.0 / 1000.0
   cco_g = {}
   d_t = 1.50 / 1000
   cco_g['D'] = (22.50 * in_m) + 2.0*d_t
   R = cco_g['D'] + gap
   # 4 rows of drums (y-direction)
   nrows    = 4
   #width of drum array (y-direction)
   g['thickness'] = (nrows - 1)*R*math.sin(math.pi/3.0) + cco_g['D']
   #Define the fine element size in the Y-direction
   H_y = H_xz * 1.0

if rapidly_coarsen:
    #Define the radius of the fine region
    R_fine = [g['room_width'] * 0.80, (g['room_top_elev'] - g['room_bot_elev']) * 2.0]
    #Define the coarsening rate
    coarsen_rate = 0.5
```

```
else:
    #Define the radius of the fine region
    R_fine = [g['room_width'] * 1.25, (g['room_top_elev'] - g['room_bot_elev']) * 2]
    #Define the coarsening rate
    coarsen_rate = 0.36

#Define any problem surfaces that need to be meshed first
prob_surfs = []

#Define stratigraphy
raw = np.genfromtxt(strat_defn + '-stratigraphy.csv', delimiter = ', ', names = True, dtype = None,
↪  encoding=None)
layers = dict(material = raw['material'], bot_elev_wrt_G = raw['bot_elev_wrt_G'], clay = raw['clay'])
#Make sure we have 1-d arrays even if there is only one layer.
for key in layers.keys():
    layers[key] = np.atleast_1d(layers[key])
layers['bot_elev_wrt_G'][0] = g['bot_elev']

if seam_slip_defn == 'SAND88_2948':
    #In SAND2012-7525 and SAND88-2948 the clay seams are labeled A through M, yet they
    #only make D through L (the nine nearest the room) active.  Thus, we turn off the
    #clay seams at -30.60 m, -16.41 m, 28.30 m.
    no_clay_names = ['A', 'B', 'M']
    for no_clay_name in no_clay_names:
        ndx = np.where(layers['clay'] == no_clay_name)[0][0]
        layers['clay'][ndx] = 'none'
elif seam_slip_defn == 'all':
    print("All clay seams active")
elif seam_slip_defn == 'none':
    #Switch all clay seams to non-slipping interfaces, if desired.
    layers['clay'][:] = 'none'
else:
    raise IOError('ERROR: did not recognize clay seam slip definition')

#Calculate the top elevation values
layers['top_elev_wrt_G'] = np.hstack([layers['bot_elev_wrt_G'][1:], g['top_elev']])
layers['thickness'] = layers['top_elev_wrt_G'] - layers['bot_elev_wrt_G']

#Generate the block
cubit.cmd('rotate -90 about X')
cubit.cmd('brick x %r y %r z %r' %(g['width']/2.0, g['thickness'], g['top_elev'] - g['bot_elev']))
cubit.cmd('move volume 1 x %r y %r z %r' \
    %(g['width']/4.0, g['thickness'] / 2.0, (g['top_elev'] - g['bot_elev'])/2.0 + g['bot_elev']))

#Cut out the room
cubit.cmd('create curve location 0 0 %r location %r 0 %r' \
    %(g['room_top_elev'], g['room_width']/2.0 - g['room_fillet_radius'], g['room_top_elev']))
cubit.cmd('create curve location %r 0 %r location %r 0 %r' \
    %(g['room_width']/2.0, g['room_top_elev'] - g['room_fillet_radius'], g['room_width']/2.0, \
    g['room_bot_elev'] + g['room_fillet_radius']))
cubit.cmd('create curve location %r 0 %r location 0 0 %r' \
    %(g['room_width']/2.0 - g['room_fillet_radius'], g['room_bot_elev'], g['room_bot_elev']))
cubit.cmd('create curve location 0 0 %r location 0 0 %r' %(g['room_bot_elev'], g['room_top_elev']))
if rounded_corners:
    cubit.cmd('create curve arc vertex 11 10 radius %r normal 0 -1 0' %(g['room_fillet_radius']))
    cubit.cmd('create curve arc vertex 13 12 radius %r normal 0 -1 0' %(g['room_fillet_radius']))
    cubit.cmd('create surface curve 13 14 15 16 17 18')
else:
    cubit.cmd('create surface curve 13 14 15 16')
cubit.cmd('sweep surface 7 direction 0 1 0 distance %r' %(g['thickness']))
cubit.cmd('chop volume 1 with volume 2')
cubit.cmd('delete volume 3')

#Slice the block at the layers
for bot, clay in zip(layers['bot_elev_wrt_G'], layers['clay']):
    if bot >= g['bot_elev'] and bot < g['top_elev']:
        if clay == 'none':
            cubit.cmd('webcut volume all with plane zplane offset %r imprint merge' %(bot))
```

```
        else:
            cubit.cmd('webcut volume all with plane zplane offset %r noimprint nomerge' %(bot))
print('For some reason I need a print here or else the layers are not created.')

#Add a slice at the mid height of the room, so that it is easy to extract variables along
#a line.
cubit.cmd('webcut volume all with plane zplane offset %r imprint merge' \
    %((g['room_top_elev'] + g['room_bot_elev'])/2.0))
cubit.cmd('webcut volume all with plane xplane offset 0.0 imprint merge')

#Cut volumes around room to assist with meshing
cubit.cmd('create surface ellipse major radius %r minor radius %r yplane' %(R_fine[0], R_fine[1]))
surface_list = cubit.parse_cubit_list('surface', 'with x_coord == 0 and y_coord == 0 and z_coord == 0')
ellipse_ID = surface_list[0]
cubit.cmd('move Surface ' + str(ellipse_ID) + ' location %r 0 %r include_merged' %(g['room_ctr'][0],
↪  g['room_ctr'][1]))
cubit.cmd('webcut volume all sweep surface ' + str(ellipse_ID) + ' perpendicular distance %r outward'
↪  %(g['thickness']))
cubit.cmd('delete surface ' + str(ellipse_ID))

#Imprint and merge the layers (we will add the clay seams later)
cubit.cmd('imprint all')
cubit.cmd('merge all')

#Group each layer's volumes together
layers['volumes'] = []
for bot, top in zip(layers['bot_elev_wrt_G'], layers['top_elev_wrt_G']):
    layers['volumes'].append(\
        cubit.parse_cubit_list('volume', \
        "with z_coord >= " + str(bot) + " and with z_coord <= " + str(top)))

#Specify the mesh

#Define some functions to help with meshing.
tol = 0.0001
def _curve_vertex_coordinates(curve_ID, ctr):
    #Order vertices based on their distance from the room
    vertex_IDs = cubit.get_relatives('curve', curve_ID, 'vertex')
    vertex_dist = []
    for vertex_ID in vertex_IDs:
        vertex = cubit.vertex(vertex_ID)
        vertex_dist.append(math.sqrt((vertex.coordinates()[0]-ctr[0])**2.0 \
            + (vertex.coordinates()[2]-ctr[1])**2.0))
    vertex_IDs = [vertex_IDs[vertex_dist.index(min(vertex_dist))], \
        vertex_IDs[vertex_dist.index(max(vertex_dist))]]
    #Get the vertex coordinates
    vertex_pos = []
    for vertex_ID in vertex_IDs:
        vertex = cubit.vertex(vertex_ID)
        vertex_pos.append(vertex.coordinates())
    return(vertex_IDs, vertex_pos)

def set_size_based_on_dist(curve_IDs, H_0, ctr, coarsen_rate, R_fine):
    for curve_ID in curve_IDs:
        [vertex_IDs, vertex_pos] = _curve_vertex_coordinates(curve_ID, ctr)
        [H_1, H_2] = _calc_size_based_on_dist(H_0, ctr, coarsen_rate, vertex_pos, R_fine)
        cubit.cmd('curve ' + str(curve_ID) + ' scheme bias fine size ' + str(H_1) \
            + ' coarse size ' + str(H_2) + ' start vertex ' + str(vertex_IDs[0]))
        cubit.cmd('curve ' + str(curve_ID) + ' interval soft')

def _calc_dists(ctr, R_fine, pt):
    #Find distance from point to the center
    ctr_2_pt_dist = math.sqrt((pt[0] - ctr[0])**2.0 + (pt[1] - ctr[1])**2.0)
    #Find angle of vertex to center of the fine region
    psi = math.atan2(pt[1] - ctr[0], pt[0] - ctr[1])
    #Find closest point on edge of fine region
    fine_pt = [ctr[0] + R_fine[0] * math.cos(psi), ctr[1] + R_fine[1] * math.sin(psi)]
    #Find the distance from center to fine point
```

```
    ctr_2_fine_pt_dist = math.sqrt((fine_pt[0] - ctr[0])**2.0 + (fine_pt[1] - ctr[1])**2.0)
    return(ctr_2_pt_dist, ctr_2_fine_pt_dist)

def  _calc_size_based_on_dist(H_0, ctr, coarsen_rate, vertex_pos, R_fine):
    #Set to H_0 inside R_fine, otherwise, calculate the element sizes based on
    #radial distance from the fine region
    [ctr_2_pt_dist, ctr_2_fine_pt_dist] = _calc_dists(ctr, R_fine, [vertex_pos[0][0], vertex_pos[0][2]])
    if ctr_2_pt_dist < ctr_2_fine_pt_dist:
        H_1 = H_0
    else:
        H_1 = H_0 * (1.0 + (ctr_2_pt_dist-ctr_2_fine_pt_dist) * coarsen_rate)
    [ctr_2_pt_dist, ctr_2_fine_pt_dist]  = _calc_dists(ctr, R_fine, [vertex_pos[1][0], vertex_pos[1][2]])
    if ctr_2_pt_dist < ctr_2_fine_pt_dist:
        H_2 = H_0
    else:
        H_2 = H_0 * (1.0 + (ctr_2_pt_dist-ctr_2_fine_pt_dist) * coarsen_rate)
    return(H_1, H_2)


#Specify the mesh sizes on the front surfaces

#Specify the problematic surfaces first
prob_surfs = []
if len(prob_surfs) > 0:
    prob_surfs_str = str(prob_surfs)[1:-1]
    prob_curves = cubit.parse_cubit_list('curve', 'with y_coord <= ' + str(tol) + ' in surface ' +
    ↪  prob_surfs_str)
    set_size_based_on_dist(prob_curves, H_xz, g['room_ctr'], coarsen_rate, R_fine)
else:
    prob_curves = []

#Carefully specify the mesh on the thin layers
thin_layer_front_surfs = []
for (thickness, top_elev, bot_elev, vol_ids) in zip(layers['thickness'], layers['top_elev_wrt_G'],
↪  layers['bot_elev_wrt_G'], layers['volumes']):
    if thickness < 0.5 and len(vol_ids) > 0:
        #Get the front surfaces of the thin layer
        thin_layer_vol_str = str(vol_ids)[1:-1]
        thin_layer_front_surf = cubit.parse_cubit_list('surface', 'with y_coord <= ' + str(tol) + ' in volume '
        ↪  + thin_layer_vol_str)
        thin_layer_front_surfs.extend(thin_layer_front_surf)
        thin_layer_front_surf_str = str(thin_layer_front_surf)[1:-1]
        #Specify the element sizes at the layer top
        thin_layer_front_top_curves = cubit.parse_cubit_list('curve', 'with y_coord <= ' + str(tol) + ' and
        ↪  with z_coord >= ' + str(top_elev - tol) + ' in surface ' + thin_layer_front_surf_str)
        set_size_based_on_dist(thin_layer_front_top_curves, H_xz, g['room_ctr'], coarsen_rate, R_fine)
        #Cubit struggles to mesh a one element thick layer if the top and bottom have different element sizes,
        #so set the element sizes at the layer bottom to be the same as the top.
        thin_layer_front_bot_curves = cubit.parse_cubit_list('curve', 'with y_coord <= ' + str(tol) + ' and
        ↪  with z_coord <= ' + str(bot_elev + tol) + ' in surface ' + thin_layer_front_surf_str)
        fake_room_ctr = [0, g['room_ctr'][1] - thickness]
        set_size_based_on_dist(thin_layer_front_bot_curves, H_xz, fake_room_ctr, coarsen_rate, R_fine)
        #Set element sizes on the left and right sides of layer
        thin_layer_front_curves =   cubit.parse_cubit_list('curve', ' in surface ' + thin_layer_front_surf_str)
        thin_layer_left_right_front_curves = list(set(thin_layer_front_curves) -
        ↪  set(thin_layer_front_top_curves) - set(thin_layer_front_bot_curves))
        set_size_based_on_dist(thin_layer_left_right_front_curves, H_xz, g['room_ctr'], coarsen_rate, R_fine)
thin_layer_front_surfs_str = str(thin_layer_front_surfs)[1:-1]
#Paving thin layers doesn't always work very well, so we map them
cubit.cmd('surface ' + thin_layer_front_surfs_str + ' scheme map')
cubit.cmd('surface ' + thin_layer_front_surfs_str + ' sizing function linear neighbor')
thin_layer_front_curves = []
if len(thin_layer_front_surfs):
    thin_layer_front_curves =  cubit.parse_cubit_list('curve', 'with y_coord <= ' + str(tol) + ' in surface ' +
    ↪  thin_layer_front_surfs_str)

#Specify the mesh on the rest of the front surfaces
all_front_curves = cubit.parse_cubit_list('curve', 'with y_coord <= ' + str(tol))
```

```
thick_layer_front_curves = list(set(all_front_curves) - set(thin_layer_front_curves) - set(prob_curves))
set_size_based_on_dist(thick_layer_front_curves, H_xz, g['room_ctr'], coarsen_rate, R_fine)
all_front_surfs = cubit.parse_cubit_list('surface', 'with y_coord <= ' + str(tol))
thick_layer_front_surfs = list(set(all_front_surfs) - set(thin_layer_front_surfs) - set(prob_surfs))
thick_layer_front_surfs_str = str(thick_layer_front_surfs)[1:-1]
cubit.cmd('surface ' + thick_layer_front_surfs_str + ' scheme pave')
cubit.cmd('surface ' + thick_layer_front_surfs_str + ' sizing function linear neighbor')

#Mesh the front surfaces
if len(prob_surfs) + len(thin_layer_front_surfs) > 0:
    first_surfs = []
    first_surfs.extend(thin_layer_front_surfs)
    first_surfs.extend(prob_surfs)
    first_surfs = list(set(first_surfs))
    first_surfs_str = str(first_surfs)[1:-1]
    cubit.cmd('mesh surface ' + first_surfs_str)
#Mesh the rest of the front surfaces
cubit.cmd('mesh surface ' + thick_layer_front_surfs_str)

#Perform a uniform refinement if requested
if split_elements:
    front_surf = cubit.parse_cubit_list('surface', 'with y_coord <= 0')
    cubit.cmd('volume all scale x 1 y 0.5 z 1')
    g['thickness'] = g['thickness'] * 0.5
    cubit.cmd('refine surface ' + str(front_surf)[1:-1] + ' numsplit 1')

#Sweep the mesh through the thickness
cubit.cmd('volume all scheme sweep vector 0 1 0')
#Set 'redistribute nodes on' so to preserve the bias during the sweep. (This does the
#same thing as the 'propagate bias' parameter in the sweep-source-target command)
cubit.cmd('volume all redistribute nodes on')

#Mesh thru the thickness
cubit.cmd('volume all size %r' %(H_y))
cubit.cmd('mesh volume all')

if not x_sym:
    #Mirror and merge
    cubit.cmd('volume all copy reflect x')
    cubit.cmd('merge all')

#Group each layer's volumes together
layers['volumes'] = []
for bot, top in zip(layers['bot_elev_wrt_G'], layers['top_elev_wrt_G']):
    layers['volumes'].append(\
        cubit.parse_cubit_list('volume', \
        "with z_coord >= " + str(bot) + " and with z_coord <= " + str(top)))

#Find which volumes pertain to which materials
material_names = []
vol_IDs = []
material_dict = dict()
for matl, vols in zip(layers['material'], layers['volumes']):
    match = re.match(r'(\w+)', matl)
    material_names.append(match.group(1))
    vol_IDs.append(vols)
#Initialize the dictionary with just the unique materials
unique_material_names = set(material_names)
for unique_material_name in unique_material_names:
    material_dict[unique_material_name] = []
#Populate the dictionary
for material_name, vol_list in zip(material_names, vol_IDs):
    material_dict[material_name].extend(vol_list)

#Identify interior room surfaces
roof_surf = cubit.parse_cubit_list('surface', \
    'with z_coord <= ' + str(g['room_top_elev'] + tol) \
    + ' and with z_coord >= ' + str(g['room_top_elev']-tol) \
```

```
    + ' and with y_coord > 0.0 ' \
    + ' and with y_coord < ' + str(g['thickness']) \
    + ' and with x_coord <= ' + str(g['room_width']/2.0 + tol) \
    + ' and with x_coord >= ' + str(-(g['room_width']/2.0 + tol)))
floor_surf = cubit.parse_cubit_list('surface', \
    'with z_coord <= ' + str(g['room_bot_elev'] + tol) \
    + ' and with z_coord >= ' + str(g['room_bot_elev']-tol) \
    + ' and with y_coord > 0.0 ' \
    + ' and with y_coord < ' + str(g['thickness']) \
    + ' and with x_coord <= ' + str(g['room_width']/2.0 + tol) \
    + ' and with x_coord >= ' + str(-(g['room_width']/2.0 + tol)))
right_wall_surf = cubit.parse_cubit_list('surface', \
    'with z_coord <= ' + str(g['room_top_elev'] + tol) \
    + ' and with z_coord >= ' + str(g['room_bot_elev'] - tol) \
    + ' and with y_coord > 0.0 ' \
    + ' and with y_coord < ' + str(g['thickness']) \
    + ' and with x_coord <= ' + str(g['room_width']/2.0 + tol) \
    + ' and with x_coord >= ' + str(g['room_width']/2.0 - g['room_fillet_radius']))
if not x_sym:
    left_wall_surf = cubit.parse_cubit_list('surface', \
        'with z_coord <= ' + str(g['room_top_elev'] + tol) \
        + ' and with z_coord >= ' + str(g['room_bot_elev'] - tol) \
        + ' and with y_coord > 0.0 ' \
        + ' and with y_coord < ' + str(g['thickness']) \
        + ' and with x_coord >= ' + str(-(g['room_width']/2.0 + tol)) \
        + ' and with x_coord <= ' + str(-(g['room_width']/2.0 - g['room_fillet_radius'])))
room_surf = []
room_surf.extend(roof_surf)
room_surf.extend(floor_surf)
if not x_sym:
    room_surf.extend(left_wall_surf)
room_surf.extend(right_wall_surf)
room_surf_str = str(room_surf)[1:-1]

#Only add in the slip lines after the rest of the mesh has been generated
#This way, the mesh will be identical, regardless of whether you have the slip lines
#on or off.
i = 1000
j = 0
for clay, bot, vols in zip(layers['clay'], layers['bot_elev_wrt_G'], layers['volumes']):
    if clay != 'none':
        merged_surfaces = cubit.parse_cubit_list('surface', \
            'with z_coord >= ' + str(bot-tol) \
            + ' and with z_coord <= ' + str(bot+tol))
        cubit.cmd('unmerge surface ' + str(merged_surfaces)[1:-1])
        #(Note: you cannot assume that the previously merged surfaces all
        #remain on the top or the bottom of the clay seam.  Cubit can randomly
        #chose which surfaces remain on the top and which are on the bottom.
        #Instead we explicitly specify that the master surfaces must be in the
        #volumes above the clay seam.)
        master_surfaces = cubit.parse_cubit_list('surface', \
            'in volume ' + str(vols)[1:-1] \
            + ' with z_coord >= ' + str(bot - tol) \
            + ' and with z_coord <= ' + str(bot + tol))
        #Get the slave surfaces by subtracting the master surfaces from all the
        #surfaces at the clay seam
        surfaces = cubit.parse_cubit_list('surface', \
            'with z_coord >= ' + str(bot - tol) \
            + ' and with z_coord <= ' + str(bot + tol))
        slave_surfaces = list(set(surfaces) - set(master_surfaces))
        #Make sure the clay seam surfaces do not include either the room floor or ceiling
        master_surfaces = list(set(master_surfaces) - set(room_surf))
        slave_surfaces = list(set(slave_surfaces) - set(room_surf))
        #Define the sidesets
        j = j + 1
        i = i + 1
        cubit.cmd('sideset ' + str(i) + ' surface ' + str(master_surfaces)[1:-1])
        cubit.cmd('sideset ' + str(i) + ' name ' \
```

```
            + '\'SS_clay_' + clay + '_master\'')
        i = i + 1
        cubit.cmd('sideset ' + str(i) + ' surface ' + str(slave_surfaces)[1:-1])
        cubit.cmd('sideset ' + str(i) + ' name ' \
            + '\'SS_clay_' +  clay + '_slave\'')
        #Print the results for troubleshooting purposes
        print("Slipping clay seam " + clay + " created at elevation = " + str(bot) + " m.")
        print("Master surfaces = " + str(master_surfaces)[1:-1])
        print("Slave surfaces = " + str(slave_surfaces)[1:-1])


i = 1
if room_surf_blocks:
    for key in material_dict.keys():
        i = i + 1
        cubit.cmd('Block ' + str(i) + 'hex in volume ' + str(material_dict[key])[1:-1] + ' except hex in edge
        ↪  in surface ' + room_surf_str)
        cubit.cmd('Block ' + str(i) + ' name \'B_' + key + '\'')
    for key in material_dict.keys():
        i = i + 1
        cubit.cmd('Block ' + str(i) + 'hex in volume ' + str(material_dict[key])[1:-1] + ' in edge in surface '
        ↪  + room_surf_str)
        cubit.cmd('Block ' + str(i) + ' name \'B_' + key + '_room_surf\'')
else:
    for key in material_dict.keys():
        i = i + 1
        cubit.cmd('Block ' + str(i) + ' volume ' + str(material_dict[key])[1:-1])
        cubit.cmd('Block ' + str(i) + ' name \'B_' + key + '\'')

#Create the nodesets and sidesets on the geologic mesh
#Plane strain surfaces
front_surf = cubit.parse_cubit_list('surface', 'with y_coord <= 0')
cubit.cmd('nodeset 1 surface ' + str(front_surf)[1:-1])
cubit.cmd('nodeset 1 name \'NS_front_surf\'')
back_surf = cubit.parse_cubit_list('surface', 'with y_coord >= ' + str(g['thickness']-tol))
cubit.cmd('nodeset 2 surface ' + str(back_surf)[1:-1])
cubit.cmd('nodeset 2 name \'NS_back_surf\'')
#Left and right surfaces
if not x_sym:
    left_surf_x = g['width']/2.0
else:
    left_surf_x = 0.0
left_surf = cubit.parse_cubit_list('surface', "with x_coord <= " + str(-(left_surf_x - tol)))
cubit.cmd('nodeset 3 surface ' + str(left_surf)[1:-1])
cubit.cmd('nodeset 3 name \'NS_left_surf\'')
cubit.cmd('sideset 3 surface ' + str(left_surf)[1:-1])
cubit.cmd('sideset 3 name \'SS_left_surf\'')
right_surf = cubit.parse_cubit_list('surface', 'with x_coord >= ' + str(g['width']/2.0 - tol))
cubit.cmd('nodeset 4 surface ' + str(right_surf)[1:-1])
cubit.cmd('nodeset 4 name \'NS_right_surf\'')
cubit.cmd('sideset 4 surface ' + str(right_surf)[1:-1])
cubit.cmd('sideset 4 name \'SS_right_surf\'')
#Top and bottom surfaces
bot_surf = cubit.parse_cubit_list('surface', 'with z_coord <= ' + str(g['bot_elev'] + tol))
cubit.cmd('nodeset 5 surface ' + str(bot_surf)[1:-1])
cubit.cmd('nodeset 5 name \'NS_bot_surf\'')
cubit.cmd('sideset 5 surface ' + str(bot_surf)[1:-1])
cubit.cmd('sideset 5 name \'SS_bot_surf\'')
top_surf = cubit.parse_cubit_list('surface', 'with z_coord >= ' + str(g['top_elev'] - tol))
cubit.cmd('nodeset 6 surface ' + str(top_surf)[1:-1])
cubit.cmd('nodeset 6 name \'NS_top_surf\'')
cubit.cmd('sideset 6 surface ' + str(top_surf)[1:-1])
cubit.cmd('sideset 6 name \'SS_top_surf\'')
#Interior room surface
cubit.cmd('sideset 7 surface ' + room_surf_str)
cubit.cmd('sideset 7 name \'SS_room_surf\'')

#Room nodesets for history traces
```

```
roof_vertex = cubit.parse_cubit_list('vertex', \
    'with y_coord <= 0 \
    and with x_coord >= ' + str(0 - tol) \
    + ' and with x_coord <= ' + str(0 + tol) \
    + ' and with z_coord >= ' + str(g['room_top_elev'] - tol) \
    + ' and with z_coord <= ' + str(g['room_top_elev'] + tol))
cubit.cmd('nodeset 8 vertex ' + str(roof_vertex)[1:-1])
cubit.cmd('nodeset 8 name \'NS_roof_ctr\'')
floor_vertex = cubit.parse_cubit_list('vertex', \
    'with y_coord <= 0 \
    and with x_coord >= ' + str(0 - tol) \
    + ' and with x_coord <= ' + str(0 + tol) \
    + ' and with z_coord >= ' + str(g['room_bot_elev'] - tol) \
    + ' and with z_coord <= ' + str(g['room_bot_elev'] + tol))
cubit.cmd('nodeset 9 vertex ' + str(floor_vertex)[1:-1])
cubit.cmd('nodeset 9 name \'NS_floor_ctr\'')
right_wall_vertex = cubit.parse_cubit_list('vertex', \
    'with y_coord <= 0 \
    and with x_coord >= ' + str(g['room_width']/2.0 - tol) \
    + ' and with x_coord <= ' + str(g['room_width']/2.0 + tol) \
    + ' and with z_coord >= ' + str(g['room_ctr'][1] - tol) \
    + ' and with z_coord <= ' + str(g['room_ctr'][1] + tol))
cubit.cmd('nodeset 10 vertex ' + str(right_wall_vertex)[1:-1])
cubit.cmd('nodeset 10 name \'NS_right_wall_ctr\'')
if not x_sym:
    left_wall_vertex = cubit.parse_cubit_list('vertex', \
        'with y_coord <= 0 \
        and with x_coord >= ' + str(-(g['room_width']/2.0 + tol)) \
        + ' and with x_coord <= ' + str(-(g['room_width']/2.0 - tol)) \
        + ' and with z_coord >= ' + str(g['room_ctr'][1] - tol) \
        + ' and with z_coord <= ' + str(g['room_ctr'][1] + tol))
    cubit.cmd('nodeset 11 vertex ' + str(left_wall_vertex)[1:-1])
    cubit.cmd('nodeset 11 name \'NS_left_wall_ctr\'')

# Calculate patches of nodes for better estimates of closure when
# there are multiple elements through the thickness.  Can be used in the
# discrete canister (CCO and POC) crush simulations.
roof_ctr_nodes = cubit.parse_cubit_list('node', \
    'with y_coord >= 0.0 \
    and with y_coord <= ' + str(g['thickness']) \
    + ' and with x_coord >= ' + str(0  -  (H_xz + tol)) \
    + ' and with x_coord <= ' + str(0 + (H_xz + tol)) \
    + ' and with z_coord >= ' + str(g['room_top_elev'] - tol) \
    + ' and with z_coord <= ' + str(g['room_top_elev'] + tol))
cubit.cmd('nodeset 12 node ' + str(roof_ctr_nodes)[1:-1])
cubit.cmd('nodeset 12 name \'NS_roof_ctr_avg\'')

if not x_sym:
    left_wall_ctr_nodes = cubit.parse_cubit_list('node', \
        'with y_coord >= 0.0 \
        and with y_coord <= ' + str(g['thickness']) \
        + ' and with x_coord >= ' + str(-(g['room_width']/2.0 + tol)) \
        + ' and with x_coord <= ' + str(-(g['room_width']/2.0 - tol)) \
        + ' and with z_coord >= ' + str(g['room_ctr'][1] - (1.1*H_xz + tol)) \
        + ' and with z_coord <= ' + str(g['room_ctr'][1] + (1.1*H_xz + tol)))
    cubit.cmd('nodeset 13 node ' + str(left_wall_ctr_nodes)[1:-1])
    cubit.cmd('nodeset 13 name \'NS_left_wall_ctr_avg\'')

right_wall_ctr_nodes = cubit.parse_cubit_list('node', \
    'with y_coord >= 0.0 \
    and with y_coord <= ' + str(g['thickness']) \
    + ' and with x_coord >= ' + str((g['room_width']/2.0 - tol)) \
    + ' and with x_coord <= ' + str((g['room_width']/2.0 + tol)) \
    + ' and with z_coord >= ' + str(g['room_ctr'][1] - (1.1*H_xz + tol))\
    + ' and with z_coord <= ' + str(g['room_ctr'][1] + (1.1*H_xz + tol)))
cubit.cmd('nodeset 14 node ' + str(right_wall_ctr_nodes)[1:-1])
cubit.cmd('nodeset 14 name \'NS_right_wall_ctr_avg\'')
```

```
floor_ctr_nodes = cubit.parse_cubit_list('node', \
    'with y_coord >= 0.0 \
    and with y_coord <= ' + str(g['thickness']) \
    + ' and with x_coord >= ' + str(0 - (H_xz + tol)) \
    + ' and with x_coord <= ' + str(0 + (H_xz + tol)) \
    + ' and with z_coord >= ' + str(g['room_bot_elev'] - tol) \
    + ' and with z_coord <= ' + str(g['room_bot_elev'] + tol))
cubit.cmd('nodeset 15 node ' + str(floor_ctr_nodes)[1:-1])
cubit.cmd('nodeset 15 name \'NS_floor_ctr_avg\'')

#Move mesh so it is centered on y=0.
cubit.cmd('move volume all x 0.0 y %r z 0.0 include_merged' %(-g['thickness'] / 2.0))

# Add a block for waste if needed
if not empty_room:
  # Include waste block mesh, nodesets and sidesets
  #All dimensions are in meters.

  #Define in-plane geometry of waste block
  #Width (see SAND97-0795, page 18)
  g['W'] = 3.675 * 2

  #Height (see SAND97-0795, page 14)
  g['H'] = 2.676
  #Define out-of-plane geometry (depth) = g['thickness']

  if x_sym:
    #Width
    g['W'] = 3.675

  #Generate geometry
  cubit.cmd('create brick x %r y %r z %r' %(g['W'], g['thickness'], g['H']))
  waste_vol_id = str(cubit.get_last_id("volume"))
  #print(waste_vol_id)

  #Define some coordinate limits (*_p = plus *_m = minus)
  top_p    = str(g['H']/2 + tol)
  top_m    = str(g['H']/2 - tol)
  bot_p    = str(-(g['H']/2 - tol))
  bot_m    = str(-(g['H']/2 + tol))
  right_p  = str(g['W']/2 + tol)
  right_m = str(g['W']/2 - tol)
  left_p    = str(-(g['W']/2 - tol))
  left_m   = str(-(g['W']/2 + tol))
  front_p  = str(-(g['thickness']/2 - tol))
  front_m = str(-(g['thickness']/2 + tol))
  back_p  = str(g['thickness']/2 + tol)
  back_m = str(g['thickness']/2 - tol)
  # front face (normal = -y)
  front_waste_surf = cubit.parse_cubit_list('surface', \
         ' in volume all with x_coord <= ' + right_p \
      + ' and with x_coord >= ' + left_m \
      + ' and with z_coord <= ' + top_p \
      + ' and with z_coord >= ' + bot_m \
      + ' and with y_coord <= ' + front_p \
      + ' and with y_coord >= ' + front_m)
  front_list_str = str(front_waste_surf)[1:-1]

  cubit.cmd('surface ' + front_list_str + 'size  %r' %(H_xz_o))
  cubit.cmd('mesh surface ' + front_list_str )
#Perform a uniform refinement if requested
  if split_elements:
    cubit.cmd('refine surface ' + front_list_str + ' numsplit 1')

  #Sweep the mesh through the thickness
  cubit.cmd('volume ' + waste_vol_id + ' scheme sweep vector 0 1 0')
  #Set 'redistribute nodes on' so to preserve the bias during the sweep. (This does the
  #same thing as the 'propagate bias' parameter in the sweep-source-target command)
```

```
cubit.cmd('volume ' + waste_vol_id + 'redistribute nodes on')

#Mesh thru the thickness
cubit.cmd('volume ' +  waste_vol_id  + 'size %r' %(H_y))
cubit.cmd('mesh volume '+ waste_vol_id)

#Generate mesh entities
cubit.cmd('block 1 vol ' + waste_vol_id)
cubit.cmd('block 1 name \'B_homogenized_can_block\'')

# right face (normal = +x)
right_waste_surf = cubit.parse_cubit_list('surface', \
       ' in volume all with x_coord <= ' + right_p \
    + ' and with x_coord >= ' + right_m \
    + ' and with z_coord <= ' + top_p \
    + ' and with z_coord >= ' + bot_m \
    + ' and with y_coord <= ' + back_p \
    + ' and with y_coord >= ' + front_m)

right_list_str = str(right_waste_surf)[1:-1]
cubit.cmd('nodeset 16 surface ' + right_list_str)
cubit.cmd('nodeset 16 name \'NS_homogenized_can_block_right_surf\' ')
cubit.cmd('sideset 8 surface ' + right_list_str)
cubit.cmd('sideset 8 name \'SS_homogenized_can_block_right_surf\' ')

# left face (normal = -x)
left_waste_surf = cubit.parse_cubit_list('surface', \
       ' in volume all with x_coord <= ' + left_p \
    + ' and with x_coord >= ' + left_m \
    + ' and with z_coord <= ' + top_p \
    + ' and with z_coord >= ' + bot_m \
    + ' and with y_coord <= ' + back_p \
    + ' and with y_coord >= ' + front_m)

left_list_str = str(left_waste_surf)[1:-1]
cubit.cmd('nodeset 17 surface ' + left_list_str)
cubit.cmd('nodeset 17 name \'NS_homogenized_can_block_left_surf\' ')
cubit.cmd('sideset 9 surface ' + left_list_str)
cubit.cmd('sideset 9 name \'SS_homogenized_can_block_left_surf\' ')

# top face (normal = +z)
top_waste_surf = cubit.parse_cubit_list('surface', \
       ' in volume all with x_coord <= ' + right_p \
    + ' and with x_coord >= ' + left_m \
    + ' and with z_coord <= ' + top_p \
    + ' and with z_coord >= ' + top_m \
    + ' and with y_coord <= ' + back_p \
    + ' and with y_coord >= ' + front_m)

top_list_str = str(top_waste_surf)[1:-1]
cubit.cmd('nodeset 18 surface ' + top_list_str)
cubit.cmd('nodeset 18 name \'NS_homogenized_can_block_top_surf\' ')
cubit.cmd('sideset 10 surface ' + top_list_str)
cubit.cmd('sideset 10 name \'SS_homogenized_can_block_top_surf\' ')

# bottom face (normal = -z)
bot_waste_surf = cubit.parse_cubit_list('surface', \
       ' in volume all with x_coord <= ' + right_p \
    + ' and with x_coord >= ' + left_m \
    + ' and with z_coord <= ' + bot_p \
    + ' and with z_coord >= ' + bot_m \
    + ' and with y_coord <= ' + back_p \
    + ' and with y_coord >= ' + front_m)

bot_list_str = str(bot_waste_surf)[1:-1]
cubit.cmd('nodeset 19 surface ' + bot_list_str)
cubit.cmd('nodeset 19 name \'NS_homogenized_can_block_bot_surf\' ')
cubit.cmd('sideset 11 surface ' + bot_list_str)
```

```
  cubit.cmd('sideset 11 name \'SS_homogenized_can_block_bot_surf\' ')

  # front face (normal = -y)
  front_waste_surf = cubit.parse_cubit_list('surface', \
         ' in volume all with x_coord <= ' + right_p \
      + ' and with x_coord >= ' + left_m \
      + ' and with z_coord <= ' + top_p \
      + ' and with z_coord >= ' + bot_m \
      + ' and with y_coord <= ' + front_p \
      + ' and with y_coord >= ' + front_m)

  front_list_str = str(front_waste_surf)[1:-1]
  cubit.cmd('nodeset 20 surface ' + front_list_str)
  cubit.cmd('nodeset 20 name \'NS_homogenized_can_block_front_surf\' ')
  cubit.cmd('sideset 12 surface ' + front_list_str)
  cubit.cmd('sideset 12 name \'SS_homogenized_can_block_front_surf\' ')

  # back face (normal = +y)
  back_waste_surf = cubit.parse_cubit_list('surface', \
         ' in volume all with x_coord <= ' + right_p \
      + ' and with x_coord >= ' + left_m \
      + ' and with z_coord <= ' + top_p \
      + ' and with z_coord >= ' + bot_m \
      + ' and with y_coord <= ' + back_p \
      + ' and with y_coord >= ' + back_m)

  back_list_str = str(back_waste_surf)[1:-1]
  cubit.cmd('nodeset 21 surface ' + back_list_str)
  cubit.cmd('nodeset 21 name \'NS_homogenized_can_block_back_surf\' ')
  cubit.cmd('sideset 13 surface ' + back_list_str)
  cubit.cmd('sideset 13 name \'SS_homogenized_can_block_back_surf\' ')

  #Exposed waste block surfaces
  if x_sym:
    exp_list_str = top_list_str + right_list_str + bot_list_str
  else:
    exp_list_str = top_list_str + right_list_str + left_list_str + bot_list_str

  cubit.cmd('nodeset 22 surface ' + exp_list_str )
  cubit.cmd('nodeset 22 name \'NS_homogenized_can_block_exposed_surf\' ')
  cubit.cmd('sideset 14 surface ' + exp_list_str)
  cubit.cmd('sideset 14 name \'SS_homogenized_can_block_exposed_surf\' ')

  #Move waste block mesh so it rests on the floor of the room.
  y_shift = 0.0
  x_shift = 0.0
  if x_sym:
     x_shift = g['W']/2
  z_shift = g['room_bot_elev'] + g['H']/2.0
  cubit.cmd('move volume ' + waste_vol_id + ' x %r y %r  z %r include_merged' %(x_shift, y_shift, z_shift))

# Add nodesets and sidesets for the room sufaces (roof, walls, floor) in case they are useful
roof_surf_str = str(roof_surf)[1:-1]
cubit.cmd('nodeset 23 surface ' + roof_surf_str)
cubit.cmd('nodeset 23 name \'NS_roof_surf\' ')
cubit.cmd('sideset 15 surface ' + roof_surf_str)
cubit.cmd('sideset 15 name \'SS_roof_surf\' ')

floor_surf_str = str(floor_surf)[1:-1]
cubit.cmd('nodeset 24 surface ' + floor_surf_str)
cubit.cmd('nodeset 24 name \'NS_floor_surf\' ')
cubit.cmd('sideset 16 surface ' + floor_surf_str)
cubit.cmd('sideset 16 name \'SS_floor_surf\' ')

right_wall_surf_str = str(right_wall_surf)[1:-1]
cubit.cmd('nodeset 25 surface ' + right_wall_surf_str)
cubit.cmd('nodeset 25 name \'NS_right_wall_surf\' ')
cubit.cmd('sideset 17 surface ' + right_wall_surf_str)
```

```
cubit.cmd('sideset 17 name \'SS_right_wall_surf\' ')

if not x_sym:
   left_wall_surf_str = str(left_wall_surf)[1:-1]
   cubit.cmd('nodeset 26 surface ' + left_wall_surf_str)
   cubit.cmd('nodeset 26 name \'NS_left_wall_surf\' ')
   cubit.cmd('sideset 18 surface ' + left_wall_surf_str)
   cubit.cmd('sideset 18 name \'SS_left_wall_surf\' ')


#Export the Mesh
import os
pwd = os.getcwd()
if plane_strain:
    base_file_name = mesh_name + '-1_element_deep'
else:
    base_file_name = mesh_name + '-%d_m_thick' %(g['thickness'])
if rapidly_coarsen:
    base_file_name = base_file_name + '-rapidly_coarsening'
#add mesh extent to file name
base_file_name = base_file_name + '-domain' + domain_extent

file_name = base_file_name + '-' + horizon_defn + 'Horizon.g'
export_path = os.path.join(pwd, file_name)
print( 'export_path =', export_path)

cubit.cmd('export genesis \'%s\' overwrite' % export_path)
if room_surf_blocks:
    export_path = os.path.join(pwd, base_file_name + '.g' )
    cubit.cmd("export genesis \'%s\' block 6 7 overwrite" % export_path)

#Save the geometry values
try:
  # for python 2.x
  import cPickle as pickle
except:
  # for python 3.x
  import pickle

#cPickle can save as a binary or a text file.  Binaries are smaller, so I
#use them here.  The 'wb' option says to open the binary file with write access.
geom_path = os.path.join(pwd, base_file_name +  '-' + horizon_defn + 'Horizon-geom_values.pkl')
geom_file = open(geom_path,'wb')
#Save the file.  Protocol 2 is the faster binary protocol for Python 2.7
pickle.dump(g, geom_file, protocol = 2)
geom_file.close()

#Print the pressures at the top and bottom surfaces
p1 = -15.97e6
p2 = -13.57e6
z1 = -54.19
z2 = 52.87
p = lambda z: (p2 - p1) / (z2 - z1) * (z - z1) + p1
print( 'At z = ' + str(g['bot_elev']) + ' p = ' + str(p(g['bot_elev'])))
print( 'At z = ' + str(g['top_elev']) + ' p = ' + str(p(g['top_elev'])))

#Print the error count
error_new = cubit.get_error_count()
print( 'Cubit error count = %r' %(error_new - error_old))
```

C.2. Sierra/SM Input Files

C.2.1. Recreated Legacy Model

```
begin sierra WIPP Isothermal Disposal Room

  title Simulation of WIPP Isothermal Disposal Room

  #---------- Variables ---------

  #Define the time periods
  ${t_m_0_0 = -1.0e-2} #s
  ${t_m_0_1 = 0.0} #s
  ${t_m_1_0 = t_m_0_1} #s
  ${t_m_1_1 = 86400.0 * 365.25 * 10000.0} #s
  ${temp = 300}

  ${gasScale = 0.5}

  #---------- Directions --------

  define direction y with vector 0.0 1.0 0.0
  define direction x with vector 1.0 0.0 0.0
  define direction z with vector 0.0 0.0 1.0
  define direction negative_z with vector 0.0  0.0 -1.0
  define point origin with coordinates 0.0 0.0 0.0

  #---------- Functions ---------

  begin definition for function function_constant
    type is piecewise linear
    begin values
      -1.0e16               1.0
      1.0e16                1.0
    end values
  end definition for function function_constant

  begin function gas_pressure
    type is piecewise analytic
    expression variable: rv = global room_volume
    expression variable:  t = global time
    begin expressions
     -1.0             "0.0"
      0.0             "13608.0*(t/3.15576e7)*2494.35/(rv-551.2)"
      1.735668e10     "(3742200.0 + 6804.0*(t/3.15576e7))*2494.35/(rv-551.2)"
      3.313548e10     "10886400.0*2494.35/(rv-551.2)"
    end
  end function gas_pressure

  begin definition for function fluid_density_ramp
    #Specify the density to give the appropriate lithostatic
    # pressure at room at start of simulation and then ramp it down to zero
    type is analytic
    evaluate expression is "2300.0 / 2.0 *
                           (1.0 - cos(pi * time / {t_m_0_1 - t_m_0_0}))"
  end definition for function fluid_density_ramp

  #---------- Materials ----------

  begin property specification for material halite
    density = 2300.0
    begin parameters for model munson_dawson
      #(These parameters came from the Clean Salt values in Table 2 and
      # Table 3 of SAND97-0795.)
      bulk modulus = 20660000000.0
```

```
    shear modulus = 12400000000.0
    a1 = 8.386e+22
    q1or = 12582 #{41.94*temp}
    n1 = 5.5
    b1 = 6086000.0
    a2 = 9.672e+12
    q2or = 5.0338e3 #{16.776*temp}
    n2 = 5.0
    b2 = 0.03034
    sig0 = 20570000.0
    qlc = 5335.0
    m = 3.0
    k0 = 627500.0
    c = 9.1967e-3 #{2.759/temp}
    alpha = -17.37
    beta = -7.738
    deltalc = 0.58
    rn3 = 2.0
    amult = 0.95
  end parameters for model munson_dawson
end property specification for material halite

begin property specification for material arg_halite
  density = 2300.0
  begin parameters for model munson_dawson
    #(These parameters came from the Clean Salt values in Table 2 and
    # Table 3 of SAND97-0795.)
    bulk modulus = 20660000000.0
    shear modulus = 12400000000.0
    a1 = 1.407e+23
    q1or = 12582 #{41.94*temp}
    n1 = 5.5
    b1 = 8998000.0
    a2 = 1.314e+13
    q2or = 5.0328e3 #{16.776*temp}
    n2 = 5.0
    b2 = 0.04289
    sig0 = 20570000.0
    qlc = 5335.0
    m = 3.0
    k0 = 2470000.0
    c = 9.1967e-3 #{2.759/temp}
    alpha = -14.96
    beta = -7.738
    deltalc = 0.58
    rn3 = 2.0
    amult = 0.95
  end parameters for model munson_dawson
end property specification for material arg_halite

begin definition for function anhydrite_pressure
  type is piecewise linear
  ordinate is volumetric_strain # unitless
  abscissa is pressure # Pa
  begin values
      0       0
      1.0    8.3e10
  end values
end definition for function anhydrite_pressure

begin property specification for material anhydrite
  density = 2300.0 # kg / m^3
  # This is adapted from the SANTOS input files from SAND97-0795
  begin parameters for model soil_foam
    two mu              =   5.5630e10 # Pa
    bulk modulus        =   8.3444e10 # Pa
    A0                  =   2.338e6 # Pa
    A1                  =   2.338
```

```
    A2                  =   0.0
    pressure cutoff     =   0.0 # Pa
    pressure function   =   anhydrite_pressure
  end parameters for model soil_foam
end property specification for material anhydrite

begin definition for function pressure_volstrain_function
  #These parameters came from SAND97-0795, Table 4
  type is piecewise linear
  ordinate is volumetric_strain # unitless
  abscissa is pressure # Pa
  begin values
      0       0
      0.510   1.53e6
      0.631   2.03e6
      0.719   2.53e6
      0.786   3.03e6
      0.838   3.53e6
      0.881   4.03e6
      0.942   4.93e6
      1.14    12.0e6
  end values
end definition for function pressure_volstrain_function

begin property specification for material homogenized_can_block
  density = 559.5 #kg / m^3, see SAND97-0796, Table 5
  #These parameters came from SAND97-0796, Table 7
  #The yield function for this model is
  #phi = sqrt(3*J_2) - (a0 + a1 * p + a2 * p^2)
  #This model has a Drucker-Prager yield surface if a2 = 0
  #The Drucker-Prager yield function is often written as
  #phi = sqrt(J_2) + a * I_1 - C
  #Thus, we can write a0 and a1 in terms of a and C

  begin parameters for model soil_foam
    bulk modulus      = 222.0e6
    two mu            = 333.0e6
    a0                = 1.0e6 # Pa
    a1                = 3.0 # unitless
    a2                = 0.0
    pressure cutoff   = 0.0 # Pa
    pressure function = pressure_volstrain_function
  end parameters for model soil_foam
end property specification for material homogenized_can_block

begin solid section solid_1
  formulation = mean_quadrature
  strain incrementation = strongly_objective
end solid section solid_1

#---------- Finite Element Model -----------

begin finite element model room
  Database name = mesh/disposal_room_CMStone-1_element_deep.g
  Database type = exodusII

  begin block defaults
    hourglass stiffness =0.005 # default is 0.05
  end

  begin parameters for block b_halite
    material halite
    solid mechanics use model munson_dawson
    section = solid_1
  end parameters for block b_halite

  begin parameters for block b_arg_halite
    material arg_halite
```

```
    solid mechanics use model munson_dawson
    section = solid_1
  end parameters for block b_arg_halite

  begin parameters for block b_arg_halite_a
    material arg_halite
    solid mechanics use model munson_dawson
    section = solid_1
  end parameters for block b_arg_halite_a

  begin parameters for block b_arg_halite_b
    material arg_halite
    solid mechanics use model munson_dawson
    section = solid_1
  end parameters for block b_arg_halite_b

  begin parameters for block b_arg_halite_c
    material arg_halite
    solid mechanics use model munson_dawson
    section = solid_1
  end parameters for block b_arg_halite_c

  begin parameters for block b_anhydrite
    material anhydrite
    solid mechanics use model soil_foam
    section = solid_1
  end parameters for block b_anhydrite

  begin parameters for block b_homogenized_can_block
    material homogenized_can_block
    solid mechanics use model soil_foam
    section = solid_1
  end parameters for block b_homogenized_can_block

end finite element model room

begin adagio procedure The_Procedure.1

  begin time control

    begin time stepping block p0
      start time = {t_m_0_0}
      begin parameters for adagio region SmRegion.1
        time increment = 5e-4
      end parameters for adagio region SmRegion.1
    end time stepping block p0

    begin time stepping block p1
      start time = {t_m_1_0}
      begin parameters for adagio region SmRegion.1
        time increment = 0.1
      end parameters for adagio region SmRegion.1
    end time stepping block p1

    termination time = {t_m_1_1}

  end time control

  #---------- Time Step Control ----------

  begin adagio region SmRegion.1

    use finite element model room

    begin adaptive time stepping time
      method = material
      cutback factor = 0.999  during p0
      cutback factor = 0.999 # 0.8  during p1
```

```
  growth factor  = 1.0  during p0
  growth factor  = 1.05 during p1

  maximum multiplier = 1 during p0
  maximum multiplier = 78894000 during p1
  minimum multiplier = 1.e-8
  maximum failure cutbacks = 20
end adaptive time stepping time

#--------- Boundary Conditions ---------

begin gravity
  include all blocks
  gravitational constant = 9.79
  direction = negative_z
  function = function_constant
end gravity

begin prescribed temperature
  include all blocks
  function = function_constant
  scale factor = {temp}
end prescribed temperature

begin pressure
  surface = SS_top_surf
  function = function_constant
  scale factor = 13.57E+06
end pressure

begin pressure
  surface = SS_room_surf
  function = gas_pressure
  scale factor = {gasScale}
  external force contribution output name = pgas
end pressure

begin fixed displacement
  node set = NS_bot_surf
  components = z
end fixed displacement

begin fixed displacement
  node set = NS_left_surf
  components = x
end fixed displacement

begin fixed displacement
  node set = NS_right_surf
  components = x
end fixed displacement

begin fixed displacement
  node set = NS_back_surf
  components = y
end fixed displacement

begin fixed displacement
  node set = NS_front_surf
  components = y
end fixed displacement

begin fluid pressure
  surface = SS_room_surf
  active periods = p0
  #Specify which direction corresponds to the depth of fluid.
  fluid surface normal = z
  #The depth function is defined relative to the reference point.
```

```
  reference point = origin
  #Set the fluid height, relative to the reference point
  #p1 = -15.97e6 Pa
  #p2 = -13.57e6 Pa
  #z1 = -54.19 m
  #z2 = 52.87 m
  #slope = (p2-p1)/(z2-z1)
  #p = slope*(z-z1)+p1
  #z0 = depth = elevation of fluid surface
  #depth = -p1 / slope + z1
  depth = 658.2050833333333 #m = height
  #Specify the function to ramp the fluid density down by time = 0
  density function = fluid_density_ramp
  gravitational constant = 9.79
end fluid_pressure

#--------- Contact ---------

begin contact definition frictionless

  search = acme
  enforcement = kinematic

  begin interaction defaults
    constraint formulation = node_face
    general contact = on
  end

  begin contact surface homogenized_can_block_surf
    surface = SS_homogenized_can_block_exposed_surf
  end

  begin contact surface room_right_wall_surf
    surface = SS_right_wall_surf
  end

  begin contact surface room_roof_surf
    surface = SS_roof_surf
  end

  begin contact surface room_floor_surf
    surface = SS_floor_surf
  end

  begin constant friction model salt_to_can_friction_model
    friction coefficient = 0.0
  end

  begin constant friction model salt_to_salt_friction_model
    friction coefficient = 0.0
  end

  #salt to salt interaction
  begin interaction roof_wall
    master = room_roof_surf
    slave  = room_right_wall_surf
    friction model = salt_to_salt_friction_model
    normal tolerance = 1e-02
    tangential tolerance = 1e-02
    capture tolerance = 1e-04
    tension release = 1.0e8 iterations = 5
    interaction behavior = sliding
  end

  begin interaction floor_wall
    master = room_floor_surf
    slave  = room_right_wall_surf
    friction model = salt_to_salt_friction_model
```

```
    normal tolerance = 1e-02
    tangential tolerance = 1e-02
    capture tolerance = 1e-04
    tension release = 1.0e8 iterations = 5
    interaction behavior = sliding
  end

  #salt-waste contact
  begin interaction floor_waste
    master = room_floor_surf
    slave  = homogenized_can_block_surf
    friction model = salt_to_can_friction_model
    normal tolerance = 1e-02
    tangential tolerance = 1e-02
    capture tolerance = 1e-04
    tension release = 1.0e8 iterations = 5
    interaction behavior = sliding
  end

  begin interaction wall_waste
    master = room_right_wall_surf
    slave  = homogenized_can_block_surf
    friction model = salt_to_can_friction_model
    normal tolerance = 1e-02
    tangential tolerance = 1e-02
    capture tolerance = 1e-04
    tension release = 1.0e8 iterations = 5
    interaction behavior = sliding
  end

  begin interaction roof_waste
    master = room_roof_surf
    slave  = homogenized_can_block_surf
    friction model = salt_to_can_friction_model
    normal tolerance = 1e-02
    tangential tolerance = 1e-02
    capture tolerance = 1e-04
    tension release = 1.0e8 iterations = 5
    interaction behavior = sliding
  end

end contact definition frictionless

#--------- Initial Conditions ---------

begin initial condition
  block = b_halite b_arg_halite b_anhydrite b_arg_halite_a
          b_arg_halite_b b_arg_halite_c
  #It is important to initialize unrotated_stress and not stress,
  #stress is just an output that gets calculated as needed, while
  #unrotated_stress gets stored and used by the constitutive models.
  #As of November 2015, initializing stress does nothing.
  initialize variable name = unrotated_stress
  variable type = element
  subroutine real parameter: top = 52.87
  subroutine real parameter: bot = -54.19
  subroutine real parameter: p1 = -13.57e6
  subroutine real parameter: po = -15.97e6
  subroutine real parameter: kvert_xx = 1.0
  subroutine real parameter: kvert_yy = 1.0
  subroutine real parameter: kvert_zz = 1.0
  subroutine real parameter: kvert_xy = 0.0
  subroutine real parameter: kvert_yz = 0.0
  subroutine real parameter: kvert_zx = 0.0
  subroutine string parameter: dir = Z
  element block subroutine = geo_is
end initial condition
```

```
#--------- User Output Variable Definitions ----------

begin user output
  compute element el_avg_stress as average of element cauchy_stress
  compute element el_avg_mean_stress as average of
          element hydrostatic_stress
  compute element el_avg_log_strain as average of
          element unrotated_log_strain
end user output

begin user output
  node set = NS_roof_ctr
  compute global roof_disp as average of nodal displacement
end

begin user output
  node set = NS_floor_ctr
  compute global floor_disp as average of nodal displacement
end

begin user output
  node set = NS_right_wall_ctr
  compute global right_wall_disp as average of nodal displacement
end

begin user variable room_volume
  type = global real length = 1
  global operator = sum
  initial value = 3.6427501440e+03   # W (10.06) * L (91.44) * H (3.96)
end user variable

begin user output
  surface = SS_room_surf
  surface subroutine = aupst_cavity_volume
  subroutine string parameter: outputVarName = room_volume
  subroutine real parameter: cavitysymmetrypoint_x = 0.0
  subroutine real parameter: cavitysymmetrypoint_y = 0.5
  subroutine real parameter: cavitysymmetrypoint_z = -4.41
  subroutine real parameter: volumeScale = 274.32
  # volumeScale is 1.5 (correction factor)*2 (for W symmetry)*91.44 (L)
  compute at every step
end

begin user output
  block = b_homogenized_can_block
  compute global waste_area as sum of element volume
end

begin user output
  compute global waste_volume from expression "waste_area*2*87.85"
end

#--------- Results Output ---------

begin results output output_1
  database name = efiles/%B-r.e
  database type = exodusII
  At time {t_m_0_0}, increment = {(t_m_0_1 - t_m_0_0) / 2.0}
  At time {t_m_1_0}, increment = {86400.0 * 365.25 * 10.0}
  nodal variables = displacement as disp
  nodal variables = contact_accumulated_slip
  nodal variables = residual
  element variables = el_avg_stress
  element variables = el_avg_mean_stress
  element variables = el_avg_eq_stress
  element variables = el_avg_eq_tr_strain
  element variables = el_avg_eq_vp_strain
  element variables = el_avg_log_strain
```

```
end results output output_1

#--------- History Output ---------

begin history output output_3
  database name = history/%B-h.e
  database type = exodusII
  At time {t_m_0_0}, increment = {(t_m_0_1 - t_m_0_0) / 5.0}
  at time {t_m_1_0 + 0} increment = 0.0864 #s
  at time {t_m_1_0 + 0.864} increment = 0.864 #s
  at time {t_m_1_0 + 8.64} increment = 8.64 #s
  at time {t_m_1_0 + 86.4} increment = 86.4 #s
  at time {t_m_1_0 + 864} increment = 864 #s
  at time {t_m_1_0 + 8640} increment = 8640 #s
  at time {t_m_1_0 + 86400} increment = 86400 #s
  at time {t_m_1_0 + 864000} increment = 864000 #s
  at time {t_m_1_0 + 31557600} increment = {86400.0*365.25*0.25} #s


  global time
  global wall_clock_time as run_time
  global roof_disp
  global floor_disp
  global right_wall_disp
  global room_volume
  global waste_volume
end history output output_3

#--------- Heartbeat Output ---------

begin heartbeat output heartbeat_adagio
  stream name = wipp.hb
  append = off
  precision = 10
  legend = on
  At time {t_m_0_0}, increment = {(t_m_0_1 - t_m_0_0) / 5.0}
  at time {t_m_1_0 + 0} increment = 0.0864 #s
  at time {t_m_1_0 + 0.864} increment = 0.864 #s
  at time {t_m_1_0 + 8.64} increment = 8.64 #s
  at time {t_m_1_0 + 86.4} increment = 86.4 #s
  at time {t_m_1_0 + 864} increment = 864 #s
  at time {t_m_1_0 + 8640} increment = 8640 #s
  at time {t_m_1_0 + 86400} increment = 86400 #s
  at time {t_m_1_0 + 864000} increment = 864000 #s
  at time {t_m_1_0 + 31557600} increment = {86400.0*365.25*0.25} #s
  global time as Time
  global timestep as tstep
  global room_volume
  global waste_volume
  face pressure nearest location 0.0 0.0 -2.43 as roof_pressure
  labels = off
  timestamp format = ""
end heartbeat output heartbeat_adagio

#--------- Restart ---------

begin restart data restart_1
  database name = restart/%B.rsout
  overwrite = True
  at wall time 0.0h increment = 11.95h
end restart data restart_1

#--------- Solver ---------

begin solver

begin loadstep predictor
  type = scale_factor
```

```
        scale factor = 0.0 0.0
      end loadstep predictor

      begin control contact
        level = 1
        target relative residual = 1e-4
        acceptable relative residual = 1e-4
        target residual = 1e-4
        acceptable residual = 1e-4
        maximum iterations = 100
        lagrange adaptive penalty = off
        #developer lagrange target gap = 1.0e-5
      end control contact

      begin cg
        target relative residual = 1.0e-4
        acceptable relative residual = 1.0e30
        target residual = 1.0e-4
        acceptable residual = 1.0e30
        maximum iterations = 3000
        iteration print = 100 #10
      end cg

      end solver

    end adagio region SmRegion.1

  end adagio procedure The_Procedure.1

  begin feti equation solver my_feti
    corner algorithm = 14
  end

end sierra WIPP Isothermal Disposal Room
```

C.2.2. New Model

```
begin sierra WIPP Isothermal Disposal Room

   title Simulation of WIPP Isothermal Disposal Room

   restart = automatic

   #---------- Variables ---------

   #-----------------------------------
   #---------- Room geometry  ---------
   #-----------------------------------

   #Define mesh name
   ${mesh_name = "disposal_room_lower_waste_base.g"}

   #Define the disposal room horizon ('lower' or 'upper')
   ${horizon = "lower"}

   #Define if disposal room empty or with waste ('empty' or 'waste')
   ${iswaste = "waste"}

   #Define element thickness (m)
   ${element_thickness = 1.0}

   #-----------------------------------
   #---------- Waste model  -----------
   #-----------------------------------
```

```
#Define waste material model ('soil_foam', 'foam_damage', or 'elastic')
${waste_model = "foam_damage"}

#Define foam damage model ('model_F2', 'model_F3', or 'model_F4')
${foam_model = "model_F3"}

#-----------------------------------
#---------- Gas generation  --------
#-----------------------------------

#Set the gas generation curve ('stone1997' or 'king2021')
# Stone: SAND97-0795, King: ERMS-575793
${gasCurve = "king2021"}

#Set the gas generation factor
${gasScale = 0.0}

#Define if gas generation pressure masking active ('mask' or 'nomask')
${masking = "nomask"}

#Define if gas generation pressure applied to clay seams ('yes' or 'no')
${clay_pressure = "yes"}

#-----------------------------------
#---------- Contact options  -------
#-----------------------------------

#Define friction coefficients
${clay_seam_friction  = 0.2}
${clay_seam_frictionF = 0.42}
${salt_salt_friction  = 0.5}
${salt_waste_friction = 0.4}

#Define if individual clay seams are tied ('yes' or 'no')
${tied_A = "no"}
${tied_B = "no"}
${tied_D = "no"}
${tied_E = "no"}
${tied_F = "no"}
${tied_G = "no"}
${tied_H = "no"}
${tied_I = "no"}
${tied_J = "no"}
${tied_K = "no"}
${tied_L = "no"}
${tied_M = "no"}

#-----------------------------------
#--- Simulation time and scaling ---
#-----------------------------------

#Define simulation time period (yrs)
${time_period = 10000}

#Define time integration method ('implicit', or 'explicit')
${time_integration = "explicit"}

{if (gasCurve=="stone1997")}
  $yr1 = {yr1 = 550.0}  end of first gas generation period
  $yr2 = {yr2 = 1050.0} end of second gas generation period
{elseif (gasCurve=="king2021")}
  $yr1 = {yr1 = 1200.0} end of first gas generation period
  $yr2 = {yr2 = 2700.0} end of second gas generation period
{endif}

{if (time_integration=="implicit")}

#Define the time periods
```

```
${t_0_0 = -0.01}     #s
${t_0_1 = 0.0}       #s
${t_1_0 = t_0_1}     #s
${t_1_1 = 86400.0 * 365.25 * time_period} #s

#Define the gas generation periods
${t1 = yr1 * 86400.0 * 365.25}
${t2 = yr2 * 86400.0 * 365.25}

{else}

#Define the time periods in material time (sec)
${t_m_0_0 = -0.5}    #s
${t_m_0_1 = 0.0}     #s
${t_m_1_0 = t_m_0_1} #s
${t_m_1_1 = 86400.0 * 365.25 * time_period} #s

#Define the scale factors
${s_1_0 = 1.0e-2}
${s_ramp = 2e9}

#Define the time periods in momentum balance time (sec)
$t_mb_m_0_0  = {t_mb_m_0_0 = -0.01} #s
$t_mb_m_0_1  = {t_mb_m_0_1 = (-s_1_0 + sqrt(s_1_0^2 + 2 * s_ramp * (t_m_0_1))) / s_ramp} #s
$t_mb_m_1_0  = {t_mb_m_1_0 = t_m_0_1}
$t_mb_m_1_1  = {t_mb_m_1_1 = (-s_1_0 + sqrt(s_1_0^2 + 2 * s_ramp * (t_m_1_1))) / s_ramp} #s

#Define the gas generation periods in momentum balance time (sec)
$ t1 = {t1 = (-s_1_0 + sqrt(s_1_0^2 + 2 * s_ramp * (yr1 * 86400.0 * 365.25))) / s_ramp }
$ t2 = {t2 = (-s_1_0 + sqrt(s_1_0^2 + 2 * s_ramp * (yr2 * 86400.0 * 365.25))) / s_ramp }

{endif}

#---------- Directions --------

define direction y with vector 0.0 1.0 0.0
define direction x with vector 1.0 0.0 0.0
define direction z with vector 0.0 0.0 1.0
define direction negative_z with vector 0.0  0.0 -1.0
define point origin with coordinates 0.0 0.0 0.0

#---------- Functions ---------

begin definition for function function_constant
   type is piecewise linear
   begin values
     -1.0e16               1.0
      1.0e16               1.0
   end values
end definition for function function_constant

begin function gas_pressure
  type is piecewise analytic
  expression variable: rv        = global room_volume
  {if (time_integration=="implicit")}
  expression variable:  t        = global time
  {else}
  expression variable:  t        = global mat_time
  {endif}
  expression variable: fricModel = nodal contact_friction_index
  {if (masking=="mask")}
    expression variable: cstrn   = nodal contact_strength
  {else}
    expression variable: cstrn   = global cstrn_off
  {endif}
  {if (gasCurve=="stone1997")}
    begin expressions
     -1.0  "0.0"
```

```
      0.0  "fricModel==5 ? (1.0 - min(1.0,cstrn))*13608.0*(t/3.15576e7)*2494.35/(rv-302.0) :
      ↪  13608.0*(t/3.15576e7)*2494.35/(rv-302.0)"
      {t1} "fricModel==5 ? (1.0 - min(1.0,cstrn))*(3742200.0 + 6804.0*(t/3.15576e7))*2494.35/(rv-302.0) :
      ↪  (3742200.0 + 6804.0*(t/3.15576e7))*2494.35/(rv-302.0)"
      {t2} "fricModel==5 ? (1.0 - min(1.0,cstrn))*10886400.0*2494.35/(rv-302.0) :
      ↪  10886400.0*2494.35/(rv-302.0)"
    end
  {elseif (gasCurve=="king2021")}
    begin expressions
     -1.0  "0.0"
      0.0  "fricModel==5 ? (1.0 - min(1.0,cstrn))*9846.38*(t/3.15576e7)*2494.35/(rv-302.0) :
      ↪  9846.38*(t/3.15576e7)*2494.35/(rv-302.0)"
      {t1} "fricModel==5 ? (1.0 - min(1.0,cstrn))*(9396876.0 + 2015.65*(t/3.15576e7))*2494.35/(rv-302.0) :
      ↪  (9396876.0 + 2015.65*(t/3.15576e7))*2494.35/(rv-302.0)"
      {t2} "fricModel==5 ? (1.0 - min(1.0,cstrn))*(13244376.0 + 590.65*(t/3.15576e7))*2494.35/(rv-302.0) :
      ↪  (13244376.0 + 590.65*(t/3.15576e7))*2494.35/(rv-302.0)"
    end
  {endif}
end function gas_pressure

begin function gas_pressure_claySeams
  type is piecewise analytic
  expression variable: rv = global room_volume
  {if (time_integration=="implicit")}
  expression variable:  t        = global time
  {else}
  expression variable:  t        = global mat_time
  {endif}
  expression variable: cstrn = nodal contact_strength
  {if (gasCurve=="stone1997")}
    begin expressions
       -1.0 "0.0"
       0.0  "(1.0 - min(1.0,cstrn))*13608.0*(t/3.15576e7)*2494.35/(rv-302.0)"
       {t1} "(1.0 - min(1.0,cstrn))*(3742200.0 + 6804.0*(t/3.15576e7))*2494.35/(rv-302.0)"
       {t2} "(1.0 - min(1.0,cstrn))*10886400.0*2494.35/(rv-302.0)"
    end
  {elseif (gasCurve=="king2021")}
    begin expressions
       -1.0 "0.0"
       0.0  "(1.0 - min(1.0,cstrn))*9846.38*(t/3.15576e7)*2494.35/(rv-302.0)"
       {t1} "(1.0 - min(1.0,cstrn))*(9396876.0 + 2015.65*(t/3.15576e7))*2494.35/(rv-302.0)"
       {t2} "(1.0 - min(1.0,cstrn))*(13244376.0 + 590.65*(t/3.15576e7))*2494.35/(rv-302.0)"
    end
  {endif}
end function gas_pressure_claySeams

 begin definition for function fluid_density_ramp
    #Specify the density to give the appropriate lithostatic pressure at room at start of simulation and then
    ↪  ramp it down to zero
    type is analytic
    {if (time_integration=="implicit")}
    evaluate expression is "2300.0 / 2.0 * (1.0 - cos(pi * time / {t_0_1 - t_0_0}))"
    {else}
    evaluate expression is "2300.0 / 2.0 * (1.0 - cos(pi * time / {t_m_0_1 - t_m_0_0}))"
    {endif}
 end definition for function fluid_density_ramp

 {if (time_integration=="explicit")}
 #---------- Viscoplastic Rate Scaling Functions ---------

 begin function stored_time_function
    type is analytic
    expression variable: t_stored = global time
    evaluate expression = "t_stored"
 end

 begin function vp_rate_scale_factor_function
    type is piecewise analytic
```

```
   begin expressions
      -0.5              "{s_1_0}"
      1e-10             "{s_1_0} + {s_ramp} * (time - 0)"
   end expressions
end

begin function vp_rate_scale_factor_broadcast_function
   type is analytic
   expression variable: vp_rate_scale_factor = global vp_rate_scale_factor
   evaluate expression = "vp_rate_scale_factor"
end

begin function mat_time_function
   type is analytic
   expression variable: t = global time
   expression variable: dt = global timestep
   expression variable: t_stored = global stored_time
   expression variable: t_m = global mat_time
   expression variable: s = global vp_rate_scale_factor
   evaluate expression = "                                      \#
      (t != t_stored) ? (                                       \#
      t_m + s * dt                                             \#
      ) : (                                                     \#
      t_m                                                      \#
      )                                                         \#
   "
end
{endif}

#---------- Materials ----------

includefile include/salt-md_viscoplastic-cal_3b.txt

includefile include/anhydrite-cal_4.txt

includefile include/polyhalite-cal_1.txt

{if (waste_model=="foam_damage")}
  {if (foam_model=="model_F2")}
    includefile include/foamDamageModel_F2.txt
  {elseif (foam_model=="model_F3")}
    includefile include/foamDamageModel_F3.txt
  {elseif (foam_model=="model_F4")}
    includefile include/foamDamageModel_F4.txt
  {endif}
{else}
  includefile include/soil_and_foam.txt
{endif}

begin solid section solid_1
   formulation = selective_deviatoric
   strain incrementation = strongly_objective
end solid section solid_1

#---------- Finite Element Model -----------

begin finite element model room
   Database name = {mesh_name}
   Database type = exodusII

   begin parameters for block b_halite
      material halite
      solid mechanics use model md_viscoplastic
      section = solid_1
   end parameters for block b_halite

   begin parameters for block b_arg_halite
      material halite
```

```
      solid mechanics use model md_viscoplastic
      section = solid_1
   end parameters for block b_arg_halite

   begin parameters for block b_anhydrite
      material anhydrite
      solid mechanics use model kayenta
      section = solid_1
   end parameters for block b_anhydrite

   begin parameters for block b_polyhalite
      material polyhalite
      solid mechanics use model soil_foam
      section = solid_1
   end parameters for block b_polyhalite

   {if (iswaste=="waste")}
   begin parameters for block b_homogenized_can_block
     material homogenized_can_block
     solid mechanics use model {waste_model}
     section = solid_1
   end parameters for block b_homogenized_can_block
   {endif}

end finite element model room

   {if (time_integration=="implicit")}

   begin adagio procedure The_Procedure.1

   begin time control

       begin time stepping block p0
         start time = {t_0_0}
         begin parameters for adagio region SmRegion.1
           time increment = {(t_0_1 - t_0_0) / 100.0}
         end
       end

       begin time stepping block p1
         start time = {t_1_0}
         begin parameters for adagio region SmRegion.1
           time increment = 1.0e-3
         end
       end

       termination time = {t_1_1}

   {else}

   begin presto procedure The_Procedure.1

   begin time control

      begin time stepping block p0
         start time = {t_mb_m_0_0}
         begin parameters for presto region SmRegion.1
            time step scale factor = 1
            time step increase factor = 5
         end
      end

      begin time stepping block p1
         start time = 0
         begin parameters for presto region SmRegion.1
            time step scale factor = 1
            time step increase factor = 5
         end
```

```
   end

   termination time = {t_mb_m_1_1}
   {endif}

end time control

#---------- Time Step Control ----------

{if (time_integration=="implicit")}
begin adagio region SmRegion.1

   begin adaptive time stepping time
       method = material during p1
       cutback factor = 0.5
       growth factor  = 1.1
       minimum multiplier = 1.e0 during p0
       minimum multiplier = 1.e-3 during p1
       maximum multiplier = 1e14
       maximum failure cutbacks = 50
   end adaptive time stepping time

{else}
begin presto region SmRegion.1
{endif}

   use finite element model room

   #--------- Boundary Conditions ---------

   begin gravity
      include all blocks
      gravitational constant = 9.79  # SAND88-2948 used 9.79 m/s^2 and so did the Germans in JPIII.  9.79
      ↪  m/s^2 is close to the local value of gravity at WIPP (9.79483 m/s^2).
      direction = negative_z
      function = function_constant
   end gravity

   begin prescribed temperature
      block = b_halite b_arg_halite b_polyhalite b_anhydrite
      function = function_constant
      scale factor = 300.0
   end prescribed temperature

   {if (iswaste=="waste")}
   begin prescribed temperature
      block = b_homogenized_can_block
      {if (waste_model=="foam_damage" && time_integration=="explicit")}
        function = vp_rate_scale_factor_function
        scale factor = 1.0
      {else}
        function = function_constant
        scale factor = 300.0
     {endif}
   end prescribed temperature
   {endif}

   begin pressure
      surface = SS_top_surf
      function = function_constant
      scale factor = 13.57E+06
   end pressure

   begin pressure
     surface = SS_room_surf
     function = gas_pressure
     scale factor = {gasScale}
     external force contribution output name = pgas_room
```

```
end pressure

{if (clay_pressure=="yes")}
begin pressure
  {if (horizon=="lower")}
  surface = SS_clay_F_master SS_clay_F_slave
  {elseif (horizon=="upper")}
  surface = SS_clay_F_master SS_clay_F_slave SS_clay_G_master SS_clay_G_slave
  {endif}
  function = gas_pressure_claySeams
  scale factor = {gasScale}
  external force contribution output name = pgas_clay

end pressure
{endif}

begin fixed displacement
   node set = NS_bot_surf
   components = z
end fixed displacement

begin fixed displacement
   node set = NS_left_surf
   components = x
end fixed displacement

begin fixed displacement
   node set = NS_right_surf
   components = x
end fixed displacement

begin fixed displacement
   node set = NS_back_surf
   components = y
end fixed displacement

begin fixed displacement
   node set = NS_front_surf
   components = y
end fixed displacement

{if (iswaste=="waste")}
begin fixed displacement
   node set = NS_homogenized_can_block_left_surf
   components = x
end fixed displacement

begin fixed displacement
   node set = NS_homogenized_can_block_back_surf
   components = y
end fixed displacement

begin fixed displacement
   node set = NS_homogenized_can_block_front_surf
   components = y
end fixed displacement
{endif}

begin fluid pressure
   surface = SS_room_surf
   active periods = p0
   #Specify which direction corresponds to the depth of fluid.
   fluid surface normal = z
   #The depth function is defined relative to the reference point.
   #See the figure in the fluid pressure section of the Sierra/SM manual for more info.
   reference point = origin
```

```
    #Set the fluid height, relative to the reference point, to give the appropriate lithostatic
    ↪  pressure at room
    #p1 = -15.97e6 Pa
    #p2 = -13.57e6 Pa
    #z1 = -54.19 m
    #z2 = 52.87 m
    #slope = (p2-p1)/(z2-z1)
    #p = slope*(z-z1)+p1
    #z0 = depth = elevation of fluid surface
    #depth = -p1 / slope + z1
    depth = 658.2050833333333 #m = height
    #Specify the function to ramp the fluid density down by time = 0
    density function = fluid_density_ramp
    gravitational constant = 9.79
end fluid_pressure

    #      --------- CONTACT MODEL --------------

 begin contact definition contact_defn

    begin enforcement options
       {if (time_integration=="explicit")}
       momentum balance iterations = 20
       {endif}
    end

    contact surface clay_A_master contains SS_clay_A_master
    contact surface clay_A_slave  contains SS_clay_A_slave
    contact surface clay_B_master contains SS_clay_B_master
    contact surface clay_B_slave  contains SS_clay_B_slave
    contact surface clay_D_master contains SS_clay_D_master
    contact surface clay_D_slave  contains SS_clay_D_slave
    contact surface clay_E_master contains SS_clay_E_master
    contact surface clay_E_slave  contains SS_clay_E_slave
    contact surface clay_F_master contains SS_clay_F_master
    contact surface clay_F_slave  contains SS_clay_F_slave
    contact surface clay_G_master contains SS_clay_G_master
    contact surface clay_G_slave  contains SS_clay_G_slave
    contact surface clay_H_master contains SS_clay_H_master
    contact surface clay_H_slave  contains SS_clay_H_slave
    contact surface clay_I_master contains SS_clay_I_master
    contact surface clay_I_slave  contains SS_clay_I_slave
    contact surface clay_J_master contains SS_clay_J_master
    contact surface clay_J_slave  contains SS_clay_J_slave
    contact surface clay_K_master contains SS_clay_K_master
    contact surface clay_K_slave  contains SS_clay_K_slave
    contact surface clay_L_master contains SS_clay_L_master
    contact surface clay_L_slave  contains SS_clay_L_slave
    contact surface clay_M_master contains SS_clay_M_master
    contact surface clay_M_slave  contains SS_clay_M_slave

    begin interaction defaults
       general contact = on
       constraint formulation = face_face
    end

    begin constant friction model clay_seam_model
       friction coefficient = {clay_seam_friction}
    end

    begin constant friction model clay_seam_modelF
       friction coefficient = {clay_seam_frictionF}
    end

    begin interaction clay_A
       surfaces = clay_A_master clay_A_slave
       {if (tied_A=="yes")}
       friction model = tied
```

```
   {else}
   friction model = clay_seam_model
   {endif}
end interaction

begin interaction clay_B
   surfaces = clay_B_master clay_B_slave
   {if (tied_B=="yes")}
   friction model = tied
   {else}
   friction model = clay_seam_model
   {endif}
end interaction

begin interaction clay_D
   surfaces = clay_D_master clay_D_slave
   {if (tied_D=="yes")}
   friction model = tied
   {else}
   friction model = clay_seam_model
   {endif}
end interaction

begin interaction clay_E
   surfaces = clay_E_master clay_E_slave
   {if (tied_E=="yes")}
   friction model = tied
   {else}
   friction model = clay_seam_model
   {endif}
end interaction

begin interaction clay_F
   surfaces = clay_F_master clay_F_slave
   {if (tied_F=="yes")}
   friction model = tied
   {else}
   friction model = clay_seam_modelF
   {endif}
end interaction

begin interaction clay_G
   surfaces = clay_G_master clay_G_slave
   {if (tied_G=="yes")}
   friction model = tied
   {else}
   friction model = clay_seam_model
   {endif}
end interaction

begin interaction clay_H
   surfaces = clay_H_master clay_H_slave
   {if (tied_H=="yes")}
   friction model = tied
   {else}
   friction model = clay_seam_model
   {endif}
end interaction

begin interaction clay_I
   surfaces = clay_I_master clay_I_slave
   {if (tied_I=="yes")}
   friction model = tied
   {else}
   friction model = clay_seam_model
   {endif}
end interaction
```

```
begin interaction clay_J
   surfaces = clay_J_master clay_J_slave
   {if (tied_J=="yes")}
   friction model = tied
   {else}
   friction model = clay_seam_model
   {endif}
end interaction

begin interaction clay_K
   surfaces = clay_K_master clay_K_slave
   {if (tied_K=="yes")}
   friction model = tied
   {else}
   friction model = clay_seam_model
   {endif}
end interaction

begin interaction clay_L
   surfaces = clay_L_master clay_L_slave
   {if (tied_L=="yes")}
   friction model = tied
   {else}
   friction model = clay_seam_model
   {endif}
end interaction

begin interaction clay_M
   surfaces = clay_M_master clay_M_slave
   {if (tied_M=="yes")}
   friction model = tied
   {else}
   friction model = clay_seam_model
   {endif}
end interaction

begin constant friction model salt_to_salt_friction_model
   friction coefficient = {salt_salt_friction}
end

begin contact surface room_surf
   surface = SS_room_surf
end

begin interaction room_surf_to_room_surf
   surfaces = room_surf room_surf
   friction model = salt_to_salt_friction_model
end

begin interaction room_surf_to_clay_F_master
   surfaces = room_surf clay_F_master
   friction model = salt_to_salt_friction_model
end

begin interaction room_surf_to_clay_F_slave
   surfaces = room_surf clay_F_slave
   friction model = salt_to_salt_friction_model
end

{if (horizon=="upper")}
begin interaction room_surf_to_clay_G_master
   surfaces = room_surf clay_G_master
   friction model = salt_to_salt_friction_model
end

begin interaction room_surf_to_clay_G_slave
   surfaces = room_surf clay_G_slave
   friction model = salt_to_salt_friction_model
```

```
   end
   {endif}

   {if (iswaste=="waste")}
   begin constant friction model salt_to_waste_friction_model
      friction coefficient = {salt_waste_friction}
   end

   begin contact surface homogenized_can_block_surf
      surface = SS_homogenized_can_block_exposed_surf
   end

   begin interaction room_surf_to_waste_surf
      surfaces = room_surf homogenized_can_block_surf
      friction model = salt_to_waste_friction_model
   end
   {endif}

   begin dash options
      subdivision level = 3
   end

end contact definition contact_defn

#--------- Initial Conditions ---------

begin initial condition
   block = b_halite b_arg_halite b_polyhalite b_anhydrite
   #It is important to initialize unrotated_stress and not stress, because
   #stress is just an output that gets calculated as needed, while
   #unrotated_stress gets stored and used by the constitutive models.
   #As of November 2015, initializing stress does nothing.
   initialize variable name = unrotated_stress
   variable type = element
   subroutine real parameter: top = 52.87
   subroutine real parameter: bot = -54.19
   subroutine real parameter: p1 = -13.57e6
   subroutine real parameter: po = -15.97e6
   subroutine real parameter: kvert_xx = 1.0
   subroutine real parameter: kvert_yy = 1.0
   subroutine real parameter: kvert_zz = 1.0
   subroutine real parameter: kvert_xy = 0.0
   subroutine real parameter: kvert_yz = 0.0
   subroutine real parameter: kvert_zx = 0.0
   subroutine string parameter: dir = Z
   element block subroutine = geo_is
end initial condition

{if (time_integration=="explicit")}
#--------- Viscoplastic Rate Scaling ---------

# See note above stored_time_function.
begin user variable stored_time
   type = global real length = 1
   global operator = min
   initial value = -0.5
end

begin user variable mat_time
   type = global real length = 1
   global operator = min
   #edit the following line for restart runs!
   initial value = -0.01
end

begin user variable vp_rate_scale_factor
   type = global real length = 1
   global operator = min
```

```
   initial value = 0.02
end
{endif}

#--------- User Output Variable Definitions ----------

begin user output
   compute element el_avg_stress as average of element cauchy_stress
   compute element el_avg_mean_stress as average of element hydrostatic_stress
   compute element el_avg_eq_stress as average of element eq_stress
   compute element el_avg_eq_tr_strain as average of element eq_tr_strain
   compute element el_avg_eq_vp_strain as average of element eq_vp_strain
   compute element el_avg_log_strain as average of element unrotated_log_strain
end user output

begin user output
   node set = NS_roof_ctr
   compute global roof_disp as average of nodal displacement
end

begin user output
   node set = NS_floor_ctr
   compute global floor_disp as average of nodal displacement
end

begin user output
   node set = NS_right_wall_ctr
   compute global right_wall_disp as average of nodal displacement
end

begin user variable room_volume
   type = global real length = 1
   global operator = sum
   initial value = 3.64275014400e+03   # W (10.06) * L (91.44) * H (3.96)
end user variable

begin user output
   {if (horizon=="lower")}
   surface = SS_room_surf SS_clay_F_master SS_clay_F_slave
   {elseif (horizon=="upper")}
   surface = SS_room_surf SS_clay_F_master SS_clay_F_slave SS_clay_G_master SS_clay_G_slave
   {endif}
   surface subroutine = aupst_cavity_volume
   subroutine string parameter: outputVarName = room_volume
   subroutine real parameter: cavitysymmetrypoint_x = 0.0
   subroutine real parameter: cavitysymmetrypoint_y = 0.0 #0.5
   {if (horizon=="lower")}
   subroutine real parameter: cavitysymmetrypoint_z = -4.41
   {elseif (horizon=="upper")}
   subroutine real parameter: cavitysymmetrypoint_z = -1.98
   {endif}
   subroutine real parameter: volumeScale = {274.32/element_thickness}
   # volumeScale is 1.5 (correction factor)*2 (for W symmetry)*91.44 (L) * (1/element_thickness)
   ↪  (converts volume per element thickness to volume per unit thickness)
   compute at every step
end

begin user variable cstrn_off
   type = global real length = 1
   global operator = sum
   initial value = 0.0
end user variable

{if (iswaste=="waste")}
begin user output
  block = b_homogenized_can_block
  compute global waste_sum as sum of element volume
end
```

```
 begin user output
   compute global waste_volume from expression "waste_sum*2*87.85/{element_thickness}"
   # waste_volume = waste_sum * 2 (for symmetry) * 87.85 (for length of waste in room) *
   ↪  (1/element_thickness) (converts volume per element thickness to volume per unit thickness)
 end
 {endif}

{if (time_integration=="explicit")}
 begin user output
    block = b_halite b_arg_halite
    compute global vp_rate_scale_factor as function vp_rate_scale_factor_function
    # Although vp_scale_factor is really a global variable, it needs to be at the integration points
    # so the material model can read it.
    compute element vp_rate_scale_factor(1) as function vp_rate_scale_factor_broadcast_function
    compute element vp_rate_scale_factor(2) as function vp_rate_scale_factor_broadcast_function
    compute element vp_rate_scale_factor(3) as function vp_rate_scale_factor_broadcast_function
    compute element vp_rate_scale_factor(4) as function vp_rate_scale_factor_broadcast_function
    compute element vp_rate_scale_factor(5) as function vp_rate_scale_factor_broadcast_function
    compute element vp_rate_scale_factor(6) as function vp_rate_scale_factor_broadcast_function
    compute element vp_rate_scale_factor(7) as function vp_rate_scale_factor_broadcast_function
    compute element vp_rate_scale_factor(8) as function vp_rate_scale_factor_broadcast_function
    compute at every step
 end

 begin user output
    compute global mat_time as function mat_time_function
    # See note above stored_time_function.  Note that stored_time must be calculated
    # AFTER other functions that use it.
    compute global stored_time as function stored_time_function
    compute at every step
 end
 {endif}

 #--------- Results Output ---------

 begin results output output_1
    database name = efiles/%B-r.e
    database type = exodusII
    {if (time_integration=="implicit")}
    At time 0, increment = {86400.0 * 365.25 * 10.0}
    At time {86400.0 * 365.25 * 2000.0}, increment = {86400.0 * 365.25 * 500.0}
    global time
    nodal variables = residual
    {else}
    #Output data every 10 years of material time from 0 to 1000 yrs
    ${yr = -10}
    {Loop(101)}
    ${yr += 10} yr
    additional times = {(-s_1_0 + sqrt(s_1_0^2 + 2 * s_ramp * (yr * 86400.0 * 365.25))) / s_ramp}
    {EndLoop}
    #Output data every 50 years of material time from 1000 to 2000 yrs
    {Loop(20)}
    ${yr += 50} yr
    additional times = {(-s_1_0 + sqrt(s_1_0^2 + 2 * s_ramp * (yr * 86400.0 * 365.25))) / s_ramp}
    {EndLoop}
    #Output data every 100 years of material time from 2000 to 5000 yrs
    {Loop(30)}
    ${yr += 100} yr
    additional times = {(-s_1_0 + sqrt(s_1_0^2 + 2 * s_ramp * (yr * 86400.0 * 365.25))) / s_ramp}
    {EndLoop}
    #Output data every 200 years of material time from 5000 to 10000 yrs
    {Loop(25)}
    ${yr += 200} yr
    additional times = {(-s_1_0 + sqrt(s_1_0^2 + 2 * s_ramp * (yr * 86400.0 * 365.25))) / s_ramp}
    {EndLoop}
    global time as mom_bal_time
    global mat_time
```

```
   {endif}
   global variables = room_volume
   nodal variables = displacement as disp
   nodal variables = contact_accumulated_slip
   nodal variables = contact_friction_index as cfi
   nodal variables = force_external as f_ext
   nodal variables = force_contact as f_cont
   nodal variables = contact_strength as cstr
   nodal variables = contact_status as cstat
   nodal variables = contact_normal_force_magnitude as cnfor
   nodal variables = pgas_room
   {if (clay_pressure=="yes")}
   nodal variables = pgas_clay
   {endif}
   element variables = el_avg_stress
   element variables = el_avg_mean_stress
   element variables = el_avg_eq_stress
   element variables = el_avg_eq_tr_strain
   element variables = el_avg_eq_vp_strain
   element variables = el_avg_log_strain
   element variables = log_strain_invariant_1
   element variables = effective_log_strain
   element variables = green_lagrange_strain_rate
   element variables = damage
   element variables = emax
   element variables = epvol
   element variables = eqps
   element variables = fa
   element variables = fb
   element variables = phi
   element variables = pwork
   element variables = von_mises
   element variables = cauchy_stress
end results output output_1

#--------- History Output ---------

begin history output output_3
   database name = history/%B-h.e
   database type = exodusII
   {if (time_integration=="implicit")}
   at time 0.0 increment = 8.64 #s
   at time 8.64 increment = 86.4 #s
   at time 86.4 increment = 864.0 #s
   at time 864 increment = 8640 #s
   at time 8640 increment = 86400 #s
   at time 86400 increment = 864000 #s
   at time 864000 increment = 8640000 #s
   at time {86400 * 365.25} increment = {86400 * 365.25} #s
   at time {86400 * 365.25 * 10.0} increment = {86400 * 365.25 * 10.0} #s
   at time {86400 * 365.25 * 1000.0} increment = {86400 * 365.25 * 50.0} #s
   global time
   {else}
   #Output data every 0.0864 sec of material time from 0 to 0.864 sec
   ${sec = -0.0864}
   {Loop(11)}
   ${sec += 0.0864} sec
   additional times = {(-s_1_0 + sqrt(s_1_0^2 + 2 * s_ramp * sec)) / s_ramp}
   {EndLoop}
   #Output data every 0.864 sec of material time from 0.864 to 8.64 sec
   {Loop(9)}
   ${sec += 0.864} sec
   additional times = {(-s_1_0 + sqrt(s_1_0^2 + 2 * s_ramp * sec)) / s_ramp}
   {EndLoop}
   #Output data every 8.64 sec of material time from 8.64 to 86.4 sec
   {Loop(9)}
   ${sec += 8.64} sec
   additional times = {(-s_1_0 + sqrt(s_1_0^2 + 2 * s_ramp * sec)) / s_ramp}
```

```
{EndLoop}
#Output data every 86.4 sec of material time from 86.4 to 864 sec
{Loop(9)}
${sec += 86.4} sec
additional times = {(-s_1_0 + sqrt(s_1_0^2 + 2 * s_ramp * sec)) / s_ramp}
{EndLoop}
#Output data every 864 sec of material time from 864 to 8640 sec
{Loop(9)}
${sec += 864.0} sec
additional times = {(-s_1_0 + sqrt(s_1_0^2 + 2 * s_ramp * sec)) / s_ramp}
{EndLoop}
#Output data every 8640 sec of material time from 8640 to 86400 sec
{Loop(9)}
${sec += 8640.0} sec
additional times = {(-s_1_0 + sqrt(s_1_0^2 + 2 * s_ramp * sec)) / s_ramp}
{EndLoop}
#Output data every day = 86400 sec of material time from 1 day to 10 days
{Loop(9)}
${sec += 86400.0} sec
additional times = {(-s_1_0 + sqrt(s_1_0^2 + 2 * s_ramp * sec)) / s_ramp}
{EndLoop}
#Output data every 10 days of material time from 10 days to 1 yr
{Loop(34)}
${sec += 864000.0} sec
additional times = {(-s_1_0 + sqrt(s_1_0^2 + 2 * s_ramp * sec)) / s_ramp}
{EndLoop}
#Output data at 1 year
${sec = 86400.0*365.25} sec
${yr  = 1} yr
additional times = {(-s_1_0 + sqrt(s_1_0^2 + 2 * s_ramp * sec)) / s_ramp}
#Output data every 1 yrs = 86400.0*365.25 sec of material time from 1 yr to 10 yrs
{Loop(9)}
${sec += 86400.0*365.25} sec
${yr  += 1} yr
additional times = {(-s_1_0 + sqrt(s_1_0^2 + 2 * s_ramp * sec)) / s_ramp}
{EndLoop}
#Output data every 10 yrs = 10*86400.0*365.25 sec of material time from 10 yr to 1000 yrs
{Loop(99)}
${sec += 10*86400.0*365.25} sec
${yr  += 10} yr
additional times = {(-s_1_0 + sqrt(s_1_0^2 + 2 * s_ramp * sec)) / s_ramp}
{EndLoop}
#Output data every 50 years of material time from 1000 to 2000 yrs
{Loop(20)}
${yr += 50} yr
additional times = {(-s_1_0 + sqrt(s_1_0^2 + 2 * s_ramp * (yr * 86400.0 * 365.25))) / s_ramp}
{EndLoop}
#Output data every 100 years of material time from 2000 to 5000 yrs
{Loop(30)}
${yr += 100} yr
additional times = {(-s_1_0 + sqrt(s_1_0^2 + 2 * s_ramp * (yr * 86400.0 * 365.25))) / s_ramp}
{EndLoop}
#Output data every 200 years of material time from 5000 to 10000 yrs
{Loop(25)}
${yr += 200} yr
additional times = {(-s_1_0 + sqrt(s_1_0^2 + 2 * s_ramp * (yr * 86400.0 * 365.25))) / s_ramp}
{EndLoop}
global time as mom_bal_time
global mat_time
global timestep as tstep
{endif}
global wall_clock_time as run_time
global vp_rate_scale_factor
global roof_disp
global floor_disp
global right_wall_disp
global room_volume
{if (iswaste=="waste")}
```

```
   global waste_volume
   {endif}
   {if (horizon=="lower")}
   face pressure nearest location 0.19 0.0 -2.43 as roof_pressure
   {elseif (horizon=="upper")}
   face pressure nearest location 0.1934615 0.0 0.0 as roof_pressure
   {endif}
end history output output_3

#--------- Heartbeat Output ---------

begin heartbeat output heartbeat_presto
   stream name = %B.hb
   append = off
   precision = 10
   legend = on
   {if (time_integration=="implicit")}
   at time 0.0 increment = 8.64 #s
   at time 8.64 increment = 86.4 #s
   at time 86.4 increment = 864.0 #s
   at time 864 increment = 8640 #s
   at time 8640 increment = 86400 #s
   at time 86400 increment = 864000 #s
   at time 864000 increment = 8640000 #s
   at time {86400 * 365.25} increment = {86400 * 365.25} #s
   at time {86400 * 365.25 * 10.0} increment = {86400 * 365.25 * 10.0} #s
   at time {86400 * 365.25 * 1000.0} increment = {86400 * 365.25 * 50.0} #s
   {else}
   #Output data every 0.0864 sec of material time from 0 to 0.864 sec
   ${sec = -0.0864}
   {Loop(11)}
   ${sec += 0.0864} sec
   additional times = {(-s_1_0 + sqrt(s_1_0^2 + 2 * s_ramp * sec)) / s_ramp}
   {EndLoop}

   #Output data every 0.864 sec of material time from 0.864 to 8.64 sec
   {Loop(9)}
   ${sec += 0.864} sec
   additional times = {(-s_1_0 + sqrt(s_1_0^2 + 2 * s_ramp * sec)) / s_ramp}
   {EndLoop}

   #Output data every 8.64 sec of material time from 8.64 to 86.4 sec
   {Loop(9)}
   ${sec += 8.64} sec
   additional times = {(-s_1_0 + sqrt(s_1_0^2 + 2 * s_ramp * sec)) / s_ramp}
   {EndLoop}

   #Output data every 86.4 sec of material time from 86.4 to 864 sec
   {Loop(9)}
   ${sec += 86.4} sec
   additional times = {(-s_1_0 + sqrt(s_1_0^2 + 2 * s_ramp * sec)) / s_ramp}
   {EndLoop}

   #Output data every 864 sec of material time from 864 to 8640 sec
   {Loop(9)}
   ${sec += 864.0} sec
   additional times = {(-s_1_0 + sqrt(s_1_0^2 + 2 * s_ramp * sec)) / s_ramp}
   {EndLoop}

   #Output data every 8640 sec of material time from 8640 to 86400 sec
   {Loop(9)}
   ${sec += 8640.0} sec
   additional times = {(-s_1_0 + sqrt(s_1_0^2 + 2 * s_ramp * sec)) / s_ramp}
   {EndLoop}

   #Output data every day = 86400 sec of material time from 1 day to 10 days
   {Loop(9)}
   ${sec += 86400.0} sec
```

```
   additional times = {(-s_1_0 + sqrt(s_1_0^2 + 2 * s_ramp * sec)) / s_ramp}
   {EndLoop}

   #Output data every 10 days of material time from 10 days to 1 yr
   {Loop(34)}
   ${sec += 864000.0} sec
   additional times = {(-s_1_0 + sqrt(s_1_0^2 + 2 * s_ramp * sec)) / s_ramp}
   {EndLoop}

   #Output data at 1 year
   ${sec = 86400.0*365.25} sec
   ${yr  = 1} yr
   additional times = {(-s_1_0 + sqrt(s_1_0^2 + 2 * s_ramp * sec)) / s_ramp}

   #Output data every 1 yrs = 86400.0*365.25 sec of material time from 1 yr to 10 yrs
   {Loop(9)}
   ${sec += 86400.0*365.25} sec
   ${yr  += 1} yr
   additional times = {(-s_1_0 + sqrt(s_1_0^2 + 2 * s_ramp * sec)) / s_ramp}
   {EndLoop}

   #Output data every 10 yrs = 10*86400.0*365.25 sec of material time from 10 yr to 1000 yrs
   {Loop(99)}
   ${sec += 10*86400.0*365.25} sec
   ${yr  += 10} yr
   additional times = {(-s_1_0 + sqrt(s_1_0^2 + 2 * s_ramp * sec)) / s_ramp}
   {EndLoop}

   #Output data every 50 years of material time from 1000 to 2000 yrs
   {Loop(20)}
   ${yr += 50} yr
   additional times = {(-s_1_0 + sqrt(s_1_0^2 + 2 * s_ramp * (yr * 86400.0 * 365.25))) / s_ramp}
   {EndLoop}

   #Output data every 100 years of material time from 2000 to 5000 yrs
   {Loop(30)}
   ${yr += 100} yr
   additional times = {(-s_1_0 + sqrt(s_1_0^2 + 2 * s_ramp * (yr * 86400.0 * 365.25))) / s_ramp}
   {EndLoop}

   #Output data every 200 years of material time from 5000 to 10000 yrs
   {Loop(25)}
   ${yr += 200} yr
   additional times = {(-s_1_0 + sqrt(s_1_0^2 + 2 * s_ramp * (yr * 86400.0 * 365.25))) / s_ramp}
   {EndLoop}
   {endif}
   global time as mom_bal_time
   global mat_time
   global timestep as tstep
   global wall_clock_time as run_time
   global vp_rate_scale_factor
   global room_volume
   {if (iswaste=="waste")}
   global waste_volume
   {endif}
   {if (horizon=="lower")}
   face pressure nearest location 0.19 0.0 -2.43 as roof_pressure
   {elseif (horizon=="upper")}
   face pressure nearest location 0.1934615 0.0 0.0 as roof_pressure
   {endif}
   global roof_disp
   global floor_disp
   global right_wall_disp
   labels = off
   timestamp format = ""
end heartbeat output heartbeat_presto

#--------- Restart ---------
```

```
         begin restart data restart_1
            database name = restart/%B.rsout
            overwrite = True
            at wall time 0.0h increment = 11.95h
         end restart data restart_1

   {if (time_integration=="implicit")}

        includefile include/mySolver.in

      end adagio region SmRegion.1

   end adagio procedure The_Procedure.1

   includefile include/equationSolvers.in

   {else}
      end presto region SmRegion.1

   end presto procedure The_Procedure.1
   {endif}

end sierra WIPP Isothermal Disposal Room
```

C.2.2.1. salt-md_viscoplastic-cal_3b.txt

```
begin property specification for material halite

    density = 2300.0

    begin parameters for model md_viscoplastic

        #Intact salt parameters
        #(These parameters correspond to Cal 3B in SAND2018-12601 and Reedlunn et al. (2022).)
        bulk modulus  = 20.7e9 # Pa  compute bulk modulus from E=31e+09 Pa and nu = 0.25
        shear modulus = 12.4e9  # Pa
        a0            = 5.617e1 # 1/sec
        q0/R          = 5123 # K
        n0            = 1.595
        a1            = 8.386e22 # 1/sec
        q1/R          = 12580.5 # K = 25000 cal / mol / 1.9872035 cal / (mol K)
        n1            = 5.5
        b1            = 6.086e6 # 1/sec
        a2            = 4.415e16 # 1/sec
        q2/R          = 5123 # K
        n2            = 6.279
        b2            = 3.034e-2 # 1/sec
        sigma_g       = 20570000.0 # Pa
        q             = 5335.0
        m0            = 0.9201
        k0            = 5.277e-2
        c0            = 8.882e-3 # 1/K
        m1            = 5.282
        k1            = 3.052e12
        c1            = 8.882e-3 # 1/K
        alpha_h       = 3.367
        beta_h        = -0.6838
        alpha_r       = 0.58
        a             = 16.0
        alpha         = 45.0e-6
    end parameters for model md_viscoplastic

end property specification for material halite
```

C.2.2.2. anhydrite-cal_4.txt

```
begin property specification for material anhydrite
    density = 2300.0 # kg / m^3
    #Sierra/SM needs to have elastic parameters defined with these names, so we repeat
    #the values in the "begin parameters ..." block.
    bulk modulus = 83.4444444e9 # Pa = bulk modulus
    shear modulus = 27814814814 # Pa = shear modulus

    #These Drucker-Prager parameters came from SAND97-0795, Table 6, except it does not
    #mention a dilation angle.  They almost certainly used the soil and foam model, which
    #has a dilatation angle of 0 degrees.  Here we have switched to associated flow.
    #The Drucker-Prager yield function is often written as phi = sqrt(J_2) + a * I_1 - C
    #B0 = bulk modulus = 83.4444444e9 Pa
    #G0 = shear modulus = 27814814814 Pa
    #C = 1.35
    #a = 0.45
    #alpha = dilatation angle = 24.227745 deg = atan(0.45)

    #Reduce Kayenta to Drucker-Prager
    begin parameters for model kayenta
        B0 = 83.4444444e9   # Pa = bulk modulus
        G0 = 27814814814    # Pa = shear modulus
        J3TYPE = 1          # Sets the dependence on J_3.  J3TYPE = 1 is a Von-Mises dependence.
        A1 = 1350000        # Pa
        A2 = 0.0
        A3 = 0.0
        A4 = 0.45
        RK = 1.0
        P0 = -1.0e99        # Put the compression cap at virtually infinity
        P1 = 0.0            # No cap
        P2 = 0.0            # No cap
        P3 = 0.0            # Zero porosity
        CR = 0.001          # Minimize the size of the curved part of the cap
        HC = 0.0            # Disable kinematic hardening
        RN = 0.0            # Disable kinematic hardening
    end parameters for model kayenta
end property specification for material anhydrite
```

C.2.2.3. polyhalite-cal_1.txt

```
begin definition for function polyhalite_pressure_volstrain_function
    type is piecewise linear
    ordinate is volumetric_strain
    abscissa is pressure
    begin values
        -1  -6.583333333e+10 # -65.83333333 GPa
        0  0
        1  6.583333333e+10 # 65.83333333 GPa = bulk modulus = E / (3*(1-2*nu)), where E = 55.3 GPa and nu =
        ↪  0.36
    end values
end definition for function polyhalite_pressure_volstrain_function

begin property specification for material polyhalite

    #These parameters came from SAND97-0796, Pages A-40 through A-41, Section 2.5.2

    #The yield function for this model is
    #phi = sqrt(3*J_2) - (a0 + a1 * p + a2 * p^2)
    #This model has a Drucker-Prager yield surface if a2 = 0
    #The Drucker-Prager yield function is often written as
    #phi = sqrt(J_2) + a * I_1 - C
    #Thus, we can write a0 and a1 in terms of a and C
```

```
    density = 2300.0
    begin parameters for model soil_foam
        poissons ratio  = 0.36
        youngs modulus  = 5.53e+10 # Pa
        a0              = 2459512.147 # Pa = sqrt(3) * C, where C = 1.42 MPa
        a1              = 2.457780096 # unitless = 3 * sqrt(3) * a, where a = 0.473
        a2              = 0.0
        pressure cutoff = -1000000.0 # Pa
        pressure function = polyhalite_pressure_volstrain_function
    end parameters for model soil_foam
end property specification for material polyhalite
```

C.2.2.4. foamDamageModel_F3.txt

```
   ###
   ### Material property definitions
   ###
   ##
   ##  Input block for Container
   ##  N, kg, m, seconds, C  Stress: Pa,  Temperature: C
   ##
   ##

   begin property specification for material homogenized_can_block
      density = 580.0              ## kg/m^3
      thermal engineering strain function = container_Thermal
      begin parameters for model foam_damage
         youngs modulus    = 4000.0e6   ## locked up Pa
         poissons ratio    =  0.30
         phi               =   0.175   ## volume fraction solids
         flow rate         =  1.000
         power exponent    =  1.000
         tensile strength  =  100.0e6 ## high so no fail in tension
         adam              =  1.000
         bdam              =  0.330
         youngs function   =  container_Modulus
         poissons function =  container_PR
         rate function     =  container_Rate
         exponent function =  container_Expo
         shear hardening function = container_Shear
         hydro hardening function = container_Hydro
         beta function            = container_Beta
         youngs phi function      = container_E
         poissons phi function    = container_Constant
         damage function          = container_Damage
      end parameters for model foam_damage
   end property specification for material homogenized_can_block

   begin definition for function container_Damage
      type is piecewise linear
      begin values
          0.00000     0.000
          0.50000     0.000
          0.60000     0.000
        100.00000     0.000
      end values
   end definition for function container_Damage

   ## flow direction 1 = radial, 0 = associated
   begin definition for function container_Beta
      type is piecewise linear
      begin values
         0.000   0.7
         0.200   0.7
         0.250   0.65
```

```
      0.30    0.55
      0.35    0.4
      0.40    0.22
      0.45    0.15
      0.50    0.075
      0.640   0.0
      1.000   0.0
      10.00   0.0
   end values
end definition for function container_Beta
##
## from unloading slopes (function values are multiplied x reference value above)
##
begin definition for function container_E
   type is piecewise linear
   begin values
       0.000    0.01
       0.250    0.015
       0.400    0.025
       0.500    0.075
       0.650    0.128
       1.000    0.500
       2.000    1.000
     100.000    1.000
   end values
end definition for function container_E

begin definition for function container_PR
   type is constant
   begin values
      1.000
   end values
end definition for function container_PR

begin definition for function container_Constant
   type is constant
   begin values
      1.0
   end values
end definition for function container_Constant

# Eliminated thermal strains and temperature dependence of the Young's
# modulus, so that temperature changes have no effect on the model, except
# to change the viscoplastic rate scaling via the container_Rate value when
# explicit time integration is being used.

begin definition for function container_Thermal
   type is piecewise linear
   ordinate is strain
   abscissa is temperature
   begin values
      -500.0    -0.0
         0.0     0.0
       500.0     0.0
   end values
end definition for function container_Thermal

begin definition for function container_Modulus
   type is piecewise linear
   ordinate is temperature
   abscissa is time
   begin values
       -1.0e5          1.0
        2.0e2          1.0
        1.3e5          1.0
   end values
end definition for function container_Modulus
```

```
# parameter "h" in \dot(\lambda) = exp(h) * < \sigma^* / a - 1 >
# (see equation 9 in SAND2015-4352)
# (Note we are using h to speed up the viscoplastic strain rate according to
# d(\lambda) / d(t^(mb)) = s * exp(h_r) * < \sigma^* / a - 1 >,
# where t^(mb) is the momentum balance time, t is material time,
# s = d(t)/d(t^(mb)) is the vp_rate_scale_factor, and h_r is the real value
# for h.  To pull s into exp(), we use s * exp(h_r) = exp(h_r + ln(s)), hence
# the expression below.)
# (Note that the expression below appears to use natural log of time, but the
# foam damage model treats "t" as temperature, and we elsewhere set temperature
# equal to the vp_rate_scale_factor "s".)
# (Note that if one tells Sierra/SM to evaluate the container_Rate for output
# purposes, then the output will treat the "t" as momentum balance time, not
# temperature.  This means the output evaluation of the container_Rate function
# and the foam damage model evalation of the container_Rate function will
# disagree, but it does not mean something went wrong in the simulation.)
   begin definition for function container_Rate
      type is analytic
      {if (time_integration=="explicit" && s_ramp!=0.0)}
        evaluate expression = " -55.0 + ln(t) "
      {else}
        evaluate expression = " -55.0 "
      {endif}
   end definition for function container_Rate

# parameter "n"
   begin definition for function container_Expo
      type is constant
      begin values
         23.0
     end values
   end definition for function container_Expo

   begin function container_Shear
      type is piecewise linear
      x scale  = 1.12
      begin values
         0.00      0.02e6
         0.10      0.02e6
         0.25      0.02e6
         0.30      0.02e6
         0.35      0.04e6
         0.40      0.07e6
         0.42      0.12e6
         0.44      0.19e6
         0.45      0.22e6
         0.50      0.36e6
         0.52      0.46e6
         0.55      0.72e6
         0.60      1.32e6
         0.62      1.74e6
         0.65      2.80e6
         0.70      4.42e6
         0.80     10.52e6
         0.90     14.62e6
         1.00     30.00e6
        10.00    500.00e6
       100.00   1600.00e6
      end values
   end function

   begin function container_Hydro
      type is piecewise linear
      x scale  = 1.12
      begin values
         0.00     0.012e6
         0.25     0.012e6
         0.30     0.036e6
```

```
        0.40     0.132e6
        0.45     0.240e6
        0.50     0.480e6
        0.60     1.440e6
        0.70    12.000e6
        0.80    45.600e6
        0.90    84.000e6
        1.00   168.000e6
       10.00   960.000e6
      100.00  9600.000e6
      end values
   end function

   ###
   ### end of input block for container material
   ###
```

C.2.2.5. soil_and_foam.txt

```
begin definition for function homogenized_can_block_pressure_volstrain_function
    #These parameters came from SAND97-0796, Table 8
    type is piecewise linear
    ordinate is volumetric_strain # unitless
    abscissa is pressure # Pa
    begin values
        0       0
        0.510   1.53e6
        0.631   2.03e6
        0.719   2.53e6
        0.786   3.03e6
        0.838   3.53e6
        0.881   4.03e6
        0.942   4.93e6
        1.14    12.0e6
    end values
end definition for function homogenized_can_block_pressure_volstrain_function

begin property specification for material homogenized_can_block

    density = 559.5 #kg / m^3, see SAND97-0796, Table 5
    #These parameters came from SAND97-0796, Table 7

    #The yield function for this model is
    #phi = sqrt(3*J_2) - (a0 + a1 * p + a2 * p^2)
    #This model has a Drucker-Prager yield surface if a2 = 0
    #The Drucker-Prager yield function is often written as
    #phi = sqrt(J_2) + a * I_1 - C
    #Thus, we can write a0 and a1 in terms of a and C

    begin parameters for model soil_foam
        bulk modulus      = 222.0e6 # Pa, this value matches SAND97-0796, Table 7, but it should be bulk
        ↪  modulus = 333.0e6 according to Weatherby et al. (1991)
        two mu            = 333.0e6 # Pa, this value matches SAND97-0796, Table 7, but it should be mu =
        ↪  222.0e6 according to Weatherby et al. (1991)
        a0                = 1.0e6 # Pa
        a1                = 3.0 # unitless
        a2                = 0.0
        pressure cutoff   = 0.0 # Pa
        pressure function = homogenized_can_block_pressure_volstrain_function
    end parameters for model soil_foam

    begin parameters for model elastic
        youngs modulus = 0.1e9 # Pa
        poissons ratio = 0.33
    end parameters for model elastic
```

```
end property specification for material homogenized_can_block
```

APPENDIX D. New Porosity Response Surface Raw Data

Using the current gas storage volume of the disposal room $V_g = V_r - V_{sw}$ as discussed in Section 2.3.2 and the relation $V_{sw} = V_{w0}(1 - \phi_{w0})$ for the solid volume of the waste, the Eulerian porosity Eq. (3.1) may be written in the form,

$$\phi_E = 1 - \frac{V_{w0}(1 - \phi_{w0})}{V_r}. \tag{D.1}$$

The initial volume of the waste $V_{w0} = 1{,}728$ m^3 (see Section 2.2.2) and the initial waste porosity ϕ_{w0} (see Table 2-3) are both constants. The current volume of the disposal room V_r is numerically computed as described in Appendix B.1 and is a direct output variable of Sierra/SM used to post-process the Eulerian porosity via Eq. (D.1). The Eulerian porosity data is tabulated in Table D-1.

The Lagrangian porosity ϕ_L is related to the Eulerian porosity by the transform Eq. (3.3). Again, the only post-processing variable needed is the current volume of the disposal room V_r directly output from Sierra/SM. The Lagrangian porosity data is tabulated in Table D-2.

The gas pressure p_g in the disposal room is computed using the ideal gas law Eq. (2.4). It is coupled to the disposal room volume V_r and is a direct output of Sierra/SM tabulated in Table D-3.

Table D-1. Eulerian porosity data at each gas generation factor, f

Time [years]	Porosity f=0.0	f=0.025	f=0.05	f=0.07	f=0.085	f=0.1	f=0.125	f=0.15	f=0.175
6.5144e-11	0.91673	0.91673	0.91673	0.91673	0.91673	0.91673	0.91673	0.91673	0.91673
3.9006e-09	0.91673	0.91673	0.91673	0.91673	0.91673	0.91673	0.91673	0.91673	0.91673
7.3573e-09	0.91673	0.91673	0.91673	0.91673	0.91673	0.91673	0.91673	0.91673	0.91673
1.184e-08	0.91673	0.91673	0.91673	0.91673	0.91673	0.91673	0.91673	0.91673	0.91673
1.7348e-08	0.91673	0.91673	0.91673	0.91673	0.91673	0.91673	0.91673	0.91673	0.91673
2.3883e-08	0.91673	0.91673	0.91673	0.91673	0.91673	0.91673	0.91673	0.91673	0.91673
3.1443e-08	0.91673	0.91673	0.91673	0.91673	0.91673	0.91673	0.91673	0.91673	0.91673
6.028e-08	0.91673	0.91673	0.91673	0.91673	0.91673	0.91673	0.91673	0.91673	0.91673
9.835e-08	0.91673	0.91673	0.91673	0.91673	0.91673	0.91673	0.91673	0.91673	0.91673
1.2886e-07	0.91673	0.91673	0.91673	0.91673	0.91673	0.91673	0.91673	0.91673	0.91673
1.4565e-07	0.91673	0.91673	0.91673	0.91673	0.91673	0.91673	0.91673	0.91673	0.91673
1.8232e-07	0.91673	0.91673	0.91673	0.91673	0.91673	0.91673	0.91673	0.91673	0.91673
2.0219e-07	0.91673	0.91673	0.91673	0.91673	0.91673	0.91673	0.91673	0.91673	0.91673
2.4501e-07	0.91673	0.91673	0.91673	0.91673	0.91673	0.91673	0.91673	0.91673	0.91673
2.6796e-07	0.91673	0.91673	0.91673	0.91673	0.91673	0.91673	0.91673	0.91673	0.91673
2.9194e-07	0.91673	0.91673	0.91673	0.91673	0.91673	0.91673	0.91673	0.91673	0.91673
5.8812e-07	0.91673	0.91673	0.91673	0.91673	0.91673	0.91673	0.91673	0.91673	0.91673
8.5649e-07	0.91672	0.91672	0.91672	0.91672	0.91672	0.91672	0.91672	0.91672	0.91672
1.1265e-06	0.91672	0.91672	0.91672	0.91672	0.91672	0.91672	0.91672	0.91672	0.91672
1.4335e-06	0.91672	0.91672	0.91672	0.91672	0.91672	0.91672	0.91672	0.91672	0.91672
1.7175e-06	0.91672	0.91672	0.91672	0.91672	0.91672	0.91672	0.91672	0.91672	0.91672
1.9632e-06	0.91672	0.91672	0.91672	0.91672	0.91672	0.91672	0.91672	0.91672	0.91672
2.2253e-06	0.91672	0.91672	0.91672	0.91672	0.91672	0.91672	0.91672	0.91672	0.91672
2.5038e-06	0.91672	0.91672	0.91672	0.91672	0.91672	0.91672	0.91672	0.91672	0.91672
2.7988e-06	0.91672	0.91672	0.91672	0.91672	0.91672	0.91672	0.91672	0.91672	0.91672
5.534e-06	0.91672	0.91672	0.91672	0.91672	0.91672	0.91672	0.91672	0.91672	0.91672
8.3869e-06	0.91672	0.91672	0.91672	0.91672	0.91672	0.91672	0.91672	0.91672	0.91672
1.1065e-05	0.91672	0.91672	0.91672	0.91672	0.91672	0.91672	0.91672	0.91672	0.91672
1.3774e-05	0.91672	0.91672	0.91672	0.91672	0.91672	0.91672	0.91672	0.91672	0.91672
1.6595e-05	0.91672	0.91672	0.91672	0.91672	0.91672	0.91672	0.91672	0.91672	0.91672
1.9279e-05	0.91671	0.91671	0.91671	0.91671	0.91671	0.91671	0.91671	0.91671	0.91671

2.2164e-05	0.91671	0.91671	0.91671	0.91671	0.91671	0.91671	0.91671	0.91671	0.91671
2.4797e-05	0.91671	0.91671	0.91671	0.91671	0.91671	0.91671	0.91671	0.91671	0.91671
2.7578e-05	0.91671	0.91671	0.91671	0.91671	0.91671	0.91671	0.91671	0.91671	0.91671
5.5141e-05	0.9167	0.9167	0.9167	0.9167	0.9167	0.9167	0.9167	0.9167	0.9167
8.2429e-05	0.91669	0.91669	0.91669	0.91669	0.91669	0.91669	0.91669	0.91669	0.91669
0.0001099	0.91668	0.91668	0.91668	0.91668	0.91668	0.91668	0.91668	0.91668	0.91668
0.00013757	0.91667	0.91667	0.91667	0.91667	0.91667	0.91667	0.91667	0.91667	0.91667
0.00016483	0.91666	0.91666	0.91666	0.91666	0.91666	0.91666	0.91666	0.91666	0.91666
0.00019204	0.91666	0.91666	0.91666	0.91666	0.91666	0.91666	0.91666	0.91666	0.91666
0.00021998	0.91665	0.91665	0.91665	0.91665	0.91665	0.91665	0.91665	0.91665	0.91665
0.00024696	0.91664	0.91664	0.91664	0.91664	0.91664	0.91664	0.91664	0.91664	0.91664
0.00027475	0.91664	0.91664	0.91664	0.91664	0.91664	0.91664	0.91664	0.91664	0.91664
0.00054827	0.91659	0.91659	0.91659	0.91659	0.91659	0.91659	0.91659	0.91659	0.91659
0.00082322	0.91654	0.91654	0.91654	0.91654	0.91654	0.91654	0.91654	0.91654	0.91654
0.0010961	0.9165	0.9165	0.9165	0.9165	0.9165	0.9165	0.9165	0.9165	0.9165
0.0013709	0.91646	0.91646	0.91646	0.91646	0.91646	0.91646	0.91646	0.91646	0.91646
0.001645	0.91643	0.91643	0.91643	0.91643	0.91643	0.91643	0.91643	0.91643	0.91643
0.0019181	0.9164	0.9164	0.9164	0.9164	0.9164	0.9164	0.9164	0.9164	0.9164
0.0021932	0.91638	0.91638	0.91638	0.91638	0.91638	0.91638	0.91638	0.91638	0.91638
0.0024663	0.91636	0.91636	0.91636	0.91636	0.91636	0.91636	0.91636	0.91636	0.91636
0.0027412	0.91634	0.91634	0.91634	0.91634	0.91634	0.91634	0.91634	0.91634	0.91634
0.0054803	0.91622	0.91622	0.91622	0.91622	0.91622	0.91622	0.91622	0.91622	0.91622
0.0082175	0.91617	0.91617	0.91617	0.91617	0.91617	0.91617	0.91617	0.91617	0.91617
0.010955	0.91609	0.91609	0.91609	0.91609	0.91609	0.91609	0.91609	0.91609	0.91609
0.013697	0.91601	0.91601	0.91601	0.91601	0.91601	0.91601	0.91601	0.91601	0.91601
0.016434	0.91593	0.91593	0.91593	0.91593	0.91593	0.91593	0.91593	0.91593	0.91593
0.01917	0.91588	0.91588	0.91588	0.91588	0.91588	0.91588	0.91588	0.91588	0.91588
0.021907	0.91584	0.91584	0.91584	0.91584	0.91584	0.91584	0.91584	0.91584	0.91584
0.024649	0.91582	0.91582	0.91582	0.91582	0.91582	0.91582	0.91582	0.91582	0.91582
0.027387	0.9158	0.9158	0.9158	0.9158	0.9158	0.9158	0.9158	0.9158	0.9158
0.054771	0.91554	0.91554	0.91554	0.91554	0.91554	0.91554	0.91554	0.91554	0.91554
0.082145	0.91525	0.91525	0.91525	0.91525	0.91525	0.91525	0.91525	0.91525	0.91525
0.10952	0.91503	0.91503	0.91503	0.91503	0.91503	0.91503	0.91503	0.91503	0.91503
0.13692	0.91482	0.91482	0.91482	0.91482	0.91482	0.91482	0.91482	0.91482	0.91482
0.16428	0.91465	0.91465	0.91465	0.91465	0.91465	0.91465	0.91465	0.91465	0.91465
0.19168	0.91453	0.91453	0.91453	0.91453	0.91453	0.91453	0.91453	0.91453	0.91453
0.21905	0.91442	0.91442	0.91442	0.91442	0.91442	0.91442	0.91442	0.91442	0.91442
0.24644	0.91434	0.91434	0.91434	0.91434	0.91434	0.91434	0.91434	0.91434	0.91434
0.27382	0.91427	0.91427	0.91427	0.91427	0.91427	0.91427	0.91427	0.91427	0.91427
0.3012	0.91421	0.91421	0.91421	0.91421	0.91421	0.91421	0.91421	0.91421	0.91421
0.32858	0.91415	0.91415	0.91415	0.91415	0.91415	0.91415	0.91415	0.91415	0.91415
0.35594	0.91411	0.91411	0.91411	0.91411	0.91411	0.91411	0.91411	0.91411	0.91411
0.38333	0.91406	0.91406	0.91406	0.91406	0.91406	0.91406	0.91406	0.91406	0.91406
0.41071	0.91402	0.91402	0.91402	0.91402	0.91402	0.91402	0.91402	0.91402	0.91402
0.43808	0.91398	0.91398	0.91398	0.91398	0.91398	0.91398	0.91398	0.91398	0.91398
0.46547	0.91395	0.91395	0.91395	0.91395	0.91395	0.91395	0.91395	0.91395	0.91395
0.49283	0.91391	0.91391	0.91391	0.91391	0.91391	0.91391	0.91391	0.91391	0.91391
0.52022	0.91388	0.91388	0.91388	0.91388	0.91388	0.91388	0.91388	0.91388	0.91388
0.54761	0.91385	0.91385	0.91385	0.91385	0.91385	0.91385	0.91385	0.91385	0.91385
0.57498	0.91381	0.91381	0.91381	0.91381	0.91381	0.91381	0.91381	0.91381	0.91381
0.60236	0.91378	0.91378	0.91378	0.91378	0.91378	0.91378	0.91378	0.91378	0.91378
0.62976	0.91375	0.91375	0.91375	0.91375	0.91375	0.91375	0.91375	0.91375	0.91375
0.6571	0.91371	0.91371	0.91371	0.91371	0.91371	0.91371	0.91371	0.91371	0.91371
0.68451	0.91368	0.91368	0.91368	0.91368	0.91368	0.91368	0.91368	0.91368	0.91368
0.71186	0.91364	0.91364	0.91364	0.91364	0.91364	0.91364	0.91364	0.91364	0.91364
0.73924	0.91361	0.91361	0.91361	0.91361	0.91361	0.91361	0.91361	0.91361	0.91361
0.76662	0.91357	0.91357	0.91357	0.91357	0.91357	0.91357	0.91357	0.91357	0.91357
0.79402	0.91353	0.91353	0.91353	0.91353	0.91353	0.91353	0.91353	0.91353	0.91353
0.82141	0.9135	0.9135	0.9135	0.9135	0.9135	0.9135	0.9135	0.9135	0.9135
0.84875	0.91346	0.91346	0.91346	0.91346	0.91346	0.91346	0.91346	0.91346	0.91346
0.87617	0.91342	0.91342	0.91342	0.91342	0.91342	0.91342	0.91342	0.91342	0.91342
0.90355	0.91338	0.91338	0.91338	0.91338	0.91338	0.91338	0.91338	0.91338	0.91338
0.93091	0.91333	0.91334	0.91334	0.91334	0.91334	0.91334	0.91334	0.91334	0.91334
0.95828	0.91329	0.91329	0.91329	0.91329	0.91329	0.91329	0.91329	0.91329	0.91329
1	0.91323	0.91323	0.91323	0.91323	0.91323	0.91323	0.91323	0.91323	0.91323
2.0001	0.9118	0.9118	0.9118	0.9118	0.9118	0.9118	0.9118	0.9118	0.9118
3.0001	0.91047	0.91047	0.91047	0.91047	0.91047	0.91047	0.91047	0.91047	0.91047
4.0001	0.90914	0.90914	0.90914	0.90914	0.90914	0.90914	0.90914	0.90914	0.90914
5.0001	0.90781	0.90781	0.90781	0.90782	0.90782	0.90782	0.90782	0.90782	0.90782
6.0001	0.90648	0.90648	0.90648	0.90648	0.90649	0.90649	0.90649	0.90649	0.90649
7.0001	0.90514	0.90514	0.90514	0.90514	0.90514	0.90514	0.90515	0.90515	0.90515
8.0001	0.90378	0.90378	0.90378	0.90379	0.90379	0.90379	0.90379	0.9038	0.9038
9.0001	0.90241	0.90241	0.90241	0.90242	0.90242	0.90242	0.90242	0.90243	0.90243
10	0.90101	0.90102	0.90102	0.90103	0.90103	0.90103	0.90104	0.90104	0.90105
20	0.88589	0.88591	0.88594	0.88595	0.88597	0.88598	0.886	0.88602	0.88605
30	0.86929	0.86935	0.86941	0.86946	0.8695	0.86954	0.8696	0.86966	0.86972
40	0.84921	0.84936	0.8495	0.84962	0.8497	0.84979	0.84993	0.85007	0.85021
50	0.82597	0.82626	0.82655	0.82678	0.82696	0.82713	0.82741	0.82769	0.82797
60	0.79744	0.79802	0.7986	0.79906	0.7994	0.79974	0.8003	0.80085	0.8014
70	0.76282	0.76389	0.76495	0.76578	0.7664	0.76701	0.76802	0.76901	0.76999
80	0.72023	0.72224	0.72421	0.72575	0.72688	0.728	0.72984	0.73164	0.7334
90	0.66757	0.67118	0.67465	0.67733	0.67929	0.6812	0.6843	0.6873	0.6902
100	0.60361	0.60957	0.61526	0.61963	0.62289	0.62609	0.63124	0.63621	0.64097
110	0.53524	0.54396	0.55238	0.55883	0.5635	0.56802	0.57528	0.58222	0.58886
120	0.47608	0.48572	0.49519	0.50261	0.5081	0.51354	0.52243	0.53105	0.5394
130	0.43463	0.44329	0.45233	0.45988	0.46556	0.47114	0.48032	0.48932	0.49814
140	0.40863	0.41605	0.4238	0.43015	0.43504	0.44006	0.4487	0.4577	0.46675
150	0.38975	0.39678	0.40421	0.41022	0.41477	0.41935	0.42704	0.43491	0.44314
160	0.37537	0.3823	0.38951	0.39531	0.39972	0.40415	0.41163	0.41917	0.42674
170	0.36376	0.37074	0.37802	0.38385	0.3882	0.39256	0.39991	0.40726	0.41468
180	0.35429	0.36134	0.3687	0.37459	0.37899	0.38339	0.39073	0.39809	0.4054
190	0.34647	0.35357	0.36102	0.36698	0.37144	0.37592	0.38336	0.39076	0.39813

200	0.34009	0.34714	0.35465	0.36068	0.3652	0.36973	0.37732	0.38485	0.39229
210	0.33503	0.34181	0.34931	0.35543	0.36002	0.36461	0.37232	0.38	0.38756
220	0.33157	0.3375	0.34485	0.35101	0.35566	0.36033	0.36815	0.37599	0.3837
230	0.32948	0.33424	0.34114	0.34727	0.35197	0.35672	0.36468	0.37266	0.38052
240	0.32801	0.33217	0.33812	0.34413	0.34884	0.35365	0.36177	0.36987	0.3779
250	0.3269	0.33079	0.3358	0.34151	0.34619	0.35105	0.35931	0.36756	0.37575
260	0.32601	0.32976	0.33426	0.33934	0.34396	0.34883	0.35723	0.36564	0.374
270	0.32529	0.32897	0.3332	0.33762	0.34208	0.34695	0.35547	0.36405	0.37257
280	0.32467	0.32834	0.33242	0.3364	0.34052	0.34536	0.35399	0.36274	0.37142
290	0.32415	0.32781	0.33183	0.33555	0.33925	0.34401	0.35275	0.36166	0.3705
300	0.32369	0.32737	0.33135	0.33493	0.33829	0.34289	0.35171	0.36078	0.36978
310	0.32328	0.327	0.33097	0.33446	0.3376	0.34195	0.35084	0.36007	0.36923
320	0.32293	0.3267	0.33067	0.33411	0.3371	0.34118	0.35011	0.35951	0.36881
330	0.32261	0.32643	0.33041	0.33383	0.33674	0.34056	0.34952	0.35906	0.36851
340	0.32232	0.3262	0.33021	0.33362	0.33647	0.34008	0.34904	0.35873	0.36831
350	0.32206	0.326	0.33004	0.33347	0.33628	0.33974	0.34865	0.35848	0.36819
360	0.32182	0.32582	0.32991	0.33334	0.33614	0.3395	0.34835	0.35831	0.36814
370	0.3216	0.32566	0.3298	0.33325	0.33604	0.33933	0.34813	0.35821	0.36814
380	0.32139	0.32553	0.3297	0.33319	0.33598	0.33922	0.34796	0.35816	0.36818
390	0.3212	0.3254	0.32962	0.33314	0.33594	0.33915	0.34785	0.35816	0.36826
400	0.32102	0.32529	0.32957	0.33312	0.33593	0.33912	0.34778	0.35819	0.36836
410	0.32085	0.3252	0.32952	0.3331	0.33593	0.33912	0.34776	0.35825	0.36848
420	0.32069	0.32511	0.32949	0.3331	0.33594	0.33913	0.34776	0.35834	0.36862
430	0.32055	0.32503	0.32946	0.33311	0.33597	0.33916	0.3478	0.35844	0.36878
440	0.32041	0.32496	0.32945	0.33313	0.33601	0.33921	0.34785	0.35855	0.36894
450	0.32027	0.3249	0.32944	0.33316	0.33606	0.33926	0.34792	0.35868	0.36911
460	0.32015	0.32485	0.32944	0.33319	0.33611	0.33933	0.34801	0.35882	0.36928
470	0.32003	0.3248	0.32944	0.33323	0.33617	0.3394	0.3481	0.35896	0.36946
480	0.31991	0.32476	0.32945	0.33327	0.33623	0.33948	0.34821	0.35912	0.36965
490	0.3198	0.32472	0.32947	0.33332	0.3363	0.33957	0.34832	0.35927	0.36985
500	0.3197	0.32468	0.32949	0.33338	0.33638	0.33966	0.34844	0.35943	0.37004
510	0.31959	0.32465	0.32951	0.33343	0.33645	0.33975	0.34856	0.35959	0.37024
520	0.3195	0.32463	0.32954	0.33349	0.33653	0.33985	0.34869	0.35976	0.37045
530	0.3194	0.32461	0.32956	0.33355	0.33661	0.33995	0.34882	0.35993	0.37065
540	0.31931	0.32459	0.3296	0.33361	0.3367	0.34005	0.34896	0.36011	0.37086
550	0.31923	0.32457	0.32963	0.33368	0.33678	0.34016	0.3491	0.36029	0.37107
560	0.31914	0.32456	0.32967	0.33375	0.33687	0.34027	0.34924	0.36047	0.37129
570	0.31906	0.32455	0.32971	0.33382	0.33696	0.34037	0.34938	0.36065	0.3715
580	0.31899	0.32454	0.32975	0.33389	0.33705	0.34049	0.34952	0.36083	0.37172
590	0.31891	0.32454	0.32979	0.33396	0.33715	0.3406	0.34967	0.36102	0.37193
600	0.31884	0.32454	0.32984	0.33404	0.33724	0.34071	0.34981	0.3612	0.37215
610	0.31877	0.32454	0.32988	0.33411	0.33734	0.34082	0.34996	0.36139	0.3724
620	0.3187	0.32454	0.32993	0.33419	0.33743	0.34094	0.35011	0.36158	0.37277
630	0.31863	0.32454	0.32998	0.33426	0.33753	0.34106	0.35026	0.36177	0.37336
640	0.31857	0.32455	0.33003	0.33434	0.33763	0.34117	0.35042	0.36196	0.37428
650	0.3185	0.32455	0.33008	0.33442	0.33773	0.34129	0.35057	0.36215	0.37555
660	0.31844	0.32456	0.33013	0.3345	0.33782	0.34141	0.35072	0.36235	0.3771
670	0.31838	0.32457	0.33018	0.33458	0.33792	0.34153	0.35088	0.36254	0.37889
680	0.31832	0.32458	0.33023	0.33466	0.33802	0.34165	0.35103	0.36274	0.38087
690	0.31826	0.32459	0.33028	0.33474	0.33812	0.34177	0.35119	0.363	0.38301
700	0.3182	0.3246	0.33034	0.33482	0.33823	0.34189	0.35134	0.36342	0.38527
710	0.31815	0.32461	0.3304	0.3349	0.33833	0.34201	0.3515	0.3641	0.38763
720	0.31809	0.32463	0.33045	0.33499	0.33843	0.34213	0.35166	0.36509	0.39006
730	0.31804	0.32464	0.33051	0.33508	0.33854	0.34226	0.35182	0.36636	0.39255
740	0.31799	0.32466	0.33056	0.33516	0.33864	0.34238	0.35198	0.36785	0.39511
750	0.31794	0.32467	0.33062	0.33524	0.33875	0.34251	0.35214	0.36953	0.39772
760	0.31789	0.32469	0.33068	0.33533	0.33885	0.34263	0.3523	0.37137	0.40038
770	0.31784	0.32471	0.33074	0.33541	0.33896	0.34276	0.35247	0.37333	0.40306
780	0.31779	0.32473	0.33079	0.3355	0.33906	0.34289	0.35263	0.37539	0.40576
790	0.31775	0.32475	0.33085	0.33559	0.33917	0.34301	0.35282	0.37752	0.40846
800	0.3177	0.32477	0.33091	0.33567	0.33928	0.34314	0.35312	0.37972	0.41117
810	0.31766	0.32479	0.33097	0.33576	0.33938	0.34327	0.35364	0.38197	0.41388
820	0.31762	0.32481	0.33103	0.33585	0.33949	0.3434	0.35441	0.38426	0.41658
830	0.31757	0.32483	0.33109	0.33593	0.3396	0.34353	0.35543	0.3866	0.41928
840	0.31753	0.32486	0.33115	0.33602	0.33971	0.34366	0.35664	0.38898	0.42197
850	0.31749	0.32488	0.33121	0.33611	0.33982	0.34379	0.35802	0.39138	0.42463
860	0.31745	0.3249	0.33127	0.3362	0.33993	0.34392	0.35955	0.39381	0.42725
870	0.31741	0.32493	0.33134	0.33629	0.34004	0.34405	0.3612	0.39625	0.42979
880	0.31737	0.32495	0.3314	0.33638	0.34015	0.34418	0.36295	0.39869	0.43235
890	0.31733	0.32498	0.33146	0.33647	0.34026	0.34431	0.36477	0.40114	0.43497
900	0.3173	0.325	0.33152	0.33656	0.34037	0.34444	0.36665	0.40358	0.43759
910	0.31726	0.32503	0.33159	0.33665	0.34048	0.34458	0.36858	0.40602	0.44018
920	0.31722	0.32505	0.33165	0.33674	0.34059	0.34471	0.37055	0.40845	0.44276
930	0.31719	0.32508	0.33171	0.33683	0.3407	0.34485	0.37255	0.41087	0.44533
940	0.31715	0.3251	0.33178	0.33692	0.34082	0.34498	0.37458	0.41328	0.44787
950	0.31712	0.32513	0.33184	0.33702	0.34093	0.34513	0.37666	0.41568	0.45039
960	0.31709	0.32516	0.33191	0.33711	0.34104	0.3453	0.37876	0.41805	0.45288
970	0.31705	0.32518	0.33197	0.3372	0.34116	0.34561	0.38088	0.42034	0.45535
980	0.31702	0.32521	0.33204	0.33729	0.34127	0.34613	0.38302	0.42262	0.4578
990	0.31699	0.32524	0.3321	0.33739	0.34139	0.34684	0.38516	0.42494	0.46023
1000	0.31695	0.32527	0.33217	0.33748	0.3415	0.34773	0.38731	0.42729	0.46263
1050	0.3168	0.32541	0.3325	0.33795	0.34208	0.35396	0.39804	0.43884	0.47438
1100	0.31666	0.32556	0.33283	0.33842	0.34267	0.36184	0.40856	0.44995	0.48563
1150	0.31653	0.32572	0.33317	0.3389	0.34442	0.37039	0.41866	0.46063	0.49645
1200	0.31641	0.32587	0.33351	0.33939	0.34929	0.37934	0.42875	0.47092	0.50684
1250	0.3163	0.32593	0.33366	0.3396	0.3532	0.38549	0.43579	0.4783	0.51443
1300	0.31619	0.32597	0.33376	0.33975	0.35572	0.38923	0.44014	0.48299	0.51934
1350	0.31609	0.32601	0.33385	0.33988	0.35778	0.39212	0.44349	0.48659	0.52313
1400	0.316	0.32605	0.33394	0.34002	0.35966	0.39462	0.44633	0.48963	0.52631
1450	0.31591	0.32608	0.33403	0.34015	0.36144	0.3969	0.44888	0.49233	0.52912
1500	0.31583	0.32612	0.33412	0.34028	0.36318	0.39902	0.45124	0.49481	0.5317
1550	0.31575	0.32616	0.33421	0.34041	0.36492	0.40093	0.45349	0.49716	0.53411

1600	0.31567	0.32619	0.3343	0.34053	0.36666	0.40286	0.45564	0.4994	0.5364
1650	0.3156	0.32623	0.33439	0.34066	0.36839	0.40479	0.45773	0.50156	0.5386
1700	0.31553	0.32627	0.33447	0.34078	0.37013	0.40671	0.45977	0.50366	0.54073
1750	0.31546	0.3263	0.33456	0.34091	0.37186	0.40862	0.46177	0.50572	0.5428
1800	0.31539	0.32634	0.33465	0.34104	0.3736	0.41053	0.46374	0.50773	0.54483
1850	0.31533	0.32638	0.33473	0.34117	0.37533	0.41243	0.46569	0.50972	0.54682
1900	0.31527	0.32641	0.33482	0.34131	0.37705	0.4143	0.46761	0.51167	0.54878
1950	0.31521	0.32645	0.3349	0.3415	0.37877	0.41615	0.46951	0.5136	0.55071
2000	0.31515	0.32649	0.33499	0.34187	0.38049	0.41798	0.47139	0.51551	0.55261
2100	0.31504	0.32657	0.33515	0.34348	0.38389	0.4216	0.47511	0.51926	0.55635
2200	0.31493	0.32665	0.33532	0.3457	0.38726	0.42515	0.47876	0.52294	0.56001
2300	0.31484	0.32673	0.33548	0.34821	0.3906	0.42865	0.48236	0.52656	0.56359
2400	0.31475	0.3268	0.33565	0.35087	0.39392	0.43211	0.4859	0.53011	0.56711
2500	0.31466	0.32688	0.33581	0.35366	0.39704	0.43552	0.48939	0.53361	0.57057
2600	0.31458	0.32696	0.33597	0.35654	0.4002	0.43889	0.49283	0.53706	0.57396
2700	0.3145	0.32704	0.33613	0.35947	0.40341	0.44222	0.49623	0.54045	0.57731
2800	0.31443	0.32707	0.33622	0.36159	0.40581	0.44475	0.49889	0.54317	0.58003
2900	0.31435	0.32711	0.33629	0.36299	0.40747	0.44649	0.50079	0.54514	0.58203
3000	0.31429	0.32714	0.33636	0.36414	0.40881	0.44791	0.50233	0.54675	0.58367
3100	0.31422	0.32717	0.33642	0.36517	0.41001	0.44916	0.50367	0.54814	0.58509
3200	0.31416	0.3272	0.33648	0.36614	0.41111	0.45031	0.50489	0.5494	0.58637
3300	0.3141	0.32723	0.33654	0.36708	0.41216	0.45139	0.50603	0.55058	0.58757
3400	0.31404	0.32726	0.33661	0.36799	0.41317	0.45244	0.50713	0.55171	0.5887
3500	0.31399	0.32729	0.33666	0.36889	0.41415	0.45346	0.50819	0.55279	0.58979
3600	0.31394	0.32732	0.33672	0.36977	0.41512	0.45446	0.50923	0.55384	0.59084
3700	0.31388	0.32734	0.33678	0.37065	0.41608	0.45544	0.51025	0.55486	0.59187
3800	0.31383	0.32737	0.33683	0.37152	0.41702	0.45642	0.51125	0.55587	0.59287
3900	0.31378	0.3274	0.33689	0.37239	0.41796	0.45738	0.51224	0.55686	0.59386
4000	0.31373	0.32743	0.33694	0.37327	0.41889	0.45834	0.51322	0.55784	0.59483
4100	0.31369	0.32745	0.337	0.37414	0.41982	0.45929	0.51419	0.55881	0.59579
4200	0.31364	0.32748	0.33705	0.375	0.42074	0.46023	0.51516	0.55977	0.59674
4300	0.31359	0.32751	0.3371	0.37587	0.42166	0.46117	0.51611	0.56072	0.59768
4400	0.31354	0.32753	0.33716	0.37673	0.42257	0.46211	0.51706	0.56167	0.59862
4500	0.31349	0.32756	0.33721	0.37759	0.42348	0.46304	0.51801	0.56261	0.59954
4600	0.31345	0.32758	0.33726	0.37844	0.42438	0.46397	0.51895	0.56354	0.60046
4700	0.31342	0.32761	0.33732	0.37929	0.42528	0.46489	0.51988	0.56446	0.60137
4800	0.31338	0.32764	0.33737	0.38014	0.42618	0.46581	0.52081	0.56538	0.60227
4900	0.31334	0.32766	0.33742	0.38099	0.42708	0.46673	0.52174	0.5663	0.60317
5000	0.3133	0.32769	0.33747	0.38184	0.42797	0.46764	0.52266	0.56721	0.60406
5200	0.31323	0.32774	0.33757	0.38353	0.42974	0.46946	0.52449	0.56902	0.60584
5400	0.31316	0.32779	0.33767	0.38522	0.43151	0.47126	0.5263	0.57082	0.60759
5600	0.31309	0.32784	0.33777	0.38689	0.43326	0.47305	0.5281	0.57259	0.60932
5800	0.31302	0.32789	0.33787	0.38856	0.435	0.47482	0.52989	0.57435	0.61104
6000	0.31296	0.32794	0.33797	0.39022	0.43674	0.47658	0.53166	0.5761	0.61273
6200	0.3129	0.32798	0.33807	0.39177	0.43846	0.47833	0.53342	0.57782	0.61441
6400	0.31283	0.32803	0.33817	0.3933	0.44017	0.48007	0.53516	0.57954	0.61608
6600	0.31277	0.32808	0.33827	0.39495	0.44187	0.4818	0.53689	0.58124	0.61772
6800	0.31271	0.32813	0.33836	0.39661	0.44357	0.48352	0.5386	0.58292	0.61935
7000	0.31265	0.32818	0.33846	0.39829	0.44525	0.48523	0.5403	0.58459	0.62097
7200	0.3126	0.32823	0.33856	0.39995	0.44692	0.48692	0.54199	0.58625	0.62258
7400	0.31254	0.32827	0.33866	0.40159	0.44858	0.48861	0.54367	0.58789	0.62418
7600	0.31248	0.32832	0.33875	0.40321	0.45023	0.49028	0.54533	0.58952	0.62576
7800	0.31243	0.32837	0.33885	0.40482	0.45188	0.49195	0.54699	0.59113	0.62733
8000	0.31237	0.32842	0.33895	0.40641	0.45351	0.4936	0.54863	0.59274	0.62888
8200	0.31232	0.32847	0.33904	0.408	0.45514	0.49524	0.55026	0.59433	0.63042
8400	0.31226	0.32851	0.33914	0.40957	0.45675	0.49687	0.55187	0.5959	0.63195
8600	0.31221	0.32856	0.33924	0.41113	0.45836	0.49849	0.55348	0.59747	0.63346
8800	0.31217	0.32861	0.33933	0.41268	0.45995	0.5001	0.55507	0.59903	0.63496
9000	0.31212	0.32866	0.33943	0.41423	0.46154	0.5017	0.55665	0.60057	0.63645
9200	0.31207	0.32871	0.33958	0.41577	0.46312	0.50329	0.55822	0.6021	0.63792
9400	0.31202	0.32875	0.33998	0.4173	0.46468	0.50487	0.55978	0.60362	0.63939
9600	0.31198	0.3288	0.34097	0.41882	0.46625	0.50644	0.56133	0.60512	0.64084
9800	0.31193	0.32885	0.34219	0.42033	0.4678	0.508	0.56287	0.60661	0.64228
10000	0.31189	0.3289	0.3435	0.42184	0.46933	0.50955	0.5644	0.60809	0.64371

Time [years]	Porosity f=0.2	f=0.25	f=0.3	f=0.35	f=0.4	f=0.5	f=0.6	f=0.8	f=1.0
6.5144e-11	0.91673	0.91673	0.91673	0.91673	0.91673	0.91673	0.91673	0.91673	0.91673
3.9006e-09	0.91673	0.91673	0.91673	0.91673	0.91673	0.91673	0.91673	0.91673	0.91673
7.3573e-09	0.91673	0.91673	0.91673	0.91673	0.91673	0.91673	0.91673	0.91673	0.91673
1.184e-08	0.91673	0.91673	0.91673	0.91673	0.91673	0.91673	0.91673	0.91673	0.91673
1.7348e-08	0.91673	0.91673	0.91673	0.91673	0.91673	0.91673	0.91673	0.91673	0.91673
2.3883e-08	0.91673	0.91673	0.91673	0.91673	0.91673	0.91673	0.91673	0.91673	0.91673
3.1443e-08	0.91673	0.91673	0.91673	0.91673	0.91673	0.91673	0.91673	0.91673	0.91673
6.028e-08	0.91673	0.91673	0.91673	0.91673	0.91673	0.91673	0.91673	0.91673	0.91673
9.835e-08	0.91673	0.91673	0.91673	0.91673	0.91673	0.91673	0.91673	0.91673	0.91673
1.2886e-07	0.91673	0.91673	0.91673	0.91673	0.91673	0.91673	0.91673	0.91673	0.91673
1.4565e-07	0.91673	0.91673	0.91673	0.91673	0.91673	0.91673	0.91673	0.91673	0.91673
1.8232e-07	0.91673	0.91673	0.91673	0.91673	0.91673	0.91673	0.91673	0.91673	0.91673
2.0219e-07	0.91673	0.91673	0.91673	0.91673	0.91673	0.91673	0.91673	0.91673	0.91673
2.4501e-07	0.91673	0.91673	0.91673	0.91673	0.91673	0.91673	0.91673	0.91673	0.91673
2.6796e-07	0.91673	0.91673	0.91673	0.91673	0.91673	0.91673	0.91673	0.91673	0.91673
2.9194e-07	0.91673	0.91673	0.91673	0.91673	0.91673	0.91673	0.91673	0.91673	0.91673
5.8812e-07	0.91673	0.91673	0.91673	0.91673	0.91673	0.91673	0.91673	0.91673	0.91673
8.5649e-07	0.91672	0.91672	0.91672	0.91672	0.91672	0.91672	0.91672	0.91672	0.91672
1.1265e-06	0.91672	0.91672	0.91672	0.91672	0.91672	0.91672	0.91672	0.91672	0.91672
1.4335e-06	0.91672	0.91672	0.91672	0.91672	0.91672	0.91672	0.91672	0.91672	0.91672
1.7175e-06	0.91672	0.91672	0.91672	0.91672	0.91672	0.91672	0.91672	0.91672	0.91672
1.9632e-06	0.91672	0.91672	0.91672	0.91672	0.91672	0.91672	0.91672	0.91672	0.91672
2.2253e-06	0.91672	0.91672	0.91672	0.91672	0.91672	0.91672	0.91672	0.91672	0.91672
2.5038e-06	0.91672	0.91672	0.91672	0.91672	0.91672	0.91672	0.91672	0.91672	0.91672

2.7988e-06	0.91672	0.91672	0.91672	0.91672	0.91672	0.91672	0.91672	0.91672	0.91672
5.534e-06	0.91672	0.91672	0.91672	0.91672	0.91672	0.91672	0.91672	0.91672	0.91672
8.3869e-06	0.91672	0.91672	0.91672	0.91672	0.91672	0.91672	0.91672	0.91672	0.91672
1.1065e-05	0.91672	0.91672	0.91672	0.91672	0.91672	0.91672	0.91672	0.91672	0.91672
1.3774e-05	0.91672	0.91672	0.91672	0.91672	0.91672	0.91672	0.91672	0.91672	0.91672
1.6595e-05	0.91672	0.91672	0.91672	0.91672	0.91672	0.91672	0.91672	0.91672	0.91672
1.9279e-05	0.91671	0.91671	0.91671	0.91671	0.91671	0.91671	0.91671	0.91671	0.91671
2.2164e-05	0.91671	0.91671	0.91671	0.91671	0.91671	0.91671	0.91671	0.91671	0.91671
2.4797e-05	0.91671	0.91671	0.91671	0.91671	0.91671	0.91671	0.91671	0.91671	0.91671
2.7578e-05	0.91671	0.91671	0.91671	0.91671	0.91671	0.91671	0.91671	0.91671	0.91671
5.5141e-05	0.9167	0.9167	0.9167	0.9167	0.9167	0.9167	0.9167	0.9167	0.9167
8.2429e-05	0.91669	0.91669	0.91669	0.91669	0.91669	0.91669	0.91669	0.91669	0.91669
0.0001099	0.91668	0.91668	0.91668	0.91668	0.91668	0.91668	0.91668	0.91668	0.91668
0.00013757	0.91667	0.91667	0.91667	0.91667	0.91667	0.91667	0.91667	0.91667	0.91667
0.00016483	0.91666	0.91666	0.91666	0.91666	0.91666	0.91666	0.91666	0.91666	0.91666
0.00019204	0.91666	0.91666	0.91666	0.91666	0.91666	0.91666	0.91666	0.91666	0.91666
0.00021998	0.91665	0.91665	0.91665	0.91665	0.91665	0.91665	0.91665	0.91665	0.91665
0.00024696	0.91664	0.91664	0.91664	0.91664	0.91664	0.91664	0.91664	0.91664	0.91664
0.00027475	0.91664	0.91664	0.91664	0.91664	0.91664	0.91664	0.91664	0.91664	0.91664
0.00054827	0.91659	0.91659	0.91659	0.91659	0.91659	0.91659	0.91659	0.91659	0.91659
0.00082322	0.91654	0.91654	0.91654	0.91654	0.91654	0.91654	0.91654	0.91654	0.91654
0.0010961	0.9165	0.9165	0.9165	0.9165	0.9165	0.9165	0.9165	0.9165	0.9165
0.0013709	0.91646	0.91646	0.91646	0.91646	0.91646	0.91646	0.91646	0.91646	0.91646
0.001645	0.91643	0.91643	0.91643	0.91643	0.91643	0.91643	0.91643	0.91643	0.91643
0.0019181	0.9164	0.9164	0.9164	0.9164	0.9164	0.9164	0.9164	0.9164	0.9164
0.0021932	0.91638	0.91638	0.91638	0.91638	0.91638	0.91638	0.91638	0.91638	0.91638
0.0024663	0.91636	0.91636	0.91636	0.91636	0.91636	0.91636	0.91636	0.91636	0.91636
0.0027412	0.91634	0.91634	0.91634	0.91634	0.91634	0.91634	0.91634	0.91634	0.91634
0.0054803	0.91622	0.91622	0.91622	0.91622	0.91622	0.91622	0.91622	0.91622	0.91622
0.0082175	0.91617	0.91617	0.91617	0.91617	0.91617	0.91617	0.91617	0.91617	0.91617
0.010955	0.91609	0.91609	0.91609	0.91609	0.91609	0.91609	0.91609	0.91609	0.91609
0.013697	0.91601	0.91601	0.91601	0.91601	0.91601	0.91601	0.91601	0.91601	0.91601
0.016434	0.91593	0.91593	0.91593	0.91593	0.91593	0.91593	0.91593	0.91593	0.91593
0.01917	0.91588	0.91588	0.91588	0.91588	0.91588	0.91588	0.91588	0.91588	0.91588
0.021907	0.91584	0.91584	0.91584	0.91584	0.91584	0.91584	0.91584	0.91584	0.91584
0.024649	0.91582	0.91582	0.91582	0.91582	0.91582	0.91582	0.91582	0.91582	0.91582
0.027387	0.9158	0.9158	0.9158	0.9158	0.9158	0.9158	0.9158	0.9158	0.9158
0.054771	0.91554	0.91554	0.91554	0.91554	0.91554	0.91554	0.91554	0.91554	0.91554
0.082145	0.91525	0.91525	0.91525	0.91525	0.91525	0.91525	0.91525	0.91525	0.91525
0.10952	0.91503	0.91503	0.91503	0.91503	0.91503	0.91503	0.91503	0.91503	0.91503
0.13692	0.91482	0.91482	0.91482	0.91482	0.91482	0.91482	0.91482	0.91482	0.91482
0.16428	0.91465	0.91465	0.91465	0.91465	0.91465	0.91465	0.91465	0.91465	0.91465
0.19168	0.91453	0.91453	0.91453	0.91453	0.91453	0.91453	0.91453	0.91453	0.91453
0.21905	0.91442	0.91442	0.91442	0.91442	0.91442	0.91442	0.91442	0.91442	0.91442
0.24644	0.91434	0.91434	0.91434	0.91434	0.91434	0.91434	0.91434	0.91434	0.91434
0.27382	0.91427	0.91427	0.91427	0.91427	0.91427	0.91427	0.91427	0.91427	0.91427
0.3012	0.91421	0.91421	0.91421	0.91421	0.91421	0.91421	0.91421	0.91421	0.91421
0.32858	0.91415	0.91415	0.91415	0.91415	0.91415	0.91415	0.91415	0.91415	0.91415
0.35594	0.91411	0.91411	0.91411	0.91411	0.91411	0.91411	0.91411	0.91411	0.91411
0.38333	0.91406	0.91406	0.91406	0.91406	0.91406	0.91406	0.91406	0.91406	0.91406
0.41071	0.91402	0.91402	0.91402	0.91402	0.91402	0.91402	0.91402	0.91402	0.91402
0.43808	0.91398	0.91399	0.91399	0.91399	0.91399	0.91399	0.91399	0.91399	0.91399
0.46547	0.91395	0.91395	0.91395	0.91395	0.91395	0.91395	0.91395	0.91395	0.91395
0.49283	0.91391	0.91391	0.91391	0.91391	0.91391	0.91392	0.91392	0.91392	0.91392
0.52022	0.91388	0.91388	0.91388	0.91388	0.91388	0.91388	0.91388	0.91388	0.91388
0.54761	0.91385	0.91385	0.91385	0.91385	0.91385	0.91385	0.91385	0.91385	0.91385
0.57498	0.91381	0.91381	0.91381	0.91381	0.91381	0.91381	0.91381	0.91381	0.91381
0.60236	0.91378	0.91378	0.91378	0.91378	0.91378	0.91378	0.91378	0.91378	0.91378
0.62976	0.91375	0.91375	0.91375	0.91375	0.91375	0.91375	0.91375	0.91375	0.91375
0.6571	0.91371	0.91371	0.91371	0.91371	0.91371	0.91371	0.91371	0.91371	0.91371
0.68451	0.91368	0.91368	0.91368	0.91368	0.91368	0.91368	0.91368	0.91368	0.91368
0.71186	0.91364	0.91364	0.91364	0.91364	0.91364	0.91364	0.91364	0.91364	0.91364
0.73924	0.91361	0.91361	0.91361	0.91361	0.91361	0.91361	0.91361	0.91361	0.91361
0.76662	0.91357	0.91357	0.91357	0.91357	0.91357	0.91357	0.91357	0.91357	0.91357
0.79402	0.91353	0.91353	0.91353	0.91353	0.91353	0.91353	0.91353	0.91353	0.91354
0.82141	0.9135	0.9135	0.9135	0.9135	0.9135	0.9135	0.9135	0.9135	0.9135
0.84875	0.91346	0.91346	0.91346	0.91346	0.91346	0.91346	0.91346	0.91346	0.91346
0.87617	0.91342	0.91342	0.91342	0.91342	0.91342	0.91342	0.91342	0.91342	0.91342
0.90355	0.91338	0.91338	0.91338	0.91338	0.91338	0.91338	0.91338	0.91338	0.91338
0.93091	0.91334	0.91334	0.91334	0.91334	0.91334	0.91334	0.91334	0.91334	0.91334
0.95828	0.91329	0.91329	0.91329	0.91329	0.91329	0.91329	0.9133	0.9133	0.9133
1	0.91323	0.91323	0.91323	0.91323	0.91323	0.91323	0.91323	0.91323	0.91323
2.0001	0.9118	0.9118	0.91181	0.91181	0.91181	0.91181	0.91181	0.91181	0.91181
3.0001	0.91047	0.91047	0.91048	0.91048	0.91048	0.91048	0.91048	0.91048	0.91049
4.0001	0.90914	0.90914	0.90915	0.90915	0.90915	0.90915	0.90915	0.90916	0.90917
5.0001	0.90782	0.90782	0.90783	0.90783	0.90783	0.90784	0.90784	0.90785	0.90786
6.0001	0.90649	0.9065	0.9065	0.9065	0.90651	0.90651	0.90652	0.90653	0.90654
7.0001	0.90515	0.90516	0.90516	0.90517	0.90517	0.90518	0.90519	0.90521	0.90522
8.0001	0.9038	0.90381	0.90381	0.90382	0.90383	0.90384	0.90385	0.90387	0.9039
9.0001	0.90244	0.90244	0.90245	0.90246	0.90247	0.90248	0.9025	0.90252	0.90255
10	0.90105	0.90106	0.90107	0.90108	0.90109	0.90111	0.90112	0.90116	0.9012
20	0.88607	0.88611	0.88616	0.8862	0.88624	0.88633	0.88642	0.88659	0.88676
30	0.86978	0.8699	0.87003	0.87015	0.87027	0.87051	0.87075	0.87121	0.87167
40	0.85035	0.85063	0.85091	0.85118	0.85146	0.85199	0.85253	0.85358	0.8546
50	0.82825	0.8288	0.82935	0.82988	0.83041	0.83144	0.83245	0.83438	0.83622
60	0.80194	0.80301	0.80407	0.8051	0.80612	0.80808	0.80996	0.8135	0.81677
70	0.77095	0.77282	0.77464	0.7764	0.7781	0.78134	0.78445	0.79031	0.79562
80	0.73511	0.73841	0.74156	0.74456	0.74744	0.75285	0.75778	0.76658	0.77428
90	0.693	0.69835	0.7034	0.70814	0.71268	0.72106	0.72872	0.74214	0.75333
100	0.64553	0.65403	0.66187	0.66923	0.67607	0.68836	0.69907	0.71722	0.73236
110	0.59525	0.60718	0.61805	0.62829	0.63786	0.65496	0.66965	0.69379	0.71263
120	0.54747	0.56286	0.57689	0.5897	0.60156	0.62279	0.6414	0.67148	0.69491

130	0.50676	0.52361	0.53974	0.55493	0.56911	0.59428	0.6157	0.65131	0.67874
140	0.47562	0.49296	0.50963	0.52571	0.54105	0.56943	0.5939	0.63357	0.66448
150	0.4517	0.4693	0.48628	0.50273	0.5186	0.54844	0.5752	0.61837	0.65252
160	0.43448	0.45103	0.46815	0.48485	0.50093	0.5316	0.55962	0.60604	0.64236
170	0.42222	0.43767	0.45418	0.471	0.48721	0.51824	0.54696	0.59585	0.63386
180	0.41283	0.42797	0.44367	0.46037	0.47663	0.50786	0.53704	0.58755	0.62699
190	0.40554	0.4206	0.43596	0.45229	0.46857	0.49994	0.52934	0.58096	0.62159
200	0.39979	0.41485	0.43018	0.4462	0.4625	0.49398	0.52351	0.57585	0.61742
210	0.39517	0.41033	0.42576	0.44164	0.45799	0.48957	0.5192	0.57204	0.61434
220	0.39143	0.4068	0.42234	0.43825	0.45466	0.48638	0.51612	0.56931	0.61224
230	0.38838	0.404	0.41969	0.43577	0.45228	0.48414	0.51403	0.56747	0.61087
240	0.38591	0.4018	0.41767	0.43397	0.45063	0.48268	0.51272	0.56637	0.6101
250	0.38392	0.40009	0.41616	0.43267	0.44951	0.4818	0.51202	0.56587	0.60981
260	0.38232	0.39877	0.41505	0.43175	0.44877	0.4813	0.51172	0.56577	0.60984
270	0.38105	0.39779	0.41426	0.43113	0.44831	0.48108	0.51166	0.56587	0.61006
280	0.38006	0.39707	0.41372	0.43074	0.44808	0.48103	0.51174	0.56612	0.61047
290	0.37929	0.39656	0.41339	0.43054	0.448	0.48111	0.51192	0.56652	0.61121
300	0.37872	0.39622	0.41321	0.43047	0.44803	0.48127	0.51219	0.56724	0.6124
310	0.3783	0.39602	0.41315	0.4305	0.44816	0.4815	0.51256	0.56844	0.61405
320	0.37801	0.39594	0.41318	0.43061	0.44834	0.48179	0.5132	0.57015	0.61616
330	0.37783	0.39593	0.41328	0.43078	0.44858	0.48217	0.51435	0.57237	0.61869
340	0.37773	0.39599	0.41342	0.43099	0.44885	0.48278	0.51607	0.57503	0.62158
350	0.37771	0.3961	0.41362	0.43124	0.44916	0.48387	0.51833	0.5781	0.6248
360	0.37774	0.39624	0.41384	0.43152	0.44952	0.48556	0.52105	0.58149	0.62827
370	0.37782	0.39641	0.41408	0.43181	0.45004	0.4878	0.52419	0.58516	0.63195
380	0.37793	0.39661	0.41433	0.43214	0.45088	0.49051	0.52767	0.58905	0.63579
390	0.37806	0.39682	0.4146	0.43258	0.45227	0.49362	0.53142	0.5931	0.63968
400	0.37822	0.39705	0.41489	0.4332	0.45424	0.49706	0.5354	0.59726	0.64376
410	0.37839	0.39729	0.41519	0.43424	0.45669	0.50078	0.53953	0.60143	0.64792
420	0.37856	0.39754	0.41554	0.43585	0.45952	0.5047	0.54379	0.60575	0.65207
430	0.37875	0.3978	0.41602	0.43798	0.46269	0.50877	0.54812	0.61015	0.65624
440	0.37895	0.39806	0.41673	0.44051	0.46612	0.51297	0.55243	0.61451	0.66041
450	0.37916	0.39833	0.4179	0.44339	0.46978	0.51723	0.55678	0.61886	0.66455
460	0.37937	0.39861	0.4196	0.44654	0.4736	0.52155	0.56125	0.6232	0.66866
470	0.37959	0.3989	0.42174	0.44992	0.47754	0.52581	0.56571	0.62749	0.67272
480	0.37982	0.3993	0.42423	0.45349	0.48156	0.53007	0.57011	0.63173	0.67674
490	0.38004	0.39987	0.42701	0.4572	0.48564	0.53445	0.57449	0.63593	0.68069
500	0.38027	0.40081	0.43002	0.461	0.48975	0.53882	0.57883	0.64006	0.68459
510	0.38051	0.4022	0.43322	0.46486	0.49386	0.54312	0.58311	0.64414	0.68842
520	0.38074	0.40403	0.43658	0.46877	0.49788	0.54738	0.58734	0.64815	0.69218
530	0.38098	0.40618	0.44006	0.47271	0.50192	0.5516	0.59151	0.6521	0.69588
540	0.38122	0.40861	0.44363	0.47666	0.50605	0.55576	0.59562	0.65598	0.6995
550	0.38147	0.41126	0.44726	0.48057	0.51017	0.55988	0.59967	0.65979	0.70305
560	0.38183	0.41408	0.45092	0.48439	0.51422	0.56394	0.60366	0.66353	0.70654
570	0.38235	0.41703	0.45461	0.48828	0.51823	0.56795	0.60758	0.66721	0.70997
580	0.38322	0.42011	0.45831	0.49222	0.52221	0.5719	0.61144	0.67081	0.71333
590	0.38447	0.42329	0.46201	0.49611	0.52613	0.57579	0.61524	0.67436	0.71662
600	0.38607	0.42655	0.46565	0.49996	0.53	0.57962	0.61898	0.67784	0.71984
610	0.38795	0.42985	0.4692	0.50377	0.53383	0.5834	0.62265	0.68126	0.72301
620	0.39006	0.43318	0.47281	0.50753	0.5376	0.58711	0.62626	0.68461	0.72611
630	0.39236	0.43654	0.47647	0.51125	0.54132	0.59077	0.6298	0.6879	0.72914
640	0.3948	0.4399	0.4801	0.51492	0.54499	0.59437	0.63329	0.69113	0.73212
650	0.39736	0.44327	0.48369	0.51855	0.54862	0.59791	0.63672	0.6943	0.73504
660	0.40001	0.44662	0.48724	0.52213	0.55219	0.6014	0.64009	0.69741	0.7379
670	0.40274	0.44995	0.49076	0.52567	0.55572	0.60484	0.6434	0.70047	0.7407
680	0.40554	0.45318	0.49423	0.52917	0.55921	0.60822	0.64666	0.70346	0.74345
690	0.40841	0.4564	0.49766	0.53261	0.56264	0.61154	0.64986	0.7064	0.74615
700	0.41131	0.4597	0.50106	0.53602	0.56602	0.61482	0.65301	0.70929	0.74879
710	0.41424	0.46299	0.50441	0.53938	0.56936	0.61804	0.6561	0.71213	0.75138
720	0.41718	0.46625	0.50773	0.54269	0.57264	0.62121	0.65915	0.71491	0.75392
730	0.42013	0.46949	0.511	0.54596	0.57588	0.62434	0.66214	0.71764	0.75642
740	0.42308	0.47269	0.51423	0.54919	0.57908	0.62741	0.66508	0.72032	0.75886
750	0.42602	0.47586	0.51743	0.55238	0.58222	0.63044	0.66798	0.72295	0.76127
760	0.42896	0.47898	0.52058	0.55553	0.58533	0.63342	0.67083	0.72554	0.76362
770	0.43189	0.48208	0.52371	0.55863	0.58839	0.63636	0.67363	0.72808	0.76593
780	0.43478	0.48515	0.5268	0.56169	0.59141	0.63925	0.67639	0.73058	0.7682
790	0.43758	0.48818	0.52985	0.56471	0.59438	0.6421	0.6791	0.73304	0.77043
800	0.44037	0.49118	0.53286	0.5677	0.59732	0.64491	0.68177	0.73545	0.77262
810	0.44322	0.49415	0.53584	0.57064	0.60022	0.64768	0.6844	0.73782	0.77478
820	0.44609	0.49708	0.53878	0.57355	0.60307	0.65041	0.68698	0.74015	0.77689
830	0.44893	0.49999	0.54169	0.57642	0.60589	0.65309	0.68953	0.74245	0.77897
840	0.45174	0.50286	0.54456	0.57925	0.60867	0.65574	0.69204	0.7447	0.78101
850	0.45455	0.50571	0.5474	0.58205	0.61141	0.65835	0.69451	0.74692	0.78301
860	0.45732	0.50852	0.5502	0.58481	0.61411	0.66092	0.69694	0.74909	0.78498
870	0.46005	0.51131	0.55297	0.58753	0.61678	0.66345	0.69934	0.75124	0.78692
880	0.46276	0.51406	0.55571	0.59023	0.61941	0.66595	0.7017	0.75335	0.78882
890	0.46545	0.51679	0.55842	0.59289	0.622	0.66841	0.70402	0.75542	0.79069
900	0.46812	0.51949	0.56109	0.59552	0.62456	0.67083	0.70631	0.75746	0.79253
910	0.47077	0.52216	0.56374	0.59811	0.62708	0.67322	0.70857	0.75947	0.79434
920	0.47339	0.5248	0.56635	0.60068	0.62958	0.67558	0.71079	0.76145	0.79612
930	0.47598	0.52742	0.56893	0.60321	0.63204	0.6779	0.71298	0.76339	0.79787
940	0.47855	0.53001	0.57148	0.6057	0.63447	0.68019	0.71514	0.76531	0.79959
950	0.4811	0.53257	0.57401	0.60817	0.63687	0.68245	0.71726	0.76719	0.80128
960	0.48362	0.5351	0.5765	0.61061	0.63924	0.68468	0.71936	0.76904	0.80295
970	0.48612	0.5376	0.57897	0.61302	0.64158	0.68688	0.72142	0.77087	0.80459
980	0.4886	0.54008	0.58141	0.6154	0.64389	0.68905	0.72346	0.77267	0.80621
990	0.49106	0.54254	0.58383	0.61775	0.64617	0.69119	0.72547	0.77445	0.8078
1000	0.49349	0.54496	0.58621	0.62007	0.64842	0.6933	0.72744	0.77619	0.80936
1050	0.50534	0.55673	0.59776	0.6313	0.65928	0.70345	0.73693	0.78455	0.81685
1100	0.51666	0.56793	0.60868	0.64189	0.66951	0.71298	0.7458	0.79233	0.8238
1150	0.52749	0.57859	0.61904	0.65189	0.67915	0.72193	0.75411	0.79959	0.83028
1200	0.53786	0.58875	0.62889	0.66136	0.68826	0.73035	0.76192	0.80639	0.83632

1250	0.54556	0.59646	0.63648	0.66876	0.69546	0.73709	0.76824	0.81197	0.84132
1300	0.55062	0.60167	0.64169	0.67392	0.70053	0.74194	0.77283	0.81611	0.84507
1350	0.55453	0.6057	0.64576	0.67796	0.70452	0.74577	0.77649	0.81942	0.84809
1400	0.55781	0.60908	0.64916	0.68134	0.70785	0.74898	0.77956	0.82222	0.85064
1450	0.5607	0.61204	0.65212	0.68428	0.71075	0.75177	0.78223	0.82464	0.85286
1500	0.56333	0.61472	0.65479	0.68692	0.71334	0.75426	0.7846	0.82679	0.85482
1550	0.56577	0.61719	0.65724	0.68933	0.71571	0.75652	0.78674	0.82873	0.8566
1600	0.56809	0.61951	0.65953	0.69158	0.71791	0.75861	0.78872	0.83051	0.85822
1650	0.5703	0.62171	0.66169	0.69369	0.71997	0.76057	0.79057	0.83217	0.85972
1700	0.57243	0.62382	0.66375	0.69571	0.72193	0.76241	0.7923	0.83372	0.86113
1750	0.5745	0.62586	0.66575	0.69765	0.7238	0.76417	0.79395	0.83518	0.86245
1800	0.57652	0.62784	0.66768	0.69952	0.72561	0.76585	0.79553	0.83657	0.86371
1850	0.5785	0.62978	0.66955	0.70133	0.72735	0.76747	0.79704	0.8379	0.8649
1900	0.58044	0.63167	0.67138	0.70309	0.72904	0.76904	0.7985	0.83918	0.86604
1950	0.58235	0.63352	0.67316	0.70481	0.73069	0.77056	0.79991	0.84041	0.86714
2000	0.58424	0.63534	0.67492	0.70649	0.7323	0.77205	0.80128	0.8416	0.8682
2100	0.58793	0.63891	0.67833	0.70975	0.73542	0.7749	0.80392	0.84389	0.87022
2200	0.59154	0.64237	0.68164	0.7129	0.73843	0.77764	0.80643	0.84605	0.87213
2300	0.59506	0.64575	0.68486	0.71596	0.74134	0.78029	0.80885	0.84813	0.87395
2400	0.59852	0.64906	0.688	0.71894	0.74416	0.78285	0.81119	0.85012	0.87569
2500	0.60191	0.65229	0.69107	0.72184	0.74691	0.78533	0.81345	0.85204	0.87737
2600	0.60524	0.65547	0.69406	0.72468	0.7496	0.78775	0.81565	0.8539	0.87898
2700	0.60852	0.65858	0.697	0.72745	0.75222	0.7901	0.81778	0.85571	0.88054
2800	0.61122	0.66119	0.69949	0.72983	0.75448	0.79215	0.81966	0.8573	0.88193
2900	0.61324	0.66319	0.70143	0.73169	0.75628	0.7938	0.82119	0.85863	0.88309
3000	0.61489	0.66483	0.70304	0.73325	0.75778	0.7952	0.82249	0.85976	0.88409
3100	0.61633	0.66625	0.70443	0.73461	0.75909	0.79642	0.82363	0.86077	0.88498
3200	0.61762	0.66754	0.70569	0.73583	0.76027	0.79752	0.82465	0.86166	0.88577
3300	0.61882	0.66872	0.70684	0.73695	0.76135	0.79852	0.82559	0.86248	0.88649
3400	0.61995	0.66983	0.70791	0.73799	0.76236	0.79946	0.82646	0.86324	0.88716
3500	0.62103	0.67089	0.70893	0.73897	0.7633	0.80034	0.82727	0.86395	0.88778
3600	0.62207	0.6719	0.70991	0.73991	0.7642	0.80117	0.82804	0.86462	0.88837
3700	0.62308	0.67288	0.71085	0.74082	0.76507	0.80196	0.82877	0.86525	0.88892
3800	0.62407	0.67384	0.71176	0.74169	0.7659	0.80273	0.82947	0.86585	0.88945
3900	0.62504	0.67477	0.71266	0.74254	0.76671	0.80347	0.83015	0.86643	0.88996
4000	0.62599	0.67569	0.71353	0.74336	0.76749	0.80418	0.8308	0.86699	0.89044
4100	0.62693	0.67659	0.71438	0.74417	0.76826	0.80488	0.83144	0.86753	0.89091
4200	0.62787	0.67747	0.71522	0.74497	0.76901	0.80557	0.83206	0.86806	0.89137
4300	0.62879	0.67835	0.71605	0.74576	0.76975	0.80623	0.83267	0.86857	0.89181
4400	0.6297	0.67921	0.71687	0.74653	0.77048	0.80689	0.83327	0.86907	0.89224
4500	0.6306	0.68007	0.71767	0.74729	0.7712	0.80753	0.83385	0.86956	0.89267
4600	0.6315	0.68092	0.71847	0.74804	0.77191	0.80817	0.83443	0.87005	0.89308
4700	0.63239	0.68175	0.71926	0.74878	0.77261	0.80879	0.835	0.87052	0.89349
4800	0.63327	0.68259	0.72004	0.74952	0.7733	0.80941	0.83555	0.87098	0.89388
4900	0.63415	0.68341	0.72082	0.75025	0.77398	0.81002	0.8361	0.87144	0.89428
5000	0.63502	0.68423	0.72158	0.75096	0.77466	0.81062	0.83665	0.8719	0.89466
5200	0.63674	0.68585	0.7231	0.75238	0.776	0.81181	0.83772	0.87278	0.89542
5400	0.63845	0.68744	0.72459	0.75378	0.77731	0.81297	0.83876	0.87365	0.89615
5600	0.64014	0.68902	0.72607	0.75516	0.7786	0.81411	0.83979	0.8745	0.89687
5800	0.64181	0.69057	0.72752	0.75651	0.77987	0.81523	0.8408	0.87533	0.89758
6000	0.64346	0.69211	0.72895	0.75785	0.78113	0.81634	0.84179	0.87615	0.89827
6200	0.6451	0.69363	0.73037	0.75917	0.78236	0.81743	0.84276	0.87695	0.89895
6400	0.64671	0.69514	0.73177	0.76047	0.78358	0.8185	0.84372	0.87774	0.89962
6600	0.64831	0.69663	0.73315	0.76176	0.78478	0.81956	0.84467	0.87851	0.90028
6800	0.64989	0.6981	0.73451	0.76303	0.78596	0.82061	0.8456	0.87928	0.90092
7000	0.65146	0.69955	0.73586	0.76429	0.78713	0.82164	0.84652	0.88003	0.90156
7200	0.65301	0.70099	0.7372	0.76553	0.78829	0.82266	0.84743	0.88077	0.90219
7400	0.65455	0.70242	0.73852	0.76676	0.78943	0.82366	0.84833	0.88151	0.90281
7600	0.65608	0.70383	0.73983	0.76797	0.79056	0.82466	0.84922	0.88223	0.90342
7800	0.65759	0.70523	0.74112	0.76917	0.79168	0.82564	0.85009	0.88294	0.90402
8000	0.65908	0.70661	0.74241	0.77036	0.79279	0.82661	0.85095	0.88364	0.90462
8200	0.66056	0.70798	0.74368	0.77154	0.79388	0.82757	0.85181	0.88434	0.9052
8400	0.66203	0.70934	0.74493	0.7727	0.79496	0.82851	0.85265	0.88503	0.90578
8600	0.66349	0.71069	0.74617	0.77385	0.79603	0.82945	0.85348	0.8857	0.90636
8800	0.66493	0.71202	0.7474	0.77499	0.79709	0.83038	0.85431	0.88637	0.90692
9000	0.66636	0.71334	0.74862	0.77611	0.79814	0.83129	0.85512	0.88703	0.90748
9200	0.66778	0.71465	0.74982	0.77723	0.79917	0.8322	0.85592	0.88769	0.90803
9400	0.66919	0.71594	0.75102	0.77833	0.8002	0.8331	0.85672	0.88834	0.90858
9600	0.67058	0.71722	0.7522	0.77942	0.80121	0.83398	0.85751	0.88898	0.90911
9800	0.67196	0.71849	0.75337	0.78051	0.80221	0.83486	0.85828	0.88961	0.90964
10000	0.67333	0.71976	0.75453	0.78158	0.80321	0.83573	0.85905	0.89023	0.91017

Table D-2. Lagrangian porosity data at each gas generation factor, f

Time [years]	Porosity								
	f=0.0	f=0.025	f=0.05	f=0.07	f=0.085	f=0.1	f=0.125	f=0.15	f=0.175
6.5144e-11	0.91673	0.91673	0.91673	0.91673	0.91673	0.91673	0.91673	0.91673	0.91673
3.9006e-09	0.91673	0.91673	0.91673	0.91673	0.91673	0.91673	0.91673	0.91673	0.91673
7.3573e-09	0.91673	0.91673	0.91673	0.91673	0.91673	0.91673	0.91673	0.91673	0.91673
1.184e-08	0.91673	0.91673	0.91673	0.91673	0.91673	0.91673	0.91673	0.91673	0.91673
1.7348e-08	0.91673	0.91673	0.91673	0.91673	0.91673	0.91673	0.91673	0.91673	0.91673
2.3883e-08	0.91673	0.91673	0.91673	0.91673	0.91673	0.91673	0.91673	0.91673	0.91673
3.1443e-08	0.91673	0.91673	0.91673	0.91673	0.91673	0.91673	0.91673	0.91673	0.91673
6.028e-08	0.91673	0.91673	0.91673	0.91673	0.91673	0.91673	0.91673	0.91673	0.91673
9.835e-08	0.91673	0.91673	0.91673	0.91673	0.91673	0.91673	0.91673	0.91673	0.91673
1.2886e-07	0.91673	0.91673	0.91673	0.91673	0.91673	0.91673	0.91673	0.91673	0.91673
1.4565e-07	0.91673	0.91673	0.91673	0.91673	0.91673	0.91673	0.91673	0.91673	0.91673

1.8232e-07	0.91673	0.91673	0.91673	0.91673	0.91673	0.91673	0.91673	0.91673	0.91673
2.0219e-07	0.91673	0.91673	0.91673	0.91673	0.91673	0.91673	0.91673	0.91673	0.91673
2.4501e-07	0.91673	0.91673	0.91673	0.91673	0.91673	0.91673	0.91673	0.91673	0.91673
2.6796e-07	0.91673	0.91673	0.91673	0.91673	0.91673	0.91673	0.91673	0.91673	0.91673
2.9194e-07	0.91673	0.91673	0.91673	0.91673	0.91673	0.91673	0.91673	0.91673	0.91673
5.8812e-07	0.91672	0.91672	0.91672	0.91672	0.91672	0.91672	0.91672	0.91672	0.91672
8.5649e-07	0.91672	0.91672	0.91672	0.91672	0.91672	0.91672	0.91672	0.91672	0.91672
1.1265e-06	0.91672	0.91672	0.91672	0.91672	0.91672	0.91672	0.91672	0.91672	0.91672
1.4335e-06	0.91672	0.91672	0.91672	0.91672	0.91672	0.91672	0.91672	0.91672	0.91672
1.7175e-06	0.91671	0.91671	0.91671	0.91671	0.91671	0.91671	0.91671	0.91671	0.91671
1.9632e-06	0.91671	0.91671	0.91671	0.91671	0.91671	0.91671	0.91671	0.91671	0.91671
2.2253e-06	0.91671	0.91671	0.91671	0.91671	0.91671	0.91671	0.91671	0.91671	0.91671
2.5038e-06	0.91671	0.91671	0.91671	0.91671	0.91671	0.91671	0.91671	0.91671	0.91671
2.7988e-06	0.91671	0.91671	0.91671	0.91671	0.91671	0.91671	0.91671	0.91671	0.91671
5.534e-06	0.91669	0.91669	0.91669	0.91669	0.91669	0.91669	0.91669	0.91669	0.91669
8.3869e-06	0.91667	0.91667	0.91667	0.91667	0.91667	0.91667	0.91667	0.91667	0.91667
1.1065e-05	0.91665	0.91665	0.91665	0.91665	0.91665	0.91665	0.91665	0.91665	0.91665
1.3774e-05	0.91663	0.91663	0.91663	0.91663	0.91663	0.91663	0.91663	0.91663	0.91663
1.6595e-05	0.91662	0.91662	0.91662	0.91662	0.91662	0.91662	0.91662	0.91662	0.91662
1.9279e-05	0.9166	0.9166	0.9166	0.9166	0.9166	0.9166	0.9166	0.9166	0.9166
2.2164e-05	0.91658	0.91658	0.91658	0.91658	0.91658	0.91658	0.91658	0.91658	0.91658
2.4797e-05	0.91657	0.91657	0.91657	0.91657	0.91657	0.91657	0.91657	0.91657	0.91657
2.7578e-05	0.91656	0.91656	0.91656	0.91656	0.91656	0.91656	0.91656	0.91656	0.91656
5.5141e-05	0.91642	0.91642	0.91642	0.91642	0.91642	0.91642	0.91642	0.91642	0.91642
8.2429e-05	0.9163	0.9163	0.9163	0.9163	0.9163	0.9163	0.9163	0.9163	0.9163
0.0001099	0.91619	0.91619	0.91619	0.91619	0.91619	0.91619	0.91619	0.91619	0.91619
0.00013757	0.91609	0.91609	0.91609	0.91609	0.91609	0.91609	0.91609	0.91609	0.91609
0.00016483	0.916	0.916	0.916	0.916	0.916	0.916	0.916	0.916	0.916
0.00019204	0.91591	0.91591	0.91591	0.91591	0.91591	0.91591	0.91591	0.91591	0.91591
0.00021998	0.91583	0.91583	0.91583	0.91583	0.91583	0.91583	0.91583	0.91583	0.91583
0.00024696	0.91575	0.91575	0.91575	0.91575	0.91575	0.91575	0.91575	0.91575	0.91575
0.00027475	0.91568	0.91568	0.91568	0.91568	0.91568	0.91568	0.91568	0.91568	0.91568
0.00054827	0.91505	0.91505	0.91505	0.91505	0.91505	0.91505	0.91505	0.91505	0.91505
0.00082322	0.9145	0.9145	0.9145	0.9145	0.9145	0.9145	0.9145	0.9145	0.9145
0.0010961	0.91402	0.91402	0.91402	0.91402	0.91402	0.91402	0.91402	0.91402	0.91402
0.0013709	0.91359	0.91359	0.91359	0.91359	0.91359	0.91359	0.91359	0.91359	0.91359
0.001645	0.91321	0.91321	0.91321	0.91321	0.91321	0.91321	0.91321	0.91321	0.91321
0.0019181	0.91287	0.91287	0.91287	0.91287	0.91287	0.91287	0.91287	0.91287	0.91287
0.0021932	0.91257	0.91257	0.91257	0.91257	0.91257	0.91257	0.91257	0.91257	0.91257
0.0024663	0.91231	0.91231	0.91231	0.91231	0.91231	0.91231	0.91231	0.91231	0.91231
0.0027412	0.91209	0.91209	0.91209	0.91209	0.91209	0.91209	0.91209	0.91209	0.91209
0.0054803	0.91071	0.91071	0.91071	0.91071	0.91071	0.91071	0.91071	0.91071	0.91071
0.0082175	0.91005	0.91005	0.91005	0.91005	0.91005	0.91005	0.91005	0.91005	0.91005
0.010955	0.90916	0.90916	0.90916	0.90916	0.90916	0.90916	0.90916	0.90916	0.90916
0.013697	0.9082	0.9082	0.9082	0.9082	0.9082	0.9082	0.9082	0.9082	0.9082
0.016434	0.90733	0.90733	0.90733	0.90733	0.90733	0.90733	0.90733	0.90733	0.90733
0.01917	0.90668	0.90668	0.90668	0.90668	0.90668	0.90668	0.90668	0.90668	0.90668
0.021907	0.90622	0.90622	0.90622	0.90622	0.90622	0.90622	0.90622	0.90622	0.90622
0.024649	0.90593	0.90593	0.90593	0.90593	0.90593	0.90593	0.90593	0.90593	0.90593
0.027387	0.90575	0.90575	0.90575	0.90575	0.90575	0.90575	0.90575	0.90575	0.90575
0.054771	0.90268	0.90268	0.90268	0.90268	0.90268	0.90268	0.90268	0.90268	0.90268
0.082145	0.89932	0.89932	0.89932	0.89932	0.89932	0.89932	0.89932	0.89932	0.89932
0.10952	0.89679	0.89679	0.89679	0.89679	0.89679	0.89679	0.89679	0.89679	0.89679
0.13692	0.8944	0.8944	0.8944	0.8944	0.8944	0.8944	0.8944	0.8944	0.8944
0.16428	0.89247	0.89247	0.89247	0.89247	0.89247	0.89247	0.89247	0.89247	0.89247
0.19168	0.89099	0.89099	0.89099	0.89099	0.89099	0.89099	0.89099	0.89099	0.89099
0.21905	0.88982	0.88982	0.88982	0.88982	0.88982	0.88982	0.88982	0.88982	0.88982
0.24644	0.88887	0.88887	0.88887	0.88887	0.88887	0.88887	0.88887	0.88887	0.88887
0.27382	0.88808	0.88808	0.88808	0.88808	0.88808	0.88808	0.88808	0.88808	0.88808
0.3012	0.88739	0.88739	0.88739	0.88739	0.88739	0.88739	0.88739	0.88739	0.88739
0.32858	0.88676	0.88676	0.88676	0.88676	0.88676	0.88676	0.88676	0.88676	0.88676
0.35594	0.88622	0.88622	0.88622	0.88622	0.88622	0.88622	0.88622	0.88622	0.88622
0.38333	0.88574	0.88574	0.88574	0.88574	0.88574	0.88574	0.88574	0.88574	0.88574
0.41071	0.88528	0.88528	0.88528	0.88528	0.88528	0.88528	0.88528	0.88528	0.88528
0.43808	0.88487	0.88487	0.88487	0.88487	0.88487	0.88487	0.88487	0.88487	0.88487
0.46547	0.88447	0.88447	0.88447	0.88447	0.88447	0.88447	0.88447	0.88447	0.88447
0.49283	0.88408	0.88408	0.88408	0.88408	0.88408	0.88408	0.88408	0.88408	0.88408
0.52022	0.8837	0.8837	0.8837	0.8837	0.8837	0.8837	0.8837	0.8837	0.8837
0.54761	0.88331	0.88331	0.88331	0.88332	0.88332	0.88332	0.88332	0.88332	0.88332
0.57498	0.88294	0.88294	0.88294	0.88294	0.88294	0.88294	0.88294	0.88294	0.88294
0.60236	0.88256	0.88256	0.88256	0.88256	0.88256	0.88256	0.88256	0.88256	0.88256
0.62976	0.88219	0.88219	0.88219	0.88219	0.88219	0.88219	0.88219	0.88219	0.88219
0.6571	0.88181	0.88181	0.88181	0.88181	0.88181	0.88181	0.88181	0.88181	0.88181
0.68451	0.88142	0.88142	0.88142	0.88142	0.88142	0.88142	0.88142	0.88142	0.88142
0.71186	0.88103	0.88103	0.88103	0.88103	0.88103	0.88103	0.88103	0.88103	0.88103
0.73924	0.88064	0.88064	0.88064	0.88064	0.88064	0.88064	0.88064	0.88064	0.88064
0.76662	0.88023	0.88023	0.88023	0.88023	0.88023	0.88023	0.88023	0.88023	0.88023
0.79402	0.87981	0.87981	0.87981	0.87981	0.87981	0.87981	0.87982	0.87982	0.87982
0.82141	0.87939	0.87939	0.87939	0.87939	0.87939	0.87939	0.87939	0.87939	0.87939
0.84875	0.87895	0.87896	0.87896	0.87896	0.87896	0.87896	0.87896	0.87896	0.87896
0.87617	0.87852	0.87852	0.87852	0.87852	0.87852	0.87852	0.87852	0.87852	0.87852
0.90355	0.87806	0.87807	0.87807	0.87807	0.87807	0.87807	0.87807	0.87807	0.87807
0.93091	0.87761	0.87761	0.87761	0.87761	0.87761	0.87761	0.87761	0.87761	0.87761
0.95828	0.87715	0.87715	0.87715	0.87715	0.87715	0.87715	0.87715	0.87715	0.87716
1	0.87645	0.87645	0.87645	0.87645	0.87645	0.87645	0.87645	0.87646	0.87646
2.0001	0.86091	0.86091	0.86092	0.86092	0.86092	0.86092	0.86092	0.86093	0.86093
3.0001	0.84686	0.84686	0.84687	0.84687	0.84687	0.84687	0.84688	0.84688	0.84689
4.0001	0.83321	0.83322	0.83323	0.83323	0.83324	0.83324	0.83325	0.83326	0.83327
5.0001	0.82004	0.82006	0.82007	0.82008	0.82008	0.82009	0.8201	0.82011	0.82012
6.0001	0.80717	0.80719	0.8072	0.80721	0.80722	0.80723	0.80725	0.80726	0.80728
7.0001	0.79456	0.79458	0.7946	0.79462	0.79463	0.79464	0.79466	0.79468	0.7947
8.0001	0.78218	0.7822	0.78223	0.78225	0.78227	0.78228	0.78231	0.78234	0.78236

9.0001	0.77	0.77003	0.77006	0.77009	0.77011	0.77013	0.77016	0.77019	0.77023
10	0.75799	0.75803	0.75807	0.7581	0.75812	0.75815	0.75819	0.75823	0.75827
20	0.64651	0.64665	0.64679	0.64691	0.64699	0.64708	0.64722	0.64736	0.6475
30	0.55381	0.55411	0.55442	0.55466	0.55484	0.55502	0.55532	0.55563	0.55593
40	0.46898	0.46952	0.47005	0.47047	0.47079	0.47111	0.47163	0.47216	0.47268
50	0.39522	0.39603	0.39684	0.39748	0.39796	0.39844	0.39923	0.40002	0.40081
60	0.32783	0.32902	0.33021	0.33115	0.33186	0.33256	0.33372	0.33487	0.33603
70	0.26782	0.26942	0.271	0.27226	0.2732	0.27414	0.27569	0.27724	0.27877
80	0.21438	0.21654	0.21868	0.22037	0.22163	0.22288	0.22497	0.22704	0.22908
90	0.16723	0.16998	0.17268	0.17481	0.17638	0.17794	0.1805	0.18303	0.18552
100	0.12681	0.13002	0.13317	0.13566	0.13755	0.13944	0.14255	0.14563	0.14867
110	0.095904	0.099331	0.10276	0.10548	0.1075	0.1095	0.1128	0.11605	0.11927
120	0.075671	0.07865	0.081686	0.08415	0.086019	0.08791	0.091097	0.094302	0.097522
130	0.064019	0.066309	0.068779	0.070904	0.072542	0.074187	0.076968	0.079792	0.082657
140	0.057543	0.059332	0.061248	0.06286	0.064126	0.065447	0.067777	0.070283	0.072891
150	0.053186	0.054776	0.056496	0.057923	0.05902	0.060141	0.062067	0.064091	0.066268
160	0.050043	0.051541	0.053133	0.054441	0.055452	0.056483	0.05826	0.060098	0.061989
170	0.04761	0.049062	0.050613	0.051879	0.05284	0.053817	0.055496	0.057218	0.058998
180	0.045691	0.047115	0.048635	0.049877	0.050822	0.051778	0.053405	0.055077	0.056777
190	0.044149	0.045549	0.04705	0.048276	0.04921	0.050161	0.051772	0.053412	0.055086
200	0.042917	0.044278	0.045763	0.046981	0.047909	0.04885	0.050462	0.052098	0.053757
210	0.041955	0.043247	0.044705	0.045919	0.046845	0.047786	0.049395	0.05104	0.052698
220	0.041309	0.042423	0.043833	0.045039	0.045965	0.04691	0.04852	0.050177	0.051845
230	0.040919	0.041807	0.043118	0.044304	0.04523	0.046178	0.047801	0.049467	0.051151
240	0.040648	0.041421	0.042541	0.043695	0.044613	0.045564	0.047203	0.04888	0.050586
250	0.040443	0.041163	0.042102	0.043188	0.044094	0.045047	0.046702	0.048397	0.050126
260	0.040281	0.040972	0.041811	0.042774	0.043661	0.044611	0.046281	0.047999	0.049752
270	0.040148	0.040825	0.041612	0.042445	0.043298	0.044243	0.045928	0.047671	0.049449
280	0.040036	0.040708	0.041467	0.042215	0.042998	0.043932	0.045632	0.047401	0.049206
290	0.03994	0.040612	0.041356	0.042055	0.042756	0.043671	0.045384	0.047181	0.049013
300	0.039857	0.04053	0.041267	0.041937	0.042573	0.043453	0.045178	0.047001	0.048862
310	0.039783	0.040463	0.041196	0.041849	0.042442	0.043272	0.045006	0.046857	0.048746
320	0.039717	0.040406	0.04114	0.041782	0.042348	0.043125	0.044863	0.046742	0.048659
330	0.039659	0.040357	0.041093	0.041731	0.042278	0.043007	0.044746	0.046652	0.048596
340	0.039607	0.040315	0.041055	0.041692	0.042228	0.042915	0.044651	0.046584	0.048553
350	0.03956	0.040278	0.041024	0.041662	0.042192	0.042849	0.044576	0.046533	0.048528
360	0.039516	0.040245	0.040999	0.04164	0.042166	0.042803	0.044517	0.0465	0.048517
370	0.039476	0.040217	0.040978	0.041623	0.042147	0.042772	0.044472	0.046479	0.048518
380	0.039439	0.040191	0.040961	0.04161	0.042135	0.042751	0.04444	0.046469	0.048527
390	0.039404	0.040169	0.040946	0.041602	0.042128	0.042738	0.044418	0.046469	0.048543
400	0.039372	0.040149	0.040935	0.041597	0.042125	0.042732	0.044405	0.046475	0.048564
410	0.039342	0.040131	0.040927	0.041594	0.042126	0.04273	0.0444	0.046488	0.04859
420	0.039313	0.040115	0.040921	0.041594	0.042129	0.042733	0.044401	0.046505	0.048619
430	0.039287	0.040101	0.040916	0.041596	0.042134	0.042739	0.044408	0.046525	0.048651
440	0.039261	0.040088	0.040913	0.0416	0.042141	0.042748	0.044418	0.046549	0.048685
450	0.039237	0.040077	0.040912	0.041605	0.04215	0.042758	0.044432	0.046575	0.04872
460	0.039215	0.040067	0.040912	0.041611	0.04216	0.042771	0.044448	0.046603	0.048756
470	0.039193	0.040058	0.040912	0.041618	0.042171	0.042785	0.044467	0.046632	0.048795
480	0.039172	0.040051	0.040914	0.041626	0.042183	0.0428	0.044488	0.046663	0.048834
490	0.039152	0.040044	0.040917	0.041635	0.042196	0.042817	0.04451	0.046694	0.048875
500	0.039133	0.040038	0.040921	0.041645	0.04221	0.042834	0.044533	0.046727	0.048916
510	0.039115	0.040032	0.040925	0.041656	0.042225	0.042852	0.044558	0.04676	0.048959
520	0.039098	0.040028	0.04093	0.041667	0.04224	0.042871	0.044583	0.046794	0.049002
530	0.039081	0.040024	0.040935	0.041678	0.042255	0.04289	0.044609	0.046829	0.049045
540	0.039065	0.04002	0.040941	0.04169	0.042271	0.04291	0.044636	0.046864	0.049089
550	0.039049	0.040017	0.040947	0.041703	0.042287	0.04293	0.044663	0.0469	0.049133
560	0.039034	0.040015	0.040954	0.041715	0.042304	0.04295	0.04469	0.046937	0.049178
570	0.03902	0.040013	0.040962	0.041728	0.042321	0.042971	0.044718	0.046974	0.049223
580	0.039006	0.040012	0.040969	0.041742	0.042339	0.042992	0.044746	0.047012	0.049268
590	0.038993	0.040011	0.040977	0.041755	0.042356	0.043013	0.044774	0.047049	0.049314
600	0.038979	0.040011	0.040985	0.041769	0.042374	0.043035	0.044804	0.047087	0.049361
610	0.038967	0.040011	0.040994	0.041783	0.042392	0.043057	0.044833	0.047125	0.049414
620	0.038954	0.040011	0.041003	0.041798	0.04241	0.043079	0.044863	0.047164	0.049492
630	0.038942	0.040012	0.041012	0.041812	0.042429	0.043101	0.044892	0.047203	0.049617
640	0.038931	0.040012	0.041021	0.041827	0.042447	0.043124	0.044922	0.047242	0.049812
650	0.038919	0.040014	0.04103	0.041841	0.042466	0.043147	0.044952	0.047281	0.050081
660	0.038908	0.040015	0.04104	0.041856	0.042485	0.043169	0.044983	0.047321	0.050414
670	0.038897	0.040016	0.041049	0.041871	0.042503	0.043192	0.045013	0.047361	0.050799
680	0.038886	0.040018	0.041059	0.041886	0.042522	0.043215	0.045044	0.047402	0.051228
690	0.038876	0.04002	0.041069	0.041902	0.042542	0.043238	0.045075	0.047454	0.051694
700	0.038865	0.040022	0.04108	0.041917	0.042561	0.043261	0.045106	0.04754	0.052191
710	0.038855	0.040025	0.04109	0.041932	0.04258	0.043284	0.045137	0.047682	0.052712
720	0.038846	0.040027	0.0411	0.041948	0.0426	0.043309	0.045168	0.047886	0.053255
730	0.038836	0.04003	0.04111	0.041965	0.04262	0.043332	0.0452	0.048148	0.053815
740	0.038827	0.040033	0.041121	0.04198	0.04264	0.043356	0.045232	0.048458	0.054394
750	0.038818	0.040036	0.041131	0.041996	0.04266	0.04338	0.045264	0.048809	0.054992
760	0.038809	0.040039	0.041142	0.042012	0.04268	0.043405	0.045296	0.049195	0.055604
770	0.0388	0.040042	0.041152	0.042028	0.0427	0.043429	0.045329	0.049609	0.056227
780	0.038792	0.040046	0.041163	0.042045	0.04272	0.043453	0.045362	0.050047	0.056861
790	0.038784	0.04005	0.041174	0.042061	0.04274	0.043478	0.045398	0.050505	0.057502
800	0.038776	0.040053	0.041185	0.042077	0.042761	0.043503	0.045458	0.050979	0.058149
810	0.038768	0.040057	0.041196	0.042094	0.042781	0.043527	0.045561	0.051467	0.058803
820	0.03876	0.040061	0.041207	0.04211	0.042802	0.043552	0.045716	0.051968	0.059462
830	0.038753	0.040065	0.041219	0.042127	0.042823	0.043577	0.045919	0.052484	0.060125
840	0.038745	0.040069	0.04123	0.042143	0.042843	0.043602	0.046162	0.053012	0.060791
850	0.038738	0.040073	0.041241	0.04216	0.042864	0.043627	0.046442	0.053552	0.061459
860	0.038731	0.040078	0.041253	0.042177	0.042885	0.043652	0.046751	0.054099	0.06212
870	0.038724	0.040082	0.041264	0.042194	0.042906	0.043678	0.047087	0.054654	0.062767
880	0.038717	0.040086	0.041276	0.042211	0.042927	0.043703	0.047444	0.055214	0.063427
890	0.03871	0.040091	0.041287	0.042228	0.042949	0.043728	0.047818	0.05578	0.064107
900	0.038703	0.040095	0.041299	0.042245	0.04297	0.043754	0.048207	0.05635	0.064793
910	0.038697	0.0401	0.041311	0.042262	0.042991	0.04378	0.048609	0.056923	0.065479

920	0.03869	0.040105	0.041323	0.042279	0.043013	0.043806	0.049022	0.0575	0.066167
930	0.038684	0.04011	0.041334	0.042296	0.043034	0.043833	0.049445	0.058078	0.066859
940	0.038678	0.040114	0.041346	0.042314	0.043056	0.043859	0.049876	0.058659	0.067551
950	0.038672	0.040119	0.041358	0.042331	0.043077	0.043887	0.050319	0.059242	0.06824
960	0.038665	0.040124	0.041371	0.042349	0.043099	0.04392	0.050771	0.059821	0.06893
970	0.03866	0.040129	0.041383	0.042366	0.043121	0.043981	0.051231	0.060387	0.06962
980	0.038654	0.040134	0.041395	0.042384	0.043143	0.044081	0.051697	0.060953	0.070311
990	0.038648	0.040139	0.041407	0.042402	0.043165	0.044221	0.052167	0.061536	0.071002
1000	0.038642	0.040145	0.041419	0.04242	0.043187	0.044395	0.052643	0.062131	0.071694
1050	0.038615	0.040171	0.041481	0.042509	0.043297	0.045626	0.055064	0.065124	0.075156
1100	0.03859	0.040198	0.041543	0.042599	0.043412	0.047218	0.057525	0.068119	0.078622
1150	0.038567	0.040226	0.041607	0.04269	0.04375	0.048989	0.059972	0.071118	0.082101
1200	0.038545	0.040255	0.04167	0.042782	0.0447	0.050896	0.062501	0.074121	0.085584
1250	0.038525	0.040266	0.041698	0.042823	0.045475	0.05224	0.06432	0.076348	0.088224
1300	0.038506	0.040273	0.041717	0.042851	0.045977	0.053068	0.065468	0.077794	0.089977
1350	0.038488	0.04028	0.041734	0.042877	0.046393	0.053716	0.066362	0.078924	0.091352
1400	0.038472	0.040287	0.041752	0.042903	0.046772	0.054283	0.06713	0.07989	0.092525
1450	0.038456	0.040293	0.041769	0.042928	0.047136	0.054803	0.067826	0.080758	0.093575
1500	0.038441	0.0403	0.041785	0.042952	0.047492	0.055289	0.068477	0.081564	0.094548
1550	0.038427	0.040307	0.041802	0.042977	0.04785	0.055732	0.0691	0.082333	0.095467
1600	0.038413	0.040314	0.041819	0.043001	0.04821	0.056181	0.069703	0.083074	0.09635
1650	0.038401	0.04032	0.041835	0.043025	0.048571	0.056634	0.070293	0.083796	0.097207
1700	0.038388	0.040327	0.041852	0.043049	0.048935	0.057087	0.070873	0.084504	0.098044
1750	0.038375	0.040334	0.041868	0.043074	0.0493	0.05754	0.071446	0.085202	0.098866
1800	0.038364	0.040341	0.041884	0.043098	0.049667	0.057996	0.072015	0.085891	0.099678
1850	0.038352	0.040348	0.0419	0.043123	0.050035	0.058452	0.07258	0.086575	0.10048
1900	0.038341	0.040354	0.041916	0.043151	0.050404	0.058904	0.073142	0.087255	0.10128
1950	0.038331	0.040361	0.041932	0.043186	0.050774	0.059355	0.073703	0.087931	0.10207
2000	0.038321	0.040368	0.041948	0.043259	0.051145	0.059805	0.074262	0.088605	0.10286
2100	0.038301	0.040383	0.041979	0.043568	0.051887	0.060699	0.075377	0.089947	0.10443
2200	0.038282	0.040397	0.04201	0.043998	0.052631	0.061589	0.076489	0.091284	0.10599
2300	0.038266	0.040412	0.042041	0.044488	0.053376	0.062477	0.077599	0.092617	0.10754
2400	0.038249	0.040426	0.042072	0.045013	0.054124	0.063363	0.078707	0.093949	0.1091
2500	0.038234	0.04044	0.042103	0.045566	0.054836	0.064249	0.079815	0.095279	0.11065
2600	0.038219	0.040454	0.042134	0.046142	0.055563	0.065135	0.080921	0.096608	0.11219
2700	0.038206	0.040468	0.042164	0.046735	0.056311	0.066021	0.082028	0.097936	0.11373
2800	0.038192	0.040476	0.04218	0.047166	0.056874	0.066701	0.082907	0.099014	0.11501
2900	0.03818	0.040482	0.042194	0.047452	0.057265	0.067175	0.083538	0.099805	0.11596
3000	0.038168	0.040487	0.042206	0.047688	0.057586	0.067562	0.084054	0.10045	0.11675
3100	0.038156	0.040493	0.042219	0.047902	0.057871	0.067903	0.084506	0.10102	0.11743
3200	0.038145	0.040499	0.04223	0.048103	0.058135	0.068219	0.084919	0.10154	0.11805
3300	0.038135	0.040504	0.042242	0.048297	0.058387	0.068519	0.085309	0.10202	0.11864
3400	0.038125	0.04051	0.042254	0.048487	0.05863	0.068808	0.085684	0.10248	0.11919
3500	0.038115	0.040515	0.042264	0.048675	0.058869	0.069092	0.086049	0.10293	0.11973
3600	0.038106	0.04052	0.042275	0.04886	0.059104	0.069371	0.086407	0.10337	0.12025
3700	0.038097	0.040525	0.042286	0.049044	0.059338	0.069647	0.08676	0.1038	0.12076
3800	0.038087	0.04053	0.042296	0.049228	0.059569	0.069921	0.087109	0.10423	0.12127
3900	0.038079	0.040535	0.042307	0.049412	0.0598	0.070193	0.087455	0.10465	0.12176
4000	0.03807	0.04054	0.042317	0.049596	0.060029	0.070464	0.087798	0.10506	0.12226
4100	0.038062	0.040545	0.042328	0.049781	0.060258	0.070735	0.088141	0.10548	0.12275
4200	0.038054	0.04055	0.042338	0.049965	0.060487	0.071005	0.088481	0.10589	0.12323
4300	0.038045	0.040555	0.042348	0.05015	0.060714	0.071274	0.088821	0.1063	0.12371
4400	0.038036	0.04056	0.042358	0.050334	0.060942	0.071543	0.08916	0.10671	0.12419
4500	0.038028	0.040565	0.042368	0.050518	0.061169	0.071811	0.089498	0.10712	0.12467
4600	0.038021	0.040569	0.042378	0.050702	0.061396	0.07208	0.089836	0.10752	0.12515
4700	0.038014	0.040574	0.042388	0.050886	0.061623	0.072348	0.090173	0.10793	0.12563
4800	0.038007	0.040579	0.042398	0.05107	0.061849	0.072616	0.090509	0.10833	0.1261
4900	0.038	0.040584	0.042408	0.051254	0.062076	0.072884	0.090845	0.10874	0.12658
5000	0.037994	0.040589	0.042417	0.051439	0.062302	0.073152	0.091181	0.10914	0.12705
5200	0.037981	0.040598	0.042437	0.051809	0.062756	0.073687	0.091853	0.10995	0.12799
5400	0.037968	0.040608	0.042456	0.052179	0.063209	0.074221	0.092523	0.11076	0.12894
5600	0.037956	0.040616	0.042475	0.05255	0.063662	0.074756	0.093194	0.11156	0.12988
5800	0.037944	0.040626	0.042494	0.052921	0.064116	0.07529	0.093864	0.11237	0.13082
6000	0.037933	0.040635	0.042513	0.053291	0.064569	0.075823	0.094533	0.11317	0.13176
6200	0.037922	0.040643	0.042531	0.05364	0.065022	0.076356	0.095203	0.11398	0.13269
6400	0.037911	0.040652	0.04255	0.053984	0.065476	0.076891	0.095872	0.11478	0.13363
6600	0.0379	0.040661	0.042569	0.054357	0.065929	0.077426	0.096541	0.11558	0.13456
6800	0.03789	0.04067	0.042587	0.054738	0.066383	0.077961	0.097209	0.11639	0.1355
7000	0.037879	0.040679	0.042606	0.055123	0.066837	0.078495	0.097877	0.11719	0.13643
7200	0.037869	0.040688	0.042624	0.055505	0.067291	0.07903	0.098544	0.11799	0.13737
7400	0.037859	0.040697	0.042643	0.055885	0.067744	0.079565	0.099212	0.11879	0.13831
7600	0.037849	0.040706	0.042661	0.056263	0.068198	0.0801	0.099881	0.1196	0.13924
7800	0.037839	0.040714	0.04268	0.05664	0.068653	0.080634	0.10055	0.1204	0.14018
8000	0.03783	0.040723	0.042698	0.057016	0.069107	0.081169	0.10122	0.1212	0.14111
8200	0.03782	0.040732	0.042716	0.057391	0.069561	0.081704	0.10189	0.122	0.14205
8400	0.03781	0.040741	0.042735	0.057765	0.070015	0.082238	0.10255	0.1228	0.14298
8600	0.037801	0.04075	0.042753	0.05814	0.07047	0.082773	0.10322	0.1236	0.14392
8800	0.037794	0.040758	0.042772	0.058514	0.070924	0.083308	0.10389	0.12441	0.14485
9000	0.037785	0.040767	0.042791	0.058888	0.071379	0.083843	0.10456	0.12521	0.14578
9200	0.037776	0.040776	0.042819	0.059262	0.071833	0.084378	0.10522	0.12601	0.14672
9400	0.037768	0.040785	0.042895	0.059636	0.072287	0.084913	0.10589	0.12681	0.14765
9600	0.03776	0.040794	0.043084	0.060011	0.072742	0.085448	0.10656	0.12761	0.14858
9800	0.037753	0.040803	0.04332	0.060385	0.073197	0.085983	0.10723	0.12841	0.14952
10000	0.037745	0.040812	0.043572	0.06076	0.073651	0.086518	0.1079	0.12921	0.15045

Time [years]	Porosity f=0.2	f=0.25	f=0.3	f=0.35	f=0.4	f=0.5	f=0.6	f=0.8	f=1.0
6.5144e-11	0.91673	0.91673	0.91673	0.91673	0.91673	0.91673	0.91673	0.91673	0.91673
3.9006e-09	0.91673	0.91673	0.91673	0.91673	0.91673	0.91673	0.91673	0.91673	0.91673
7.3573e-09	0.91673	0.91673	0.91673	0.91673	0.91673	0.91673	0.91673	0.91673	0.91673
1.184e-08	0.91673	0.91673	0.91673	0.91673	0.91673	0.91673	0.91673	0.91673	0.91673

1.7348e-08	0.91673	0.91673	0.91673	0.91673	0.91673	0.91673	0.91673	0.91673	0.91673
2.3883e-08	0.91673	0.91673	0.91673	0.91673	0.91673	0.91673	0.91673	0.91673	0.91673
3.1443e-08	0.91673	0.91673	0.91673	0.91673	0.91673	0.91673	0.91673	0.91673	0.91673
6.028e-08	0.91673	0.91673	0.91673	0.91673	0.91673	0.91673	0.91673	0.91673	0.91673
9.835e-08	0.91673	0.91673	0.91673	0.91673	0.91673	0.91673	0.91673	0.91673	0.91673
1.2886e-07	0.91673	0.91673	0.91673	0.91673	0.91673	0.91673	0.91673	0.91673	0.91673
1.4565e-07	0.91673	0.91673	0.91673	0.91673	0.91673	0.91673	0.91673	0.91673	0.91673
1.8232e-07	0.91673	0.91673	0.91673	0.91673	0.91673	0.91673	0.91673	0.91673	0.91673
2.0219e-07	0.91673	0.91673	0.91673	0.91673	0.91673	0.91673	0.91673	0.91673	0.91673
2.4501e-07	0.91673	0.91673	0.91673	0.91673	0.91673	0.91673	0.91673	0.91673	0.91673
2.6796e-07	0.91673	0.91673	0.91673	0.91673	0.91673	0.91673	0.91673	0.91673	0.91673
2.9194e-07	0.91673	0.91673	0.91673	0.91673	0.91673	0.91673	0.91673	0.91673	0.91673
5.8812e-07	0.91672	0.91672	0.91672	0.91672	0.91672	0.91672	0.91672	0.91672	0.91672
8.5649e-07	0.91672	0.91672	0.91672	0.91672	0.91672	0.91672	0.91672	0.91672	0.91672
1.1265e-06	0.91672	0.91672	0.91672	0.91672	0.91672	0.91672	0.91672	0.91672	0.91672
1.4335e-06	0.91672	0.91672	0.91672	0.91672	0.91672	0.91672	0.91672	0.91672	0.91672
1.7175e-06	0.91671	0.91671	0.91671	0.91671	0.91671	0.91671	0.91671	0.91671	0.91671
1.9632e-06	0.91671	0.91671	0.91671	0.91671	0.91671	0.91671	0.91671	0.91671	0.91671
2.2253e-06	0.91671	0.91671	0.91671	0.91671	0.91671	0.91671	0.91671	0.91671	0.91671
2.5038e-06	0.91671	0.91671	0.91671	0.91671	0.91671	0.91671	0.91671	0.91671	0.91671
2.7988e-06	0.91671	0.91671	0.91671	0.91671	0.91671	0.91671	0.91671	0.91671	0.91671
5.534e-06	0.91669	0.91669	0.91669	0.91669	0.91669	0.91669	0.91669	0.91669	0.91669
8.3869e-06	0.91667	0.91667	0.91667	0.91667	0.91667	0.91667	0.91667	0.91667	0.91667
1.1065e-05	0.91665	0.91665	0.91665	0.91665	0.91665	0.91665	0.91665	0.91665	0.91665
1.3774e-05	0.91663	0.91663	0.91663	0.91663	0.91663	0.91663	0.91663	0.91663	0.91663
1.6595e-05	0.91662	0.91662	0.91662	0.91662	0.91662	0.91662	0.91662	0.91662	0.91662
1.9279e-05	0.9166	0.9166	0.9166	0.9166	0.9166	0.9166	0.9166	0.9166	0.9166
2.2164e-05	0.91658	0.91658	0.91658	0.91658	0.91658	0.91658	0.91658	0.91658	0.91658
2.4797e-05	0.91657	0.91657	0.91657	0.91657	0.91657	0.91657	0.91657	0.91657	0.91657
2.7578e-05	0.91656	0.91656	0.91656	0.91656	0.91656	0.91656	0.91656	0.91656	0.91656
5.5141e-05	0.91642	0.91642	0.91642	0.91642	0.91642	0.91642	0.91642	0.91642	0.91642
8.2429e-05	0.9163	0.9163	0.9163	0.9163	0.9163	0.9163	0.9163	0.9163	0.9163
0.0001099	0.91619	0.91619	0.91619	0.91619	0.91619	0.91619	0.91619	0.91619	0.91619
0.00013757	0.91609	0.91609	0.91609	0.91609	0.91609	0.91609	0.91609	0.91609	0.91609
0.00016483	0.916	0.916	0.916	0.916	0.916	0.916	0.916	0.916	0.916
0.00019204	0.91591	0.91591	0.91591	0.91591	0.91591	0.91591	0.91591	0.91591	0.91591
0.00021998	0.91583	0.91583	0.91583	0.91583	0.91583	0.91583	0.91583	0.91583	0.91583
0.00024696	0.91575	0.91575	0.91575	0.91575	0.91575	0.91575	0.91575	0.91575	0.91575
0.00027475	0.91568	0.91568	0.91568	0.91568	0.91568	0.91568	0.91568	0.91568	0.91568
0.00054827	0.91505	0.91505	0.91505	0.91505	0.91505	0.91505	0.91505	0.91505	0.91505
0.00082322	0.9145	0.9145	0.9145	0.9145	0.9145	0.9145	0.9145	0.9145	0.9145
0.0010961	0.91402	0.91402	0.91402	0.91402	0.91402	0.91402	0.91402	0.91402	0.91402
0.0013709	0.91359	0.91359	0.91359	0.91359	0.91359	0.91359	0.91359	0.91359	0.91359
0.001645	0.91321	0.91321	0.91321	0.91321	0.91321	0.91321	0.91321	0.91321	0.91321
0.0019181	0.91287	0.91287	0.91287	0.91287	0.91287	0.91287	0.91287	0.91287	0.91287
0.0021932	0.91257	0.91257	0.91257	0.91257	0.91257	0.91257	0.91257	0.91257	0.91257
0.0024663	0.91231	0.91231	0.91231	0.91231	0.91231	0.91231	0.91231	0.91231	0.91231
0.0027412	0.91209	0.91209	0.91209	0.91209	0.91209	0.91209	0.91209	0.91209	0.91209
0.0054803	0.91071	0.91071	0.91071	0.91071	0.91071	0.91071	0.91071	0.91071	0.91071
0.0082175	0.91005	0.91005	0.91005	0.91005	0.91005	0.91005	0.91005	0.91005	0.91005
0.010955	0.90916	0.90916	0.90916	0.90916	0.90916	0.90916	0.90916	0.90916	0.90916
0.013697	0.9082	0.9082	0.9082	0.9082	0.9082	0.9082	0.9082	0.9082	0.9082
0.016434	0.90733	0.90733	0.90733	0.90733	0.90733	0.90733	0.90733	0.90733	0.90733
0.01917	0.90668	0.90668	0.90668	0.90668	0.90668	0.90668	0.90668	0.90668	0.90668
0.021907	0.90622	0.90622	0.90622	0.90622	0.90622	0.90622	0.90622	0.90622	0.90622
0.024649	0.90593	0.90593	0.90593	0.90593	0.90593	0.90593	0.90593	0.90593	0.90593
0.027387	0.90575	0.90575	0.90575	0.90575	0.90575	0.90575	0.90575	0.90575	0.90575
0.054771	0.90268	0.90268	0.90268	0.90268	0.90268	0.90268	0.90268	0.90268	0.90268
0.082145	0.89932	0.89932	0.89932	0.89932	0.89932	0.89932	0.89932	0.89932	0.89932
0.10952	0.89679	0.89679	0.89679	0.89679	0.89679	0.89679	0.89679	0.89679	0.89679
0.13692	0.8944	0.8944	0.8944	0.8944	0.8944	0.8944	0.89441	0.89441	0.89441
0.16428	0.89247	0.89247	0.89247	0.89247	0.89247	0.89247	0.89247	0.89247	0.89247
0.19168	0.89099	0.89099	0.89099	0.89099	0.891	0.891	0.891	0.891	0.891
0.21905	0.88982	0.88982	0.88982	0.88982	0.88982	0.88982	0.88982	0.88982	0.88982
0.24644	0.88887	0.88887	0.88887	0.88887	0.88887	0.88888	0.88888	0.88888	0.88888
0.27382	0.88808	0.88808	0.88808	0.88808	0.88808	0.88808	0.88808	0.88808	0.88808
0.3012	0.88739	0.88739	0.88739	0.88739	0.8874	0.8874	0.8874	0.8874	0.8874
0.32858	0.88676	0.88676	0.88676	0.88676	0.88676	0.88676	0.88676	0.88676	0.88677
0.35594	0.88622	0.88622	0.88622	0.88623	0.88623	0.88623	0.88623	0.88623	0.88623
0.38333	0.88574	0.88575	0.88575	0.88575	0.88575	0.88575	0.88575	0.88575	0.88575
0.41071	0.88528	0.88528	0.88528	0.88528	0.88528	0.88528	0.88528	0.88529	0.88529
0.43808	0.88487	0.88487	0.88487	0.88487	0.88487	0.88487	0.88487	0.88487	0.88488
0.46547	0.88447	0.88447	0.88447	0.88447	0.88447	0.88447	0.88447	0.88448	0.88448
0.49283	0.88408	0.88408	0.88408	0.88408	0.88408	0.88408	0.88408	0.88409	0.88409
0.52022	0.8837	0.8837	0.8837	0.8837	0.8837	0.8837	0.8837	0.8837	0.88371
0.54761	0.88332	0.88332	0.88332	0.88332	0.88332	0.88332	0.88332	0.88332	0.88333
0.57498	0.88294	0.88294	0.88294	0.88294	0.88294	0.88294	0.88295	0.88295	0.88295
0.60236	0.88256	0.88256	0.88256	0.88257	0.88257	0.88257	0.88257	0.88257	0.88257
0.62976	0.88219	0.8822	0.8822	0.8822	0.8822	0.8822	0.8822	0.8822	0.88221
0.6571	0.88181	0.88181	0.88181	0.88181	0.88182	0.88182	0.88182	0.88182	0.88182
0.68451	0.88142	0.88142	0.88142	0.88142	0.88142	0.88143	0.88143	0.88143	0.88143
0.71186	0.88103	0.88104	0.88104	0.88104	0.88104	0.88104	0.88104	0.88105	0.88105
0.73924	0.88064	0.88064	0.88064	0.88064	0.88064	0.88064	0.88065	0.88065	0.88065
0.76662	0.88023	0.88023	0.88023	0.88023	0.88023	0.88024	0.88024	0.88024	0.88025
0.79402	0.87982	0.87982	0.87982	0.87982	0.87982	0.87982	0.87982	0.87983	0.87983
0.82141	0.87939	0.87939	0.87939	0.8794	0.8794	0.8794	0.8794	0.8794	0.87941
0.84875	0.87896	0.87896	0.87896	0.87896	0.87896	0.87897	0.87897	0.87897	0.87898
0.87617	0.87852	0.87852	0.87852	0.87852	0.87852	0.87853	0.87853	0.87853	0.87854
0.90355	0.87807	0.87807	0.87807	0.87807	0.87807	0.87808	0.87808	0.87808	0.87809
0.93091	0.87761	0.87761	0.87762	0.87762	0.87762	0.87762	0.87762	0.87763	0.87763
0.95828	0.87716	0.87716	0.87716	0.87716	0.87716	0.87716	0.87717	0.87717	0.87718
1	0.87646	0.87646	0.87646	0.87646	0.87646	0.87647	0.87647	0.87647	0.87648

2.0001	0.86093	0.86093	0.86094	0.86094	0.86095	0.86096	0.86097	0.86098	0.861
3.0001	0.84689	0.8469	0.84691	0.84692	0.84693	0.84695	0.84697	0.847	0.84704
4.0001	0.83327	0.83329	0.8333	0.83332	0.83333	0.83336	0.83339	0.83345	0.83352
5.0001	0.82013	0.82016	0.82018	0.8202	0.82022	0.82027	0.82031	0.8204	0.82049
6.0001	0.8073	0.80733	0.80736	0.80739	0.80742	0.80748	0.80755	0.80767	0.80779
7.0001	0.79472	0.79476	0.79481	0.79485	0.79489	0.79497	0.79505	0.79522	0.79538
8.0001	0.78239	0.78244	0.7825	0.78255	0.7826	0.78271	0.78281	0.78302	0.78323
9.0001	0.77026	0.77033	0.77039	0.77046	0.77052	0.77065	0.77078	0.77105	0.77131
10	0.75831	0.75839	0.75847	0.75855	0.75863	0.75879	0.75895	0.75926	0.75958
20	0.64764	0.64792	0.6482	0.64848	0.64876	0.64932	0.64988	0.651	0.65209
30	0.55623	0.55683	0.55743	0.55803	0.55863	0.55981	0.561	0.56334	0.56566
40	0.4732	0.47424	0.47528	0.47631	0.47733	0.47937	0.48141	0.48546	0.48944
50	0.40159	0.40316	0.40471	0.40624	0.40776	0.41078	0.41374	0.41954	0.42517
60	0.33717	0.33947	0.34175	0.34401	0.34624	0.35063	0.35492	0.36324	0.37121
70	0.28029	0.28329	0.28625	0.28915	0.29201	0.29756	0.30305	0.31385	0.32418
80	0.2311	0.23506	0.23894	0.24273	0.24644	0.25366	0.26052	0.27349	0.28566
90	0.18798	0.19279	0.19749	0.20205	0.20656	0.21527	0.22369	0.23967	0.25432
100	0.15165	0.15743	0.16301	0.16849	0.1738	0.18394	0.19345	0.21121	0.22787
110	0.12247	0.12872	0.13475	0.14075	0.14668	0.15807	0.16881	0.18868	0.20651
120	0.10075	0.10723	0.11354	0.11969	0.12573	0.13749	0.14894	0.17021	0.18967
130	0.085556	0.091531	0.097655	0.10383	0.10999	0.12198	0.13342	0.15555	0.17594
140	0.07553	0.080962	0.086545	0.092304	0.098172	0.11013	0.12179	0.14399	0.16492
150	0.068604	0.073641	0.078827	0.084191	0.08971	0.10114	0.11276	0.13494	0.15638
160	0.063979	0.068419	0.073302	0.078378	0.083585	0.094511	0.10582	0.1281	0.14957
170	0.060854	0.064813	0.069294	0.074144	0.079122	0.089582	0.10054	0.12278	0.14417
180	0.058549	0.062302	0.066411	0.071043	0.075837	0.085936	0.096599	0.11863	0.13998
190	0.056809	0.060451	0.064365	0.068767	0.073425	0.083256	0.093656	0.11545	0.13679
200	0.055467	0.059038	0.062868	0.067095	0.071656	0.081294	0.091492	0.11306	0.13439
210	0.054408	0.057949	0.061741	0.065867	0.070365	0.079873	0.089925	0.11131	0.13265
220	0.053562	0.057108	0.060884	0.064967	0.069428	0.078858	0.088824	0.11008	0.13148
230	0.05288	0.056448	0.060227	0.064315	0.068765	0.078154	0.088082	0.10926	0.13073
240	0.052333	0.055934	0.059728	0.063846	0.068309	0.077698	0.087623	0.10877	0.1303
250	0.051894	0.055537	0.059357	0.06351	0.068	0.077424	0.087377	0.10854	0.13015
260	0.051545	0.055234	0.059087	0.063272	0.067796	0.077272	0.087272	0.1085	0.13016
270	0.051268	0.055007	0.058895	0.063111	0.067671	0.077201	0.087251	0.10855	0.13029
280	0.051052	0.054842	0.058765	0.063012	0.067606	0.077186	0.08728	0.10866	0.13051
290	0.050886	0.054726	0.058685	0.062959	0.067585	0.077211	0.087344	0.10883	0.13092
300	0.050762	0.054649	0.058641	0.062941	0.067594	0.077262	0.087438	0.10915	0.13157
310	0.050672	0.054603	0.058627	0.06295	0.067628	0.077334	0.087565	0.10969	0.13249
320	0.050609	0.054583	0.058634	0.062978	0.067679	0.077424	0.087791	0.11046	0.13368
330	0.05057	0.054581	0.058658	0.063021	0.067743	0.07754	0.088195	0.11146	0.13511
340	0.05055	0.054595	0.058693	0.063077	0.067818	0.077731	0.088804	0.11268	0.13679
350	0.050545	0.054619	0.058739	0.06314	0.067902	0.07807	0.089611	0.1141	0.13867
360	0.050553	0.054652	0.058792	0.063211	0.068002	0.0786	0.090596	0.11571	0.14074
370	0.050569	0.054691	0.058851	0.063287	0.068146	0.079309	0.091741	0.11747	0.14299
380	0.050592	0.054737	0.058913	0.063372	0.068377	0.080174	0.093031	0.11936	0.14537
390	0.050621	0.054786	0.058979	0.063485	0.068762	0.081176	0.094444	0.12138	0.14784
400	0.050654	0.054838	0.059049	0.063647	0.069311	0.082302	0.095963	0.12349	0.15048
410	0.050691	0.054893	0.059122	0.063918	0.069997	0.083534	0.097574	0.12566	0.15325
420	0.050729	0.05495	0.059206	0.064337	0.070802	0.084855	0.099261	0.12795	0.15607
430	0.05077	0.055009	0.059323	0.064895	0.071709	0.08625	0.10101	0.13033	0.15897
440	0.050813	0.05507	0.059497	0.065566	0.072707	0.087709	0.10279	0.13275	0.16194
450	0.050858	0.055132	0.059785	0.066335	0.073782	0.089221	0.10461	0.13521	0.16497
460	0.050904	0.055195	0.060204	0.067187	0.074922	0.090776	0.10653	0.13773	0.16805
470	0.050952	0.055262	0.060735	0.068113	0.076114	0.092339	0.10848	0.14027	0.17117
480	0.051	0.055354	0.061359	0.069102	0.07735	0.093932	0.11044	0.14285	0.17433
490	0.051049	0.055486	0.06206	0.070142	0.078624	0.095599	0.11243	0.14546	0.17752
500	0.051099	0.055704	0.062827	0.071224	0.079928	0.097294	0.11445	0.14809	0.18075
510	0.05115	0.056028	0.063652	0.07234	0.081253	0.098992	0.11648	0.15073	0.18399
520	0.0512	0.056454	0.064528	0.073485	0.082571	0.10071	0.11852	0.1534	0.18726
530	0.051252	0.056962	0.065447	0.074655	0.083917	0.10244	0.12058	0.15609	0.19054
540	0.051304	0.057537	0.066401	0.075848	0.085316	0.10418	0.12266	0.15879	0.19385
550	0.05136	0.05817	0.067383	0.077045	0.086732	0.10593	0.12474	0.1615	0.19716
560	0.051437	0.058851	0.068389	0.078233	0.08815	0.1077	0.12683	0.16422	0.2005
570	0.051552	0.059571	0.069415	0.07946	0.089578	0.10947	0.12893	0.16696	0.20385
580	0.05174	0.06033	0.070457	0.080723	0.091016	0.11125	0.13104	0.1697	0.20721
590	0.052014	0.061123	0.071513	0.08199	0.092458	0.11303	0.13316	0.17245	0.21059
600	0.052367	0.061942	0.072569	0.08326	0.093906	0.11482	0.13528	0.17521	0.21397
610	0.052785	0.062783	0.073612	0.084539	0.09536	0.11662	0.13741	0.17799	0.21736
620	0.053255	0.063642	0.074685	0.085822	0.096818	0.11841	0.13954	0.18076	0.22077
630	0.053771	0.064517	0.075789	0.087107	0.09828	0.12022	0.14167	0.18355	0.22418
640	0.054325	0.065404	0.0769	0.088398	0.099744	0.12202	0.14381	0.18634	0.22759
650	0.054909	0.066302	0.078013	0.089692	0.10121	0.12383	0.14595	0.18914	0.23102
660	0.055519	0.06721	0.079132	0.090989	0.10269	0.12565	0.1481	0.19194	0.23445
670	0.056153	0.06812	0.080253	0.092289	0.10416	0.12746	0.15025	0.19474	0.23788
680	0.056811	0.069014	0.081375	0.093592	0.10565	0.12928	0.1524	0.19755	0.24132
690	0.057489	0.069917	0.0825	0.094897	0.10713	0.1311	0.15456	0.20036	0.24477
700	0.058183	0.070851	0.083628	0.096204	0.10861	0.13292	0.15671	0.20318	0.24822
710	0.05889	0.071797	0.084757	0.097512	0.1101	0.13474	0.15887	0.206	0.25167
720	0.059607	0.072744	0.085889	0.098823	0.11159	0.13657	0.16104	0.20882	0.25514
730	0.060334	0.073695	0.087021	0.10014	0.11307	0.1384	0.1632	0.21165	0.2586
740	0.061068	0.07465	0.088155	0.10145	0.11456	0.14023	0.16537	0.21448	0.26207
750	0.061809	0.075603	0.089289	0.10276	0.11605	0.14206	0.16754	0.21731	0.26554
760	0.062556	0.076557	0.090425	0.10408	0.11755	0.14389	0.16971	0.22014	0.26902
770	0.063307	0.077513	0.091565	0.1054	0.11904	0.14573	0.17188	0.22298	0.2725
780	0.064057	0.078471	0.092706	0.10672	0.12053	0.14756	0.17406	0.22582	0.27598
790	0.06479	0.079429	0.093848	0.10804	0.12203	0.1494	0.17623	0.22866	0.27947
800	0.065529	0.080388	0.09499	0.10936	0.12353	0.15125	0.17841	0.2315	0.28297
810	0.066291	0.081348	0.096134	0.11068	0.12502	0.15309	0.18059	0.23435	0.28647
820	0.067065	0.082309	0.097279	0.112	0.12652	0.15493	0.18277	0.2372	0.28997
830	0.067839	0.08327	0.098424	0.11332	0.12802	0.15678	0.18495	0.24006	0.29348
840	0.068616	0.084233	0.09957	0.11465	0.12952	0.15862	0.18713	0.24291	0.29699

850	0.069396	0.085198	0.10072	0.11597	0.13102	0.16047	0.18932	0.24577	0.3005
860	0.070175	0.086163	0.10186	0.11729	0.13253	0.16231	0.19151	0.24862	0.30401
870	0.070952	0.087128	0.10301	0.11862	0.13403	0.16416	0.1937	0.25148	0.30753
880	0.071731	0.088095	0.10416	0.11995	0.13553	0.16601	0.19589	0.25434	0.31105
890	0.072511	0.089062	0.10531	0.12128	0.13703	0.16786	0.19808	0.25721	0.31458
900	0.073293	0.09003	0.10646	0.12261	0.13853	0.16971	0.20027	0.26007	0.3181
910	0.074075	0.090999	0.10761	0.12393	0.14003	0.17156	0.20247	0.26294	0.32163
920	0.074858	0.091968	0.10876	0.12526	0.14154	0.17341	0.20466	0.26581	0.32517
930	0.07564	0.092938	0.10991	0.12659	0.14304	0.17526	0.20686	0.26868	0.3287
940	0.076424	0.093908	0.11106	0.12792	0.14454	0.17711	0.20906	0.27155	0.33224
950	0.077207	0.094878	0.11221	0.12925	0.14605	0.17897	0.21126	0.27442	0.33579
960	0.077992	0.095849	0.11336	0.13058	0.14756	0.18082	0.21346	0.27729	0.33933
970	0.078777	0.096819	0.11451	0.13192	0.14906	0.18267	0.21566	0.28017	0.34288
980	0.079562	0.09779	0.11567	0.13325	0.15057	0.18453	0.21786	0.28305	0.34643
990	0.080348	0.098761	0.11682	0.13458	0.15208	0.18639	0.22006	0.28593	0.34999
1000	0.081134	0.099732	0.11798	0.13591	0.15358	0.18824	0.22226	0.28881	0.35355
1050	0.085071	0.10459	0.12375	0.14258	0.16114	0.19754	0.23327	0.30325	0.3714
1100	0.089016	0.10946	0.12953	0.14926	0.1687	0.20686	0.24432	0.31773	0.38934
1150	0.092965	0.11433	0.13532	0.15594	0.17627	0.2162	0.25539	0.33225	0.40738
1200	0.096919	0.11922	0.14112	0.16264	0.18386	0.22555	0.2665	0.34685	0.42549
1250	0.099972	0.12309	0.1458	0.16813	0.19017	0.23347	0.27603	0.35961	0.44151
1300	0.10204	0.12578	0.14914	0.17211	0.1948	0.23942	0.28331	0.36957	0.45421
1350	0.10366	0.12792	0.15181	0.17531	0.19855	0.24429	0.28931	0.37789	0.46492
1400	0.10505	0.12975	0.15408	0.17805	0.20177	0.24848	0.2945	0.38513	0.47428
1450	0.10629	0.13137	0.15611	0.18049	0.20462	0.2522	0.29912	0.3916	0.48268
1500	0.10743	0.13286	0.15796	0.18271	0.20723	0.2556	0.30332	0.39749	0.49034
1550	0.1085	0.13426	0.15968	0.18478	0.20965	0.25875	0.30722	0.40294	0.49743
1600	0.10953	0.13559	0.16131	0.18673	0.21193	0.26171	0.31087	0.40805	0.50408
1650	0.11052	0.13686	0.16287	0.18859	0.2141	0.26453	0.31435	0.4129	0.51038
1700	0.11149	0.13809	0.16439	0.1904	0.21619	0.26723	0.31767	0.41753	0.51639
1750	0.11243	0.1393	0.16586	0.19215	0.21823	0.26984	0.32088	0.42198	0.52215
1800	0.11337	0.14049	0.16731	0.19386	0.22021	0.27238	0.324	0.42628	0.52772
1850	0.11429	0.14166	0.16873	0.19554	0.22215	0.27486	0.32703	0.43046	0.53312
1900	0.11521	0.14281	0.17013	0.1972	0.22406	0.27729	0.33	0.43454	0.53838
1950	0.11612	0.14396	0.17152	0.19883	0.22594	0.27968	0.33291	0.43854	0.54352
2000	0.11702	0.14509	0.17289	0.20045	0.2278	0.28204	0.33578	0.44247	0.54856
2100	0.11882	0.14734	0.17561	0.20363	0.23147	0.28668	0.34141	0.45015	0.5584
2200	0.1206	0.14958	0.1783	0.20678	0.23509	0.29124	0.34694	0.45766	0.56798
2300	0.12237	0.1518	0.18097	0.20991	0.23867	0.29574	0.35238	0.46504	0.57738
2400	0.12414	0.15401	0.18363	0.21301	0.24222	0.30021	0.35777	0.47233	0.58663
2500	0.12591	0.15622	0.18628	0.2161	0.24576	0.30465	0.36312	0.47955	0.59578
2600	0.12768	0.15843	0.18892	0.21919	0.24929	0.30907	0.36844	0.48672	0.60484
2700	0.12944	0.16063	0.19156	0.22227	0.25281	0.31346	0.37373	0.49384	0.61383
2800	0.13092	0.16251	0.19384	0.22495	0.25591	0.31737	0.37849	0.50031	0.62205
2900	0.13204	0.16397	0.19564	0.2271	0.2584	0.32057	0.38244	0.50577	0.62904
3000	0.13296	0.16518	0.19715	0.22891	0.26052	0.32333	0.38585	0.51055	0.63519
3100	0.13377	0.16624	0.19847	0.23051	0.2624	0.32578	0.38889	0.51482	0.64071
3200	0.13451	0.1672	0.19967	0.23195	0.2641	0.328	0.39164	0.5187	0.64574
3300	0.13519	0.1681	0.20078	0.23329	0.26567	0.33005	0.39419	0.52229	0.65039
3400	0.13584	0.16894	0.20183	0.23455	0.26715	0.33197	0.39658	0.52565	0.65473
3500	0.13646	0.16975	0.20283	0.23575	0.26855	0.3338	0.39883	0.52882	0.65882
3600	0.13707	0.17054	0.20379	0.23691	0.26989	0.33554	0.40098	0.53183	0.66271
3700	0.13766	0.1713	0.20472	0.23802	0.27119	0.33723	0.40305	0.53471	0.66643
3800	0.13824	0.17204	0.20564	0.23911	0.27245	0.33886	0.40505	0.53749	0.67001
3900	0.13881	0.17278	0.20653	0.24017	0.27368	0.34045	0.407	0.54019	0.67347
4000	0.13938	0.1735	0.20742	0.24121	0.27489	0.342	0.4089	0.54281	0.67683
4100	0.13994	0.17421	0.20829	0.24224	0.27607	0.34352	0.41076	0.54537	0.6801
4200	0.1405	0.17492	0.20915	0.24326	0.27724	0.34502	0.41259	0.54787	0.68331
4300	0.14106	0.17562	0.21	0.24426	0.2784	0.3465	0.4144	0.55034	0.68645
4400	0.14161	0.17632	0.21084	0.24526	0.27955	0.34796	0.41618	0.55276	0.68954
4500	0.14216	0.17702	0.21168	0.24625	0.28069	0.3494	0.41794	0.55516	0.69258
4600	0.14271	0.17771	0.21252	0.24724	0.28182	0.35083	0.41968	0.55752	0.69558
4700	0.14325	0.17839	0.21335	0.24821	0.28294	0.35225	0.42141	0.55987	0.69854
4800	0.1438	0.17908	0.21418	0.24918	0.28406	0.35366	0.42312	0.56219	0.70148
4900	0.14434	0.17976	0.21501	0.25015	0.28517	0.35506	0.42482	0.56449	0.70439
5000	0.14489	0.18044	0.21583	0.25111	0.28628	0.35645	0.42651	0.56678	0.70727
5200	0.14597	0.1818	0.21747	0.25303	0.28849	0.35922	0.42987	0.57132	0.71299
5400	0.14705	0.18316	0.2191	0.25494	0.29068	0.36197	0.4332	0.57582	0.71864
5600	0.14814	0.18451	0.22072	0.25684	0.29286	0.36471	0.43651	0.58027	0.72424
5800	0.14921	0.18585	0.22234	0.25874	0.29503	0.36743	0.4398	0.5847	0.7298
6000	0.15029	0.18719	0.22396	0.26062	0.29719	0.37013	0.44307	0.5891	0.73533
6200	0.15137	0.18854	0.22557	0.26251	0.29935	0.37284	0.44634	0.59348	0.74084
6400	0.15244	0.18988	0.22718	0.26439	0.3015	0.37554	0.44959	0.59785	0.74632
6600	0.15351	0.19122	0.22879	0.26627	0.30365	0.37824	0.45284	0.60219	0.75179
6800	0.15458	0.19256	0.23039	0.26814	0.30579	0.38093	0.45608	0.60653	0.75724
7000	0.15565	0.19389	0.232	0.27001	0.30793	0.38361	0.45932	0.61086	0.76268
7200	0.15672	0.19523	0.2336	0.27189	0.31007	0.3863	0.46255	0.61519	0.76811
7400	0.15779	0.19656	0.2352	0.27376	0.3122	0.38897	0.46578	0.6195	0.77354
7600	0.15886	0.1979	0.2368	0.27563	0.31434	0.39165	0.469	0.62381	0.77896
7800	0.15992	0.19923	0.2384	0.27749	0.31647	0.39432	0.47222	0.62812	0.78438
8000	0.16099	0.20056	0.24001	0.27936	0.31861	0.39699	0.47544	0.63242	0.78979
8200	0.16205	0.2019	0.24161	0.28122	0.32074	0.39966	0.47865	0.63672	0.79519
8400	0.16312	0.20323	0.24321	0.28309	0.32287	0.40233	0.48187	0.64101	0.8006
8600	0.16419	0.20456	0.2448	0.28495	0.325	0.405	0.48508	0.64531	0.806
8800	0.16526	0.20589	0.2464	0.28682	0.32713	0.40767	0.4883	0.6496	0.8114
9000	0.16632	0.20723	0.24799	0.28868	0.32926	0.41034	0.49151	0.6539	0.8168
9200	0.16739	0.20855	0.24959	0.29054	0.33139	0.413	0.49472	0.65819	0.82219
9400	0.16845	0.20988	0.25119	0.2924	0.33351	0.41566	0.49793	0.66249	0.82758
9600	0.16952	0.21121	0.25278	0.29426	0.33564	0.41833	0.50113	0.66678	0.83297
9800	0.17058	0.21254	0.25438	0.29612	0.33776	0.42099	0.50433	0.67107	0.83836
10000	0.17165	0.21388	0.25597	0.29798	0.33989	0.42366	0.50754	0.67536	0.84376

Table D-3. Pressure data at each gas generation factor, f

Time [years]	Pressure [MPa]								
	f=0.0	f=0.025	f=0.05	f=0.07	f=0.085	f=0.1	f=0.125	f=0.15	f=0.175
6.5144e-11	0	0	0	0	0	0	0	0	0
3.9006e-09	0	2.7109e-07	5.4218e-07	7.5905e-07	9.217e-07	1.0844e-06	1.3554e-06	1.6265e-06	1.8976e-06
7.3573e-09	0	7.1937e-07	1.4387e-06	2.0142e-06	2.4459e-06	2.8775e-06	3.5968e-06	4.3162e-06	5.0356e-06
1.184e-08	0	1.3569e-06	2.7137e-06	3.7992e-06	4.6133e-06	5.4274e-06	6.7843e-06	8.1411e-06	9.498e-06
1.7348e-08	0	2.1835e-06	4.3671e-06	6.1139e-06	7.424e-06	8.7342e-06	1.0918e-05	1.3101e-05	1.5285e-05
2.3883e-08	0	3.1994e-06	6.3989e-06	8.9584e-06	1.0878e-05	1.2798e-05	1.5997e-05	1.9197e-05	2.2396e-05
3.1443e-08	0	4.4045e-06	8.8091e-06	1.2333e-05	1.4975e-05	1.7618e-05	2.2023e-05	2.6427e-05	3.0832e-05
6.028e-08	0	9.1551e-06	1.831e-05	2.5634e-05	3.1127e-05	3.662e-05	4.5775e-05	5.493e-05	6.4085e-05
9.835e-08	0	1.5608e-05	3.1217e-05	4.3704e-05	5.3069e-05	6.2434e-05	7.8042e-05	9.365e-05	0.00010926
1.2886e-07	0	2.0857e-05	4.1713e-05	5.8399e-05	7.0913e-05	8.3427e-05	0.00010428	0.00012514	0.000146
1.4565e-07	0	2.3765e-05	4.7529e-05	6.6541e-05	8.08e-05	9.5058e-05	0.00011882	0.00014259	0.00016635
1.8232e-07	0	3.0148e-05	6.0296e-05	8.4415e-05	0.0001025	0.00012059	0.00015074	0.00018089	0.00021104
2.0219e-07	0	3.3624e-05	6.7247e-05	9.4146e-05	0.00011432	0.00013449	0.00016812	0.00020174	0.00023537
2.4501e-07	0	4.1142e-05	8.2285e-05	0.0001152	0.00013988	0.00016457	0.00020571	0.00024685	0.000288
2.6796e-07	0	4.5186e-05	9.0371e-05	0.00012652	0.00015363	0.00018074	0.00022593	0.00027111	0.0003163
2.9194e-07	0	4.9418e-05	9.8836e-05	0.00013837	0.00016802	0.00019767	0.00024709	0.00029651	0.00034593
5.8812e-07	0	0.00010215	0.0002043	0.00028602	0.0003473	0.00040859	0.00051074	0.00061289	0.00071504
8.5649e-07	0	0.00015032	0.00030064	0.00042089	0.00051108	0.00060127	0.00075159	0.00090191	0.0010522
1.1265e-06	0	0.00019899	0.00039797	0.00055716	0.00067655	0.00079594	0.00099493	0.0011939	0.0013929
1.4335e-06	0	0.00025446	0.00050893	0.0007125	0.00086518	0.0010179	0.0012723	0.0015268	0.0017813
1.7175e-06	0	0.0003059	0.0006118	0.00085652	0.0010401	0.0012236	0.0015295	0.0018354	0.0021413
1.9632e-06	0	0.00035046	0.00070091	0.00098128	0.0011916	0.0014018	0.0017523	0.0021027	0.0024532
2.2253e-06	0	0.00039804	0.00079608	0.0011145	0.0013533	0.0015922	0.0019902	0.0023882	0.0027863
2.5038e-06	0	0.00044865	0.0008973	0.0012562	0.0015254	0.0017946	0.0022432	0.0026919	0.0031405
2.7988e-06	0	0.00050229	0.0010046	0.0014064	0.0017078	0.0020091	0.0025114	0.0030137	0.003516
5.534e-06	0	0.0010011	0.0020022	0.002803	0.0034037	0.0040043	0.0050054	0.0060065	0.0070075
8.3869e-06	0	0.0015227	0.0030455	0.0042637	0.0051773	0.006091	0.0076137	0.0091364	0.010659
1.1065e-05	0	0.002013	0.0040261	0.0056365	0.0068443	0.0080521	0.010065	0.012078	0.014091
1.3774e-05	0	0.0025096	0.0050193	0.007027	0.0085328	0.010039	0.012548	0.015058	0.017567
1.6595e-05	0	0.003027	0.006054	0.0084756	0.010292	0.012108	0.015135	0.018162	0.021189
1.9279e-05	0	0.0035194	0.0070389	0.0098544	0.011966	0.014078	0.017597	0.021117	0.024636
2.2164e-05	0	0.004049	0.008098	0.011337	0.013767	0.016196	0.020245	0.024294	0.028343
2.4797e-05	0	0.0045324	0.0090649	0.012691	0.01541	0.01813	0.022662	0.027195	0.031727
2.7578e-05	0	0.0050431	0.010086	0.014121	0.017147	0.020173	0.025216	0.030259	0.035302
5.5141e-05	0	0.010111	0.020221	0.02831	0.034376	0.040443	0.050553	0.060664	0.070775
8.2429e-05	0	0.015133	0.030266	0.042373	0.051452	0.060532	0.075665	0.090798	0.10593
0.0001099	0	0.020192	0.040384	0.056538	0.068653	0.080769	0.10096	0.12115	0.14135
0.00013757	0	0.02529	0.050581	0.070813	0.085987	0.10116	0.12645	0.15174	0.17703
0.00016483	0	0.030316	0.060632	0.084884	0.10307	0.12126	0.15158	0.1819	0.21221
0.00019204	0	0.035333	0.070665	0.098931	0.12013	0.14133	0.17666	0.212	0.24733
0.00021998	0	0.040486	0.080971	0.11336	0.13765	0.16194	0.20243	0.24291	0.2834
0.00024696	0	0.045463	0.090926	0.1273	0.15457	0.18185	0.22731	0.27278	0.31824
0.00027475	0	0.05059	0.10118	0.14165	0.17201	0.20236	0.25295	0.30354	0.35413
0.00054827	0	0.1011	0.20221	0.28309	0.34375	0.40441	0.50552	0.60662	0.70772
0.00082322	0	0.15195	0.3039	0.42546	0.51663	0.6078	0.75975	0.9117	1.0637
0.0010961	0	0.20247	0.40494	0.56692	0.6884	0.80989	1.0124	1.2148	1.4173
0.0013709	0	0.25338	0.50676	0.70946	0.86149	1.0135	1.2669	1.5203	1.7737
0.001645	0	0.3042	0.60839	0.85175	1.0343	1.2168	1.521	1.8252	2.1294
0.0019181	0	0.35487	0.70975	0.99365	1.2066	1.4195	1.7744	2.1292	2.4841
0.0021932	0	0.40591	0.81183	1.1366	1.3801	1.6237	2.0296	2.4355	2.8414
0.0024663	0	0.45662	0.91325	1.2785	1.5525	1.8265	2.2831	2.7397	3.1964
0.0027412	0	0.50768	1.0154	1.4215	1.7261	2.0307	2.5384	3.0461	3.5537
0.0054803	0	1.0167	2.0335	2.8469	3.4569	4.0669	5.0837	6.1004	7.1172
0.0082175	0	1.5259	3.0517	4.2724	5.1879	6.1034	7.6293	9.1551	10.681
0.010955	0	2.0363	4.0727	5.7018	6.9236	8.1454	10.182	12.218	14.254
0.013697	0	2.5487	5.0974	7.1363	8.6656	10.195	12.743	15.292	17.841
0.016434	0	3.0612	6.1223	8.5713	10.408	12.245	15.306	18.367	21.428
0.01917	0	3.5733	7.1466	10.005	12.149	14.293	17.866	21.44	25.013
0.021907	0	4.0857	8.1714	11.44	13.891	16.343	20.428	24.514	28.6
0.024649	0	4.5986	9.1973	12.876	15.635	18.395	22.993	27.592	32.19
0.027387	0	5.1106	10.221	14.31	17.376	20.443	25.553	30.664	35.775
0.054771	0	10.256	20.513	28.718	34.871	41.025	51.281	61.538	71.794
0.082145	0	15.44	30.88	43.232	52.496	61.76	77.2	92.64	108.08
0.10952	0	20.645	41.289	57.805	70.192	82.578	103.22	123.87	144.51
0.13692	0	25.877	51.754	72.456	87.982	103.51	129.39	155.26	181.14
0.16428	0	31.117	62.235	87.129	105.8	124.47	155.59	186.7	217.82
0.19168	0	36.366	72.733	101.83	123.65	145.47	181.83	218.2	254.56
0.21905	0	41.616	83.232	116.52	141.49	166.46	208.08	249.7	291.31
0.24644	0	46.868	93.736	131.23	159.35	187.47	234.34	281.21	328.08
0.27382	0	52.122	104.24	145.94	177.22	208.49	260.61	312.73	364.86
0.3012	0	57.379	114.76	160.66	195.09	229.51	286.89	344.27	401.65
0.32858	0	62.64	125.28	175.39	212.98	250.56	313.2	375.84	438.48
0.35594	0	67.897	135.79	190.11	230.85	271.59	339.49	407.38	475.28
0.38333	0	73.161	146.32	204.85	248.75	292.64	365.81	438.97	512.13
0.41071	0	78.429	156.86	219.6	266.66	313.72	392.15	470.57	549
0.43808	0	83.695	167.39	234.35	284.56	334.78	418.47	502.17	585.86
0.46547	0	88.968	177.94	249.11	302.49	355.87	444.84	533.81	622.77
0.49283	0	94.239	188.48	263.87	320.41	376.95	471.19	565.43	659.67
0.52022	0	99.519	199.04	278.65	338.37	398.08	497.6	597.11	696.63
0.54761	0	104.8	209.61	293.45	356.34	419.22	524.02	628.83	733.63
0.57498	0	110.09	220.18	308.25	374.31	440.36	550.45	660.54	770.63
0.60236	0	115.38	230.76	323.07	392.3	461.53	576.91	692.29	807.67
0.62976	0	120.68	241.36	337.9	410.31	482.72	603.4	724.08	844.76
0.6571	0	125.98	251.95	352.73	428.32	503.9	629.88	755.85	881.83
0.68451	0	131.29	262.58	367.61	446.38	525.15	656.44	787.72	919.01
0.71186	0	136.59	273.19	382.46	464.42	546.37	682.97	819.56	956.15

0.73924	0	141.91	283.82	397.35	482.5	567.65	709.56	851.47	993.38
0.76662	0	147.24	294.47	412.26	500.6	588.95	736.18	883.42	1030.7
0.79402	0	152.57	305.14	427.2	518.74	610.28	762.85	915.42	1068
0.82141	0	157.91	315.82	442.14	536.89	631.63	789.54	947.45	1105.4
0.84875	0	163.25	326.49	457.09	555.04	652.99	816.23	979.48	1142.7
0.87617	0	168.6	337.21	472.09	573.25	674.42	843.02	1011.6	1180.2
0.90355	0	173.96	347.92	487.09	591.47	695.85	869.81	1043.8	1217.7
0.93091	0	179.32	358.65	502.1	609.7	717.29	896.61	1075.9	1255.3
0.95828	0	184.69	369.38	517.14	627.95	738.77	923.46	1108.1	1292.8
1	0	192.89	385.79	540.1	655.83	771.57	964.46	1157.4	1350.2
2.0001	0	392.76	785.51	1099.7	1335.4	1571	1963.8	2356.5	2749.3
3.0001	0	598.9	1197.8	1676.9	2036.2	2395.6	2994.5	3593.3	4192.2
4.0001	0	811.62	1623.2	2272.5	2759.4	3246.4	4057.9	4869.5	5681
5.0001	0	1030.8	2061.6	2886.2	3504.6	4123.1	5153.7	6184.4	7215
6.0001	0	1256.7	2513.3	3518.6	4272.5	5026.4	6282.9	7539.4	8795.8
7.0001	0	1489.4	2978.7	4170.1	5063.6	5957	7446.1	8935.1	10424
8.0001	0	1729.1	3458	4841.1	5878.4	6915.6	8644.2	10373	12101
9.0001	0	1976	3951.8	5532.3	6717.6	7902.8	9878.1	11853	13828
10	0	2230.3	4460.3	6244.1	7581.9	8919.6	11149	13378	15607
20	0	5228.7	10455	14634	17768	20901	26120	31338	36553
30	0	9152.5	18295	25602	31078	36550	45663	54766	63859
40	0	14402	28771	40243	48833	57412	71685	85926	1.0014e+05
50	0	21341	42596	59538	72210	84851	1.0585e+05	1.2677e+05	1.4761e+05
60	0	30824	61426	85751	1.0391e+05	1.2198e+05	1.5195e+05	1.8171e+05	2.1127e+05
70	0	43913	87313	1.2167e+05	1.4724e+05	1.7263e+05	2.1457e+05	2.5605e+05	2.9708e+05
80	0	62437	1.2365e+05	1.7178e+05	2.0741e+05	2.4264e+05	3.0048e+05	3.573e+05	4.1313e+05
90	0	89467	1.7614e+05	2.436e+05	2.9316e+05	3.4187e+05	4.2127e+05	4.9855e+05	5.7383e+05
100	0	1.2994e+05	2.5373e+05	3.487e+05	4.1761e+05	4.8466e+05	5.9261e+05	6.9609e+05	7.9552e+05
110	0	1.8704e+05	3.6159e+05	4.9319e+05	5.8763e+05	6.7873e+05	8.2365e+05	9.6069e+05	1.0906e+06
120	0	2.5762e+05	4.9611e+05	6.7425e+05	8.0096e+05	9.2206e+05	1.1123e+06	1.2895e+06	1.4548e+06
130	0	3.3094e+05	6.3815e+05	8.6668e+05	1.0287e+06	1.1834e+06	1.4259e+06	1.6506e+06	1.859e+06
140	0	3.9823e+05	7.7159e+05	1.0526e+06	1.2529e+06	1.4443e+06	1.7435e+06	2.0177e+06	2.2699e+06
150	0	4.6209e+05	8.961e+05	1.2237e+06	1.4584e+06	1.6838e+06	2.0395e+06	2.3703e+06	2.6747e+06
160	0	5.2378e+05	1.0162e+06	1.3886e+06	1.6555e+06	1.9122e+06	2.3174e+06	2.696e+06	3.0495e+06
170	0	5.8457e+05	1.1334e+06	1.5481e+06	1.8457e+06	2.1321e+06	2.5847e+06	3.0084e+06	3.4041e+06
180	0	6.4447e+05	1.2487e+06	1.7048e+06	2.0317e+06	2.3462e+06	2.8436e+06	3.3089e+06	3.7451e+06
190	0	7.0361e+05	1.3624e+06	1.8591e+06	2.2147e+06	2.5562e+06	3.0961e+06	3.6014e+06	4.0742e+06
200	0	7.6184e+05	1.4744e+06	2.0107e+06	2.3944e+06	2.7628e+06	3.3435e+06	3.8864e+06	4.3945e+06
210	0	8.1896e+05	1.5846e+06	2.16e+06	2.5711e+06	2.9654e+06	3.5863e+06	4.1652e+06	4.7068e+06
220	0	8.7458e+05	1.693e+06	2.3069e+06	2.745e+06	3.1645e+06	3.8246e+06	4.4383e+06	5.0118e+06
230	0	9.2777e+05	1.7993e+06	2.4517e+06	2.9163e+06	3.3606e+06	4.0585e+06	4.7066e+06	5.3106e+06
240	0	9.7711e+05	1.9029e+06	2.5939e+06	3.0851e+06	3.5539e+06	4.2885e+06	4.97e+06	5.6032e+06
250	0	1.0242e+06	2.0028e+06	2.7336e+06	3.2513e+06	3.7443e+06	4.515e+06	5.2287e+06	5.8902e+06
260	0	1.0701e+06	2.0974e+06	2.8704e+06	3.4148e+06	3.9321e+06	4.7382e+06	5.4829e+06	6.1717e+06
270	0	1.1152e+06	2.1884e+06	3.0038e+06	3.5758e+06	4.1173e+06	4.9582e+06	5.7327e+06	6.4482e+06
280	0	1.1599e+06	2.2774e+06	3.132e+06	3.734e+06	4.2999e+06	5.1751e+06	5.9788e+06	6.72e+06
290	0	1.2041e+06	2.3651e+06	3.2562e+06	3.8893e+06	4.48e+06	5.3891e+06	6.2212e+06	6.9873e+06
300	0	1.2482e+06	2.4519e+06	3.3779e+06	4.0407e+06	4.6576e+06	5.6003e+06	6.4603e+06	7.2506e+06
310	0	1.2919e+06	2.5379e+06	3.4978e+06	4.1882e+06	4.833e+06	5.8091e+06	6.6962e+06	7.5101e+06
320	0	1.3355e+06	2.6234e+06	3.6164e+06	4.3329e+06	5.0059e+06	6.0155e+06	6.9292e+06	7.7662e+06
330	0	1.3788e+06	2.7084e+06	3.734e+06	4.4756e+06	5.1764e+06	6.2197e+06	7.1594e+06	8.0193e+06
340	0	1.4221e+06	2.7931e+06	3.8507e+06	4.6167e+06	5.3446e+06	6.4218e+06	7.3872e+06	8.2695e+06
350	0	1.4653e+06	2.8774e+06	3.9668e+06	4.7566e+06	5.5103e+06	6.6218e+06	7.6126e+06	8.5171e+06
360	0	1.5084e+06	2.9614e+06	4.0824e+06	4.8955e+06	5.6738e+06	6.82e+06	7.8358e+06	8.7624e+06
370	0	1.5514e+06	3.0452e+06	4.1975e+06	5.0336e+06	5.8357e+06	7.0164e+06	8.057e+06	9.0057e+06
380	0	1.5943e+06	3.1288e+06	4.3122e+06	5.1712e+06	5.9964e+06	7.2112e+06	8.2764e+06	9.2474e+06
390	0	1.6372e+06	3.2123e+06	4.4266e+06	5.3081e+06	6.156e+06	7.4047e+06	8.4944e+06	9.4876e+06
400	0	1.68e+06	3.2956e+06	4.5406e+06	5.4446e+06	6.3148e+06	7.5967e+06	8.7109e+06	9.7266e+06
410	0	1.7227e+06	3.3786e+06	4.6544e+06	5.5807e+06	6.4728e+06	7.7875e+06	8.9264e+06	9.9645e+06
420	0	1.7654e+06	3.4616e+06	4.7679e+06	5.7164e+06	6.6303e+06	7.9772e+06	9.1408e+06	1.0201e+07
430	0	1.8081e+06	3.5444e+06	4.8812e+06	5.8518e+06	6.7872e+06	8.166e+06	9.3543e+06	1.0438e+07
440	0	1.8507e+06	3.6271e+06	4.9943e+06	5.9869e+06	6.9437e+06	8.354e+06	9.567e+06	1.0673e+07
450	0	1.8933e+06	3.7096e+06	5.1072e+06	6.1217e+06	7.0997e+06	8.5412e+06	9.7789e+06	1.0908e+07
460	0	1.9359e+06	3.7921e+06	5.22e+06	6.2562e+06	7.2553e+06	8.7277e+06	9.9903e+06	1.1142e+07
470	0	1.9784e+06	3.8745e+06	5.3325e+06	6.3905e+06	7.4106e+06	8.9137e+06	1.0201e+07	1.1375e+07
480	0	2.0209e+06	3.9567e+06	5.4449e+06	6.5246e+06	7.5656e+06	9.0992e+06	1.0411e+07	1.1608e+07
490	0	2.0634e+06	4.0389e+06	5.5571e+06	6.6585e+06	7.7203e+06	9.2841e+06	1.0621e+07	1.184e+07
500	0	2.1058e+06	4.1209e+06	5.6692e+06	6.7921e+06	7.8746e+06	9.4686e+06	1.083e+07	1.2071e+07
510	0	2.1482e+06	4.2029e+06	5.7811e+06	6.9256e+06	8.0288e+06	9.6527e+06	1.1039e+07	1.2302e+07
520	0	2.1906e+06	4.2848e+06	5.8929e+06	7.0589e+06	8.1827e+06	9.8364e+06	1.1247e+07	1.2532e+07
530	0	2.2329e+06	4.3666e+06	6.0046e+06	7.192e+06	8.3363e+06	1.002e+07	1.1455e+07	1.2762e+07
540	0	2.2752e+06	4.4484e+06	6.1161e+06	7.3249e+06	8.4897e+06	1.0203e+07	1.1662e+07	1.2991e+07
550	0	2.3175e+06	4.5301e+06	6.2276e+06	7.4577e+06	8.6429e+06	1.0385e+07	1.1869e+07	1.322e+07
560	0	2.3598e+06	4.6117e+06	6.3389e+06	7.5903e+06	8.7958e+06	1.0568e+07	1.2076e+07	1.3448e+07
570	0	2.4021e+06	4.6932e+06	6.45e+06	7.7228e+06	8.9486e+06	1.075e+07	1.2282e+07	1.3675e+07
580	0	2.4443e+06	4.7746e+06	6.5611e+06	7.855e+06	9.1011e+06	1.0932e+07	1.2487e+07	1.3903e+07
590	0	2.4865e+06	4.856e+06	6.672e+06	7.9871e+06	9.2534e+06	1.1113e+07	1.2692e+07	1.4129e+07
600	0	2.5286e+06	4.9373e+06	6.7829e+06	8.1191e+06	9.4055e+06	1.1294e+07	1.2897e+07	1.4355e+07
610	0	2.5708e+06	5.0186e+06	6.8936e+06	8.2509e+06	9.5574e+06	1.1475e+07	1.3101e+07	1.4579e+07
620	0	2.6129e+06	5.0998e+06	7.0042e+06	8.3826e+06	9.7092e+06	1.1655e+07	1.3305e+07	1.4794e+07
630	0	2.655e+06	5.1809e+06	7.1148e+06	8.5141e+06	9.8607e+06	1.1835e+07	1.3509e+07	1.4995e+07
640	0	2.6971e+06	5.2619e+06	7.2252e+06	8.6455e+06	1.0012e+07	1.2015e+07	1.3712e+07	1.5174e+07
650	0	2.7392e+06	5.343e+06	7.3355e+06	8.7767e+06	1.0163e+07	1.2195e+07	1.3915e+07	1.5328e+07
660	0	2.7812e+06	5.4239e+06	7.4457e+06	8.9078e+06	1.0314e+07	1.2374e+07	1.4117e+07	1.5461e+07
670	0	2.8232e+06	5.5048e+06	7.5558e+06	9.0388e+06	1.0465e+07	1.2553e+07	1.4319e+07	1.5577e+07
680	0	2.8653e+06	5.5857e+06	7.6658e+06	9.1696e+06	1.0615e+07	1.2732e+07	1.452e+07	1.5677e+07
690	0	2.9072e+06	5.6664e+06	7.7757e+06	9.3003e+06	1.0766e+07	1.291e+07	1.4717e+07	1.5765e+07
700	0	2.9492e+06	5.747e+06	7.8856e+06	9.4308e+06	1.0916e+07	1.3088e+07	1.4903e+07	1.5841e+07
710	0	2.9912e+06	5.8277e+06	7.9953e+06	9.5611e+06	1.1066e+07	1.3266e+07	1.5072e+07	1.5909e+07
720	0	3.0331e+06	5.9083e+06	8.1049e+06	9.6914e+06	1.1216e+07	1.3444e+07	1.5219e+07	1.5969e+07
730	0	3.075e+06	5.9889e+06	8.2141e+06	9.8214e+06	1.1365e+07	1.3621e+07	1.5347e+07	1.6023e+07
740	0	3.1169e+06	6.0694e+06	8.3236e+06	9.9512e+06	1.1514e+07	1.3798e+07	1.5457e+07	1.607e+07

750	0	3.1588e+06	6.1498e+06	8.4329e+06	1.0081e+07	1.1664e+07	1.3974e+07	1.5554e+07	1.611e+07
760	0	3.2007e+06	6.2302e+06	8.5421e+06	1.0211e+07	1.1813e+07	1.4151e+07	1.5638e+07	1.6146e+07
770	0	3.2425e+06	6.3106e+06	8.6512e+06	1.034e+07	1.1961e+07	1.4326e+07	1.5712e+07	1.6177e+07
780	0	3.2843e+06	6.3909e+06	8.7602e+06	1.0469e+07	1.211e+07	1.4502e+07	1.5777e+07	1.6205e+07
790	0	3.3262e+06	6.4711e+06	8.869e+06	1.0599e+07	1.2258e+07	1.4676e+07	1.5835e+07	1.623e+07
800	0	3.3679e+06	6.5513e+06	8.9779e+06	1.0728e+07	1.2406e+07	1.4842e+07	1.5886e+07	1.6253e+07
810	0	3.4097e+06	6.6314e+06	9.0865e+06	1.0857e+07	1.2554e+07	1.4994e+07	1.5933e+07	1.6273e+07
820	0	3.4515e+06	6.7114e+06	9.1951e+06	1.0985e+07	1.2702e+07	1.5128e+07	1.5974e+07	1.6292e+07
830	0	3.4932e+06	6.7914e+06	9.3036e+06	1.1114e+07	1.285e+07	1.5245e+07	1.601e+07	1.6309e+07
840	0	3.5349e+06	6.8714e+06	9.4119e+06	1.1243e+07	1.2997e+07	1.5347e+07	1.6042e+07	1.6325e+07
850	0	3.5767e+06	6.9513e+06	9.5202e+06	1.1371e+07	1.3144e+07	1.5437e+07	1.607e+07	1.634e+07
860	0	3.6183e+06	7.0311e+06	9.6284e+06	1.1499e+07	1.3291e+07	1.5515e+07	1.6095e+07	1.6357e+07
870	0	3.66e+06	7.1109e+06	9.7364e+06	1.1627e+07	1.3438e+07	1.5584e+07	1.6117e+07	1.6377e+07
880	0	3.7017e+06	7.1906e+06	9.8444e+06	1.1755e+07	1.3585e+07	1.5645e+07	1.6137e+07	1.6393e+07
890	0	3.7433e+06	7.2703e+06	9.9523e+06	1.1883e+07	1.3731e+07	1.5699e+07	1.6155e+07	1.6404e+07
900	0	3.785e+06	7.3499e+06	1.006e+07	1.201e+07	1.3877e+07	1.5748e+07	1.6172e+07	1.6413e+07
910	0	3.8266e+06	7.4295e+06	1.0168e+07	1.2138e+07	1.4023e+07	1.5791e+07	1.6187e+07	1.6422e+07
920	0	3.8682e+06	7.509e+06	1.0275e+07	1.2265e+07	1.4169e+07	1.583e+07	1.6201e+07	1.643e+07
930	0	3.9098e+06	7.5884e+06	1.0383e+07	1.2392e+07	1.4314e+07	1.5866e+07	1.6214e+07	1.6437e+07
940	0	3.9513e+06	7.6678e+06	1.049e+07	1.2519e+07	1.4459e+07	1.5898e+07	1.6227e+07	1.6443e+07
950	0	3.9929e+06	7.7471e+06	1.0597e+07	1.2646e+07	1.4604e+07	1.5926e+07	1.6239e+07	1.6451e+07
960	0	4.0344e+06	7.8263e+06	1.0705e+07	1.2773e+07	1.4746e+07	1.5951e+07	1.6251e+07	1.6458e+07
970	0	4.076e+06	7.9056e+06	1.0812e+07	1.2899e+07	1.4879e+07	1.5973e+07	1.6266e+07	1.6465e+07
980	0	4.1174e+06	7.9847e+06	1.0918e+07	1.3025e+07	1.4999e+07	1.5992e+07	1.6282e+07	1.6471e+07
990	0	4.1589e+06	8.0639e+06	1.1025e+07	1.3152e+07	1.5104e+07	1.601e+07	1.6292e+07	1.6478e+07
1000	0	4.2004e+06	8.1429e+06	1.1132e+07	1.3278e+07	1.5197e+07	1.6026e+07	1.63e+07	1.6484e+07
1050	0	4.4075e+06	8.5374e+06	1.1664e+07	1.3906e+07	1.5527e+07	1.6089e+07	1.6329e+07	1.6512e+07
1100	0	4.6143e+06	8.9305e+06	1.2194e+07	1.453e+07	1.572e+07	1.6135e+07	1.6356e+07	1.6536e+07
1150	0	4.8206e+06	9.3223e+06	1.2721e+07	1.5073e+07	1.5841e+07	1.6182e+07	1.638e+07	1.6557e+07
1200	0	5.0266e+06	9.7127e+06	1.3245e+07	1.5395e+07	1.5912e+07	1.6203e+07	1.64e+07	1.6574e+07
1250	0	5.0681e+06	9.7892e+06	1.3346e+07	1.5263e+07	1.5636e+07	1.588e+07	1.6058e+07	1.6216e+07
1300	0	5.1101e+06	9.8676e+06	1.345e+07	1.5224e+07	1.5522e+07	1.5734e+07	1.5894e+07	1.6035e+07
1350	0	5.1521e+06	9.9461e+06	1.3554e+07	1.5215e+07	1.5464e+07	1.5653e+07	1.5798e+07	1.5926e+07
1400	0	5.1941e+06	1.0025e+07	1.3659e+07	1.5217e+07	1.543e+07	1.5603e+07	1.5737e+07	1.5856e+07
1450	0	5.2361e+06	1.0103e+07	1.3764e+07	1.5224e+07	1.541e+07	1.557e+07	1.5696e+07	1.5807e+07
1500	0	5.278e+06	1.0182e+07	1.3868e+07	1.5234e+07	1.54e+07	1.5548e+07	1.5669e+07	1.5773e+07
1550	0	5.32e+06	1.026e+07	1.3973e+07	1.5243e+07	1.5402e+07	1.5534e+07	1.5648e+07	1.5748e+07
1600	0	5.3619e+06	1.0339e+07	1.4077e+07	1.5251e+07	1.5402e+07	1.5523e+07	1.5634e+07	1.5729e+07
1650	0	5.4038e+06	1.0417e+07	1.4182e+07	1.5259e+07	1.5401e+07	1.5516e+07	1.5623e+07	1.5715e+07
1700	0	5.4457e+06	1.0496e+07	1.4286e+07	1.5266e+07	1.54e+07	1.5511e+07	1.5615e+07	1.5705e+07
1750	0	5.4876e+06	1.0574e+07	1.439e+07	1.5272e+07	1.5399e+07	1.5508e+07	1.5609e+07	1.5696e+07
1800	0	5.5294e+06	1.0652e+07	1.4494e+07	1.5278e+07	1.5397e+07	1.5506e+07	1.5605e+07	1.569e+07
1850	0	5.5713e+06	1.0731e+07	1.4598e+07	1.5283e+07	1.5396e+07	1.5504e+07	1.5601e+07	1.5685e+07
1900	0	5.6131e+06	1.0809e+07	1.4701e+07	1.5288e+07	1.5395e+07	1.5503e+07	1.5599e+07	1.5681e+07
1950	0	5.6549e+06	1.0887e+07	1.4801e+07	1.5292e+07	1.5395e+07	1.5503e+07	1.5597e+07	1.5678e+07
2000	0	5.6967e+06	1.0965e+07	1.4888e+07	1.5296e+07	1.5395e+07	1.5503e+07	1.5595e+07	1.5676e+07
2100	0	5.7801e+06	1.1122e+07	1.5004e+07	1.5304e+07	1.5396e+07	1.5503e+07	1.5594e+07	1.5673e+07
2200	0	5.8635e+06	1.1278e+07	1.5078e+07	1.5312e+07	1.5398e+07	1.5504e+07	1.5593e+07	1.567e+07
2300	0	5.9469e+06	1.1434e+07	1.5129e+07	1.5318e+07	1.5401e+07	1.5505e+07	1.5593e+07	1.5669e+07
2400	0	6.0302e+06	1.159e+07	1.5168e+07	1.5324e+07	1.5404e+07	1.5507e+07	1.5593e+07	1.5668e+07
2500	0	6.1135e+06	1.1745e+07	1.5196e+07	1.534e+07	1.5407e+07	1.5508e+07	1.5593e+07	1.5668e+07
2600	0	6.1966e+06	1.19e+07	1.5217e+07	1.5351e+07	1.541e+07	1.551e+07	1.5593e+07	1.5668e+07
2700	0	6.2797e+06	1.2056e+07	1.5231e+07	1.5356e+07	1.5413e+07	1.5512e+07	1.5594e+07	1.5668e+07
2800	0	6.3036e+06	1.2099e+07	1.5152e+07	1.5265e+07	1.5317e+07	1.5409e+07	1.5486e+07	1.5556e+07
2900	0	6.3277e+06	1.2143e+07	1.5121e+07	1.5221e+07	1.5269e+07	1.5353e+07	1.5424e+07	1.549e+07
3000	0	6.3518e+06	1.2187e+07	1.5106e+07	1.5196e+07	1.5242e+07	1.5319e+07	1.5385e+07	1.5447e+07
3100	0	6.3758e+06	1.2232e+07	1.5098e+07	1.5181e+07	1.5225e+07	1.5297e+07	1.536e+07	1.5417e+07
3200	0	6.3999e+06	1.2276e+07	1.5093e+07	1.5171e+07	1.5214e+07	1.5283e+07	1.5341e+07	1.5396e+07
3300	0	6.4241e+06	1.2321e+07	1.5092e+07	1.5165e+07	1.5207e+07	1.5272e+07	1.5328e+07	1.538e+07
3400	0	6.4482e+06	1.2365e+07	1.5091e+07	1.5161e+07	1.5202e+07	1.5265e+07	1.5318e+07	1.5368e+07
3500	0	6.4723e+06	1.241e+07	1.5091e+07	1.5158e+07	1.5198e+07	1.5259e+07	1.531e+07	1.5359e+07
3600	0	6.4964e+06	1.2455e+07	1.5092e+07	1.5156e+07	1.5196e+07	1.5254e+07	1.5304e+07	1.5351e+07
3700	0	6.5206e+06	1.25e+07	1.5094e+07	1.5154e+07	1.5194e+07	1.5251e+07	1.5299e+07	1.5345e+07
3800	0	6.5447e+06	1.2544e+07	1.5095e+07	1.5153e+07	1.5192e+07	1.5248e+07	1.5295e+07	1.5339e+07
3900	0	6.5688e+06	1.2589e+07	1.5096e+07	1.5152e+07	1.5191e+07	1.5246e+07	1.5292e+07	1.5335e+07
4000	0	6.593e+06	1.2634e+07	1.5097e+07	1.5152e+07	1.519e+07	1.5244e+07	1.529e+07	1.5331e+07
4100	0	6.6171e+06	1.2678e+07	1.5098e+07	1.5152e+07	1.5189e+07	1.5242e+07	1.5287e+07	1.5328e+07
4200	0	6.6413e+06	1.2723e+07	1.5099e+07	1.5151e+07	1.5189e+07	1.5241e+07	1.5285e+07	1.5325e+07
4300	0	6.6654e+06	1.2768e+07	1.51e+07	1.5151e+07	1.5188e+07	1.5239e+07	1.5284e+07	1.5323e+07
4400	0	6.6896e+06	1.2813e+07	1.5101e+07	1.5151e+07	1.5188e+07	1.5238e+07	1.5282e+07	1.5321e+07
4500	0	6.7137e+06	1.2857e+07	1.5103e+07	1.5152e+07	1.5188e+07	1.5237e+07	1.5281e+07	1.5319e+07
4600	0	6.7379e+06	1.2902e+07	1.5104e+07	1.5152e+07	1.5187e+07	1.5237e+07	1.528e+07	1.5317e+07
4700	0	6.762e+06	1.2947e+07	1.5105e+07	1.5152e+07	1.5187e+07	1.5236e+07	1.5279e+07	1.5316e+07
4800	0	6.7861e+06	1.2992e+07	1.5106e+07	1.5152e+07	1.5187e+07	1.5235e+07	1.5278e+07	1.5314e+07
4900	0	6.8103e+06	1.3036e+07	1.5107e+07	1.5152e+07	1.5187e+07	1.5235e+07	1.5277e+07	1.5313e+07
5000	0	6.8344e+06	1.3081e+07	1.5108e+07	1.5153e+07	1.5187e+07	1.5234e+07	1.5276e+07	1.5312e+07
5200	0	6.8827e+06	1.317e+07	1.511e+07	1.5153e+07	1.5187e+07	1.5233e+07	1.5274e+07	1.531e+07
5400	0	6.9308e+06	1.326e+07	1.5112e+07	1.5154e+07	1.5186e+07	1.5232e+07	1.5273e+07	1.5308e+07
5600	0	6.9792e+06	1.3349e+07	1.5113e+07	1.5154e+07	1.5186e+07	1.5232e+07	1.5272e+07	1.5306e+07
5800	0	7.0274e+06	1.3438e+07	1.5115e+07	1.5154e+07	1.5186e+07	1.5231e+07	1.527e+07	1.5305e+07
6000	0	7.0756e+06	1.3528e+07	1.5116e+07	1.5155e+07	1.5187e+07	1.5231e+07	1.5269e+07	1.5304e+07
6200	0	7.1239e+06	1.3617e+07	1.5124e+07	1.5155e+07	1.5187e+07	1.523e+07	1.5268e+07	1.5303e+07
6400	0	7.1721e+06	1.3706e+07	1.5133e+07	1.5156e+07	1.5187e+07	1.523e+07	1.5268e+07	1.5302e+07
6600	0	7.2203e+06	1.3795e+07	1.5133e+07	1.5156e+07	1.5187e+07	1.5229e+07	1.5267e+07	1.5301e+07
6800	0	7.2684e+06	1.3884e+07	1.5132e+07	1.5156e+07	1.5187e+07	1.5229e+07	1.5266e+07	1.53e+07
7000	0	7.3166e+06	1.3973e+07	1.5129e+07	1.5157e+07	1.5187e+07	1.5228e+07	1.5265e+07	1.53e+07
7200	0	7.3647e+06	1.4062e+07	1.5127e+07	1.5157e+07	1.5186e+07	1.5228e+07	1.5265e+07	1.5299e+07
7400	0	7.4128e+06	1.4151e+07	1.5126e+07	1.5157e+07	1.5186e+07	1.5228e+07	1.5264e+07	1.5298e+07
7600	0	7.4609e+06	1.4239e+07	1.5125e+07	1.5157e+07	1.5186e+07	1.5228e+07	1.5264e+07	1.5297e+07
7800	0	7.509e+06	1.4328e+07	1.5125e+07	1.5158e+07	1.5186e+07	1.5227e+07	1.5263e+07	1.5296e+07
8000	0	7.557e+06	1.4417e+07	1.5125e+07	1.5158e+07	1.5186e+07	1.5227e+07	1.5262e+07	1.5295e+07
8200	0	7.6051e+06	1.4505e+07	1.5125e+07	1.5158e+07	1.5186e+07	1.5227e+07	1.5262e+07	1.5295e+07

8400	0	7.6531e+06	1.4594e+07	1.5125e+07	1.5158e+07	1.5186e+07	1.5226e+07	1.5261e+07	1.5294e+07
8600	0	7.7011e+06	1.4682e+07	1.5126e+07	1.5158e+07	1.5186e+07	1.5226e+07	1.5261e+07	1.5293e+07
8800	0	7.7491e+06	1.4771e+07	1.5126e+07	1.5158e+07	1.5186e+07	1.5226e+07	1.526e+07	1.5293e+07
9000	0	7.797e+06	1.4859e+07	1.5126e+07	1.5158e+07	1.5186e+07	1.5225e+07	1.526e+07	1.5292e+07
9200	0	7.8449e+06	1.4943e+07	1.5127e+07	1.5159e+07	1.5186e+07	1.5225e+07	1.5259e+07	1.5292e+07
9400	0	7.8928e+06	1.5011e+07	1.5127e+07	1.5159e+07	1.5185e+07	1.5225e+07	1.5259e+07	1.5291e+07
9600	0	7.9407e+06	1.5039e+07	1.5127e+07	1.5159e+07	1.5185e+07	1.5225e+07	1.5259e+07	1.5291e+07
9800	0	7.9885e+06	1.5051e+07	1.5127e+07	1.5159e+07	1.5185e+07	1.5225e+07	1.5258e+07	1.529e+07
10000	0	8.0364e+06	1.5057e+07	1.5128e+07	1.5159e+07	1.5185e+07	1.5224e+07	1.5258e+07	1.529e+07

Time	Pressure [MPa]								
[years]	f=0.2	f=0.25	f=0.3	f=0.35	f=0.4	f=0.5	f=0.6	f=0.8	f=1.0
6.5144e-11	0	0	0	0	0	0	0	0	0
3.9006e-09	2.1687e-06	2.7109e-06	3.2531e-06	3.7952e-06	4.3374e-06	5.4218e-06	6.5061e-06	8.6748e-06	1.0844e-05
7.3573e-09	5.7549e-06	7.1937e-06	8.6324e-06	1.0071e-05	1.151e-05	1.4387e-05	1.7265e-05	2.302e-05	2.8775e-05
1.184e-08	1.0855e-05	1.3569e-05	1.6282e-05	1.8996e-05	2.171e-05	2.7137e-05	3.2564e-05	4.3419e-05	5.4274e-05
1.7348e-08	1.7468e-05	2.1835e-05	2.6202e-05	3.057e-05	3.4937e-05	4.3671e-05	5.2405e-05	6.9873e-05	8.7342e-05
2.3883e-08	2.5595e-05	3.1994e-05	3.8393e-05	4.4792e-05	5.1191e-05	6.3989e-05	7.6786e-05	0.00010238	0.00012798
3.1443e-08	3.5236e-05	4.4045e-05	5.2854e-05	6.1663e-05	7.0473e-05	8.8091e-05	0.00010571	0.00014095	0.00017618
6.028e-08	7.324e-05	9.1551e-05	0.00010986	0.00012817	0.00014648	0.0001831	0.00021972	0.00029296	0.0003662
9.835e-08	0.00012487	0.00015608	0.0001873	0.00021852	0.00024973	0.00031217	0.0003746	0.00049947	0.00062434
1.2886e-07	0.00016685	0.00020857	0.00025028	0.00029199	0.00033371	0.00041713	0.00050056	0.00066741	0.00083427
1.4565e-07	0.00019012	0.00023765	0.00028518	0.0003327	0.00038023	0.00047529	0.00057035	0.00076047	0.00095058
1.8232e-07	0.00024118	0.00030148	0.00036178	0.00042207	0.00048237	0.00060296	0.00072355	0.00096474	0.0012059
2.0219e-07	0.00026899	0.00033624	0.00040348	0.00047073	0.00053798	0.00067247	0.00080697	0.001076	0.0013449
2.4501e-07	0.00032914	0.00041142	0.00049371	0.00057599	0.00065828	0.00082285	0.00098742	0.0013166	0.0016457
2.6796e-07	0.00036148	0.00045186	0.00054223	0.0006326	0.00072297	0.00090371	0.0010845	0.0014459	0.0018074
2.9194e-07	0.00039534	0.00049418	0.00059302	0.00069185	0.00079069	0.00098836	0.001186	0.0015814	0.0019767
5.8812e-07	0.00081719	0.0010215	0.0012258	0.0014301	0.0016344	0.002043	0.0024516	0.0032688	0.0040859
8.5649e-07	0.0012025	0.0015032	0.0018038	0.0021045	0.0024051	0.0030064	0.0036076	0.0048102	0.0060127
1.1265e-06	0.0015919	0.0019899	0.0023878	0.0027858	0.0031838	0.0039797	0.0047757	0.0063675	0.0079594
1.4335e-06	0.0020357	0.0025446	0.0030536	0.0035625	0.0040714	0.0050893	0.0061072	0.0081429	0.010179
1.7175e-06	0.0024472	0.003059	0.0036708	0.0042826	0.0048944	0.006118	0.0073416	0.0097888	0.012236
1.9632e-06	0.0028036	0.0035046	0.0042055	0.0049064	0.0056073	0.0070091	0.0084109	0.011215	0.014018
2.2253e-06	0.0031843	0.0039804	0.0047765	0.0055725	0.0063686	0.0079608	0.0095529	0.012737	0.015922
2.5038e-06	0.0035892	0.0044865	0.0053838	0.0062811	0.0071784	0.008973	0.010768	0.014357	0.017946
2.7988e-06	0.0040183	0.0050229	0.0060274	0.007032	0.0080366	0.010046	0.012055	0.016073	0.020091
5.534e-06	0.0080086	0.010011	0.012013	0.014015	0.016017	0.020022	0.024026	0.032034	0.040043
8.3869e-06	0.012182	0.015227	0.018273	0.021318	0.024364	0.030455	0.036546	0.048728	0.06091
1.1065e-05	0.016104	0.02013	0.024156	0.028182	0.032208	0.040261	0.048313	0.064417	0.080521
1.3774e-05	0.020077	0.025096	0.030116	0.035135	0.040154	0.050193	0.060231	0.080308	0.10039
1.6595e-05	0.024216	0.03027	0.036324	0.042378	0.048432	0.06054	0.072648	0.096864	0.12108
1.9279e-05	0.028156	0.035194	0.042233	0.049272	0.056311	0.070389	0.084467	0.11262	0.14078
2.2164e-05	0.032392	0.04049	0.048588	0.056686	0.064784	0.08098	0.097176	0.12957	0.16196
2.4797e-05	0.03626	0.045324	0.054389	0.063454	0.072519	0.090649	0.10878	0.14504	0.1813
2.7578e-05	0.040345	0.050431	0.060518	0.070604	0.08069	0.10086	0.12104	0.16138	0.20173
5.5141e-05	0.080885	0.10111	0.12133	0.14155	0.16177	0.20221	0.24266	0.32354	0.40443
8.2429e-05	0.12106	0.15133	0.1816	0.21186	0.24213	0.30266	0.36319	0.48426	0.60532
0.0001099	0.16154	0.20192	0.24231	0.28269	0.32307	0.40384	0.48461	0.64615	0.80769
0.00013757	0.20232	0.2529	0.30348	0.35407	0.40465	0.50581	0.60697	0.80929	1.0116
0.00016483	0.24253	0.30316	0.36379	0.42442	0.48505	0.60632	0.72758	0.97011	1.2126
0.00019204	0.28266	0.35333	0.42399	0.49466	0.56532	0.70665	0.84798	1.1306	1.4133
0.00021998	0.32388	0.40486	0.48583	0.5668	0.64777	0.80971	0.97165	1.2955	1.6194
0.00024696	0.3637	0.45463	0.54555	0.63648	0.72741	0.90926	1.0911	1.4548	1.8185
0.00027475	0.40472	0.5059	0.60709	0.70827	0.80945	1.0118	1.2142	1.6189	2.0236
0.00054827	0.80883	1.011	1.2132	1.4154	1.6177	2.0221	2.4265	3.2353	4.0441
0.00082322	1.2156	1.5195	1.8234	2.1273	2.4312	3.039	3.6468	4.8624	6.078
0.0010961	1.6198	2.0247	2.4297	2.8346	3.2395	4.0494	4.8593	6.4791	8.0989
0.0013709	2.027	2.5338	3.0406	3.5473	4.0541	5.0676	6.0811	8.1081	10.135
0.001645	2.4336	3.042	3.6504	4.2588	4.8671	6.0839	7.3007	9.7343	12.168
0.0019181	2.839	3.5487	4.2585	4.9682	5.678	7.0975	8.517	11.356	14.195
0.0021932	3.2473	4.0591	4.871	5.6828	6.4946	8.1183	9.7419	12.989	16.237
0.0024663	3.653	4.5662	5.4795	6.3927	7.306	9.1325	10.959	14.612	18.265
0.0027412	4.0614	5.0768	6.0921	7.1075	8.1228	10.154	12.184	16.246	20.307
0.0054803	8.1339	10.167	12.201	14.234	16.268	20.335	24.402	32.536	40.669
0.0082175	12.207	15.259	18.31	21.362	24.414	30.517	36.62	48.827	61.034
0.010955	16.291	20.363	24.436	28.509	32.582	40.727	48.872	65.163	81.454
0.013697	20.39	25.487	30.584	35.682	40.779	50.974	61.169	81.558	101.95
0.016434	24.489	30.612	36.734	42.856	48.979	61.223	73.468	97.957	122.45
0.01917	28.586	35.733	42.879	50.026	57.172	71.466	85.759	114.34	142.93
0.021907	32.686	40.857	49.028	57.2	65.371	81.714	98.057	130.74	163.43
0.024649	36.789	45.986	55.184	64.381	73.578	91.973	110.37	147.16	183.95
0.027387	40.885	51.106	61.328	71.549	81.77	102.21	122.66	163.54	204.43
0.054771	82.05	102.56	123.08	143.59	164.1	205.13	246.15	328.2	410.25
0.082145	123.52	154.4	185.28	216.16	247.04	308.8	370.56	494.08	617.6
0.10952	165.16	206.45	247.73	289.02	330.31	412.89	495.47	660.63	825.78
0.13692	207.02	258.77	310.53	362.28	414.03	517.54	621.05	828.07	1035.1
0.16428	248.94	311.17	373.41	435.64	497.88	622.35	746.82	995.75	1244.7
0.19168	290.93	363.66	436.39	509.13	581.86	727.32	872.79	1163.7	1454.6
0.21905	332.93	416.16	499.39	582.62	665.85	832.32	998.78	1331.7	1664.6
0.24644	374.95	468.68	562.42	656.15	749.89	937.36	1124.8	1499.8	1874.7
0.27382	416.98	521.22	625.47	729.71	833.95	1042.4	1250.9	1667.9	2084.9
0.3012	459.03	573.78	688.54	803.3	918.05	1147.6	1377.1	1836.1	2295.1
0.32858	501.12	626.4	751.68	876.96	1002.2	1252.8	1503.4	2004.5	2505.6
0.35594	543.18	678.97	814.76	950.56	1086.4	1357.9	1629.5	2172.7	2715.9
0.38333	585.29	731.61	877.93	1024.3	1170.6	1463.2	1755.9	2341.1	2926.4
0.41071	627.43	784.29	941.15	1098	1254.9	1568.6	1882.3	2509.7	3137.1
0.43808	669.56	836.95	1004.3	1171.7	1339.1	1673.9	2008.7	2678.2	3347.8
0.46547	711.74	889.67	1067.6	1245.5	1423.5	1779.3	2135.2	2846.9	3558.7
0.49283	753.91	942.39	1130.9	1319.3	1507.8	1884.8	2261.7	3015.6	3769.5
0.52022	796.15	995.19	1194.2	1393.3	1592.3	1990.4	2388.4	3184.6	3980.7

0.54761	838.44	1048	1257.7	1467.3	1676.9	2096.1	2515.3	3353.7	4192.1
0.57498	880.72	1100.9	1321.1	1541.3	1761.4	2201.8	2642.2	3522.9	4403.6
0.60236	923.05	1153.8	1384.6	1615.3	1846.1	2307.6	2769.1	3692.2	4615.2
0.62976	965.44	1206.8	1448.2	1689.5	1930.9	2413.6	2896.3	3861.7	4827.1
0.6571	1007.8	1259.8	1511.7	1763.6	2015.6	2519.5	3023.4	4031.2	5038.9
0.68451	1050.3	1312.9	1575.4	1838	2100.6	2625.7	3150.9	4201.1	5251.4
0.71186	1092.7	1365.9	1639.1	1912.3	2185.5	2731.9	3278.2	4370.9	5463.6
0.73924	1135.3	1419.1	1702.9	1986.8	2270.6	2838.2	3405.8	4541.1	5676.4
0.76662	1177.9	1472.4	1766.8	2061.3	2355.8	2944.7	3533.6	4711.5	5889.4
0.79402	1220.6	1525.7	1830.8	2136	2441.1	3051.4	3661.6	4882.2	6102.7
0.82141	1263.3	1579.1	1894.9	2210.7	2526.5	3158.1	3789.8	5053	6316.2
0.84875	1306	1632.5	1958.9	2285.4	2611.9	3264.9	3917.9	5223.8	6529.7
0.87617	1348.8	1686	2023.2	2360.4	2697.6	3372	4046.4	5395.2	6744
0.90355	1391.7	1739.6	2087.5	2435.4	2783.4	3479.2	4175	5566.7	6958.3
0.93091	1434.6	1793.2	2151.9	2510.5	2869.1	3586.4	4303.7	5738.2	7172.7
0.95828	1477.5	1846.9	2216.3	2585.7	2955	3693.8	4432.5	5910	7387.5
1	1543.1	1928.9	2314.7	2700.5	3086.2	3857.8	4629.3	6172.4	7715.5
2.0001	3142	3927.5	4713	5498.4	6283.9	7854.8	9425.6	12567	15709
3.0001	4791.1	5988.7	7186.4	8384.1	9581.7	11977	14372	19162	23951
4.0001	6492.5	8115.5	9738.4	11361	12984	16230	19475	25964	32453
5.0001	8245.7	10307	12368	14429	16490	20611	24732	32972	41210
6.0001	10052	12565	15077	17589	20101	25124	30147	40190	50230
7.0001	11913	14890	17867	20844	23821	29773	35724	47622	59515
8.0001	13829	17285	20741	24196	27651	34559	41466	55273	69072
9.0001	15803	19752	23700	27648	31595	39487	47377	63148	78908
10	17835	22292	26748	31202	35656	44561	53462	71252	89028
20	41766	52184	62594	72995	83387	1.0414e+05	1.2486e+05	1.662e+05	2.074e+05
30	72942	91078	1.0918e+05	1.2724e+05	1.4526e+05	1.8119e+05	2.1697e+05	2.8808e+05	3.5863e+05
40	1.1432e+05	1.4258e+05	1.7073e+05	1.9875e+05	2.2665e+05	2.8211e+05	3.371e+05	4.4572e+05	5.5262e+05
50	1.6837e+05	2.0964e+05	2.5061e+05	2.9127e+05	3.3164e+05	4.1151e+05	4.9027e+05	6.4467e+05	7.9517e+05
60	2.4063e+05	2.9875e+05	3.5611e+05	4.1274e+05	4.6866e+05	5.785e+05	6.858e+05	8.9347e+05	1.0929e+06
70	3.3769e+05	4.1764e+05	4.9599e+05	5.7285e+05	6.4828e+05	7.9523e+05	9.3699e+05	1.2063e+06	1.4599e+06
80	4.6803e+05	5.7518e+05	6.7901e+05	7.7984e+05	8.7781e+05	1.0661e+06	1.2456e+06	1.5821e+06	1.8934e+06
90	6.4725e+05	7.8889e+05	9.2416e+05	1.0538e+06	1.1781e+06	1.4131e+06	1.6319e+06	2.0308e+06	2.3924e+06
100	8.9131e+05	1.0733e+06	1.2439e+06	1.4041e+06	1.5556e+06	1.8373e+06	2.0966e+06	2.5604e+06	2.9666e+06
110	1.2139e+06	1.4437e+06	1.655e+06	1.8485e+06	2.0274e+06	2.3516e+06	2.6426e+06	3.1525e+06	3.6007e+06
120	1.6094e+06	1.8903e+06	2.1423e+06	2.3712e+06	2.5798e+06	2.9492e+06	3.267e+06	3.8121e+06	4.2765e+06
130	2.0527e+06	2.3986e+06	2.698e+06	2.9606e+06	3.1944e+06	3.6008e+06	3.9508e+06	4.5188e+06	4.9943e+06
140	2.5036e+06	2.9199e+06	3.2781e+06	3.5861e+06	3.8537e+06	4.2945e+06	4.6607e+06	5.2569e+06	5.7375e+06
150	2.9529e+06	3.439e+06	3.8556e+06	4.212e+06	4.5179e+06	5.0099e+06	5.3931e+06	6.0099e+06	6.483e+06
160	3.377e+06	3.9477e+06	4.4222e+06	4.8255e+06	5.1718e+06	5.7183e+06	6.1293e+06	6.7521e+06	7.2297e+06
170	3.7719e+06	4.4274e+06	4.9699e+06	5.4195e+06	5.8046e+06	6.4095e+06	6.8542e+06	7.4852e+06	7.9693e+06
180	4.1508e+06	4.8765e+06	5.4903e+06	5.9884e+06	6.4119e+06	7.0742e+06	7.5531e+06	8.2024e+06	8.6903e+06
190	4.5153e+06	5.3047e+06	5.9792e+06	6.5299e+06	6.9901e+06	7.7072e+06	8.2228e+06	8.8961e+06	9.3865e+06
200	4.8677e+06	5.7174e+06	6.4436e+06	7.0446e+06	7.5393e+06	8.3084e+06	8.8602e+06	9.5621e+06	1.0057e+07
210	5.2104e+06	6.1158e+06	6.889e+06	7.5346e+06	8.0613e+06	8.8789e+06	9.4651e+06	1.0198e+07	1.0698e+07
220	5.5446e+06	6.5012e+06	7.3184e+06	8.0025e+06	8.5591e+06	9.4212e+06	1.0039e+07	1.0803e+07	1.1307e+07
230	5.8712e+06	6.8761e+06	7.7345e+06	8.4509e+06	9.0342e+06	9.9381e+06	1.0583e+07	1.1379e+07	1.189e+07
240	6.1904e+06	7.2408e+06	8.138e+06	8.883e+06	9.4899e+06	1.0431e+07	1.1101e+07	1.1927e+07	1.2447e+07
250	6.5027e+06	7.5963e+06	8.53e+06	9.3021e+06	9.9302e+06	1.0904e+07	1.1596e+07	1.2449e+07	1.2981e+07
260	6.8086e+06	7.9435e+06	8.9117e+06	9.7104e+06	1.0358e+07	1.1362e+07	1.2074e+07	1.2953e+07	1.3498e+07
270	7.1085e+06	8.2829e+06	9.2846e+06	1.011e+07	1.0777e+07	1.181e+07	1.2542e+07	1.3445e+07	1.4004e+07
280	7.4029e+06	8.6155e+06	9.6497e+06	1.05e+07	1.1186e+07	1.225e+07	1.3002e+07	1.3929e+07	1.4498e+07
290	7.6923e+06	8.9421e+06	1.0008e+07	1.0885e+07	1.159e+07	1.2683e+07	1.3457e+07	1.4403e+07	1.4969e+07
300	7.977e+06	9.2634e+06	1.0361e+07	1.1263e+07	1.1988e+07	1.3112e+07	1.3906e+07	1.4856e+07	1.5408e+07
310	8.2575e+06	9.5802e+06	1.0709e+07	1.1637e+07	1.2381e+07	1.3537e+07	1.4348e+07	1.5277e+07	1.5812e+07
320	8.5344e+06	9.8929e+06	1.1053e+07	1.2007e+07	1.2771e+07	1.3957e+07	1.4773e+07	1.566e+07	1.6177e+07
330	8.8079e+06	1.0202e+07	1.1394e+07	1.2374e+07	1.3157e+07	1.4372e+07	1.5165e+07	1.6004e+07	1.6505e+07
340	9.0784e+06	1.0509e+07	1.1732e+07	1.2738e+07	1.3541e+07	1.4771e+07	1.5518e+07	1.631e+07	1.6798e+07
350	9.3462e+06	1.0813e+07	1.2067e+07	1.3099e+07	1.3922e+07	1.5139e+07	1.583e+07	1.6581e+07	1.7057e+07
360	9.6119e+06	1.1115e+07	1.2401e+07	1.3458e+07	1.4299e+07	1.5467e+07	1.6106e+07	1.6819e+07	1.7286e+07
370	9.8757e+06	1.1416e+07	1.2733e+07	1.3815e+07	1.4665e+07	1.5755e+07	1.6347e+07	1.7027e+07	1.7488e+07
380	1.0138e+07	1.1715e+07	1.3063e+07	1.417e+07	1.5011e+07	1.6006e+07	1.6556e+07	1.7209e+07	1.7667e+07
390	1.0399e+07	1.2012e+07	1.3392e+07	1.4517e+07	1.5319e+07	1.6225e+07	1.6738e+07	1.7369e+07	1.7829e+07
400	1.0658e+07	1.2309e+07	1.3719e+07	1.4851e+07	1.5588e+07	1.6414e+07	1.6896e+07	1.751e+07	1.7965e+07
410	1.0917e+07	1.2604e+07	1.4045e+07	1.5158e+07	1.5821e+07	1.6576e+07	1.7032e+07	1.7639e+07	1.8082e+07
420	1.1175e+07	1.2898e+07	1.4367e+07	1.5427e+07	1.6023e+07	1.6717e+07	1.7152e+07	1.7746e+07	1.8189e+07
430	1.1432e+07	1.3191e+07	1.468e+07	1.5659e+07	1.6198e+07	1.6838e+07	1.7256e+07	1.7836e+07	1.8282e+07
440	1.1688e+07	1.3483e+07	1.4977e+07	1.5859e+07	1.6347e+07	1.6943e+07	1.7353e+07	1.7919e+07	1.8364e+07
450	1.1943e+07	1.3774e+07	1.5244e+07	1.6032e+07	1.6476e+07	1.7035e+07	1.7438e+07	1.7993e+07	1.8437e+07
460	1.2197e+07	1.4064e+07	1.5475e+07	1.6181e+07	1.6586e+07	1.7116e+07	1.7505e+07	1.8057e+07	1.8501e+07
470	1.2451e+07	1.4352e+07	1.5673e+07	1.6308e+07	1.6681e+07	1.7192e+07	1.7565e+07	1.8115e+07	1.8559e+07
480	1.2704e+07	1.4633e+07	1.5844e+07	1.6417e+07	1.6764e+07	1.7261e+07	1.762e+07	1.8167e+07	1.861e+07
490	1.2956e+07	1.4902e+07	1.5992e+07	1.6511e+07	1.6837e+07	1.7313e+07	1.7669e+07	1.8213e+07	1.8657e+07
500	1.3207e+07	1.5147e+07	1.6119e+07	1.6592e+07	1.6901e+07	1.7359e+07	1.7712e+07	1.8255e+07	1.8698e+07
510	1.3458e+07	1.5361e+07	1.6229e+07	1.6664e+07	1.6958e+07	1.7403e+07	1.7752e+07	1.8293e+07	1.8736e+07
520	1.3709e+07	1.5544e+07	1.6323e+07	1.6726e+07	1.7015e+07	1.7442e+07	1.7787e+07	1.8328e+07	1.877e+07
530	1.3958e+07	1.5702e+07	1.6404e+07	1.6781e+07	1.7064e+07	1.7477e+07	1.782e+07	1.8359e+07	1.8802e+07
540	1.4207e+07	1.5839e+07	1.6474e+07	1.6829e+07	1.7101e+07	1.751e+07	1.785e+07	1.8388e+07	1.883e+07
550	1.4455e+07	1.5957e+07	1.6535e+07	1.6875e+07	1.7134e+07	1.7539e+07	1.7877e+07	1.8414e+07	1.8857e+07
560	1.4695e+07	1.6059e+07	1.6588e+07	1.6921e+07	1.7165e+07	1.7566e+07	1.7902e+07	1.8438e+07	1.888e+07
570	1.4925e+07	1.6149e+07	1.6635e+07	1.6957e+07	1.7194e+07	1.7591e+07	1.7925e+07	1.8461e+07	1.8902e+07
580	1.5131e+07	1.6226e+07	1.6677e+07	1.6985e+07	1.7219e+07	1.7613e+07	1.7946e+07	1.8481e+07	1.8921e+07
590	1.5311e+07	1.6292e+07	1.6714e+07	1.7012e+07	1.7243e+07	1.7635e+07	1.7965e+07	1.85e+07	1.8939e+07
600	1.5466e+07	1.6349e+07	1.675e+07	1.7036e+07	1.7265e+07	1.7654e+07	1.7984e+07	1.8517e+07	1.8956e+07
610	1.56e+07	1.64e+07	1.6789e+07	1.7059e+07	1.7286e+07	1.7672e+07	1.8e+07	1.8532e+07	1.8971e+07
620	1.5715e+07	1.6444e+07	1.6819e+07	1.7079e+07	1.7305e+07	1.769e+07	1.8016e+07	1.8547e+07	1.8985e+07
630	1.5816e+07	1.6483e+07	1.6842e+07	1.7099e+07	1.7323e+07	1.7706e+07	1.8032e+07	1.856e+07	1.8998e+07
640	1.5904e+07	1.6518e+07	1.6862e+07	1.7117e+07	1.734e+07	1.7721e+07	1.8046e+07	1.8573e+07	1.901e+07
650	1.5981e+07	1.6549e+07	1.6882e+07	1.7134e+07	1.7355e+07	1.7735e+07	1.8059e+07	1.8584e+07	1.9021e+07
660	1.6049e+07	1.6577e+07	1.69e+07	1.715e+07	1.737e+07	1.7748e+07	1.8071e+07	1.8595e+07	1.9031e+07
670	1.6108e+07	1.6604e+07	1.6916e+07	1.7165e+07	1.7383e+07	1.7761e+07	1.8083e+07	1.8605e+07	1.9041e+07

680	1.616e+07	1.6634e+07	1.6932e+07	1.7179e+07	1.7395e+07	1.7772e+07	1.8093e+07	1.8614e+07	1.9049e+07
690	1.6204e+07	1.6661e+07	1.6947e+07	1.7192e+07	1.7407e+07	1.7784e+07	1.8104e+07	1.8623e+07	1.9058e+07
700	1.6243e+07	1.6679e+07	1.6961e+07	1.7205e+07	1.7418e+07	1.7794e+07	1.8113e+07	1.8631e+07	1.9065e+07
710	1.6278e+07	1.6695e+07	1.6975e+07	1.7216e+07	1.7429e+07	1.7804e+07	1.8123e+07	1.8639e+07	1.9072e+07
720	1.6309e+07	1.671e+07	1.6987e+07	1.7228e+07	1.7439e+07	1.7814e+07	1.8131e+07	1.8646e+07	1.9078e+07
730	1.6337e+07	1.6724e+07	1.6999e+07	1.7238e+07	1.7449e+07	1.7823e+07	1.8139e+07	1.8653e+07	1.9084e+07
740	1.6362e+07	1.6737e+07	1.7011e+07	1.7248e+07	1.7458e+07	1.7832e+07	1.8147e+07	1.8659e+07	1.909e+07
750	1.6384e+07	1.6749e+07	1.7022e+07	1.7258e+07	1.7467e+07	1.784e+07	1.8154e+07	1.8665e+07	1.9095e+07
760	1.6405e+07	1.6761e+07	1.7033e+07	1.7267e+07	1.7475e+07	1.7848e+07	1.8161e+07	1.867e+07	1.9099e+07
770	1.6424e+07	1.6773e+07	1.7042e+07	1.7276e+07	1.7483e+07	1.7855e+07	1.8168e+07	1.8676e+07	1.9104e+07
780	1.6443e+07	1.6783e+07	1.7051e+07	1.7284e+07	1.7491e+07	1.7862e+07	1.8174e+07	1.868e+07	1.9108e+07
790	1.6466e+07	1.6794e+07	1.706e+07	1.7292e+07	1.7498e+07	1.7868e+07	1.818e+07	1.8685e+07	1.9111e+07
800	1.6486e+07	1.6804e+07	1.7068e+07	1.73e+07	1.7505e+07	1.7874e+07	1.8185e+07	1.8689e+07	1.9114e+07
810	1.6501e+07	1.6813e+07	1.7076e+07	1.7307e+07	1.7512e+07	1.788e+07	1.8191e+07	1.8693e+07	1.9117e+07
820	1.6512e+07	1.6823e+07	1.7084e+07	1.7314e+07	1.7518e+07	1.7885e+07	1.8196e+07	1.8696e+07	1.9119e+07
830	1.6523e+07	1.6831e+07	1.7091e+07	1.7321e+07	1.7524e+07	1.7891e+07	1.8201e+07	1.8699e+07	1.9121e+07
840	1.6533e+07	1.684e+07	1.7099e+07	1.7327e+07	1.753e+07	1.7896e+07	1.8205e+07	1.8702e+07	1.9123e+07
850	1.6542e+07	1.6848e+07	1.7105e+07	1.7334e+07	1.7536e+07	1.7901e+07	1.8209e+07	1.8705e+07	1.9124e+07
860	1.6551e+07	1.6855e+07	1.7112e+07	1.734e+07	1.7541e+07	1.7905e+07	1.8213e+07	1.8708e+07	1.9125e+07
870	1.6561e+07	1.6862e+07	1.7118e+07	1.7346e+07	1.7547e+07	1.791e+07	1.8217e+07	1.871e+07	1.9127e+07
880	1.6569e+07	1.6869e+07	1.7124e+07	1.7351e+07	1.7552e+07	1.7914e+07	1.822e+07	1.8712e+07	1.9128e+07
890	1.6578e+07	1.6876e+07	1.713e+07	1.7356e+07	1.7557e+07	1.7918e+07	1.8223e+07	1.8714e+07	1.9128e+07
900	1.6585e+07	1.6882e+07	1.7136e+07	1.7361e+07	1.7562e+07	1.7922e+07	1.8226e+07	1.8716e+07	1.9129e+07
910	1.6593e+07	1.6888e+07	1.7141e+07	1.7366e+07	1.7567e+07	1.7926e+07	1.8229e+07	1.8718e+07	1.9129e+07
920	1.66e+07	1.6894e+07	1.7147e+07	1.7371e+07	1.7572e+07	1.793e+07	1.8232e+07	1.8719e+07	1.9129e+07
930	1.6607e+07	1.69e+07	1.7152e+07	1.7375e+07	1.7576e+07	1.7933e+07	1.8234e+07	1.8721e+07	1.9129e+07
940	1.6614e+07	1.6905e+07	1.7157e+07	1.7379e+07	1.758e+07	1.7937e+07	1.8237e+07	1.8722e+07	1.9129e+07
950	1.662e+07	1.6911e+07	1.7161e+07	1.7384e+07	1.7584e+07	1.794e+07	1.8239e+07	1.8724e+07	1.9129e+07
960	1.6627e+07	1.6916e+07	1.7166e+07	1.7388e+07	1.7588e+07	1.7943e+07	1.8241e+07	1.8725e+07	1.9128e+07
970	1.6633e+07	1.6921e+07	1.717e+07	1.7392e+07	1.7592e+07	1.7946e+07	1.8243e+07	1.8726e+07	1.9127e+07
980	1.6639e+07	1.6926e+07	1.7175e+07	1.7396e+07	1.7595e+07	1.7949e+07	1.8245e+07	1.8727e+07	1.9126e+07
990	1.6644e+07	1.6931e+07	1.7179e+07	1.7399e+07	1.7599e+07	1.7951e+07	1.8247e+07	1.8727e+07	1.9125e+07
1000	1.665e+07	1.6935e+07	1.7183e+07	1.7403e+07	1.7602e+07	1.7954e+07	1.8249e+07	1.8727e+07	1.9124e+07
1050	1.6674e+07	1.6957e+07	1.72e+07	1.7419e+07	1.7617e+07	1.7965e+07	1.8257e+07	1.8728e+07	1.9116e+07
1100	1.6695e+07	1.6975e+07	1.7216e+07	1.7432e+07	1.7629e+07	1.7973e+07	1.8263e+07	1.8726e+07	1.9103e+07
1150	1.6713e+07	1.6991e+07	1.723e+07	1.7445e+07	1.7639e+07	1.7979e+07	1.8265e+07	1.8722e+07	1.9088e+07
1200	1.6729e+07	1.7004e+07	1.724e+07	1.7454e+07	1.7647e+07	1.7983e+07	1.8265e+07	1.8714e+07	1.907e+07
1250	1.6357e+07	1.661e+07	1.6829e+07	1.7028e+07	1.7207e+07	1.7521e+07	1.7785e+07	1.8204e+07	1.8535e+07
1300	1.6162e+07	1.6392e+07	1.6592e+07	1.6776e+07	1.694e+07	1.7231e+07	1.7475e+07	1.7863e+07	1.8169e+07
1350	1.6042e+07	1.6253e+07	1.6438e+07	1.6607e+07	1.676e+07	1.7029e+07	1.7256e+07	1.7617e+07	1.79e+07
1400	1.5963e+07	1.6158e+07	1.633e+07	1.6488e+07	1.663e+07	1.6881e+07	1.7093e+07	1.7429e+07	1.7692e+07
1450	1.5907e+07	1.609e+07	1.6251e+07	1.64e+07	1.6533e+07	1.6769e+07	1.6968e+07	1.7283e+07	1.7528e+07
1500	1.5867e+07	1.604e+07	1.6192e+07	1.6333e+07	1.6459e+07	1.6682e+07	1.687e+07	1.7166e+07	1.7395e+07
1550	1.5837e+07	1.6002e+07	1.6148e+07	1.6282e+07	1.6401e+07	1.6613e+07	1.6791e+07	1.7071e+07	1.7286e+07
1600	1.5815e+07	1.5973e+07	1.6113e+07	1.6241e+07	1.6355e+07	1.6557e+07	1.6728e+07	1.6993e+07	1.7196e+07
1650	1.5799e+07	1.5951e+07	1.6086e+07	1.6209e+07	1.6319e+07	1.6512e+07	1.6675e+07	1.6928e+07	1.7119e+07
1700	1.5786e+07	1.5934e+07	1.6064e+07	1.6183e+07	1.6289e+07	1.6474e+07	1.6631e+07	1.6873e+07	1.7054e+07
1750	1.5776e+07	1.592e+07	1.6046e+07	1.6161e+07	1.6264e+07	1.6443e+07	1.6594e+07	1.6826e+07	1.6998e+07
1800	1.5768e+07	1.5909e+07	1.6032e+07	1.6143e+07	1.6243e+07	1.6417e+07	1.6563e+07	1.6786e+07	1.695e+07
1850	1.5762e+07	1.5899e+07	1.602e+07	1.6129e+07	1.6226e+07	1.6395e+07	1.6536e+07	1.6752e+07	1.6908e+07
1900	1.5757e+07	1.5892e+07	1.601e+07	1.6116e+07	1.6211e+07	1.6376e+07	1.6513e+07	1.6722e+07	1.6872e+07
1950	1.5753e+07	1.5886e+07	1.6002e+07	1.6106e+07	1.6199e+07	1.636e+07	1.6493e+07	1.6696e+07	1.684e+07
2000	1.575e+07	1.5881e+07	1.5995e+07	1.6097e+07	1.6188e+07	1.6345e+07	1.6476e+07	1.6673e+07	1.6811e+07
2100	1.5745e+07	1.5873e+07	1.5984e+07	1.6083e+07	1.6171e+07	1.6322e+07	1.6448e+07	1.6634e+07	1.6763e+07
2200	1.5741e+07	1.5868e+07	1.5976e+07	1.6072e+07	1.6158e+07	1.6305e+07	1.6425e+07	1.6603e+07	1.6724e+07
2300	1.5739e+07	1.5863e+07	1.5969e+07	1.6064e+07	1.6147e+07	1.629e+07	1.6407e+07	1.6578e+07	1.6691e+07
2400	1.5738e+07	1.586e+07	1.5964e+07	1.6057e+07	1.6139e+07	1.6278e+07	1.6392e+07	1.6557e+07	1.6664e+07
2500	1.5737e+07	1.5857e+07	1.596e+07	1.6052e+07	1.6132e+07	1.6268e+07	1.638e+07	1.6538e+07	1.6641e+07
2600	1.5736e+07	1.5855e+07	1.5957e+07	1.6047e+07	1.6126e+07	1.626e+07	1.6369e+07	1.6522e+07	1.662e+07
2700	1.5736e+07	1.5853e+07	1.5954e+07	1.6043e+07	1.6121e+07	1.6253e+07	1.6359e+07	1.6508e+07	1.6602e+07
2800	1.562e+07	1.5732e+07	1.5829e+07	1.5914e+07	1.5989e+07	1.6117e+07	1.6218e+07	1.636e+07	1.6448e+07
2900	1.5549e+07	1.5654e+07	1.5746e+07	1.5827e+07	1.5897e+07	1.6019e+07	1.6114e+07	1.6247e+07	1.633e+07
3000	1.5502e+07	1.5601e+07	1.5687e+07	1.5763e+07	1.583e+07	1.5945e+07	1.6035e+07	1.6159e+07	1.6236e+07
3100	1.5469e+07	1.5562e+07	1.5644e+07	1.5716e+07	1.5779e+07	1.5888e+07	1.5972e+07	1.6088e+07	1.6159e+07
3200	1.5445e+07	1.5533e+07	1.5611e+07	1.5679e+07	1.5739e+07	1.5842e+07	1.5922e+07	1.603e+07	1.6096e+07
3300	1.5427e+07	1.5511e+07	1.5585e+07	1.565e+07	1.5707e+07	1.5805e+07	1.5881e+07	1.5982e+07	1.6044e+07
3400	1.5413e+07	1.5493e+07	1.5564e+07	1.5626e+07	1.5681e+07	1.5775e+07	1.5847e+07	1.5942e+07	1.5999e+07
3500	1.5402e+07	1.5479e+07	1.5548e+07	1.5607e+07	1.5659e+07	1.5749e+07	1.5818e+07	1.5908e+07	1.5961e+07
3600	1.5393e+07	1.5468e+07	1.5534e+07	1.5591e+07	1.5641e+07	1.5728e+07	1.5794e+07	1.5879e+07	1.5929e+07
3700	1.5386e+07	1.5458e+07	1.5523e+07	1.5578e+07	1.5627e+07	1.5709e+07	1.5773e+07	1.5854e+07	1.5901e+07
3800	1.538e+07	1.545e+07	1.5513e+07	1.5566e+07	1.5614e+07	1.5694e+07	1.5755e+07	1.5832e+07	1.5877e+07
3900	1.5375e+07	1.5443e+07	1.5505e+07	1.5557e+07	1.5603e+07	1.568e+07	1.574e+07	1.5813e+07	1.5855e+07
4000	1.5371e+07	1.5438e+07	1.5497e+07	1.5548e+07	1.5593e+07	1.5668e+07	1.5726e+07	1.5797e+07	1.5837e+07
4100	1.5367e+07	1.5432e+07	1.5491e+07	1.5541e+07	1.5585e+07	1.5658e+07	1.5714e+07	1.5782e+07	1.582e+07
4200	1.5363e+07	1.5428e+07	1.5485e+07	1.5534e+07	1.5578e+07	1.5648e+07	1.5703e+07	1.5769e+07	1.5805e+07
4300	1.5361e+07	1.5424e+07	1.5481e+07	1.5528e+07	1.5571e+07	1.564e+07	1.5694e+07	1.5757e+07	1.5792e+07
4400	1.5358e+07	1.542e+07	1.5476e+07	1.5523e+07	1.5566e+07	1.5633e+07	1.5685e+07	1.5747e+07	1.578e+07
4500	1.5356e+07	1.5417e+07	1.5472e+07	1.5518e+07	1.556e+07	1.5626e+07	1.5677e+07	1.5738e+07	1.5769e+07
4600	1.5353e+07	1.5414e+07	1.5469e+07	1.5514e+07	1.5555e+07	1.5621e+07	1.567e+07	1.5729e+07	1.576e+07
4700	1.5352e+07	1.5412e+07	1.5466e+07	1.551e+07	1.5551e+07	1.5615e+07	1.5664e+07	1.5721e+07	1.5751e+07
4800	1.535e+07	1.541e+07	1.5463e+07	1.5507e+07	1.5547e+07	1.561e+07	1.5658e+07	1.5714e+07	1.5743e+07
4900	1.5348e+07	1.5407e+07	1.546e+07	1.5503e+07	1.5543e+07	1.5606e+07	1.5653e+07	1.5707e+07	1.5735e+07
5000	1.5347e+07	1.5405e+07	1.5457e+07	1.5501e+07	1.554e+07	1.5602e+07	1.5648e+07	1.5701e+07	1.5728e+07
5200	1.5344e+07	1.5402e+07	1.5453e+07	1.5495e+07	1.5533e+07	1.5594e+07	1.5639e+07	1.569e+07	1.5716e+07
5400	1.5341e+07	1.5399e+07	1.5449e+07	1.5491e+07	1.5528e+07	1.5588e+07	1.5631e+07	1.568e+07	1.5706e+07
5600	1.5339e+07	1.5396e+07	1.5445e+07	1.5487e+07	1.5523e+07	1.5583e+07	1.5624e+07	1.5672e+07	1.5696e+07
5800	1.5337e+07	1.5394e+07	1.5442e+07	1.5483e+07	1.5519e+07	1.5578e+07	1.5618e+07	1.5664e+07	1.5688e+07
6000	1.5335e+07	1.5392e+07	1.544e+07	1.548e+07	1.5515e+07	1.5573e+07	1.5612e+07	1.5657e+07	1.568e+07
6200	1.5333e+07	1.539e+07	1.5437e+07	1.5477e+07	1.5512e+07	1.5569e+07	1.5607e+07	1.5651e+07	1.5673e+07
6400	1.5332e+07	1.5388e+07	1.5435e+07	1.5474e+07	1.5509e+07	1.5565e+07	1.5602e+07	1.5645e+07	1.5667e+07
6600	1.533e+07	1.5386e+07	1.5433e+07	1.5472e+07	1.5506e+07	1.5561e+07	1.5598e+07	1.564e+07	1.5661e+07
6800	1.5329e+07	1.5384e+07	1.5431e+07	1.547e+07	1.5503e+07	1.5558e+07	1.5594e+07	1.5635e+07	1.5655e+07

7000	1.5328e+07	1.5383e+07	1.5429e+07	1.5467e+07	1.5501e+07	1.5555e+07	1.559e+07	1.5631e+07	1.565e+07
7200	1.5327e+07	1.5382e+07	1.5428e+07	1.5465e+07	1.5499e+07	1.5552e+07	1.5586e+07	1.5626e+07	1.5645e+07
7400	1.5326e+07	1.5381e+07	1.5426e+07	1.5463e+07	1.5497e+07	1.5549e+07	1.5583e+07	1.5622e+07	1.564e+07
7600	1.5325e+07	1.5379e+07	1.5425e+07	1.5462e+07	1.5495e+07	1.5546e+07	1.558e+07	1.5618e+07	1.5635e+07
7800	1.5324e+07	1.5378e+07	1.5423e+07	1.546e+07	1.5493e+07	1.5544e+07	1.5576e+07	1.5615e+07	1.5631e+07
8000	1.5324e+07	1.5377e+07	1.5422e+07	1.5458e+07	1.5491e+07	1.5541e+07	1.5573e+07	1.5611e+07	1.5626e+07
8200	1.5323e+07	1.5376e+07	1.542e+07	1.5457e+07	1.5489e+07	1.5539e+07	1.5571e+07	1.5608e+07	1.5622e+07
8400	1.5322e+07	1.5375e+07	1.5419e+07	1.5455e+07	1.5487e+07	1.5537e+07	1.5568e+07	1.5604e+07	1.5618e+07
8600	1.5322e+07	1.5374e+07	1.5418e+07	1.5454e+07	1.5486e+07	1.5535e+07	1.5565e+07	1.5601e+07	1.5614e+07
8800	1.5321e+07	1.5373e+07	1.5417e+07	1.5453e+07	1.5484e+07	1.5533e+07	1.5562e+07	1.5598e+07	1.561e+07
9000	1.532e+07	1.5372e+07	1.5416e+07	1.5451e+07	1.5483e+07	1.5531e+07	1.5559e+07	1.5595e+07	1.5606e+07
9200	1.532e+07	1.5372e+07	1.5415e+07	1.545e+07	1.5481e+07	1.5529e+07	1.5557e+07	1.5592e+07	1.5603e+07
9400	1.5319e+07	1.5371e+07	1.5414e+07	1.5449e+07	1.548e+07	1.5527e+07	1.5554e+07	1.5589e+07	1.5599e+07
9600	1.5319e+07	1.537e+07	1.5413e+07	1.5448e+07	1.5479e+07	1.5525e+07	1.5552e+07	1.5586e+07	1.5595e+07
9800	1.5318e+07	1.5369e+07	1.5412e+07	1.5447e+07	1.5477e+07	1.5523e+07	1.555e+07	1.5583e+07	1.5592e+07
10000	1.5318e+07	1.5369e+07	1.5411e+07	1.5446e+07	1.5476e+07	1.5521e+07	1.5548e+07	1.558e+07	1.5589e+07

DISTRIBUTION

Email—External (encrypt for CUI)

Name	Company Email Address	Company Name
George Basabilvazo	george.basabilvazo@wipp.ws	U.S. Department of Energy Carlsbad Field Office
Anderson Ward	anderson.ward@wipp.ws	U.S. Department of Energy Carlsbad Field Office
Michael Gross	mike_gross@earthlink.net	MG Enterprises
Gordan Gjerapic	ggjerapic@gmail.com	Golder Associates
Frank Hansen	francis.d.hansen@gmail.com	N/A
J. Guadalupe Arguello	llae.arguello@att.net	N/A

Email—Internal (encrypt for CUI)

Name	Org.	Sandia Email Address
F. Beckwith	1542	fbeckwi@sandia.gov
W. Witkowski	1550	wrwitko@sandia.gov
A. Brundage	1554	albrund@sandia.gov
S. Nelson	1558	smnelso@sandia.gov
J. Coulibaly	1558	jbcouli@sandia.gov
D. O'Connor	1558	dtoconn@sandia.gov
E. Stein	8840	ergiamb@sandia.gov
E. Matteo	8842	enmatte@sandia.gov
K. Kuhlman	8842	klkuhlm@sandia.gov
R. Rechard	8842	rprecha@sandia.gov
R. C. Camphouse	8842	rccamph@sandia.gov
M. Mills	8842	mmmills@sandia.gov
R. Keith	8880	rlkeith@sandia.gov
D. Kicker	8880	dckicke@sandia.gov
G. Duran	8880	gasosa@sandia.gov
R. Kirkes	8881	grkirke@sandia.gov

Name	Org.	Sandia Email Address
S. King	8881	sking@sandia.gov
J. Long	8881	jjlong@sandia.gov
S. Wagner	8881	swagner@sandia.gov
B. Park	8912	bypark@sandia.gov
T. Zeitler	8912	tzeitle@sandia.gov
T. Ross	8912	tsross@sandia.gov
R. Jensen	8914	rpjense@sandia.gov
A. Holland	8914	aaholla@sandia.gov
S. Broome	8914	stbroom@sandia.gov
C. Herrick	8914	cgherri@sandia.gov
M. Ingraham	8914	mdingr@sandia.gov
Technical Library	1911	sanddocs@sandia.gov



Sandia National Laboratories is a multimission laboratory managed and operated by National Technology & Engineering Solutions of Sandia LLC, a wholly owned subsidiary of Honeywell International Inc., for the U.S. Department of Energy's National Nuclear Security Administration under contract DE-NA0003525.